TESIS DE LA UNIVERSIDAD DE ZARAGOZA

2024 405

María Del Pilar Arenaz Callao

In vitro studies to optimize β-lactam containing regimens for tuberculosis therapy

Director/es
Mendoza Losana, Alfonso
Ramon Garcia, Santiago

ISSN 2254-7606

Prensas de la Universidad
Universidad Zaragoza

Universidad de Zaragoza
Servicio de Publicaciones

ISSN 2254-7606

Universidad Zaragoza
1542

Tesis Doctoral

IN VITRO STUDIES TO OPTIMIZE B-LACTAM CONTAINING REGIMENS FOR TUBERCULOSIS THERAPY

Autor

María Del Pilar Arenaz Callao

Director/es

Mendoza Losana, Alfonso
Ramon Garcia, Santiago

UNIVERSIDAD DE ZARAGOZA
Escuela de Doctorado

Programa de Doctorado en Bioquímica y Biología Molecular

2022

FACULTAD DE MEDICINA

Departamento de Microbiología, Pediatría, Radiología y Salud Pública

In vitro studies to optimize β-lactam containing regimens for tuberculosis therapy

Memoria para optar al grado de Doctor presentada por:

María del Pilar Arenaz Callao

Licenciada en Bioquímica

Directores:

Santiago Ramón García

Alfonso Mendoza Losana

Dr. SANTIAGO RAMÓN GARCÍA, Investigador ARAID en el Departamento de Microbiología, Pediatría, Radiología y Salud Pública de la Facultad de Medicina de la Universidad de Zaragoza.

Dr. ALFONSO MENDOZA LOSANA, Investigador Distinguido en el Departamento de Bioingeniería de la Universidad Carlos III de Madrid.

Directores de la Tesis Doctoral presentada por **María Pilar Arenaz Callao** bajo el título:

In vitro studies to optimize β-lactam containing regimens for tuberculosis therapy

(ESTUDIOS *IN VITRO* PARA OPTIMIZAR LOS REGÍMENES QUE CONTIENEN β-LACTÁMICOS PARA EL TRATAMIENTO DE LA TUBERCULOSIS)

EXPONEN:

Que dicha Tesis Doctoral corresponde con el proyecto de tesis presentado y aprobado en su momento, no habiéndose producido ninguna variación.

Que dicha Tesis Doctoral ha sido realizada bajo su dirección y reúne los requisitos necesarios para optar al grado de Doctor.

Por lo anterior, emiten el presente **INFORME FAVORABLE**.

Zaragoza, 10 de enero de 2022

Fdo: Santiago Ramón García

Fdo: Alfonso Mendoza Losana

Esta tesis doctoral ha sido elaborada en el centro de investigación DDW (Diseases of the Developing World) de la compañía GlaxoSmithKline (GSK) en Tres Cantos (Madrid, España) en colaboración con la Fundación ARAID (Zaragoza, España) y la Universidad de British Columbia (Vancouver, Canadá). La tesis doctoral está adscrita al Departamento de Microbiología, Pediatría, Radiología y Salud Pública de la Facultad de Medicina de la Universidad de Zaragoza dentro del programa de Doctorado del Departamento de Bioquímica y Biología Molecular, habiendo sido María Pilar Arenaz Callao beneficiaria de un contrato laboral de la Fundación ARAID financiado por la Fundación Tres Cantos Open Lab.

Este trabajo ha sido realizado bajo el marco de dos proyectos de investigación financiados por la Fundación Tres Cantos Open Lab: “The development of synergistic combinations of rifampicin and cephalosporins against *Mycobacterium tuberculosis* (Ref. TC144)” y “Predicting optimal dosing schedules and clinical outcomes of beta-lactams for TB therapy using PKPD and mechanistic models Carbapenem *vs* cephem: the beta-lactam paradigm (Ref. TC256)”

Index of contents

List of abbreviations 1
Summary 5
Resumen 9
Introduction 15
History of tuberculosis 17
Pathogenesis of tuberculosis 20
Diagnosis of tuberculosis 22
Epidemics of the tuberculosis disease 23
Tuberculosis treatment and drug resistance 25
Drug discovery pipeline 29
Objectives 34
Chapter 1: Development of OPTIKA, a new technology for drug combination kinetic studies against *Mycobacterium tuberculosis* 39
1.1 Introduction 41
1.2 Material and methods 47
1.2.1 Bacterial strain, growth conditions and reagents 47
1.2.2 Growth inhibition assays. MTT Readout 47
1.2.2.1 Checkerboard assays 48
1.2.2.2 Diagonal Measurement of n-way drug interactions (DiaMOND) assay .. 49
1.2.3 Bactericidal assays 49
1.2.3.1 CARA plates preparation 49
1.2.3.2 Minimum Bactericidal Concentration (MBC) assays 49
1.2.3.3 Fractional Bactericidal Concentration Index (FBCI) assays 50
1.2.4 CFU-based time kill assays 50
1.2.5 OPTIKA (OPtimized TIme Kill Assay) protocol 51
1.2.5.1 Classification of combinations by OPTIKA 52
1.3 Results and discussion 56
1.3.1 Comparison of checkerboard and DiaMOND methodologies 56
1.3.2 *In-depth* comparison of checkerboard and DiaMOND assays data analysis . 58

1.3.3 Impact of growth inhibition parameters in the FICI calculation 61
1.3.4 CARA calibration 63
1.3.5 Fractional Bactericidal Inhibitory Concentration Index as a readout 64
1.3.6 CARA optimization and OPTIKA validation 66
1.3.6.1 Tween 80 addition to CARA plates 66
1.3.6.2 CARA pre-moistening step removal 69
1.3.6.3 OPTIKA set up and assay validation against CFU counts, the gold standard method for time kill assays 70
1.3.7 OPTIKA data analysis 74
1.3.8 Definition of OPTIKA optimal indicators according to their killing curves profiles 77
1.3.9 Study of 36 reference pair-wise combinations by OPTIKA and comparison with other methods 80
1.3.10 OPTIKA applied to triple drug combinations 81
1.4 General discussion 84
1.5 Conclusions and future perspectives 88
1.6 APPENDIX I: Chapter 1 results summary table 89
1.7 APPENDIX II: Chapter 1 Killing curves supplementary tables 90
Chapter 2: *In vitro* identification and characterization of β-lactam synergistic partners against *Mycobacterium tuberculosis* 93
2.1 Introduction 95
2.2 Material and methods 104
2.2.1 Bacterial strain, growth conditions, compound information and reagents 104
2.2.2 Growth inhibition assays. MTT Readout 105
2.2.2.1 Drug interaction studies. FICI determination 105
2.2.3 OPTIKA 107
2.2.4 β-lactam synergy screening outline 107
2.2.5 Integration of β-lactams in current anti-TB therapy 108
2.3 Results and discussion 110
2.3.1. β-lactam synergy screening outline 110
2.3.1.1 β-lactam primary synergy screening 110
2.3.1.2 β-lactam synergy screening confirmation by OPTIKA 112

2.3.1.3 OPTIKA screening of β-lactam triple drug combinations 113
2.3.1.4 Triple-drug combinations secondary validation 116
2.3.1.5 *In-depth* analysis of triple combinations containing β-lactam 117
2.3.1.5.1 Deconvolution focused on regrowth at end point 118
2.3.1.5.2 Deconvolution focused on meropenem addition to pair-wise combinations 118
2.3.1.5.3 Deconvolution focused on ethambutol and meropenem 120
2.3.2 β-lactams within currently recommended MDR-TB therapy 122
2.3.2.1 Five-drug combinations killing ability 122
2.3.2.2 Evaluation of delamanid (or β-lactam) contribution to triple and four-drug combinations 123
2.3.2.3 Negative effect of linezolid in five-drug combinations 126
2.3.2.4 Bedaquiline-pretomanid-linezolid (BPaL) deconvolution 128
2.4 General discussion and future perspectives 130
2.5 Conclusions 135
2.6 APPENDIX I: Chapter 2 results summary table 137
2.7 APPENDIX II: Chapter 2 OPTIKA killing curves suplementary tables 138
Chapter 3: Mechanism of action elucidation studies of the rifampicin/β-lactam synergy in mycobacteria 141
3.1 Introduction 143
3.2 Material and methods 148
3.2.1 Bacterial strain, growth conditions, compounds information and reagents 148
3.2.2 FICI determination. MTT assay 148
3.2.3 CFU-based time kill assays 149
3.2.4 Mechanism of action studies / experimental design 149
3.2.4.1 Mycobacterial RNA extraction 149
3.2.5 Transcriptomics 150
3.2.5.1 Selection of differentially expressed genes with statistical significance. Volcano plots 151
3.2.5.2 Functional category analysis 151
3.2.5.3 Enrichment analysis 152
3.3 Results and discussion 153

3.3.1 Confirmation of drug interaction between rifampicin and compounds targeting the cell wall in *M. bovis* BCG 153
3.3.2 General transcriptomic profile analysis 156
3.3.3 Analysis of gene differential expression 157
3.3.4 Enrichment analysis of molecular pathways 164
3.4 General discussion and future perspectives 175
3.5 Conclusions 177
3.6 APPENDIX I: Chapter 3 Killing curves supplementary tables 178
General conclusions and future perspectives 179
Conclusiones generales 185
References 189

List of abbreviations

Abs	Absorbance
ADC	Albumin dextrose catalase
AMK	Amikacin
BAC	Bacitracin
BCG	Bacilli Calmette-Guérin
BDQ	Bedaquiline
BPaL	Bedaquiline-pretomanid-linezolid
BSL3	Biosafety Level 3
CAM	Chloramphenicol
CARA	Charcoal Agar Resazurin Assay
CBA	Checkerboard assays
CDS	Coding DNA sequence
CEF	Cefdinir
CFD	Cephradine
CFM	Cefixime
CFU	Colony Forming Units
CFX	Cefadroxil
CFZ	Clofazimine
CLA	Clarithromycin
CLI	Clindamycin
CLX	Cloxacillin
CRO	Ceftriaxone
CTT	Cefotetan (YM09330)
DAP	Dapsone
DCGI	Drug Controller General of India
DDTs	D,D-transpeptidases
DEPC	Diethylpyrocarbonate
DiaMOND	Diagonal measurement of n-way drug interactions
DLM	Delamanid
DMSO	Dimethyl sulfoxide
DR-TB	Drug Resistant Tuberculosis
DS-TB	Drug Susceptible Tuberculosis
EBA	Early Bactericidal Assay
EDTA	Ethylenediaminetetraacetic acid
EMA	European Medicine Agency
EMB	Ethambutol
Emis	Emission
Eq.	Equation

ERA4TB	European Regimen Accelerator for TB
ETH	Ethionamide
ETP	Ertapenem
Exc	Excitation
FBC	Fractional Bactericidal Concentration
FDA	Food and drug administration
FDX	Fidaxomicin
FIC	Fractional Inhibitory Concentration
FICI	Fractional Inhibitory Concentration Index
FISABIO	Foundation for the Promotion of health and Biomedical Research of Valencia Region
FOS	Fosfomycin
FUS	Fusidic acid
GO	Gene ontology
HBS-TB	Hollow Fiber System
IC_{50}	Inhibitory concentration of 50%
IC_{90}	Inhibitory concentration of 90%
IGRA	Interferon Gamma Release Assay
INH	Isoniazid
IPM	Imipenem
KET	Ketoconazole
LD	Limit of detection
LDTs	L,D-transpeptidases
LVX	Levofloxacin
LZD	Linezolid
$MBC_{99.9}$	Minimum Bactericidal Concentration
MDR-TB	Multi Drug Resistant TB
MER	Meropenem
MIC	Minimum Inhibitory Concentration
MIC_{Combo}	Minimum Inhibitory Concentration of the Combination
MIC_{Exp}	Experimental MIC
MIC_{Ref}	Reference MIC
MIN	Minocycline
MOX	Moxifloxacin
Mtb	Mycobacterium tuberculosis
MTBC	Mycobacterium tuberculosis Complex
MTT	2-(3,5-diphenyltetrazol-2-ium-2-yl)-4,5-dimethyl-1,3-thiazole;bromide
NFT	Nitrofurantoin
NGS	Next generation sequencing
NO	Nitric oxide

OADC	Oleic acid albumin dextrose catalase
OD	Optical Density
OPTIKA	Optimized Time Kill Assays
p-adj	Adjusted p-value
PAE	Post antibiotic effect
PAS	*p*-amino salicilic acid
PBP	Penicillin Binding Protein
PBS	Phosphate buffer saline
PC	Primary Compound
PCA	Principal Component Analysis
PD	Pharmacodynamic
PE	Proline-glutamic acid
PK	Pharmacokinetic
PPD	Purified Protein Derivative
PPE	Proline-proline-glutamic acid
Pre-XDR-TB	Pre-Extensive Drug Resistant TB
PTD	Pretomanid
PTO	Prothionamide
RET	Retapamulin
RIF	Rifampicin
RR-TB	Rifampicin resistant TB
S/B	Signal to background
SC	Secondary Compound
SD	Standard deviation
SDS	Sodium Dodecyl Sulphate
SEA	Singular enrichment analysis
SMX	Sulfamethoxazole
SPC	Spectinomycin
SZD	Sutezolid
TB	Tuberculosis
TBDA	TB drug accelerator
TBP-PI	Tebipenem-Pivoxil
THZ	Thioacetazone
TKA	Time Kill Assays
TMP	Trimethoprim
TST	Tuberculin Skin Test
VCM	Vancomycin hydrochloride
WHO	World Health Organization
XDR-TB	Extensive Drug Resistant TB

Summary

Tuberculosis (TB) is a highly infectious airborne disease caused by *Mycobacterium tuberculosis (Mtb)*. An estimated 9.9 million people fell ill with TB in 2020 although only 5.8 million cases were diagnosed and reported. In addition, it is estimated that 1.5 million people died from TB in the same year.

TB is treatable and curable. The standard treatment for active drug-susceptible TB (DS-TB) includes the use of four anti-TB drugs for six months. This regimen has a success rate of 85%. However, the inappropriate use of drugs for decades led to the emergence of bacterial strains resistant to one or more of these anti-TB drugs. The treatment of drug resistant forms of TB (MDR-TB) is more complex and with limited options. It includes the use of second-line anti-TB drugs, which are associated with severe side effects and longer times (treatment can be extended up to two years). Moreover, patients might not have alternative treatment options if TB is caused by bacteria that do not respond to the most effective second-line TB drugs; this is known as extensively drug resistant (XDR-TB).

The increase of drug resistant strains, together with the limited protective efficacy of the available BCG vaccine against pulmonary TB, make *Mtb* one of the most infectious killers in the world. Therefore, shorter, safer, and simpler regimens to combat drug susceptible and drug resistant TB are urgently needed.

Over the last decade, the discovery of new anti-TB drugs has increased the clinical pipeline. As of December 2021, there were 23 drugs and various combination regimens in clinical trials. Such as the study that aims to reduce the standard treatment for DS-TB to four months using rifapentine and moxifloxacin instead rifampicin and ethambutol. Or, for instance, the combination of bedaquiline-pretomanid-linezolid administered for six months that was recently approved for operational research against XDR-TB.

Despite these advances, there is a lack of understanding on how to properly combine new compounds into optimal TB regimens. An initial step to this aim is *in vitro* combination assays. However, such combination studies for old and new drugs against *Mtb* is a nascent field. It is thus key to develop new methodologies to provide high quality data able to feed the rational design of future anti-TB regimens.

This Thesis is divided into three chapters, which contain their own introduction with specific concepts, as well as a final discussion of the results generated in them.

Chapter 1 deals with methodology development.

1. We first performed an *in-depth* study of currently available *in vitro* methodologies to evaluate drug combinations against *Mtb*. We included standard techniques as well as the recently published DiaMOND method. The main limitations were: (i) their basis on growth inhibition, which very often does not correlate with killing ability; (ii) their single-point measurements, which leads to a loss of valuable information as the different combinations show their maximum effect at different times, or (iii) their low throughput, which significantly limits the capability of exploring new drug interactions.

2. In the second part of this chapter, we developed a new *in vitro* methodology applied to the study of drug combinations against *Mtb*. This methodology, named OPTIKA (Optimized Time Kill Assays), overcomes current limitations of standard techniques such as the need of primary checkerboard assays based on growth inhibition to select favourable pair-wise combinations and the confirmation by technically cumbersome and low-throughput CFU-based time kill assays. In addition to the enhanced throughput of OPTIKA comparing with standard methods, its main advantage is that it allows to interrogate hundreds of combinations of *n* drugs and select favourable interactions based on killing activity in a unique assay.

In **Chapter 2**, we applied OPTIKA to study β-lactam containing drug combinations against *Mtb*. We focused our study on these drugs because it is a large family of antibiotics with exceptional records of clinical safety in humans and there has been a recently growing interest on them in the TB field. We chose two sub-families of β-lactams (*i.e.* carbapenems and cephalosporins) to perform our *in vitro* combination screenings based on bacterial killing. We screened β-lactams: (i) in combination with a panel of commercially available drugs creating combinations up to three drugs, and (ii) in combinations of up to five drugs from a set of drugs recently recommended by the World Health Organization (WHO) treat drug-resistant forms of TB. After these screenings, we robustly identified a clear favourable contribution of the β-lactams at initial times of the experiments. In addition, we found some favourable and non-favourable partners in high-order drug combinations containing β-lactams.

In **Chapter 3**, the study of β-lactam contribution to favourable drug combinations was done from a mechanistic perspective. There, we focused our work on pair-wise drug combinations containing rifampicin and cell wall inhibitors, such as β-lactams and the first-line anti-TB drug ethambutol. Through transcriptomics, we found that bacteria treated with multiple drugs were not able to mount the adaptative and protective responses that are observed when they were exposed to single drugs.

Resumen

La tuberculosis es una enfermedad infecciosa causada por *Mycobacterium tuberculosis*. Es una enfermedad de transmisión aérea y altamente contagiosa. Se estima que 9.9 millones de personas enfermaron de tuberculosis en 2020 aunque solamente 5.8 millones de casos fueron diagnosticados y notificados. Además, se calcula que 1.5 millones de personas murieron de tuberculosis en ese mismo año.

Hoy en día, la tuberculosis es una enfermedad tratable y curable. El tratamiento estándar para las formas de tuberculosis activa sensibles a fármacos consiste en el uso de cuatro antibióticos durante seis meses. La tasa de éxito de este tratamiento es de un 85%. Sin embargo, el uso incorrecto de estos fármacos a lo largo de los años condujo a la generación de resistencias y, por tanto, a la existencia de cepas bacterianas resistentes a uno o más de estos fármacos antituberculosos. El tratamiento de las formas de tuberculosis resistentes a fármacos es más complejo y con opciones limitadas. En estos casos, hay que recurrir al uso de fármacos antituberculosos de segunda línea, los cuales se asocian a efectos secundarios graves y necesitan ser administrados durante periodos de tiempo más largos (el tratamiento puede prolongarse hasta dos años). Además, los pacientes pueden no tener opciones de tratamiento alternativas si la tuberculosis está causada por bacterias que no responden a los fármacos antituberculosos de segunda línea más eficaces; es lo que se conoce como tuberculosis extremadamente resistente.

El aumento de cepas resistentes a fármacos, junto con la limitada eficacia protectora de BCG, la vacuna disponible contra la tuberculosis pulmonar, hacen de *M. tuberculosis* uno de los agentes infecciosos más mortales a nivel mundial. Por lo tanto, se necesitan urgentemente tratamientos más cortos, más seguros, más simples y más eficaces frente a formas sensibles y resistentes de tuberculosis.

Durante la última década, el descubrimiento de nuevos compuestos con actividad antituberculosa ha aumentado significativamente la lista de posibles fármacos en desarrollo clínico. A fecha de diciembre de 2021, se estaban evaluando 23 compuestos y varios regímenes de combinaciones en ensayos clínicos, con el objetivo de optimizar el uso de los fármacos recientemente descubiertos. Por ejemplo, el estudio que pretende reducir el tratamiento estándar de formas de tuberculosis sensibles a fármacos a cuatro meses mediante el uso de rifapentina y moxifloxacina en lugar de rifampicina y etambutol. O la combinación de bedaquilina, pretomanid y linezolid administrada durante seis meses que ha sido aprobada recientemente para ser utilizada en el marco de actividades de investigación operativa contra formas de tuberculosis extremadamente resistentes a fármacos.

A pesar de estos avances, no se sabe cómo combinar adecuadamente los nuevos compuestos en regímenes óptimos contra la tuberculosis. Un primer paso para ello son los ensayos de combinación *in vitro*. Sin embargo, este tipo de estudios de combinación

de fármacos antiguos y nuevos contra la tuberculosis es un campo incipiente. Por lo tanto, es fundamental desarrollar nuevas metodologías que proporcionen datos de alta calidad capaces de alimentar el diseño racional de futuros regímenes antituberculosos.

Esta tesis se divide en tres capítulos principales. Cada uno de los cuales contiene su propia introducción con conceptos específicos así como una discusión final de los resultados presentados en ellos.

El **Capítulo 1** trata del desarrollo de metodología.

1. Primero realizamos un estudio en profundidad de las metodologías *in vitro* actualmente disponibles para evaluar combinaciones de fármacos contra *M. tuberculosis*. Incluimos tanto técnicas tradicionales como el método DiaMOND, recientemente publicado. Como principales limitaciones hemos encontrado: (i) su base en la inhibición del crecimiento, que muy a menudo no se correlaciona con la capacidad de matar, (ii) sus mediciones en un solo punto, lo que conlleva una pérdida de información muy valiosa ya que las distintas combinaciones presentan su máximo efecto a distintos tiempos, o (iii) su baja capacidad, que limita significativamente la capacidad de explorar nuevas interacciones farmacológicas.

2. En la segunda parte de este capítulo, desarrollamos una nueva metodología aplicada al estudio *in vitro* de combinaciones de fármacos frente a tuberculosis. Esta metodología, denominada OPTIKA, supera las limitaciones de las técnicas actuales, como la necesidad de realizar ensayos primarios basados en inhibición de crecimiento para seleccionar las combinaciones favorables y la posterior confirmación de estas interacciones mediante las tradicionales curvas de muerte basadas en contaje de colonias viables, experimentos técnicamente engorrosos y de baja capacidad. Además de la mayor capacidad de OPTIKA en comparación con los métodos tradicionales, su principal ventaja es que permite ensayar cientos de combinaciones de *n* fármacos y seleccionar las interacciones favorables basándose en muerte celular y en un único ensayo.

En el **Capítulo 2**, aplicamos OPTIKA para llevar a cabo un estudio de las interacciones farmacológicas de combinaciones que contienen β-lactámicos frente a *M. tuberculosis*. Centramos nuestro estudio en los β-lactámicos porque se trata de una gran familia de antibióticos con registros excepcionales de seguridad clínica en humanos. Además, recientemente ha habido un creciente interés en esta familia de fármacos en el campo de la tuberculosis. Elegimos dos subfamilias de β-lactámicos (carbapenems y cefalosporinas) para llevar a cabo nuestros cribados *in vitro* de combinación basados en muerte celular. Hemos examinado los β-lactámicos: (i) en combinación con un panel de

fármacos disponibles en el mercado creando combinaciones de hasta tres fármacos, y (ii) en combinaciones de hasta cinco fármacos de un conjunto de fármacos recientemente recomendados por la organización mundial de la salud para tratar las formas de tuberculosis resistentes. Tras estos cribados, identificamos de forma robusta una clara contribución favorable de los β-lactámicos en los momentos iniciales de los experimentos. Además, encontramos contribuciones favorables y no favorables de determinados fármacos en combinaciones de más de tres compuestos que contienen β-lactámicos.

En el **Capítulo 3**, el estudio de la contribución de los β-lactámicos a las combinaciones favorables de fármacos se realiza desde una perspectiva mecanicista. En él, centramos nuestro trabajo en combinaciones de parejas de compuestos que contienen rifampicina e inhibidores de la pared celular como los β-lactámicos y el fármaco antituberculoso de primera línea etambutol. A través de la transcriptómica, descubrimos que las bacterias tratadas con múltiples fármacos no eran capaces de generar la respuesta adaptativa y protectora que se observa cuando se exponen a fármacos únicos.

Introduction

History of tuberculosis

Tuberculosis (TB) is an ancient disease whose history has been closely related with the history of humanity. Despite being one of the oldest infection diseases affecting humans, today it still remains as a public health threat around the world [1].

Bone deformities found in fossils from the Neolithic period and Egyptian mummies constituted the earliest evidence of TB in humans and animals [2, 3]. In the ancient Greece, TB was well known. Hippocrates (460-370 BC) described a lung disease with fever and cough, which he refers to as *phthisis* (from the Greek *phthiein*: to waste away describing the progressive decay of the body of patients with pulmonary TB) or consumption. He provided a remarkably accurate description of the clinical characteristics of patients with pulmonary TB and recognized the predilection of young adults for active tuberculosis [4, 5]. *Phthisis* was described as the commonest disease of that period, usually culminating in death. The Hippocratic school considered it a hereditary disease rather than an infectious disease, as it commonly occurred affecting a whole family. Contrary to the general opinion at that time, Aristotle (384-322 BC) believed in the infectious nature of *phthisis* [2, 6].

Not only the Greeks, but also the Indians and the Romans, described and studied the disease, evidencing its wide prevalence. Reviewing its evolution over the course of the history, it is clear that TB has been linked to the development of new urban areas where people have been confined, such as the establishment of the cities of the Nile Valley, the Greek polis and in Rome of the early imperial period [2].

During the Renaissance, the pathoanatomical basis of the disease began to be investigated. In 1679, Sylvius de la Böe was the first to mention tubercles as characteristic lesions in the lungs and other organs of consumptives. However, it was not until 1834 when Johann Lukas Schönlein coined the term *tuberculosis* [2, 6].

In the 18th and 19th centuries, TB caused an epidemic in Europe. At that time, it received different names such as *the robber of youth*, *the great white plague* or *the white death* (because of the paleness derived from the disease). Extra-pulmonary tubercles were also observed although it was not known that Scrofula (the name given to extra-pulmonary TB) was related with *phthisis* or consumption [6].

In 1865, the French military surgeon Jean-Antoine Villemin demonstrated the infectious nature of TB. He also noticed an increased prevalence of TB in crowded urban areas; and that in other areas, such as Australia or New Zeeland, TB had not been known until the pioneers arrived [3, 7]. However, it was not until 1882 when Robert Koch

identified and isolated the causative agent of TB, the tubercle bacillus, lately named *Mycobacterium tuberculosis (Mtb)* [8].

Mtb belongs to the *Mycobacterium tuberculosis* complex (MTBC), which includes several mycobacterial species (*M. tuberculosis, Mycobacterium bovis, Mycobacterium microti, Mycobacterium africanum, Mycobacterium pinnipedii* and *Mycobacterium caprae*). It is believed that all of them shared a common ancestor. Some studies estimated that this common ancestor was present in East Africa three million years ago, where it coexisted with early hominids [9]. In another model, it was proposed that humans had been infected with MTBC for at least 70,000 years [10]. Nevertheless, it is clear that MTBC has coevolved and globally disseminated within human population.

Historically, TB was considered an incurable disease. In the 19th century Hermann Brehmer introduced the sanatoria [11]. People suffering from TB were isolated from their regular environment and taken to sanatoria to be subjected to strict rest, fresh air and good nutrition. Patients with minimal infection showed a good recovery during sanatoria treatment. However, many patients with severe forms of the disease still died. Overall, according to long-term results of an American study, there were multiple cases in which TB appeared again some years after the sanatoria treatment. In retrospect, this improvement on patients' health could be explained as an active to latent TB disease progression rather than a complete eradication of TB [2, 3].

A turning point in the prevention of TB in the 1900s was the creation of the live attenuated BCG (bacilli Calmette-Guérin) vaccine developed by Albert Calmette and Camille Guérin [12]. After 231 passages of an *M. bovis* strain, they obtained an attenuated strain that was well tolerated and unable to produce the disease in several animal models such as guinea pigs, cows, horses, hamsters, mice, rabbits, dogs, chicken and non-human primates [13]. Immunization with this vaccine started in Paris in 1921 [2]. The original culture of BCG was rapidly sub-cultured and distributed to different laboratories around the world. Until 1960, when the lyophilized methods appeared, these laboratories maintained the strain by passaging on non-synthetic culture media and used it for local vaccine production. This parallel passaging of the culture in different media led to genetically different sub-strains of BCG still existing today [13]. To date, BCG is the only available vaccine to be used against TB. It provides a strong effective protection in children against disseminated forms of the disease, especially meningitis, but it shows variable efficacy in the protection against pulmonary TB in adults [14]. Currently, several vaccines against TB are under development [15].

Another milestone in the fight against TB was the discovery of effective antibiotics against *Mtb* (**Figure I.1**). The first one was streptomycin (1944) [16]. In the 1940s and 1960s, more antibiotics were developed for the treatment of TB (*i.e. para-*

aminosalicylic acid, isoniazid, pyrazinamide, cycloserine, ethionamide, kanamycin, capreomycin, ethambutol and rifampicin) [17]. However, the administration of these antibiotics alone rapidly produced the appearance of drug resistant strains (DR-TB) [18] and it was soon acknowledged the need of treating TB in combination therapy.

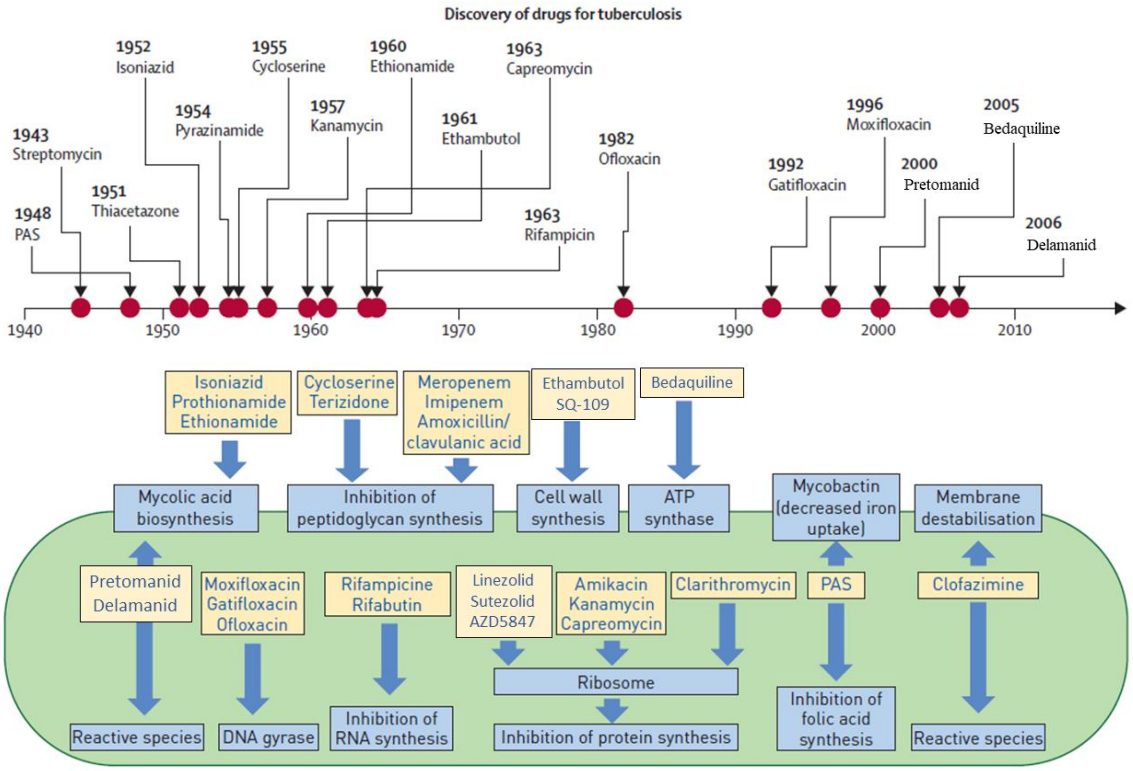

Figure I.1. History of anti-TB drugs discovery and their mechanism of action. Upper panel: Available drugs to treat TB disposed in a chronological order according to their discovery date. Repurposed drugs (clofazimine, linezolid and meropenem) and drugs currently under development in clinical trials (sutezolid and SQ109) are not included in the Figure. Adapted from [19]. Lower panel: Mechanism of action of currently available anti-TB drugs. Adapted from [20].

Due to this initial success on treating TB, public health institutions devoted less efforts and control resources on TB, which combined with an increase of immigrants from high prevalence nations to developed ones, changes in social structure, and the onset of the HIV/AIDS epidemic, produced a resurgence of the disease in the late 1980s [2, 21, 22]. The number of TB cases dangerously increased and multi-drug resistant forms of *Mtb* spread. Research was also disregarded and few anti-TB compounds were added over those decades to the TB drug armamentarium.

In response to the resurgence of TB, in 1993 the WHO declared TB a global emergency making it the first infectious disease to be declared as such [23]. Since then, several TB control strategies aiming to reduce the global burden of TB have been created. For example, in 1994, an international TB control strategy named DOTS (Direct Observed Treatment, Short-course) was launched covering different points such as

political commitment, diagnosis, standardized short-course chemotherapy, effective drug supply system, a standardized system for surveillance and programme monitoring [24]. In 2006, the WHO launched the Stop TB strategy focused on achieving universal access to diagnosis and treatment for people with TB, reducing the socioeconomic burden associated with TB, protecting vulnerable populations and supporting the development and use of new tools [25].

In 1993 the funding situation and the research strategy of the scientific community began to change [26, 27]. Small research groups became TB research units and, eventually, large and interdisciplinary consortia including several members from academic institutions and the industry were created, such as the TB alliance (Global Alliance for TB Drug Development), a non-for-profit organization that was set to the discovery and development of faster-acting and affordable drugs against TB [28], the TBDA (TB Drug Accelerator), whose main goal is to discover new drugs to get a shorter, safer and simpler regimen [29], or the ERA4TB (European Regimen Accelerator for TB) Consortium, aiming to accelerate the development of new regimens against TB [30], among others [26]. Research and development efforts across academia, pharmaceutical companies and public-private partnerships led to the clinical development and the regulatory approval of pretomanid, bedaquiline and delamanid during the last decade, which meant a great progress in the fight against DR-TB [31].

Pathogenesis of tuberculosis

Tuberculosis is an airborne infectious disease in which humans are the unique known reservoir. There are several forms of the disease affecting different parts of the body, although most cases are pulmonary TB (**Figure I.2**). When a person with active TB coughs, speaks or sings, small drops containing the bacteria, also known as aerosols, are disseminated into the air. People nearby may inhale these aerosols and become infected. After inhalation, *Mtb* reaches the lower respiratory tract and, once in the lungs, it encounters the alveolar macrophages, which are the predominant cell types that *Mtb* infects. *Mtb* is an intracellular pathogen and it has developed strategies to overcome the host defence mechanisms [32]. Once inside the macrophage, *Mtb* blocks the phagosome fusion with the lysosome and disrupts the phagosomal membrane, accessing to the cytosol, which favours its dissemination.

The progression of TB infection is fundamentally regulated by the integrity of the immune system of the host [33, 34]. If the first line defence fails to eliminate the bacteria, *Mtb* continues replicating and expanding to other macrophages and interstitial tissue. Afterwards, it reaches the parenchyma, where a multicellular host response

occurs. This multicellular response leads to the recruitment of other immune cells, such as T cells and B cells and the formation of the granuloma.

The granuloma is the hallmark of the host response to contain the infection. However, bacteria inside the granuloma might persist in a latent state instead of being eliminated. This ability of *Mtb* to live in equilibrium with immune responses makes these bacteria an extremely successful human pathogen. It can survive in this immune microenvironment for years, causing few health problems for the most part of the infected people. This phenomenon is known as latent TB infection. However, in approximately 10% of patients, a reactivation of the disease occurs when the immune system is compromised. Then, infected cells inside the granuloma die; this necrotic zone leads to the breakdown of the granuloma and the subsequent dissemination of TB to the lung and, thus, into the air through coughing [33, 35].

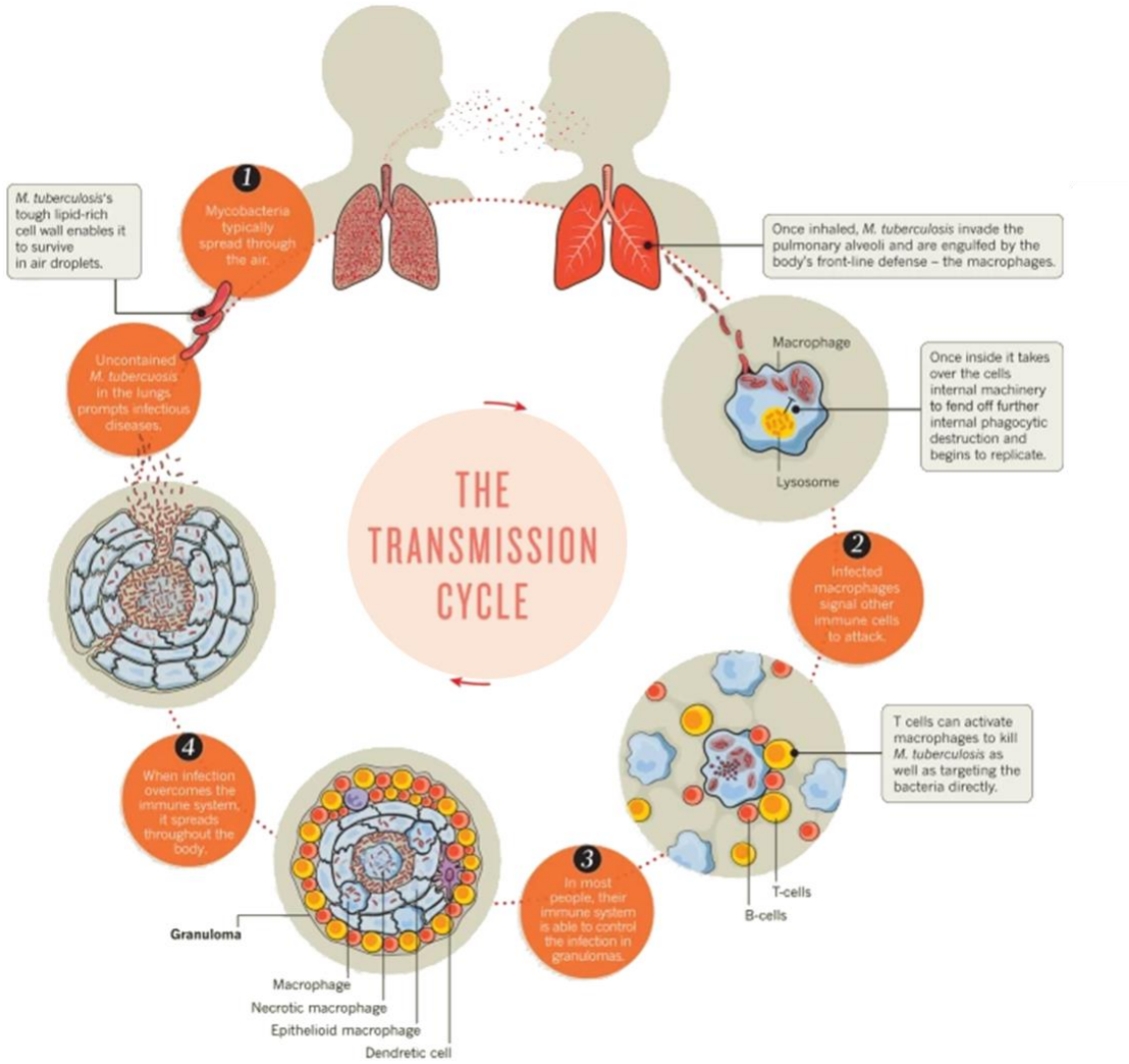

Figure I.2. Transmission cycle of *Mycobacterium tuberculosis*. 1.Human to human transmission of *Mtb* occurs airborne. 2. The disease progression depends on the immune system of the host and, in most of the cases, the bacilli are contained in the granuloma and no symptoms are

presented by infected individuals. This form of the disease is known as latent TB. 3. If the immune system is compromised, the granuloma collapses. 4. In those cases, *Mtb* spreads and active TB is developed. Adapted from [36].

Diagnosis of tuberculosis

Two immuno-based methods are widely available to detect latent TB infection, *i.e.* the Tuberculin Skin Test (TST), also known as the Mantoux and the Interferon Gamma Release Assay (IGRA). Both tests are acceptable but present low sensitivity in immunocompromised population [37]. The TST consists of an intradermal injection of tuberculin or the purified protein derivative (PPD). If the individual has developed cell-mediated immunity to these antigens due to previous exposure to the pathogen, a hypersensibility reaction is likely to occur in the next 72 hours. The main disadvantage of TST is that it cannot distinguish between people actually infected with TB, other non-TB mycobacteria or BCG-vaccinated people [38]. Quantiferon is based on IGRA and it measures the interferon gamma released by T-cells after stimulation with some *Mtb* antigens. This method allows to distinguish between *Mtb* infection and BCG vaccination, but it cannot differentiate between latent or active TB [39].

Other technologies like imaging, microscopy, culture-based methods and molecular tests are used to diagnose active TB. Chest X-rays are an established triage, but a microbiological test is needed to confirm the diagnosis due to its low specificity. The sputum smear microscopy is the most used technique in low and middle-income countries. However, it presents low sensitivity in comparison with culture-based methods, whose main limitation is the long time needed to obtain results. Some molecular methods have been developed and implemented in high-burden countries [40, 41].

To detect drug resistant forms of TB, culture-based drug susceptibility tests are the gold standard methods. However, they are time-consuming and require well-trained personnel and high biosafety-level laboratories, limiting its use in low-income and middle-income countries. As an alternative, several molecular methods have been developed (such as LPAs, Xpert MTB/RIF and Genedrive MTB/RIF ID among others). However, some significant limitations are still present. First, most of them are focused on a few genes, which implies that the same sample should be used for several tests to its complete genome characterization. Second, not all of them are suitable to be used in low-income and middle-income countries and, finally, far from being universal, sensitivity and specificity can vary in different populations [42].

Despite recent advances achieved in the field, an accurate and rapid method to early diagnose and find people infected with TB is urgently needed not only to administer the corresponding therapy before severe lung damage occurs, but also to prevent the transmission of the bacteria to uninfected people.

Epidemics of the tuberculosis disease

Despite being preventable and treatable, TB is one of the deadliest infectious diseases and the 13th leading cause of death in the world [43]. The WHO estimated that nearly 10 million people developed TB in 2020, although only 5.8 million cases diagnosed and reported. In the same year, 1.5 million people died from TB worldwide (including 214,000 people co-infected with HIV) [44].

These figures are strongly affected by the COVID-19 pandemic, which had a devastating impact on the fight against tuberculosis [45]. The most evident sign is a huge drop in the number of new cases of TB diagnosis reported. From 2019 to 2020 it dropped an 18% (from 7.1 million to 5.8 million) reaching levels of 2012. This means a clear reversal of progress achieved in previous years (**Figure I.3**). The WHO estimated that in the last year 4.1 million people fell ill with TB and were not diagnosed or officially reported, a number far from the 2.9 million people estimated for 2019. This decrease was concentrated in sixteen countries. The largest reduction in case reporting was observed in those countries that had experienced major COVID-19 outbreaks and health care service disruptions. This limitation to TB diagnosis and treatment access involved an increase in TB deaths for the first time in over a decade. These impacts are forecast to be worse in the coming years due to both: (i) the ongoing COVID-19 surges in low- and middle-income countries and, (ii) an increased TB transmission, that is expected after so many cases have been missed during the past two years [44, 46].

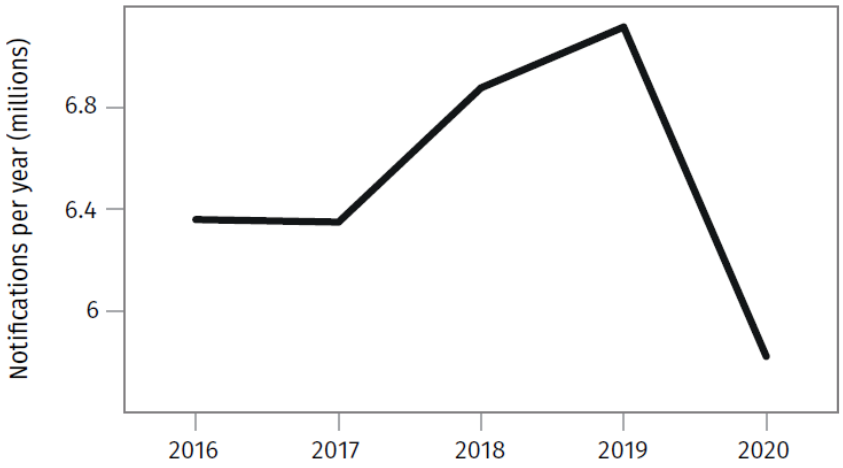

Figure I.3. Global trend of new TB cases notification. From [44]

According to WHO estimations, about 1.8 billion people (*i.e.* around one quarter of the world's population), are latently infected with *Mtb*. However, among all people infected with *Mtb* worldwide, only a small proportion of it (5-10%) will develop the disease in their lifetime. TB can affect anyone, but most cases diagnosed in 2020 were adults (56% men, 33% women and 11% children). In addition, TB is a disease linked to poverty, since 90% of the cases diagnosed every year belong to 30 high TB-burden countries, which are low-income and middle-income countries [14, 47]. The probability of developing the disease drastically increases among people suffering from poverty, undernutrition, HIV infection, diabetes, smokers or alcohol consumers [14].

The estimated incidence of TB in 2020 worldwide is shown in **Figure I.4**. Areas that accounted for most of the cases were South-East Asia, Africa, and the Western Pacific. Eighteen countries accounted for more than 100,000 cases and only eight countries *i.e.* Bangladesh, China, India, Indonesia, Nigeria, Pakistan, Philippines and South Africa accounted for two thirds of the global cases [14, 48].

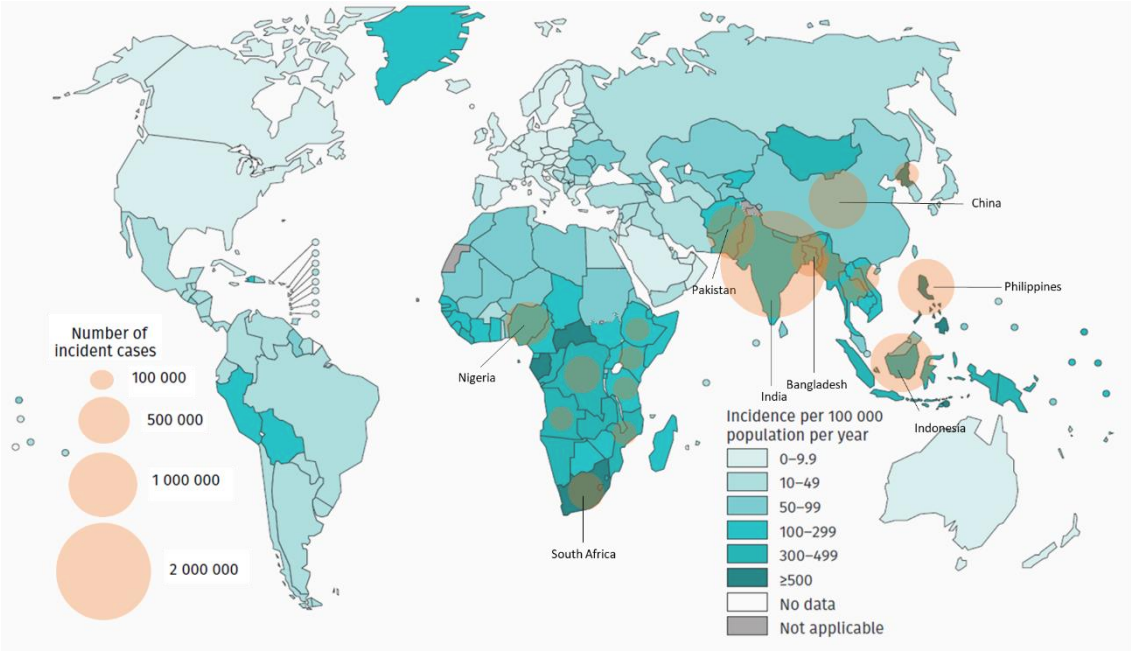

Figure I.4. Estimated tuberculosis incidence & countries with more than 100,000 estimated cases of TB in 2020. Green colour scale represents the incidence of TB in 2020. Countries with more than 100,000 estimated cases of TB are marked with orange circles. Labelled countries accounted for two thirds of the global cases. Adapted from [44].

TB not only presents a high incidence, but also a high mortality. In 2019, before the COVID-19 pandemic occurred, TB was the leading cause of death from a single infectious agent, ranking even higher than HIV [14].

In 2020, 1.3 million people (HIV negative) were estimated to have died because of TB. It is difficult to measure TB mortality among HIV positive people because deaths

of people suffering from HIV are recorded as HIV deaths, and other contributory cases are usually not recorded. However, 214,000 deaths were estimated in the same year among HIV positive people.

A similar inequity for TB incidence is observed in mortality distribution (**Figure I.5**). Globally, the number of deaths among HIV-negative is 17 per 100,000 population. However, there is less than 1 death in most high-income countries; and more than 40 deaths per 100,000 population in many countries belong to Africa, Korea and Papua New Guinea [14].

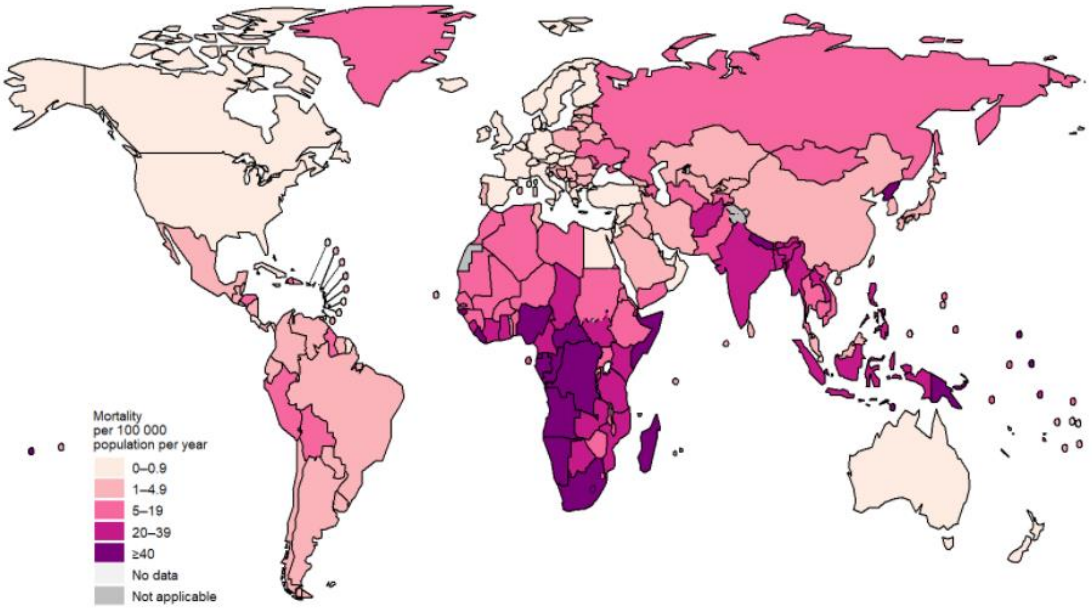

Figure I.5. Estimated TB mortality rates among HIV-negative people in 2020. High-income countries show the lowest death rate. Most of the countries with the highest number of deaths per 100,000 population belong to Africa, Korea and Papua New Guinea [14, 44].

Tuberculosis treatment and drug resistance

Drug treatment is the most effective therapy against TB, although it does not have a 100% cure rate. The latest data show a global treatment success rate of 85% for DS-TB, 59% for DR-TB and 77% for patients living with HIV [44].

Current treatment against DS-TB was developed decades ago (**Figure I.6**). In 1950, only a few years after the discovery of *p*-aminosalicylic acid and streptomycin, a clinical study demonstrated that the combination of both drugs was more effective and reduced the acquired drug resistance. In 1952, isoniazid was discovered and its

administration in combination with available anti-TB drugs at that moment was rapidly evaluated in many trials. The *triple therapy*, which included isoniazid and *p*-aminosalicylic acid for 18 to 24 months and pyrazinamide for the first six months, showed predictable cures for 90-95% of patients and constituted the standard treatment for TB for the next 15 years. In the 1960s, the substitution of *p*-aminosalicylic acid by ethambutol resulted in an 18-months regimen, which was better tolerated. In the 1970s, rifampicin was added to streptomycin, isoniazid and ethambutol, and the regimen was reduced to 9-12 months. Finally, in the 1980s, the regimen duration was reduced to six months by substituting streptomycin for pyrazinamide [19, 21, 49].

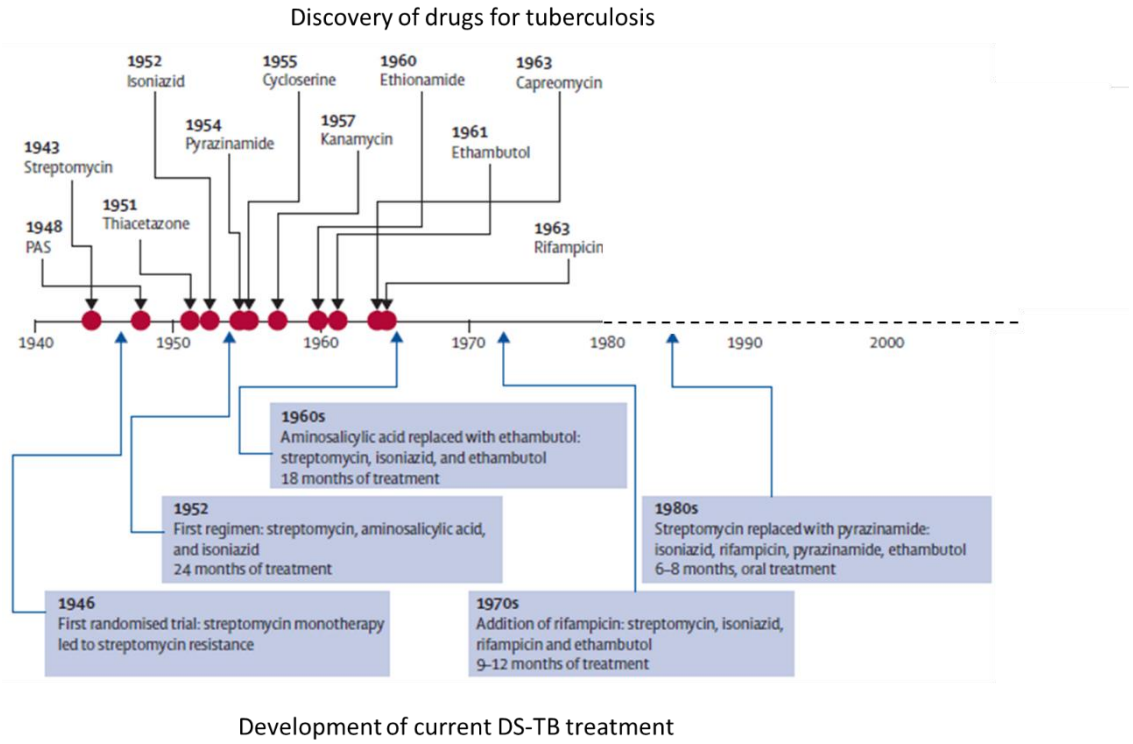

Figure I.6. History of DS-TB treatment development. Adapted from [19].

The standard treatment for patients with DS-TB currently recommended by the WHO consists of an initial two-months intensive phase of isoniazid, rifampicin, pyrazinamide and ethambutol followed by a dual therapy of isoniazid and rifampicin for four months [44]. This regimen has not changed for decades, although a shorter regimen composed of rifapentine, isoniazid, pyrazinamide and moxifloxacin for four months may soon constitute an alternative according to recent WHO recommendations [50].

While this standard regimen presents a good success rate if taken as prescribed, it implies that patients need to take an average of ten pills per day in the intensive phase. It is a long regimen; it presents hepatic toxicity, and it is not well tolerated by a considerable proportion of patients [51]. Moreover, poor adherence to treatment leads to appearance of drug-resistant bacteria.

A schema of TB drug resistance development is shown in **Figure I.7**. When a latent TB infection is reactivated to active TB, the patient is treated with available drugs. If the regimen is appropriate and completed, bacteria might be eradicated and the patient cured. However, this progression does not occur in all cases; DS-TB treatment is long and it includes at least four drugs with associate adverse effects, which calls for the existence of structured programmes to improve adherence. Limitations of control programmes are more common in places linked to poverty, high levels of people co-infected with HIV and poor access to an appropriate treatment. Once patients start with the treatment, the disease progresses form active to latent TB and symptoms disappear, but bacteria have not been completely eradicated and the patient is not completely cured. Uncompleted or unappropriated treatments lead to a higher probability of developing disease relapse and drug resistance [52].

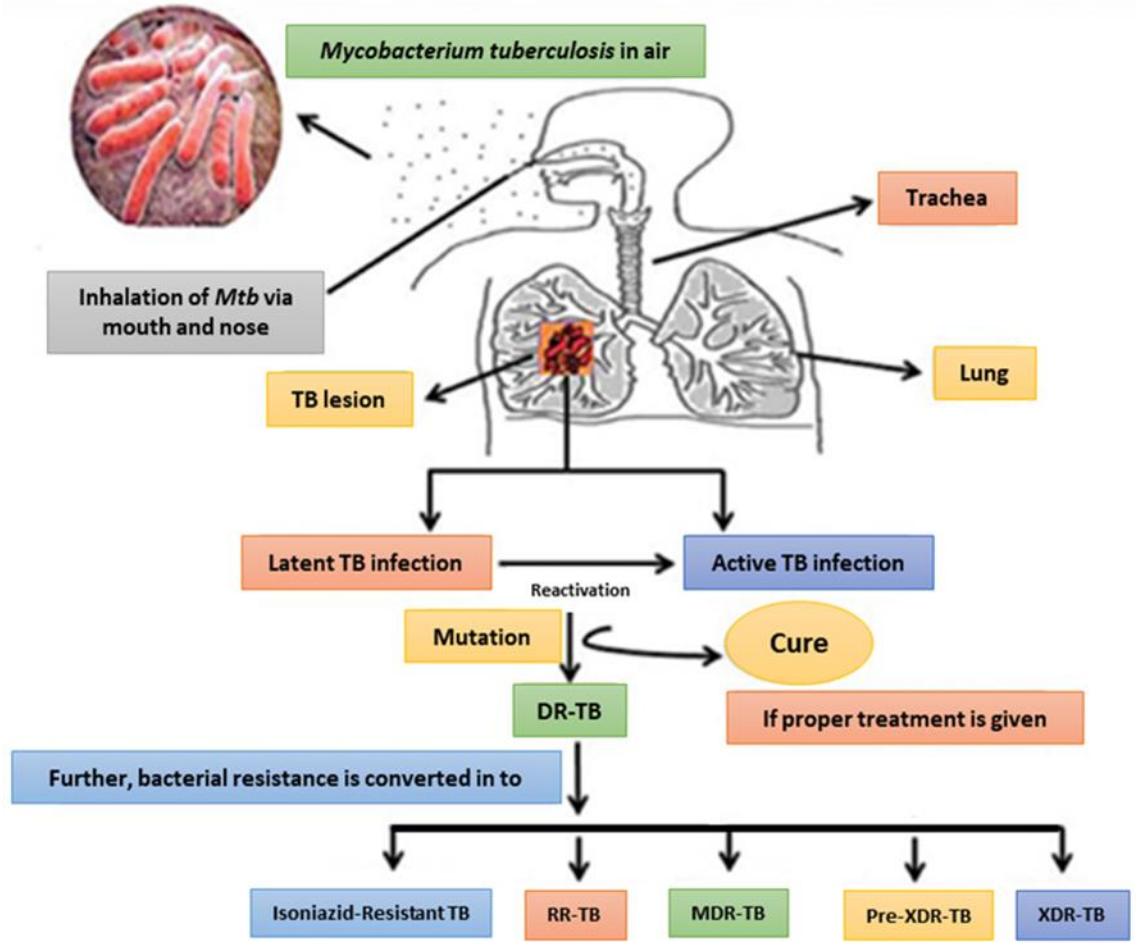

Figure I.7. Mechanism of drug resistant development. Adapted from [52].

Drug resistant strains of *Mtb* are classified by the WHO into five groups [44, 53]:

- Isoniazid-resistant TB: strains of *Mtb* resistant to isoniazid.
- Rifampicin resistant TB (RR-TB): rifampicin resistant strains of *Mtb*.

- Multi Drug Resistant TB (MDR-TB): *Mtb* strains resistant to at least isoniazid and rifampicin, the cornerstone drugs for the treatment of TB.

- Pre-Extensive Drug Resistant TB (Pre-XDR-TB): *Mtb* strains that fulfil the definition of MDR/RR-TB and are also resistant to any fluoroquinolone (levofloxacin or moxifloxacin).

- Extensive Drug Resistant TB (XDR-TB): *Mtb* strains that fulfil the definition of MDR/RR-TB, are also resistant to any fluoroquinolone (levofloxacin or moxifloxacin) plus at least one of the drugs bedaquiline or linezolid.

Individuals suffering from drug resistant forms of TB cannot be treated with the standard regimen. Treatment usually requires the use of second-line drugs for at least 9 months and up to 20 months, although an all-oral treatment of bedaquiline-pretomanid-linezolid administered for six months (BPaL regimen) has been recently approved to be used under operational research against XDR-TB [44].

DR-TB treatments need to be supported by counselling and monitoring for adverse effects. In the absence of a DR-TB standard treatment, its design faces some challenges. First, these regimens should be designed according to drug-susceptibility testing, but traditional culture techniques take too much time and alternative molecular techniques are not always available. Second, multidrug treatments for MDR- and XDR-TB are long, and patients usually lose their income due to the duration of this treatment. Third, previous medications taken by the patient, as well as the dose and duration, need to be considered to design the proper regimen. Finally, DR-TB regimens often cost up to 25 times more than the standard treatment for DS-TB, which implies that some patients are not able to cover the costs. All of these factors, together with severe side effects associated with the drugs (*i.e.* ototoxicity, nephrotoxicity, hypothyroidism, psychiatric disorders, epileptic episodes and gastrointestinal disturbance) contribute to the inefficiency of the treatment and poor adherence rates [19, 52, 54]. Treatment can be even more challenging in the case of XDR-TB, a form of the disease with even fewer treatment options.

Recently, the WHO elaborated a guide to manage DR-TB. There, available drugs for resistant forms of TB were grouped into three groups based on drug class and level of certainty in the evidence of effectiveness and safety (**Table I.1**) [55].

Group A includes the fluoroquinolones (levofloxacin and moxifloxacin), bedaquiline and linezolid. It is strongly recommended to include them in longer regimens unless there are toxicity issues or drug resistance. These medicines showed high efficacy in treatment outcomes and deaths reduction.

Group B is formed by clofazimine and cycloserine or terizidone, drugs that were effective in improving treatment outcomes but not so effective in reducing deaths.

Group C includes several drugs which are less effective than others from groups A and B (ethambutol, delamanid, pyrazinamide, ethionamide, prothionamide and p-aminosalicylic acid) or drugs with related toxicity or issues in the parenteral administration (imipinem-cilastatin, meropenem-amoxicillin/clavulanic acid, amikacin, and streptomycin).

According to the WHO most recent guidelines, a fully oral longer regimen is preferred. However, agents should be chosen based on the resistance profile, patients' known contraindications, drug-drug interaction, clinician preferences or operational considerations among others.

Longer regimens should be initiated with four drugs; three of them from the group A and one from the group B. Drugs from group C should be included in longer regimens if they cannot be constituted with agents from groups A and B.

Group A	Group B	Group C
Levofloxacin (LVX) *or* Moxifloxacin (MOX)	Clofazimine (CFZ)	Ethambutol (EMB)
Bedaquiline (BDQ)	Cycloserine (CS) *or* Terizidone (TRD)	Delamanid (DLM)
Linezolid (LZD)		Pyrazinamide (PZA)
		Imipenem-Cilastatin (IMP-CLN) *or* Meropenem (MER)
		Amikacin (AMK) *or* Streptomycin (STR)
		Ethionamide (ETH) *or* Prothionamide (PTO)
		p-aminosalicylic acid (PAS)

Table I.1. Second line drugs for TB. Meropenem administered in combination with amoxicillin/clavulanic acid. In addition to compounds included in this Table, clavulanic acid, high dose of isoniazid and gatifloxacin are considered. Adapted from [55].

Drug discovery pipeline

Despite the global efforts made over the last two decades, finding new drugs for TB remains a great challenge today. Recent advances done in the field of drug discovery

have been driven by the increased knowledge of the biology of the pathogen and its interaction with the human host [56]. From the development of the first successful chemotherapy against TB in the 1960s to the development of the last approved drugs, different approaches have been used in the drug discovery and development process [57]:

1. Early chemotherapy: the progression of the first drugs (*i.e.* isoniazid, rifampicin, ethambutol and pyrazinamide) was driven by the medical need. No chemotherapy was available before these drugs were discovered. Their anti-TB properties were assessed by *in vitro* assays followed by *in vivo* tests in animal models and rapidly introduced into humans [57]. This fast clinical progression is very different to current trials and regulatory processes, which imply different clinical phases and several years to assess safety and efficacy of the new drugs [58].

2. Modification of existing scaffolds: Multiple antibiotic candidates are chemical molecules derived from drug classes which were discovered many years ago [59, 60]. This approach identifies interesting chemical scaffolds of natural products or drugs with good *in vitro* anti-TB activity but poor drug-like properties. Molecules are redesigned to develop novel chemical entities with better antimycobacterial properties. This approach not only allows to find novel molecules which are more active against *Mtb* in contrast to the parent compound, but also to design molecules with improved chemical properties, such as better resistance profiles, safety, tolerability or pharmacokinetic (PK) and pharmacodynamic (PD) properties, thus improving the probability to be progressed into clinical phases. Following this strategy, potent analogues of existing drugs were discovered:

    - Nitroimidazole derivates: 5-nitroimidazole, an active molecule against anaerobic bacteria, which was used to treat bacterial infections affecting the gut. They served as the starting point of the recently approved pretomanid and delamanid.

    - Rifampicin derivates: rifabutin is a rifampicin derivate that shows better compatibility with anti-HIV drugs.

    - Ethambutol derivates: SQ-109 arose from a screening focused on ethambutol analogues. It is currently in development in clinical trials.

3. Drug repurposing: In some cases, existing antibacterial drugs with good anti-TB properties are tested directly in TB clinical trials. Drug repurposing or

repositioning is based on the identification of new uses for old, clinically approved drugs. This strategy reduces the development risks because chosen drugs have already gone through several phases of clinical trials and have also been safety and pharmacokinetic profiled. This approach drastically reduces development times because *in vitro* and *in vivo* testing, chemical optimization or formulation development are in many cases completed. This reduction in associated development risks, cost and time definitely facilitates their way to the market [61].

Drug repurposing was applied to TB in the 1990s, after the global emergency was declared, in order to introduce novel drugs against drug-resistant strains in the pipeline. Several drug classes were added:

- Oxazolidinones: such as linezolid, currently in use against MDR and XDR-TB, and others in clinical trials: posizolid, sutezolid, delpazolid and contezolid [56, 62].

- β-lactams: meropenem, the broad-spectrum β-lactam, possesses *in vitro* activity against *Mtb* and showed efficacy in an early bactericidal activity TB study. It has been recently recommended by the WHO to treat MDR-TB [55]. Chapters 2 and 3 of this Thesis are focused on β-lactams against TB.

- Fluoroquinolones: several fluoroquinolones showed antimycobacterial activity *in vitro*. A study performed in India showed positive results of the inclusion of oxofloxacin in the anti-TB regimen. Moxifloxacin is a member of this group and is currently used to treat MDR-TB [63, 64].

4. Target-based screening: the sequencing of the *Mtb* genome in the late 1990s allowed to identify new targets to drug candidates. However, hits identified in target-based screenings failed to progress because of poor physicochemical properties or because of its inability to penetrate the highly impermeable bacterial cell wall. For many essential targets found by genome-derived target-based approaches, specific inhibitors with drug-like properties have not been identified [57, 59].

5. Phenotypic screening: whole cell-based screenings test the potency of compounds against *in vitro* mycobacterial cultures. This approach has been very successful along the years and not only serves to identify new drugs, but also to characterize and progress potential drugs as it happened with most

of the frontline drugs [65]. Current phenotypic screening methodologies allow testing compounds under different environments such as replicating, non-replicating, or physiological states. The recently approved drug bedaquiline [66] (FDA approved it in 2012, becoming the first anti-TB drug approved in 40 years) was developed following this approach, as well as other drugs which currently are in late phases of clinical trials (BTZ043, Q203, OPC-167832).

The first anti-TB drugs were discovered more than 50 years ago. However, its use as monotherapy rapidly prompted to the appearance of resistance. Global efforts in the drug discovery field in the last two decades led to substantial progress and new compounds progressing in the clinical pipeline, but more drugs are needed to avoid drug resistance and achieve shorter regimens. Similarly, the recognition of the need for improved therapies for MDR-TB has led to an increase in the number of trials to identify novel anti-TB therapies [67] (**Figure I.8**).

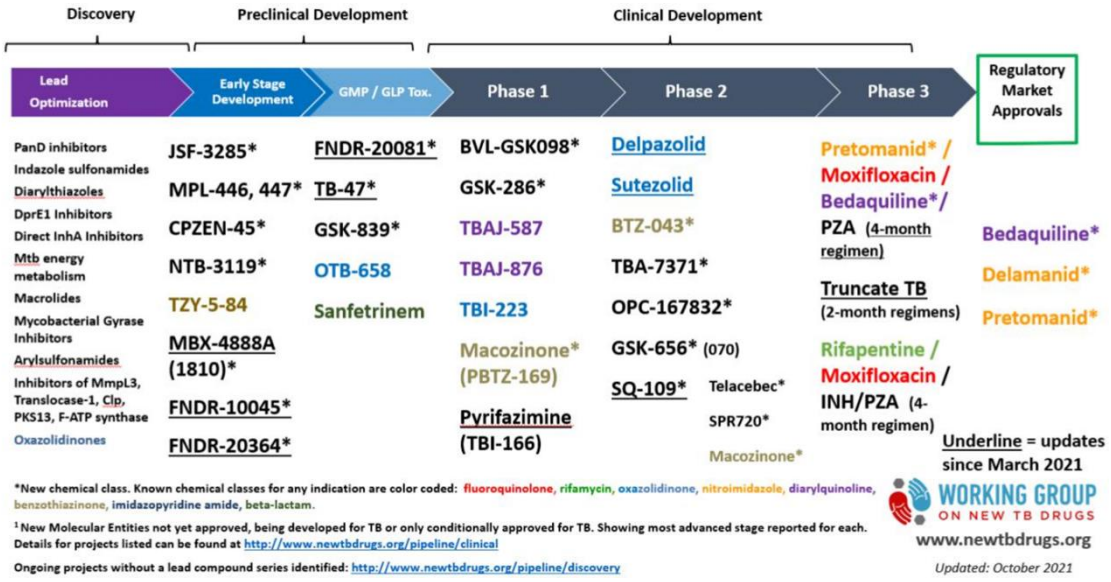

Figure I.8 New TB drug pipeline. From [67]. Accessed on 29th Oct 2021.

Treatment of TB is rooted on combinations of drugs administered for enough time to get non-relapsing cure and avoiding the selection of drug-resistant mutants. However, the design of new regimens based on recently developed drugs is challenging and needs to be rationally developed for several reasons. Firstly, it should be considered that the contribution of a particular drug could be altered by other drugs in the combination. Secondly, drug combinations should be designed with the purpose of eradicating different bacterial subpopulations to achieve cure and prevent the development of resistance. And finally, more effective, shorter, simpler, and safer regimens are urgently needed to treat DS- and DR-TB [3, 19, 56, 57].

Despite some advances done during the last decades, new anti-TB drugs are urgently needed. Single agents are unable to eradicate the disease and, thus, new regimens combining three or more new drugs are required. Drug discovery and development in tuberculosis is particularly challenging for several reasons. First, due to the nature of the disease, its pathology and the disease progression hinder the development of new drugs to get shorter regimens with respect to other diseases. The granuloma limits drug penetration and allows the co-existence of extracellular and intracellular bacteria with different metabolisms and antibiotic susceptibility. Second, *Mtb* is a slow-growing bacteria and, consequently, *in vitro* and *in vivo* assays can take months, which leads to a slower progress compared to other areas. Finally, *Mtb* research requires Biosafety Level 3 (BSL3) facilities with high level of containment and highly trained personnel [68].

The challenge for the development of new regimens for TB is not just the identification of new molecules. The need for combining three or more drugs in final anti-TB regimens requires the inclusion of drug combination assays in pre-clinical models [31, 69]. Traditional *in vitro* assays to evaluate drug combinations present low throughput, which limits its practical use. New methodologies such DiaMOND have overcome this limitation and allow the interrogation of a higher number of drug combinations under different conditions mimicking different bacterial niches [70, 71]. However, although *in vitro* growth inhibition rates of compounds are widely accepted as a determinant of response to treatment, it has been seen that, when integrating PK and PD measures from late-stages of clinical trials, measurements of growth inhibition are not optimal because they indicate inhibition of bacterial growth rather than bacterial killing [72].

To date, available *in vitro* methodologies for the preliminary evaluation of drug combination against TB are mainly based on drug inhibition assays. This Thesis describes the development and practical application of a new *in vitro* technique to study drug combinations against TB based on bacterial killing.

Objectives

The main objective of this thesis is to explore more effective drug combinations against tuberculosis. For this, the following specific objectives were considered:

1. To evaluate currently available *in vitro* methods to perform drug interaction studies.

2. To develop a new *in vitro* method with enhanced throughput and based on bacterial viability to evaluate drug combinations against *Mycobacterium tuberculosis*.

3. To explore new drug combinations containing β-lactams against *Mycobacterium tuberculosis*.

4. To understand the contribution of β-lactams in high order drug combinations.

5. To study the mechanism of action of favourable drug combinations in mycobacteria.

Chapter 1

Development of OPTIKA, a new technology for drug combination kinetic studies against *Mycobacterium tuberculosis*

1.1 Introduction

Multidrug regimens to treat active TB were implemented in the 1950s as a need to achieve cures and decrease antibiotic resistance emergence [49]. Today, the development of anti-TB multidrug regimes to reduce disease relapse, antibiotic resistance development and treatment duration remains a key principle of the third pillar of the WHO END TB strategy, which calls for an urgent impulse in research investments to develop new tools and make them available and accessible. [73]. Although drug combinations against TB have been used for more than 60 years [74], there is no a gold standard method to perform *in vitro* interaction studies.

Checkerboard assays (CBA) are the standard method to evaluate *in vitro* pair-wise drug interactions. They are typically performed in 96 or 384 multi-well plates in which drugs are assayed in pair-wise combinations titrated in two-fold serial dilutions along the X and the Y axes. Minimum Inhibitory Concentration (MIC) values (*i.e.*, the minimum drug concentration inhibiting at least 90% of bacterial growth) of the drugs alone are thus measured together with the MIC of the combination (MIC_{Combo}). To quantify the degree of drug interaction, the Fractional Inhibitory Concentration (FIC) of each drug is calculated by dividing the MIC of the drug in combination with the MIC of the drug alone. Per drug combination, the Fractional Inhibitory Concentration Index (FICI), the reference parameter to classify drug interactions, is calculated as the sum of the individual FIC of the two drugs. The FICI is used as an indication of synergy (FICI ≤0.5), antagonism (FICI >4) or no interaction (0.5< FICI ≤4) [75].

However, the main limitation of CBA is their low throughput. As an example, if eight dilutions are included for each antibiotic, 68 wells will be needed per each pair-wise combination. CBA can be applied to triple combinations by adding a fixed concentration of the third drug to every well of the previously described checkerboard. Each concentration of the third drug requires the evaluation of a completely new checkerboard plate. These three-dimensional checkerboards are technically cumbersome and impossible to be applied to more than three drugs, which definitely restricts the applicability of CBA to pair-wise combination studies.

To overcome this issue, Berenbaum described a method that reduced the two-dimensional dose response space to n+1 dose response curves, proposing to assay: *One dose response per single compound to determine the MIC value and one additional "reference combination of n agents" dose response where all the compounds are 1/n fold serially diluted and assayed together*, being "n" the number of drugs tested [76].

Results derived from *in vitro* drug susceptibility tests are influenced by the physicochemical environment of the assays. An important source of variation of drug susceptibility tests results is the preparation of an inappropriate bacterial inoculum. The standardization of the bacterial inoculum is challenging because of the size, dispersion and viability of organisms [77]. To overcome the inoculum size variation influence from one experiment to another, Berenbaum emphasised the importance of repeating the MIC determination of the compounds while the combination was being evaluated. In addition, he also highlighted the need of including replicates to minimize technical errors that could be easily detected in a traditional checkerboard layout.

More recently, Cokol *et al* applied the theoretical work of Berenbaum to a set of nine first and second-line anti TB compounds, developing DiaMOND (diagonal measurement of *n-way* drug interactions) [70]. DiaMOND gathered a great acceptance and popularity in the TB drug discovery community because of its throughput and its ability to interrogate high-order drug interactions, two key aspects in the case of TB, a slow-growing microorganism that require BSL3 laboratories. However, DiaMOND relies on MIC data, which constitutes a considerable limitation.

Briefly, DiaMOND requires previous determination of the activity of single drugs to determine their inhibitory concentration, being these values defined as the *Reference MIC* (MIC_{Ref}). Drugs are then combined in an equipotent mixture of single drugs regarding their individual MICs. A generic example of an experimental design to determine the interaction of two drugs by DiaMOND is illustrated below, where blue wells contain the desired mixture in terms of drug concentration (**Figure 1.1**). This condition will be reached if the MIC values of drugs A and B in the combination assay are the same than the MIC_{Ref} for both drugs determined beforehand. If this condition is met, the diagonal of a squared checkerboard represents the most informative zone to detect drug interactions.

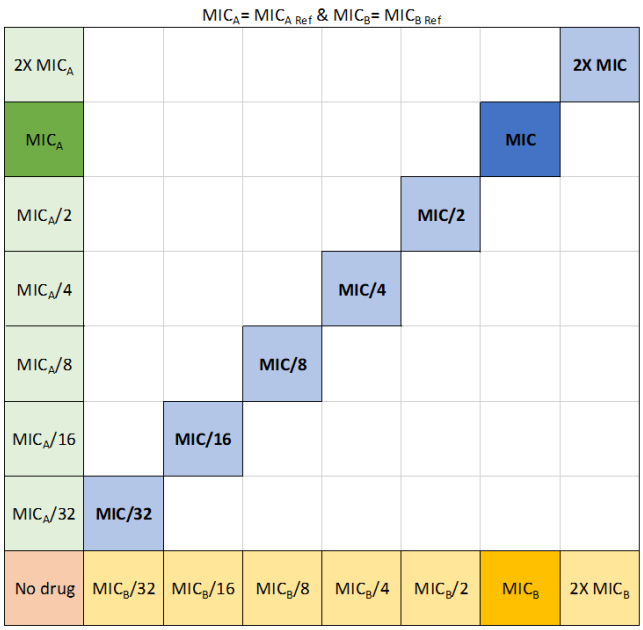

Figure 1.1. Comparison of CBA and DiaMOND layouts. Drugs A and B are displayed in a squared checkerboard layout with respect to their MIC_{Ref}. In this example, the maximum assay concentration of the single drugs is set at twice the $MIC_{Ref.}$ Green wells: dose response of drug A. Yellow wells: dose response of drug B. Wells containing equipotent mixture of drugs A and B are placed in the diagonal of the checkerboard (blue wells). In the case that IC_{50} was considered the reference value to determine the compound activity, MIC= IC_{50}.

However, MIC determination assays entail intrinsic reproducibility issues due to a ±1 dilution factor variability [78]. This variability is assumed in standard single-drug MIC determination assays and it does not impact the evaluation of pair-wise CBA, because the whole array of concentrations allows the selection of the correct MIC values and $MIC_{Combo,}$ thus minimizing intrinsic variations between MIC_{Ref} and the experimental MIC (MIC_{Exp}).

Because of its dependence on MIC values, DiaMOND is strongly affected by inter-experiment MIC variation. Two generic examples where the MIC_{Exp} of one compound varies in one dilution factor with regard to the MIC_{Ref}, either one dilution factor up, or one down are illustrated in **Figure 1.2** (**Figure 1.2** left and **Figure 1.2** right, respectively). In these examples, the diagonal of the squared checkerboard would not contain the equipotent mixture of drugs predicted by DiaMOND. As a consequence, wells of maximum probability for drug interaction determination would not be assayed and, therefore, drug interaction determination would lead to erroneous classifications. Antagonism and synergy, for instance, are overestimated in the examples shown in **Figure 1.2**, left and right, respectively.

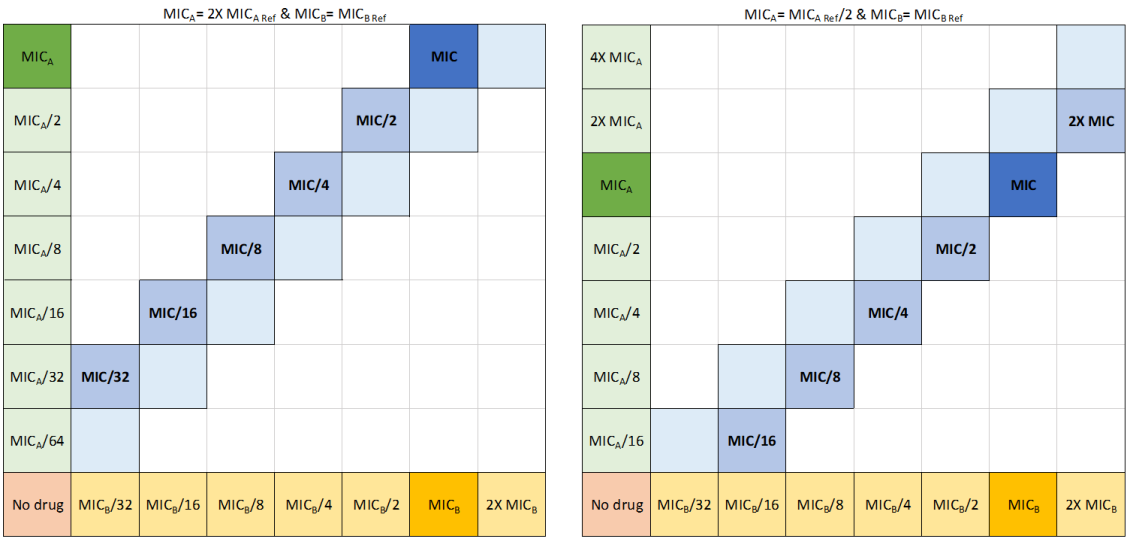

Figure 1.2. Equipotent mixture position variation in DiaMOND. Equipotent mixture of drugs A and B position (dark blue wells) might change due to intrinsic experimental variation of MIC, moving up or down in relation to their theoretical position (light blue wells). Left: example of MIC_A varying in one dilution factor up with regard to the previously determined MIC_{Ref} (green wells). Right: example of MIC_A resulting in one dilution factor down with regard to the previously determined MIC_{Ref} (green wells).

In this example only one dilution factor variation for one of the drugs was considered. However, the real situation could be easily more complex if such variations were to be observed for both drugs, or if they would vary in more than one dilution factor.

Although several mathematical models have been discussed at large on how to best define synergy [74, 79, 80], the biological relevance of such approaches for routine clinical use has been questioned when it comes to predict clinical outcomes of drug combination therapy [81]. One explanation for such discrepancies could be that both, CBA and DiaMOND, are single time point assays that remain inherently rooted in the use of the FICI, a measurement of growth inhibition, as the metric of drug activity rather than bacterial killing [82]. This brings two major limitations when it comes to identify combinations with a potential translational impact for TB therapy:

1. Growth inhibition measurements are dependent on the sensitivity of the growth indicator used, *i.e.* optical density, redox indicators (such as MTT or resazurin), or ATP-based luminescence readouts, each having a defined bacterial cell limit of detection. For example, to get a positive growth signal when using optical density, at least, a cell density of 10^8 cells/ml is needed. This threshold can be lowered to 10^7 or 10^5 cells/ml when using redox or ATP-based growth indicators, respectively [82]. Effectively, this limits the evaluation of the potential activity that drugs alone or in combination might have below the set limit of detection.

2. MIC determination against *Mtb* is typically read only once after five to seven days of incubation. Effectively, this means that essential information is missed at early and late time points of the growth curve since the longitudinal data (*i.e.* factoring time) is not computed in the drug interaction assessment. This is clearly exemplified in the case of β-lactam antibiotics, which displayed a rapid initial bactericidal killing followed by cell regrowth. Such regrowth is due to the stoppage of drug pressure due to thermal drug degradation (for example, β-lactams are highly unstable in the 7H9 assay media) [83]. Considering drug combinations, those drug interactions that produce a faster effect than the related single drugs would be overlooked if the end point is taken after the culmination of this transitory effect. The use of a single end point could be misleading due to lack of activity or lack of drug interactions.

Any potential combination identified by FICI-based readouts would thus require secondary validation by time kill assays (TKA) [81]. TKA are the most valuable assays in static *in vitro* PK and PD studies that rely on Colony Forming Units (CFU) enumeration at different time points (instead of a fixed time point as in the case of CBA or DiaMOND), being the basis of mathematical modelling of antimicrobial drug action [84]. However, this type of assays significantly and, in some cases, prohibitively increases the complexity and duration of combination testing. In TB research, performing TKA is cumbersome due to the slow growth of bacteria (which may take *ca.* 2-4 weeks to form colonies) and the need of working in BSL3 laboratories. Under these conditions, TKA throughput is typically limited to the working capacity of the technical operator (a maximum of *ca.* 30 samples can be processed per experiment), which creates a barrier to validate interactions of more than three drugs due to the large number of possible combinations.

In 2015, Gold *et al.* described the Charcoal Agar Resazurin Assay (CARA) [85], a methodology based on cell viability instead of growth inhibition that can be performed in 96 multi well-plates. In CARA, MIC is determined in liquid medium in a 96-well plate format followed by an outgrowth phase. From the liquid cultures, an aliquot is transferred to a 96-well plate containing solid growth media supplemented with activated charcoal. After a further incubation, cell viability is measured by the fluorescence based resazurin assay, and the Minimum Bactericidal Concentration ($MBC_{99.9}$) is determined.

CARA was developed to classify compounds based on bacteriostatic or bactericidal activity in both replicating and non-replicating conditions [85]. Building from this assay, CARA was adapted as a tool to perform killing curve assays of drug combinations in a 96-well plate format resulting in OPTIKA (Optimized Time Kill Assays). OPTIKA allows to replace the tedious labour of manually diluting samples and CFU counts by a resazurin-based fluorescence readout. Briefly, samples are grown in a

standard 96-well plate, at different time points aliquots are taken and then inoculated in CARA plates.

This Chapter describes the development process of OPTIKA for its use against *M. tuberculosis* and its validation by comparison with standard CBA and DiaMOND methodologies.

1.2 Material and methods

1.2.1 Bacterial strain, growth conditions and reagents

M. tuberculosis H37Rv strain was used for all experiments in Chapter 1. *Mtb* cells were routinely propagated at 37°C in Middlebrook 7H9 broth (Difco) supplemented with 10% Middlebrook albumin-dextrose-catalase (ADC) (Difco), 0.2% glycerol and 0.05% (vol/vol) tyloxapol; or on Middlebrook 7H10 agar plates (Difco) supplemented with 10% (vol/vol) oleic acid-albumin-dextrose-catalase (OADC) (Difco). An exponentially growing *Mtb* liquid culture (OD_{600} = 0.2-0.5) was aliquot, stored at -80˚C and frozen stocks CFU enumerated (5.75 $x10^6$ CFU/ml). Every experiment was started from a new aliquot. Aliquots were thawed in the appropriate assay media volume (Middlebrook 7H9 broth supplemented with 10% ADC and 0.2% glycerol) to reach the desired bacterial concentration.

Stock solutions of drugs used in this Chapter were always prepared fresh on the same day of plate preparation (10 mM in DMSO). The day before bacterial inoculation, compounds were dispensed onto the corresponding assay plate using an HP D300e Digital Dispenser, HP T8+ and D4+ Dispensehead Cassettes (Ref. F0L59A & F0L60A) and stored at -80°C.

MTT solution was prepared dissolving 5 mg/ml of MTT (2-(3,5-diphenyltetrazol-2-ium-2-yl)-4,5-dimethyl-1,3-thiazole; bromide) (Acros Organics, 158990050) in Milli-Q water containing 20% vol/vol of Tween 80 (Sigma, P4780). Once dissolved, this solution was filtered through a 0.2 µm pore size, and aliquots were stored at -20°C until use.

Resazurin solution was prepared fresh on the same day of dispensation onto the assay plate. One tablet of resazurin (Fisher Chemical, R/0040/79) was dissolved in 30 ml sterile PBS (Sigma, SLCB4705) containing 5 % (vol/vol) of Tween 80. The solution was filtered through a 0.2 µm pore size.

1.2.2 Growth inhibition assays. MTT Readout

Duplicate two-fold dilutions of the compounds were dispensed onto clear, flat-bottom 96-well plates (Costar 3599), or clear, flat-bottom 384-well plates (Greiner 781091). Plates were then inoculated with *Mtb* cells (180 µl/well or 50 µl/well in a 96-well or 384-well plates, respectively, to obtain a final cell density of 10^5 CFU/ml) and incubated at 37°C. Internal growth controls were always included, *i.e.* no drug as 100% growth control and no cells as 0% growth control. After 6 days of incubation, 30 µl/well (or 15 µl/well in 384-well plates) of the MTT solution were added and plates further

incubated at 37°C for 24 hours. Plates were then equilibrated at room temperature for 30 min and sealed with adhesive films (Perkin Elmer, 6050185). Absorbance at 580 nm was then measured with an EnVision Multilabel Plate reader (Perkin Elmer). Absorbance raw data (Abs_{Sample}) was normalized to the percentage of growth (% $Growth_{Sample}$) using the absorbance of positive and negative growth controls ($Abs_{100\%\ Growth\ control}$ and $Abs_{0\%\ Growth\ control}$, respectively) and the following formula:

$$\%\ Growth_{Sample} = \frac{Abs_{Sample} - Abs_{0\%\ Growth\ control}}{Abs_{100\%\ Growth\ control} - Abs_{0\%\ Growth\ control}}\ x\ 100 \textit{ (Eq. 1.1)}$$

Minimum drug concentration inhibiting bacterial growth by at least 90% was defined as the MIC. Similarly, minimum drug concentration inhibiting bacterial growth by 50% was defined as Inhibitory Concentration of 50% (IC_{50}).

1.2.2.1 Checkerboard assays

Drug interaction assays were performed in an 8x8 grid checkerboard format in 96-well plates. Compounds alone were placed in a two-fold dose response format in the left column and bottom row of the array. The top concentration for each compound was two-fold the MIC_{Ref} value.

MIC for each partner alone was calculated as described in section 1.2.2. Similarly, the optimal MIC of the combination (MIC_{Combo}) was calculated as the minimum drug concentration of both drugs inhibiting bacterial growth by 90%.

In order to quantify the degree of pair-wise drug interaction (combination of drugs A and B), the FICI was calculated with the following formula:

$$FICI_{90}AB = FIC_{90}A + FIC_{90}B \textit{ (Eq. 1.2)}$$

Here, the FIC for every single drug was calculated as:

$$FIC_{90}A = \frac{Concentration\ of\ drug\ A\ in\ MIC_{Combo}}{Concentration\ of\ drug\ A\ alone\ inhibiting\ bacterial\ growth\ by\ 90\%\ (MIC_A)} \textit{ (Eq.1. 3)}$$

$FICI_{50}$ was similarly calculated using IC_{50} instead of MIC.

Synergy was defined by a $FICI_{90(50)} \leq 0.5$; antagonism by $FICI_{90(50)} > 4$, and no interaction by $0.5 < FICI_{90(50)} \leq 4$.

1.2.2.2 Diagonal Measurement of n-way drug interactions (DiaMOND) assay

From the layout of a checkerboard plate, two-fold serial dilutions of the single drugs and wells constituting the diagonal of the squared checkerboard (equipotent serial dilution of the mixture predicted by DiaMOND) were selected for DiaMOND analysis using two approaches:

(i) Dose Response Curve fitting analysis. The dose response of the single drugs and the dose response of the equipotent mixture (see **Figure 1.1**) were fitted to a four-parameter logistic model by the excel add-in XL fit version 5.5.0.5 (IDBS). MIC (*i.e.* IC_{90}) and IC_{50} values were interpolated in the fitted curve equation. $FICI_{90}$ and $FICI_{50}$ were calculated using equations *(Eq. 1.2)* and *(Eq. 1.3).* When MIC or IC_{50} was a higher concentration than the highest concentration assayed this was manually replaced by the value determined in 1.2.2.1.

(ii) Monotonically decreasing analysis: % growth was converted to a monotonically decreasing curve. MIC or IC_{50} of single drugs and combinations were interpolated from the corresponding linear drug concentration interval equation.

In both approaches drug combinations were classified as described by Cokol *et al.*: synergy $FICI_{90(50)} < 0.85$; antagonism $FICI_{90(50)} > 1.1$, and additive $0.85 \leq FICI_{90(50)} \leq 1.1$.

1.2.3 Bactericidal assays

1.2.3.1 CARA plates preparation

CARA plates (96-well Costar 3599) were prepared as previously described [86]. Briefly, Middlebrook 7H10 agar (Difco) was supplemented with 0.5% glycerol, 10% (vol/vol) OADC (Difco), 0.4% (wt/vol) activated charcoal (Sigma, C9157) and 0.5% (vol/vol) of Tween 80. Media was maintained at 50°C on a heating plate with constant stirring. Then, 200 µl per well were dispensed with a multichannel pipette and plates were left for 40 minutes in the biosafety cabinet, without their lids, for agar solidification. CARA plates were stored in sealed bags at room temperature until use.

1.2.3.2 Minimum Bactericidal Concentration (MBC) assays

Bactericidal assays were coupled to growth inhibition assays as it is described in the CARA assay [87]. Briefly, growth inhibition assay plates were inoculated with the

bacterial culture and incubated at 37°C for six days. At this point, prior to MTT addition, 20 µl/well were transferred to CARA plates.

Inoculated CARA plates were placed in plastic bags and incubated at 37°C for nine days. Then, 40 µl/well of resazurin solution were added to the CARA plate, placed in plastic bags, and further incubated at 37°C for 24 hours. Plates were then equilibrated to room temperature for 30 mins, sealed with adhesive films (Perkin Elmer, 6050185) and top fluorescence (λ_{exc}=530 nm λ_{emis}=590 nm) was read with an EnVision Multilabel plate reader. Fluorescence background was calculated using wells containing media without inoculum. The $MBC_{99.9}$ was calculated as the lowest drug concentration showing a fluorescence signal below the background.

1.2.3.3 Fractional Bactericidal Concentration Index (FBCI) assays

Similar to the MBC assays, the starting point was a 6-day-old plate from a growth inhibition assay with drug combinations instead of single drugs. The CARA protocol was followed as described for MBC determination in section 1.2.3.2.

In the case of combinations, the $MBC_{99.9Combo}$ was calculated as the combination with the lowest concentrations of both drugs A and B maintaining a signal of fluorescence below the background.

Similar to equations *(Eq. 1.2)* and *(Eq. 1.3),* the Fractional Bactericidal Concentration (FBC) of each drug of the pair-wise combination was calculated as:

$$FBC_{99.9}A = \frac{Concentration\ of\ drug\ A\ in\ MBC99.9_{Combo}}{Concentration\ of\ drug\ A\ alone\ killing\ 99.9\%\ of\ bacteria\ (MBC99.9_{A})} \textit{(Eq. 1.4)}$$

Fractional Bactericidal Concentration Index (FBCI) of the combination was calculated as:

$$FBCI_{99.9}AB = FBC_{99.9}A + FBC_{99.9}B \textit{ (Eq. 1.5)}$$

1.2.4 CFU-based time kill assays

Frozen stocks of *Mtb* were thawed in 7H9 + ADC media to obtain a cell density of *ca.* 10^4 CFU/ml and incubated at 37°C for three days for bacterial recovery and exponential growth. This pre-inoculum (*ca.* 10^5 CFU/ml) was then distributed (10 ml) in 25 cm^2 tissue culture flasks, and freshly prepared drug solutions were added to the cultures at the designated concentrations.

At every time point cultures were homogenized, aliquots (50 µl) 10-fold serially diluted up to the 10^{-4} or 10^{-6} dilution in sterile PBS containing 0.1% of tyloxapol and plated (50 or 100 µl, in duplicate) in 7H10 + OADC four compartments petri dishes. Agar plates were incubated at 37°C for 2 weeks and colonies enumerated. Plates were checked again after 3 and 4 weeks of incubation to account for late growers. Cell density was reported as $\log_{10}$ CFU/ml.

1.2.5 OPTIKA (OPtimized TIme Kill Assay) protocol

Compounds were dispensed onto 96-well plates (Thermo Scientific, 267427) using a HP D300e digital dispenser. Unless indicated otherwise, sub-MIC (1/4x MIC), 1x MIC and over-MIC (4x MIC) concentrations of single drugs were assayed in quadruplicate. Combination assays were performed at these concentrations and compared to the activity of single drugs.

- OPTIKA calibration curve:

An untreated *Mtb* culture with a known cell density (OD_{600nm} = 0.125 corresponding to 10^7 CFU/ml) grown in 7H9 + ADC + 0.05% tyloxapol was 10-fold serially diluted in PBS containing 0.1% tyloxapol, and 6-8 replicates of 20 µl/well were plated onto CARA plates. The actual concentration of cells used for the calibration curves was determined by duplicate CFU plating, *i.e.* 50 µl of the diluted inoculum into four compartments petri dishes containing 7H10 agar supplemented with OADC.

Inoculated CARA plates with calibration curves were placed inside plastic bags and incubated at 37°C for nine days. A resazurin solution (40 µl/well) was then added and plates were placed in plastic bags for further 24 hours incubation at 37°C. Plates were equilibrated at room temperature for 30 minutes, adhesive films placed and top fluorescence (λ_{exc}=530 nm λ_{emis}=590 nm) measured with an EnVision Multilabel plate reader.

Fluorescence mean +/- standard deviation (SD) of 6-8 replicates *vs* $\log_{10}$ CFU/ml inoculated was plotted in GraphPad Prism version 6.07 (La Jolla, CA). Fluorescence background and lower linear range of the calibration curve defined the limit of detection for sample interpolation. The linear range of the calibration curve was fitted to a linear regression.

- OPTIKA:

Frozen stocks of *Mtb* were thawed in 7H9 + ADC to a cell density of *ca.* 10^4 CFU/ml and incubated at 37°C for three days to allow for bacterial recovery and exponential growth. Assay plates were inoculated with 250 µl/well of this pre-inoculum (*ca.* 10^5 CFU/ml) and incubated at 37°C. For the OPTIKA assay, 96-well edge plates 2.0

(Thermo Scientific) were used to minimize the plate evaporation. At day 0, and every 7-10 days, 0.7-1 ml of sterile water were added to the edge reservoirs to prevent from well evaporation. These plates constituted the mother plates. They served to inoculate CARA plates at different time points to measure the bacterial viability. Standard time points in OPTIKA assays were day -3 (pre-inoculum), day 0 (bacterial culture used for mother plates inoculation), day 1, day 2, day 4, day 7, day 14, day 21 and end point (*ca*. day 50).

At selected time points during the time-kill assay, 20 µl/well from the mother plates were transferred to CARA plates and CARA protocol was followed as described above for the OPTIKA calibration curve.

Fluorescence units were converted to $\log_{10}$ CFU/ml through data interpolation in the calculated calibration curve equation of the corresponding time point. When the calculated value was below the lower limit of detection, this was manually corrected to the limit of detection. Values above the upper limit of detection were not corrected, as absolute values of $\log_{10}$ CFU/ml were not critical to draw conclusions.

1.2.5.1 Classification of combinations by OPTIKA

GraphPad Prism software was used to calculate the mean of $\log_{10}$ CFU/ml of every drug condition at every time point. The following five parameters of the time-kill curve were selected to classify the combinations (**Figure 1.3**):

1) Bacterial killing rate. It was calculated as the mean $\log_{10}$ CFU/ml at day 2 (D2) minus the mean $\log_{10}$ CFU/ml at day 0 (D0), divided by 2. Graphically, this value corresponded to the slope of the killing curve from day 0 to day 2 *(Eq. 1.6).*

$$D2\ slope_{Sample} = \frac{D2\ Mean\ log_{10}CFU/ml_{Sample} - D0\ Mean\ log_{10}CFU/ml_{Sample}}{2} \text{ (Eq. 1.6)}$$

This value was normalized by subtracting the slope of the untreated control, calculated with (*Eq. 1.7*):

$$D2\ slope_{Control} = \frac{D2\ Mean\ log_{10}CFU/ml_{Control} - D0\ Mean\ log_{10}CFU/ml_{Control}}{2} \text{ (Eq. 1.7)}$$

And lead to the normalized slope to untreated, calculated parameter (*Eq. 1.8*):

$$Normalized\ slope = D2\ slope_{Sample} - D2\ slope_{Control} \text{ (Eq. 1.8)}$$

In order to determine whether the combination killed faster than the fastest single drug, normalized slope values of the combination were compared with values of the respective single drugs. Based on this approximation, combinations were classified as:

- Favourable Interaction (FI): if this parameter was lower for the combination than for the respective single drugs.

- Not determined (ND): if the limit of detection was reached at day 2 by both the combination and, at least, one of the single drugs.

- No Favourable Interaction (NFI): combinations were classified as no favourable interaction if they were not classified as favourable interaction or not determined.

Due to weak differences in killing rates at day 2 for some combinations and the development of OPTIKA as a methodology focused on positive interactions, antagonism was not defined according to killing rate at day 2.

2) Day 4 (D4) bacterial burden reduction. At day four, the bacterial burden of the combinations was compared with that of the related single drugs. Considering the generic pair-wise drug combination constituted by A and B, log reduction of single drugs was calculated as:

$$(D4\ log_{10}\ reduction)_A = (D4\ mean\ log_{10}\ CFU/ml)_A\ - (D4\ mean\ log_{10}\ CFU/ml)_{AB}$$

(Eq. 1.9)

$$(D4\ log_{10}\ reduction)_B = (D4\ mean\ log_{10}\ CFU/ml)_B\ - (D4\ mean\ log_{10}\ CFU/ml)_{AB}$$

(Eq.1.10)

The minimum absolute value of log reduction of A and B was selected to calculate the D4 log reduction of the combination, using the formula:

$$D4\ log_{10}\ reduction = Min_{(D4\ log_{10}CFU/ml)A,B}\ - (D4\ mean\ log_{10}\ CFU/ml)_{AB}$$ (*Eq. 1.11)*

Combinations were then classified according to the D4 log_{10} reduction parameter as:

- Favourable Interaction (FI): if this calculated parameter reached a value of 2 or more.

- No favourable Interaction (NFI): if the reduction was lower than 2-$\log_{10}$.

3) D7 Bacterial burden reduction. This parameter was calculated as described for D4 $\log_{10}$ reduction, but with the data obtained from day 7.

4) D21 Regrowth. For single drugs and combinations, regrowth was a categorical parameter, based on *Yes* or *No* answers, indicating whether the bacterial load was above or within the limit of detection (LD). It was calculated on Day 21 as:

$$D21\ mean\ log_{10}CFU > D21_{LD} = Yes$$

and,

$$D21\ mean\ log_{10}CFU = D21_{LD} = No \quad (\textit{Eq. 1.13})$$

By comparison of the D21 regrowth of combinations and related single drugs:

- Favourable Interaction (FI) was attributed to combinations that did not show regrowth (*No*), compared to the corresponding single drugs (*Yes*).

- Antagonism (A) was defined in combinations that showed bacterial regrowth (*Yes*), whereas single drugs bacterial load was at the limit of detection (*No*).

- Not determined (ND), if regrowth was not observed in the combination and in, at least, one of the single drugs.

- No Favourable Interaction (NFI) was a profile assigned to combinations that did not fit in any of the classifications described above *i.e.* FI, A and ND.

5) D_{end} Regrowth: this parameter was calculated as described for regrowth at day 21, but for the last time point of the time kill assays (*ca.* Day 50, 7 weeks of incubation).

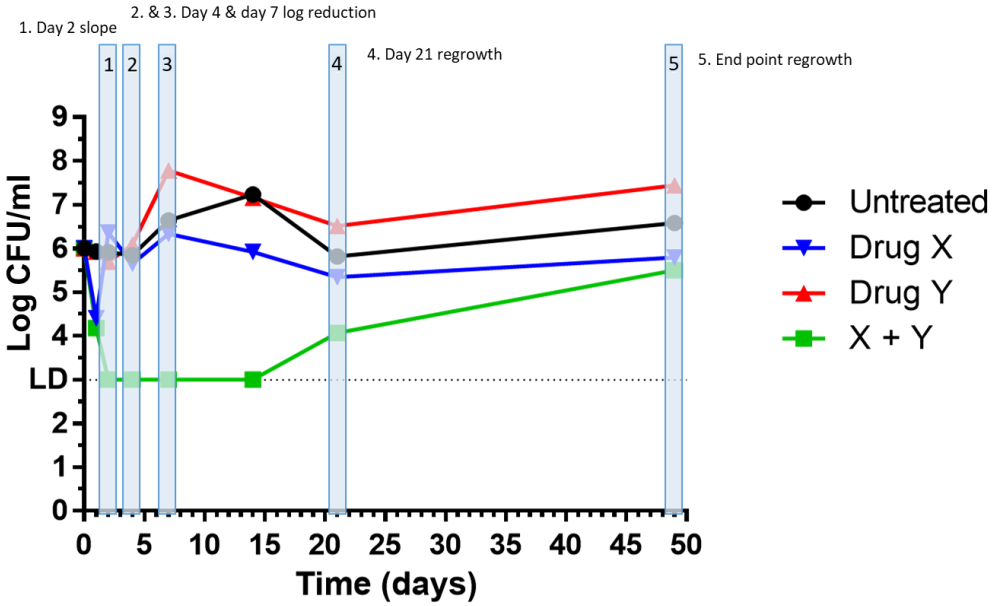

Figure 1.3. Parameters for OPTIKA analysis and classification of combinations. Interaction of combinations is determined by five parameters: slope at day 2, log reduction at days 4 and 7, and bacterial regrowth at days 21 and ~50. To analyse the combinations, the killing profile of combinations is compared with the killing profile of related single drugs. LD: Limit of detection.

Parameters described here were used to obtain a preliminary, fast classification of the combinations. However, all the classifications were revised and manually curated, if needed, by visual analysis of Graphpad killing curves, where the mean $\log_{10}$ CFU/ml *vs* time were plotted. It should be noted that SD was not included in killing curve plots for figure clearness. Mean Log CFU/ml and SD values can be found at appendix II of this Chapter. Otherwise indicated, this applies to all figures of this Chapter containing killing curves.

1.3 Results and discussion

1.3.1 Comparison of checkerboard and DiaMOND methodologies

DiaMOND layout allows a high throughput assay capacity to study drug combinations by reducing the number of conditions typically assayed in a checkerboard format to just the most informative wells in the diagonal of interaction. This reduction in the number of wells needed to interrogate a pair-wise combination allowed to increase the number of different drug combinations tested and, in consequence, the assay capacity.

In order to replicate studies performed by Cokol *et al.*, nine anti-TB drugs were assayed in all possible pair-wise combinations by CBA, using the platemap illustrated in **Figure 1.1**.

Prior to combination studies, the MIC of single drugs (**Table 1.1**) were determined by the MTT assay [88], as described in section 1.2.2.

Drug name	MIC (μM)
Bedaquiline (BDQ)	0.11
Clofazimine (CFZ)	0.31
Ethambutol (EMB)	12.50
Ethionamide (ETH)	6.00
Isoniazid (INH)	4.00
Linezolid (LZD)	1.50
Moxifloxacin (MOX)	0.40
Pretomanid (PTD)	0.50
Rifampicin (RIF)	0.30

Table 1.1. MIC values of selected compounds.

The FICI of the 36 pair-wise combinations were calculated following different methodologies:

- Traditional checkerboard assay (CBA): $FICI_{90}$ values were calculated using the whole plate layout.

- DiaMOND: from our checkerboard assay plates, $FICI_{50}$ values were calculated by using only the dose response of single drugs and the diagonal of the concentration array.

One important difference between CBA and DiaMOND is the criteria for combination classification. Although both methods use the FICI parameter, the CBA classification done here follows Odds' recommendations, which consider MIC variation when establishing the FICI cut-off (FICI ≤ 0.5 synergy, FICI > 4 antagonism, and 0.5 < FICI ≤ 4 no interaction). However, DiaMOND is based on Loewe's model, which is based on the concept that an agent cannot interact with itself in a synergistic or antagonistic manner [89]. In their work, Cokol *et al.* calculated the FICI of isoniazid combined with itself. They obtained a FICI value ranging from 0.85 to 1.1 and, thus, pair-wise interactions were classified as synergy if FICI < 0.85, antagonism if FICI > 1.1, or additive if 0.85 ≤ FICI ≤ 1.1.

To simplify, in this work, *no interaction* and *additive* from CBA and DiaMOND, respectively, were considered as equivalent parameters, and combinations with FICI between synergy and antagonism cut-offs (0.5 < FICI ≤ 4 for CBA and 0.85 ≤ FICI ≤ 1.1 for DiaMOND) were labelled as *no interaction*.

The FICI values from traditional CBA analysis of the 36 pair-wise combinations were correlated with those published by Cokol *et al.* (**Figure 1.4**). In addition, combinations were classified as synergy, no interaction or antagonism according to their respective FICI cut offs. If the classification of a particular interaction did not match by CBA and DiaMOND, it was classified as *no matching*.

Three combinations (ethambutol-rifampicin, pretomanid-rifampicin and clofazimine-rifampicin) were classified as synergy using both methods; CBA done here and data published by Cokol *et al.* Similarly, five combinations (isoniazid-linezolid, bedaquiline-pretomanid, clofazimine-pretomanid, isoniazid-pretomanid, and clofazimine-linezolid) were classified as no interaction. In total, only eight out of 36 combinations showed the classification profile that was reported by Cokol *et al.*, which suggested that the profile of interaction of pair-wise drug combinations depends on the methodology used to estimate drug interactions.

The correlation of absolute FICI values could be measured as the distance of a particular dot to the perfect correlation line. As an example, from **Figure 1.4** it could be observed that the combination clofazimine-ethionamide (CFZ-ETH) showed a similar FICI value in both assays. However, due to the FICI cut-off for combinations classification of both methods, the interaction profile by DiaMOND and CBA did not match.

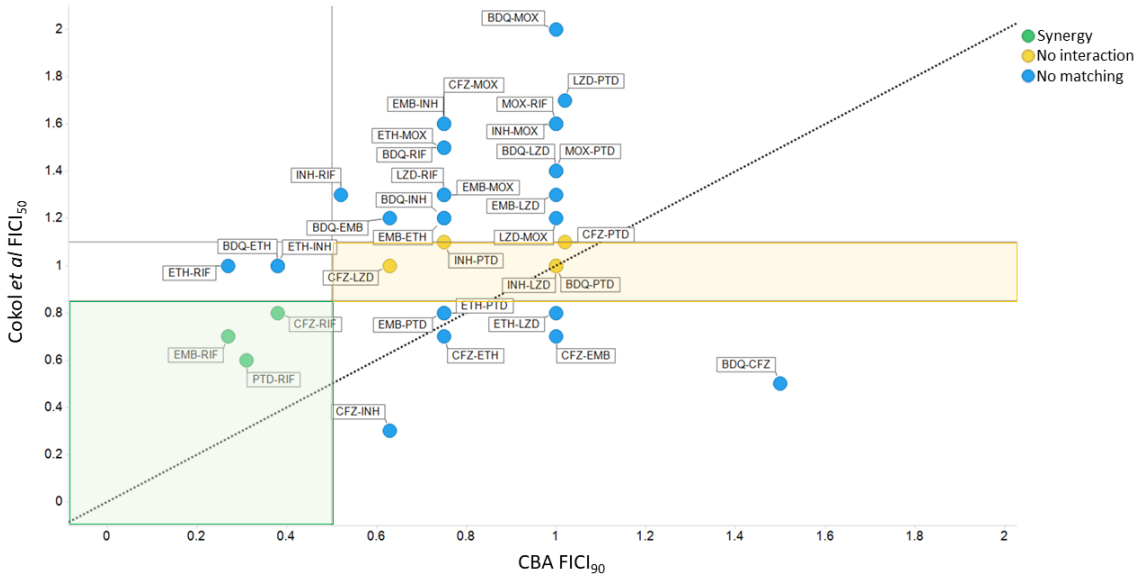

Figure 1.4. Cokol *et al.* reported $FICI_{50}$ *vs* CBA $FICI_{90}$. Circle legends: green: synergy. Yellow: no interaction. Blue: no matching combinations. Background zone legends: according to FICI cut off of DiaMOND and CBA: Green: space for synergy combinations classified by both Cokol *et al.* and CBA. Yellow: space for no interaction combinations. White: space for combinations classified differently by both methods. Straight dotted line: perfect correlation zone (x=y). Bedaquiline (BDQ), clofazimine (CFZ), ethambutol (EMB), ethionamide (ETH), isoniazid (INH), linezolid (LZD), moxifloxacin (MOX), pretomanid (PTD), rifampicin (RIF).

1.3.2 *In-depth* comparison of checkerboard and DiaMOND assays data analysis

Section 1.3.1. showed a low correlation between DiaMOND data reported by Cokol *et al*. and data generated in this Chapter with CBA methodology. To determine whether this low correlation was due to the use of a different analytical parameter ($FICI_{50}$ *vs* $FICI_{90}$), the raw data internally generated from the 36 CBA plates was analysed by DiaMOND (*i.e.* reducing the CBA plate to DiaMOND conditions, calculating $FICI_{50}$ and using DiaMOND defined cut-off for interactions classification). An improved correlation was observed between $FICI_{50}$ values reported by Cokol *et al*. (Cokol *et al*. $FICI_{50}$) and $FICI_{50}$ from our CBA analysed following DiaMOND ($FICI_{50}$ based on DiaMOND) (**Figure 1.5**). Sixteen combinations showed the same interaction profile in both assays when comparing $FICI_{50}$ data from Cokol *et al*. with our internally generated data. However, a low correlation was still observed between these two sets ($R^2 = 0.14$), indicating that the reduction of analysis differences between DiaMOND and CBA did not produce a good-result correlation.

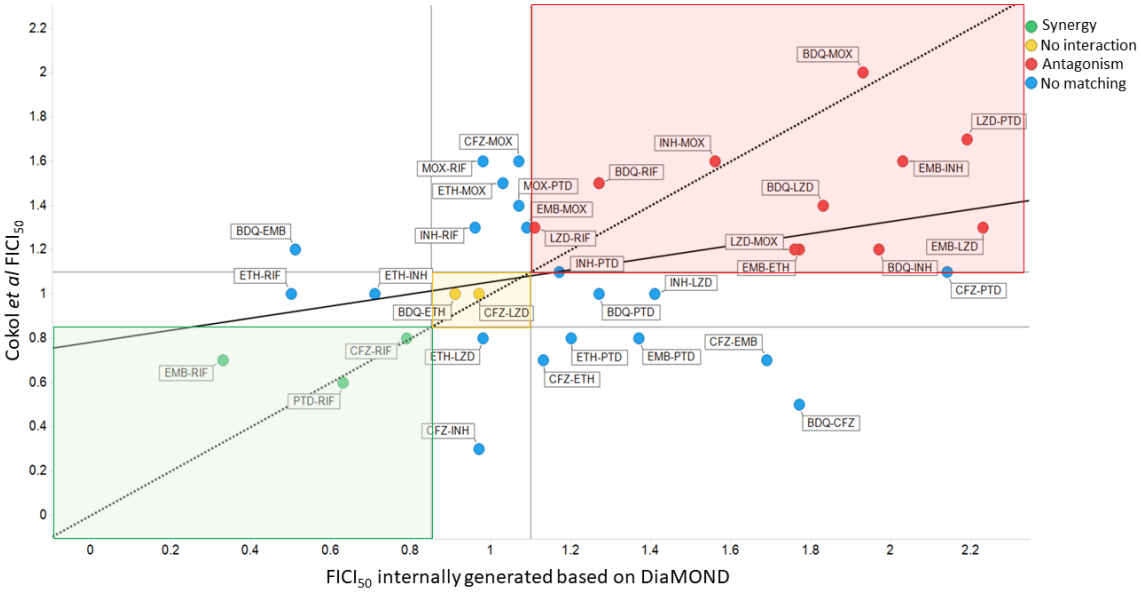

Figure 1.5. *Cokol et al* reported $FICI_{50}$ *vs* $FICI_{50}$ internally generated based on DiaMOND method. Circle legends: green: synergy. Yellow: no interaction. Red: antagonism. Blue: no matching combinations. Background zone legends; green: space for synergy combinations classified by both Cokol *et al.* and CBA; yellow: space for no interaction combinations; white: space for combinations classified differently by both methods. Straight dotted line: perfect correlation zone (x=y). Continuous line: correlation line between two sets of results ($R^2 = 0.14$). Bedaquiline (BDQ), clofazimine (CFZ), ethambutol (EMB), ethionamide (ETH), isoniazid (INH), linezolid (LZD), moxifloxacin (MOX), pretomanid (PTD), rifampicin (RIF).

It should be considered that the $FICI_{50}$ of combinations shown in **Figure 1.5** were calculated in a different manner:

1. Cokol *et al.* analysed the dose-response curves according to a **monotonically decreasing** method (described in section 1.2.2.2 (ii)).

2. In our assay, dose-response curves were fitted to the standard equation fit for *in vitro* dose-response assays [90] *i.e.* using a **four-parameter logistic regression model** (described in section 1.2.2.2 (i)).

In order to assess whether $FICI_{50}$ were comparable independently of the calculation method, from our 36 pair-wise combinations data DiaMOND $FICI_{50}$ was calculated following the two methods described above (**Figure 1.6**).

The good correlation of $FICI_{50}$ shown in **Figure 1.6** suggested that the lack of correlation observed in **Figure 1.5** could not be attributed to the calculation method. It should be noted that linezolid-pretomanid and moxifloxacin-pretomanid were excluded from this analysis because the IC_{50} of pretomanid for those combinations was not reached at the maximum assay concentration assayed.

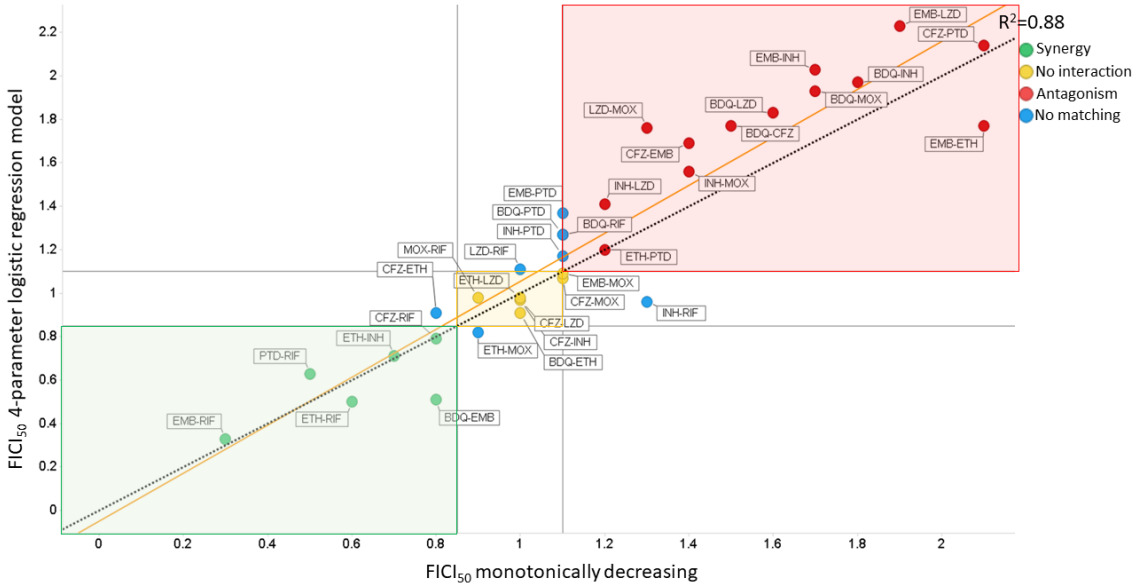

Figure 1.6. $FICI_{50}$ by four-parameter logistic regression model *vs* $FICI_{50}$ by monotonically decreasing. Circle legends: green: synergy. Yellow: no interaction. Red: antagonism. Blue: no matching combinations. Background zone legends; green: space for synergy combinations classified by both methods; yellow: space for no interaction combinations; white: space for combinations classified differently by both methods. Straight dotted line: perfect correlation zone (x=y). Orange line: correlation line between two sets of results (R^2 = 0.88). Bedaquiline (BDQ), clofazimine (CFZ), ethambutol (EMB), ethionamide (ETH), isoniazid (INH), linezolid (LZD), moxifloxacin (MOX), pretomanid (PTD), rifampicin (RIF).

In order to understand these discrepancies between data reported by Cokol *et al.* and our results additional identified differences of both methods, which are summarized below, need to be considered (**Table 1.2**):

1. **Use of detergent.** Unlike our assay, Cokol *et al.* included tween 80, a detergent, in the assay media. Detergent is usually added to reduce aggregation of mycobacterial cultures. It modifies the permeability of the cell wall, a fact that is manifested in an increased drug susceptibility [91]. Moreover, tween 80 could be used as a carbon source by mycobacteria, it alters its central carbon metabolism, and it could interfere with the antimycobacterial activity of some antibiotics [92].

2. **Readout**. Optical density (OD) is a direct method based on turbidity caused by bacterial growth while the MTT assay is an indirect method that relies on a redox indicator and detects metabolically active viable cells. Each readout for cell viability determination possesses its own intrinsic limit of detection, being 10^8 for OD and 10^7 for MTT assay. This could limit the ability to determine synergistic combinations [82].

3. **Bacterial strain**. Although the pantothenate and leucine auxotrophic strain used by Cokol *et al.* seems to show a drug susceptibility profile similar to the strain used in our work (*i.e.* H37Rv) [93], there are strong evidences suggesting that drug interactions are specie and strain dependant [94].

	Cokol *et al* (DOI: 10.1126/sciadv.1701881) [70]	**This work**
***Mtb* strain**	Panthotenate and leucine auxotrophic H37Rv	H37Rv
Bacterial growth	7H9 + ADC + Tween	7H9 + ADC
Assay format	50 µl, $4{\cdot}10^6$ CFU/ml & 384 wells plate	180 µl, 10^5 CFU/ml & 96 wells plate
Incubation for readout	5 days	6 days
Assay readout	OD_{600nm}	MTT assay

Table 1.2. Experimental differences between Cokol *et al.* and our assay.

1.3.3 Impact of growth inhibition parameters in the FICI calculation

Traditionally, the calculation of the FICI has been based on MIC values (*i.e.* 90% growth inhibition). However, more recently, the work published by Cokol *et al*. used the 50% inhibition (IC_{50}) to calculate the FICI.

To determine whether the level of growth inhibition (*i.e.* MIC or IC_{50}) influenced the FICI and, therefore, the combination classification, both $FICI_{90}$ and $FICI_{50}$ were calculated from the same dataset. In **Figure 1.7 A**, the $FICI_{50}$ (grey circles) and the $FICI_{90}$ (black circles) of every combination determined following the CBA methodology can be observed. In general, $FICI_{50}$ showed a larger value than $FICI_{90}$. Only two out of 36 combinations showed a $FICI_{50}$ of 0.5 or lower, with the vast majority of the combinations classified as no interaction.

The same profile was observed comparing $FICI_{50}$ and $FICI_{90}$ calculated with DiaMOND methodology (**Figure 1.7 B**). Due to the FICI cut-offs for interaction classification of the DiaMOND method, antagonism was clearly overrepresented when using $FICI_{50}$.

Considering this FICI reliance on the growth inhibition level, criteria for interaction classification using low inhibition levels such as $FICI_{50}$ should be re-defined to avoid the overestimation of antagonism.

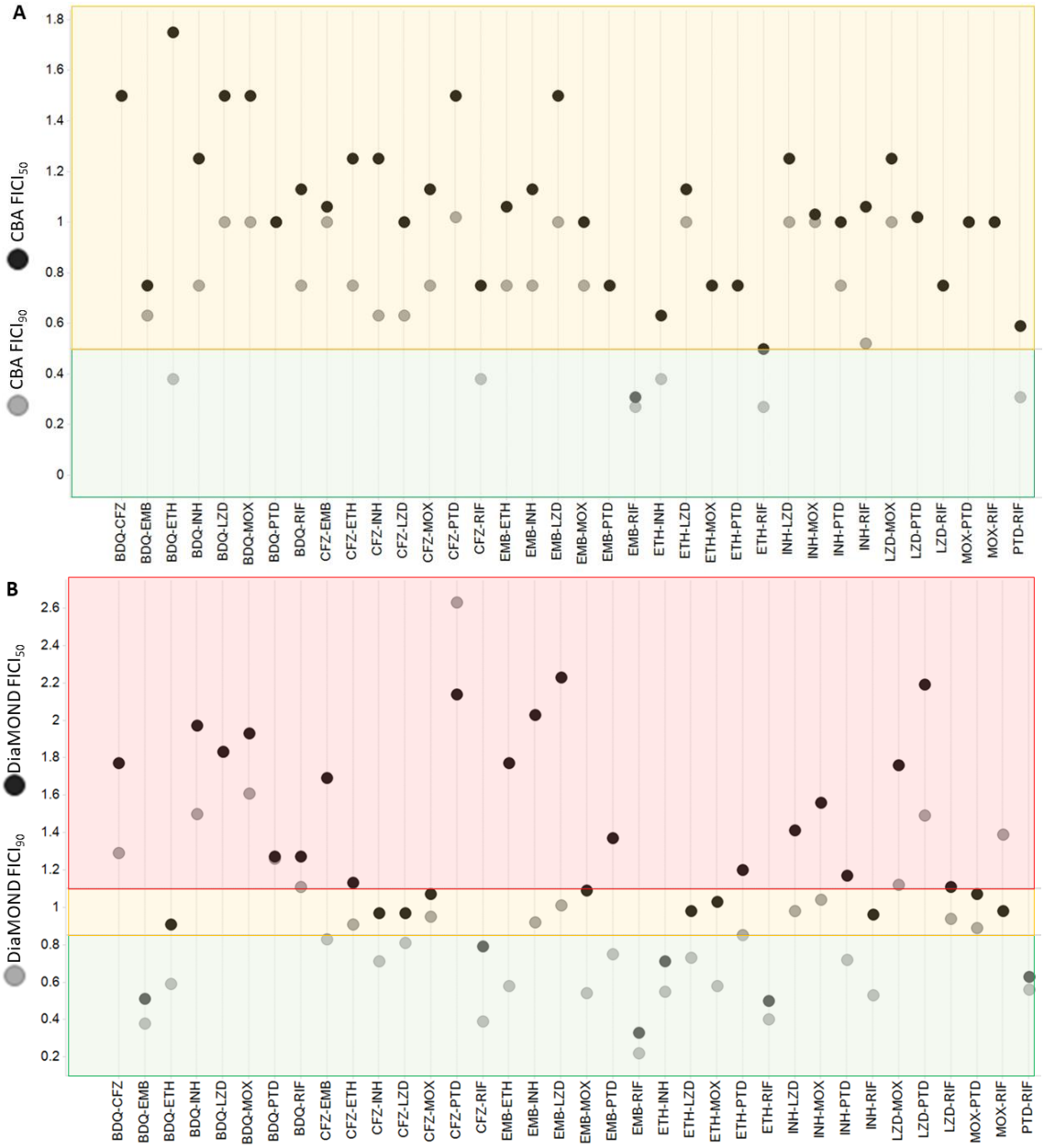

Figure 1.7. $FICI_{50}$ & $FICI_{90}$ comparison. Grey circles: $FICI_{90}$. Black circles: $FICI_{50}$ determined by **(A)** CBA **(B)** DiaMOND methods. Green background: synergy. Yellow background: no interaction. Red background: antagonism. Bedaquiline (BDQ), clofazimine (CFZ), ethambutol (EMB), ethionamide (ETH), isoniazid (INH), linezolid (LZD), moxifloxacin (MOX), pretomanid (PTD), rifampicin (RIF).

1.3.4 CARA calibration

CBA and DiaMOND methods measure growth inhibition [82]. In order to explore bacterial viability as a readout applied to drug interactions, CARA [85] was the chosen assay.

First, we assessed whether the technique described by Gold *et al*. [85] could be reproduced in our laboratory. For this, an untreated culture of *Mtb* exponentially growing was tested using three different inocula, four different times of incubation for bacterial growth in CARA plates and different times of incubation for resazurin conversion (**Table 1.3**).

The signal to background (S/B) ratio of every condition was calculated as the ratio of fluorescence of the most concentrated wells and the fluorescence of wells without cells *(Eq. 14)*.

$$S/B = \frac{Fluorescence\ mean_{Dilution\ 0}}{Fluorescence\ mean_{Blank}} \quad (Eq.\ 14)$$

Based on the S/B ratio and the standard deviation of blank, the chosen parameters for the CARA assay were 20 µl/well, 7 to 11 days for bacterial outgrowth, and 24 hours for resazurin conversion (**Table 1.3**).

Plate ID	Growth time (days)	Resazurin conversion time (hours)	Blank SD (%)	5 µl S/B	10 µl S/B	20 µl S/B	Comments
1_D4 1h	4	1	Saturated signal				
2_D4 4h	4	4	8.2	1.4	2.0	2.4	
3_D4 24h	4	24	13.4	1.3	1.7	2.2	
4_D7 1h	7	1	Saturated signal				
5_D7 4h	7	4	8.3	1.9	Saturated signal		
6_D7 24h	***7***	***24***	***6.2***	3.4	4.4	***4.6***	
7_D11 1h	11	1	16.9	8.4	11.4	13.4	Diluted resazurin solution
8_D11 4h	11	4	9.5	3.7	7.2	14.4	Diluted resazurin solution
9_D11 24h	***11***	***24***	***4.9***	5.5	5.7	***6.9***	
10_D11 48h	11	48	6.1	3.5	4.8	5.9	
11_D13 1h	13	1	27.5	7.2	11.8	14.2	Diluted resazurin solution
12_D13 4h	13	4	9.8	4.7	12.8	24.5	Diluted resazurin solution
13_D13 24h	13	24	8.5	4.9	5.5	7.4	
14_D13 48h	13	48	9.1	3.0	2.8	7.3	

Table 1.3: CARA calibration table. Chosen conditions are highlighted in red and blue. An untreated culture of *Mtb* exponentially growing in 7H9 + ADC + 0.05% Tx (OD_{600nm} = 0.4) was 10-fold serially diluted and three different inocula were plated (5, 10 and 20 µl/well) in triplicate. Background fluorescence signal (blank) was calculated with 10 µl/well 7H9 + ADC. Per condition, S/B and SD were calculated with the three replicates. Four different times of incubation for bacterial growth in CARA plates were evaluated (4, 7, 11 and 13 days). For each time point, different times of incubation for resazurin conversion were tested (1 hour, 4 hours, 24 hours, and 48 hours for later growth incubation times). For 1h and 4h, the resazurin solution needed to be 10-fold diluted because it caused saturated fluorescence signal when the plate was read.

For the conditions highlighted in **Table 1.3,** the calibration curves were plotted (**Figure 1.8**). Although more concentrated points would be needed to observe the upper curve plateau, the linear-log profile described by Gold *et al.* [85] was reproduced in our assay.

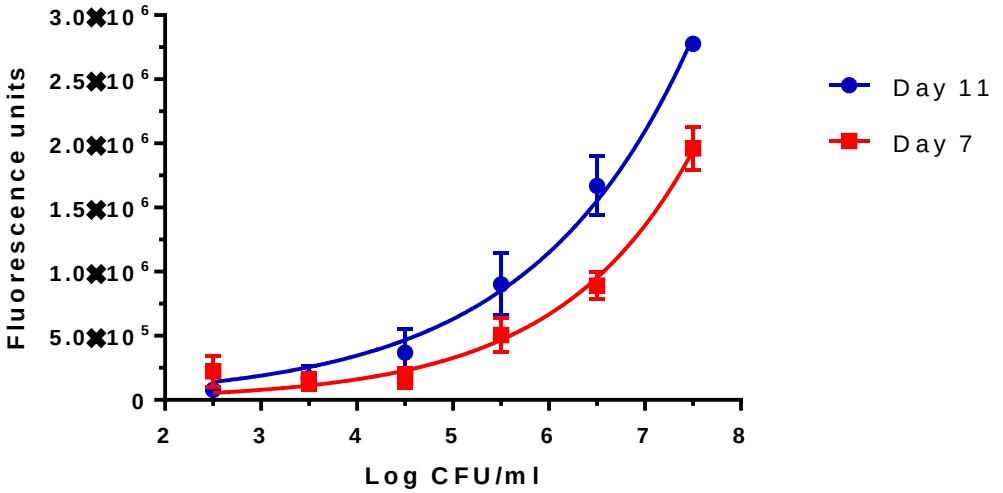

Figure 1.8: CARA validation curves. Fluorescence signal *vs* bacterial concentration. Fluorescence mean & SD of three replicates. Background fluorescence signal was subtracted from the fluorescence values to compare curves of two different times of incubation for bacterial growth: 7 days (red) and 11 days (blue).

1.3.5 Fractional Bactericidal Inhibitory Concentration Index as a readout

CARA was explored as a readout to determine drug interactions. The original 36 pair-wise combinations already tested by CBA and DiaMOND were assayed with this methodology.

As described in sections 1.2.3.2 and 1.2.3.3, 36 CARA plates were inoculated with 20 µl/well of the corresponding MTT plate. After the bacterial outgrowth, $FBCI_{99.9}$ of every combination was calculated, and the 36 combinations were classified not only based on growth inhibition readout, but also on bacterial killing.

$FBCI_{99.9}$ results are shown in **Table 1.4**. It should be noted that a bacteriostatic profile was observed in single drugs or combinations for most of the cases. The $FBCI_{99.9}$ was then calculated using 2x maximum concentration assayed. If the $MBC_{99.9}$ was not determined for both single drugs and the combination, the $FBCI_{99.9}$ reached a value of 2. If the $MBC_{99.9}$ of one single drug and the combination was not determined, the $FBCI_{99.9}$ showed a value of 3.

Combination	$MBC_{99.9}$ A	$MBC_{99.9}$ B	CBA $FBCI_{99.9}$
BDQ-CFZ	> 0.22	> 0.62	2*
BDQ-ETH	> 0.22	> 12.00	2*
BDQ-EMB	> 0.22	> 25.00	2*
BDQ-INH	> 0.22	4.00	3*
BDQ-LZD	> 0.22	> 3.00	2*
BDQ-MOX	> 0.22	0.80	3*
BDQ-PTD	> 0.22	> 1.00	2*
BDQ-RIF	> 0.22	> 0.60	≤ 0.50
CFZ-ETH	> 0.62	> 12.00	2*
CFZ-INH	> 0.62	8.00	≤ 0.50
CFZ-EMB	> 0.62	> 25.00	2*
CFZ-LZD	> 0.62	> 3.00	2*
CFZ-RIF	> 0.62	> 0.60	2*
CFZ-MOX	> 0.62	> 0.80	2*
CFZ-PTD	> 0.62	> 1.00	2*
EMB-PTD	> 25.00	> 1.00	≤ 0.50
EMB-ETH	> 25.00	> 12.00	2*
EMB-RIF	> 25.00	> 0.60	≤ 0.25

Combination	$MBC_{99.9}$ A	$MBC_{99.9}$ B	CBA $FBCI_{99.9}$
EMB-INH	> 25.00	8.00	≤ 0.75
EMB-LZD	> 25.00	> 3.00	2*
EMB-MOX	> 12.50	> 0.40	3*
ETH-INH	> 12.00	> 8.00	≤ 0.25
ETH-LZD	> 12.00	> 3.00	2*
ETH-MOX	> 12.00	> 0.80	1.5
ETH-PTD	> 12.00	> 1.00	2*
ETH-RIF	> 12.00	> 0.60	≤ 0.13
INH-LZD	4.00	> 3.00	≤ 1
INH-MOX	4.00	> 0.80	≤ 0.8
INH-PTD	> 8.00	> 1.00	2*
INH-RIF	4.00	> 0.60	≤ 0.50
LZD-MOX	> 3.00	> 0.80	2*
LZD-PTD	> 3.00	> 1.00	2*
LZD-RIF	1.50	> 0.60	≤ 0.60
MOX-PTD	0.40	> 1.00	3*
MOX-RIF	0.80	> 0.60	3*
PTD-RIF	1.00	0.60	≤ 0.50

Table 1.4: $FBCI_{99.9}$ results table. $MBC_{99.9}$: Minimal Bactericidal Concentration. CBA $FBCI_{99.9}$: Factorial Bactericidal Concentration Index, calculated from checkerboard. Modulator (≤) if $MBC_{99.9}$ of single drugs or combinations is bigger than the highest concentration assayed. In those cases, 2x highest concentration is used for calculations. $FBCI_{99.9}$= 2*: $MBC_{99.9}$A, $MBC_{99.9}$B and $FBCI_{99.9}$ were no determined. $FBCI_{99.9}$ = 3*: $MBC_{99.9}$A or $MBC_{99.9}$B and $FBCI_{99.9}$ were not determined. Bedaquiline (BDQ), Clofazimine (CFZ), Ethionamide (EHT), Ethambutol (EMB), Isoniazid (INH), Linezolid (LZD), Moxifloxacin (MOX), Pretomanid (PTD), Rifampicin (RIF).

The $FBCI_{99.9}$ of the 36 pair-wise combinations were compared with the $FICI_{50}$ determined by DiaMOND (**Figure 1.9**). For 23 combinations (66% of the combinations tested), the $FICI_{50}$ and the $FBCI_{99.9}$ could not be compared because a bacteriostatic profile was observed and the $FBCI_{99.9}$ was not accurately calculated. Four combinations were classified as favourable and one as no interaction with both methods. The seven remaining combinations were classified differently depending on bacterial killing and growth inhibition readouts.

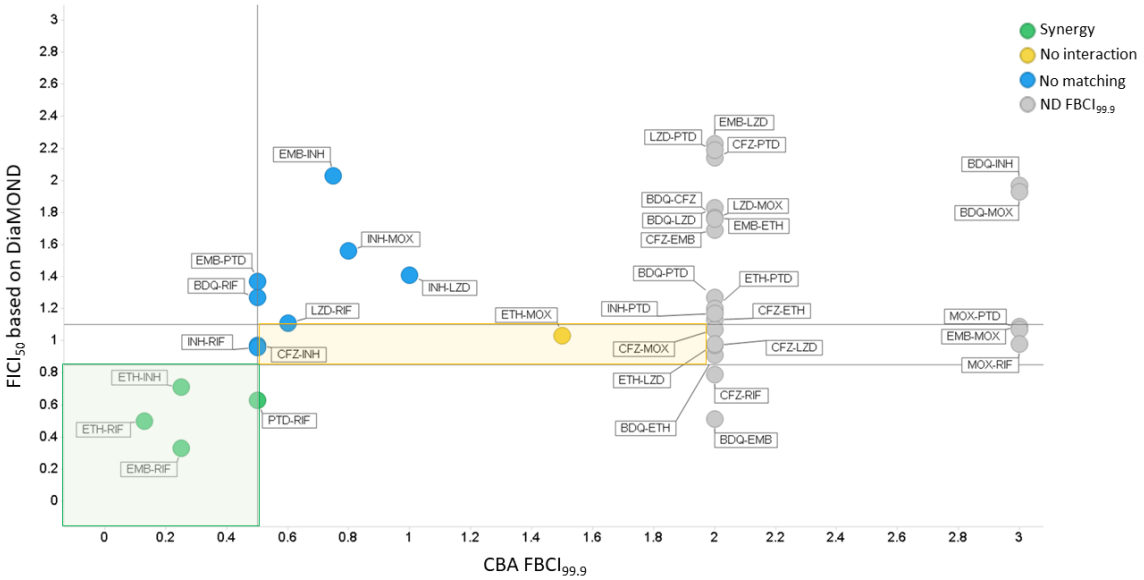

Figure 1.9. $FICI_{50}$ based on DiaMOND *vs* CBA FBCI. Circle legends: green: combinations classified as synergy by both methods. Yellow: combination classified as no interaction by both methods. Grey: combinations that did not reach 99.9% bacterial killing. Blue: no matching combinations. Plot zone legends; green: space for synergy combinations classified by both methods; yellow: space for no interaction combinations; white: space for combinations classified differently by both methods. Bedaquiline (BDQ), clofazimine (CFZ), ethambutol (EMB), ethionamide (ETH), isoniazid (INH), linezolid (LZD), moxifloxacin (MOX), pretomanid (PTD), rifampicin (RIF).

These observations highlighted again the dependence of the results on the methodology and emphasized the need of a standard method based on a reliable readout [82]. CARA was designed as a semi-quantitative method [85] and data shown in this section confirms that its low sensitivity might not fit the needs to be applied to obtain quantitative results.

1.3.6 CARA optimization and OPTIKA validation

CARA was discarded as an absolute methodology applied to study drug interactions based on the MBC and the FBCI due to its low sensitivity. However, in this Chapter, we have explored it as a tool to perform time kill assays of drug combinations with an increased throughput. This new methodology was named OPTIKA (Optimized Time Kill Assays) and previously to its validation, some optimizations described below were performed.

1.3.6.1 Tween 80 addition to CARA plates

Tween 80 is a synthetic phospholipid routinely added to growth media of mycobacterial cultures to increase the growth rate and reduce aggregation [95, 96]. In order to improve the dynamic range of CARA, four different concentrations of tween 80

in the solid assay media were evaluated: 0%, 0.05%, 0.5% and 2% (vol/vol). Four CARA plates were inoculated from the respective growth inhibition plates. To assess that tween 80 addition did not interfere in the characterization of the compounds, the MIC and $MBC_{99.9}$ of the standard bacteriostatic and bactericidal controls [85] (*i.e.* linezolid and moxifloxacin, respectively) were also included in those plates.

Plates shown in **Figure 1.10 A** shared the same plate map design. Differences in cell growth could be visually observed (**Figure 1.10 A**). As tween 80 concentrations were increased (from 0% to 2%), cells grew more dispersed and a bigger area of the wells was covered by the bacterial culture. Regarding the homogeneity of growth inside the well and bacterial morphology, isolated colonies could be easily observed in the plate containing 0% of tween 80, as well as in some wells with low bacterial growth in the plate with 0.05% of tween 80. Plates containing higher concentration of tween 80 showed a uniform mass of bacterial culture instead of isolated colonies.

For each concentration of tween 80, the S/B was calculated with the ratio of fluorescence of 100% growth and 0% growth controls (similar to section 1.3.4). According to **Figure 1.10 B**, S/B was dependent on tween 80 concentrations. It was higher as tween 80 concentrations were increased from 0% to 0.5 %. At 2%, a decrease in the S/B was observed, which could be attributed to the toxic effect of tween 80 when used at high concentrations [95].

The optimal concentration of tween 80 was 0.5% (vol/vol). To assess that this concentration did not affect the compound profiling by CARA, the MIC, $MBC_{99.9}$ and $MBC_{99.9}$/MIC ratio of moxifloxacin and linezolid were calculated from the CARA plate containing 0.5% of tween 80. Compounds were assayed in triplicate following protocols described in sections 1.2.2 and 1.2.3.2. Compounds were classified as bactericidal or bacteriostatic according to the $MBC_{99.9}$/MIC ratio, following the same criteria described by Gold *et al.* [85] (*i.e.* ≤ 4 for bactericidal and > 4 for bacteriostatic compounds). The expected profile was confirmed in both bactericidal and bacteriostatic controls, thus validating the addition of 0.5 % (vol/vol) of tween 80 in the agar of CARA plates (**Figure 1.10 C**).

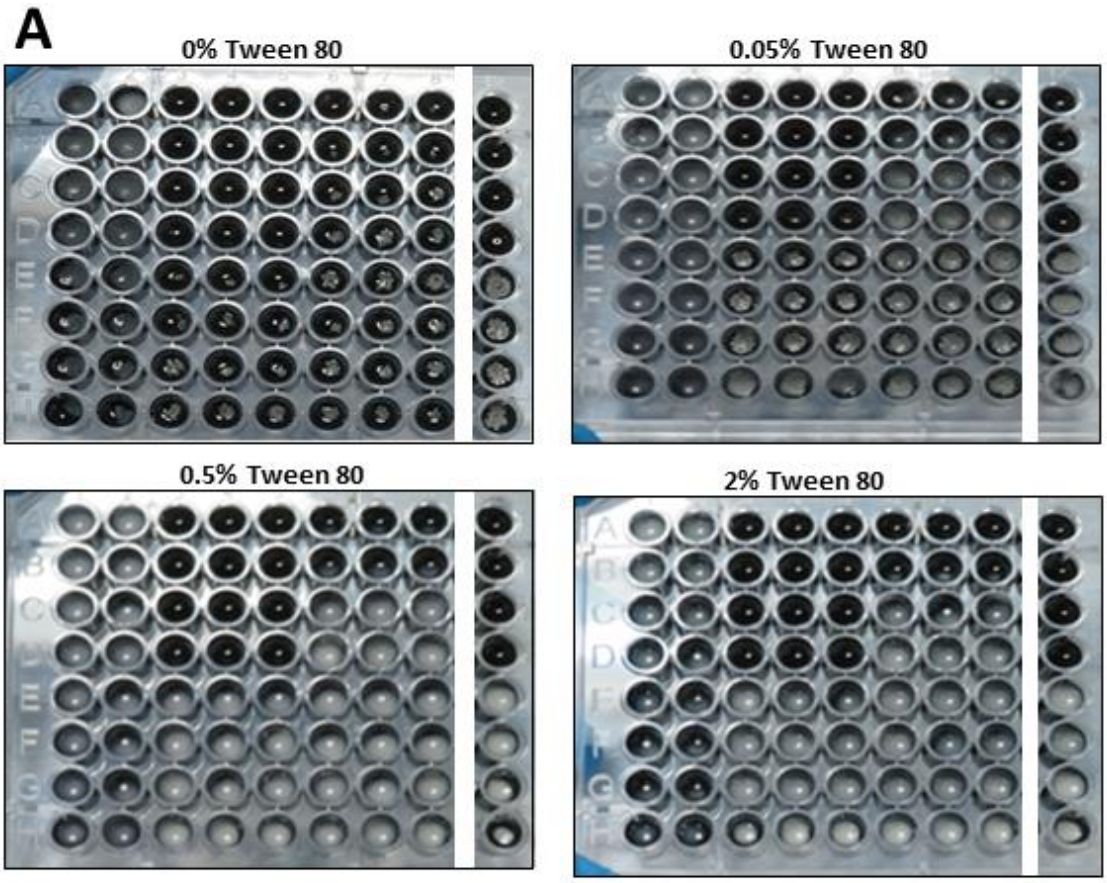

B

Tween 80 (vol/vol)	S/B ratio
0%	4
0.05%	7
0.50%	16
2%	10

C

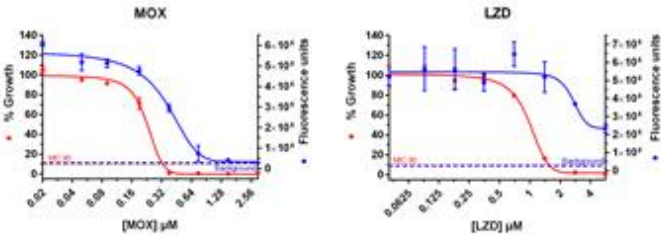

Drug	MIC (µM)	$MBC_{99.9}$ (µM)	$MBC_{99.9}$/MIC
MOX	0.38	1.5	3.9
LZD	1.59	> 5.6	≥ 7.0

Figure 1.10. Tween 80 addition to CARA plates. A: effect of tween 80 addition on bacterial growth in CARA plates. All the plates shared the same plate map design, the only difference was the concentration of tween 80 in the solid media. Columns 1 and 2, calibration curves: these columns were empty in the MIC plate. In each column of the CARA plates, a serial dilution of an untreated culture of *Mtb* exponentially growing (Starting OD_{600nm}=0.14) was plated. Columns 3, 4 and 5, bactericidal control: $MBC_{99.9}$ determination of moxifloxacin. CARA plates were inoculated from a moxifloxacin MIC determination plate, in triplicate. Columns 6, 7 and 8, bacteriostatic control: $MBC_{99.9}$ determination of linezolid. CARA plates were inoculated from a linezolid MIC determination plate, in triplicate. Column 12, 0% (rows A-D) and 100% (rows E-F) growth controls: no cells were included in the 0% growth control. An untreated inoculum of growth inhibition plate was included in 100% growth control wells. **B:** tween concentration determination according to S/B ratio. **C:** control compounds profiling in plate containing 0.5% of tween 80. For LZD, 99.9% of bacterial killing was not reached at maximum drug concentration

assayed; 2x maximum assay concentration was used for $MBC_{99.9}$/MIC ratio calculation. Moxifloxacin (MOX), linezolid (LZD).

1.3.6.2 CARA pre-moistening step removal

Gold *et al.* reccommend to moisten the CARA plates before the addition of the rezasurin developing solution [85] to avoid concentration of the sample in a small area (spot) in the agar of the CARA plates due to a rapid absorption of the solution by the agar.

However, in our conditions, dryness was not visually observed in nine-day incubated CARA plates. Before the moistening step removal, it was checked whether results could be affected by this change of the protocol. For this, eight replicates of a 10-fold serially diluted culture of *Mtb* were plated onto a CARA plate and incubated at 37°C. After 9 days, 10 µl/well of sterile PBS were added to four of the eight replicates and 40 µl/well of resazurin solution were added to all replicates. CARA protocol was followed as described in section 1.2.3.2. **Figure 1.11** shows the fluorescence *vs* the bacterial concentration of both assay conditions. Differences between linear range and fitted equations of both conditions were minimum, thus validating the removal of the pre-moistening step of the CARA assay.

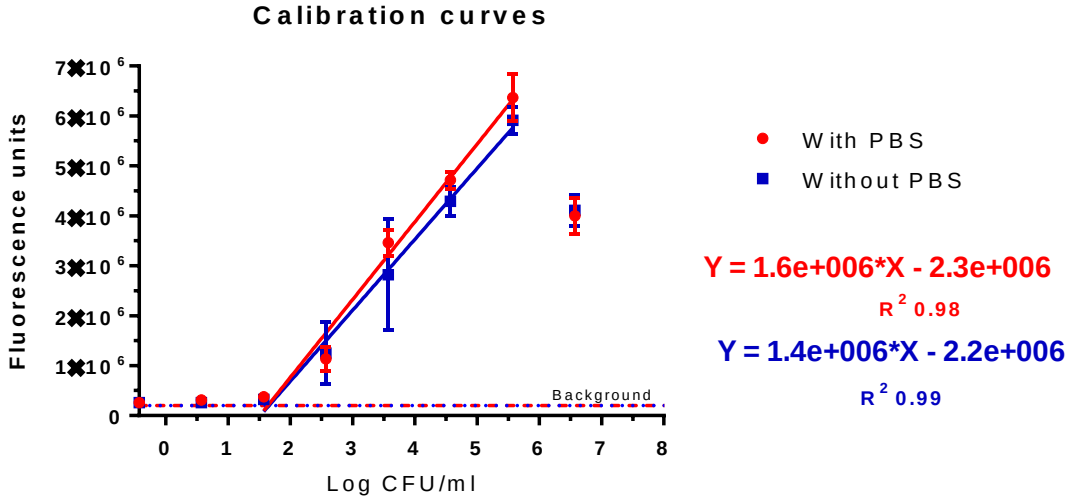

Figure 1.11. Evaluation of pre-moistening step removal. Fluorescence *vs* Log CFU/ml curves. In four replicates (red) the PBS moistening step prior to resazusin addition was performed, and in four replicates (blue) this step was skipped and resazurin was directly added to CARA plates. Similar linear range was observed with and without the pre-moistening PBS step.

1.3.6.3 OPTIKA set up and assay validation against CFU counts, the gold standard method for time kill assays

Once the CARA was adapted to our experimental needs, it was applied to perform kinetic studies of drug combinations, leading to the foundations of the OPTIKA assay. **Figure 1.12** shows the OPTIKA protocol previously described in section 1.2.5. Briefly, compound plates containing single drugs and combinations at a different concentration were inoculated with an *Mtb* culture. These plates constituted the mother plates and they were incubated at 37°C until the last time point included in the experiment. At every time point, every mother plate was taken from the incubator, cells were mixed with a multichannel pipete and an aliquot of each well was transferred to an empty CARA plate. In parallel, a calibration curve was built with an untreated culture of *Mtb* exponentially growing. The concentration of this culture was initially determined by OD measurement and exactly quantified by CFU counting. For the calibration curve, this culture was 10-fold serially diluted and plated in an empty CARA plate. Moreover, internal 100% growth and 0% growth controls were always included in each CARA plate. Inoculated CARA plates (those coming from the mother plates and the calibration curve) were incubated for bacterial outgrowth and revealed with resazurin. Fluorescence linear range of every calibration curve was fitted to a linear regression. Fluorescence of treated samples was converted to $\log_{10}$ CFU/ml with the calibration curve of the corresponding time point. Finally, $\log_{10}$ CFU/ml *vs* time of every drug combination and corresponding single drugs were plotted for killing curves comparison.

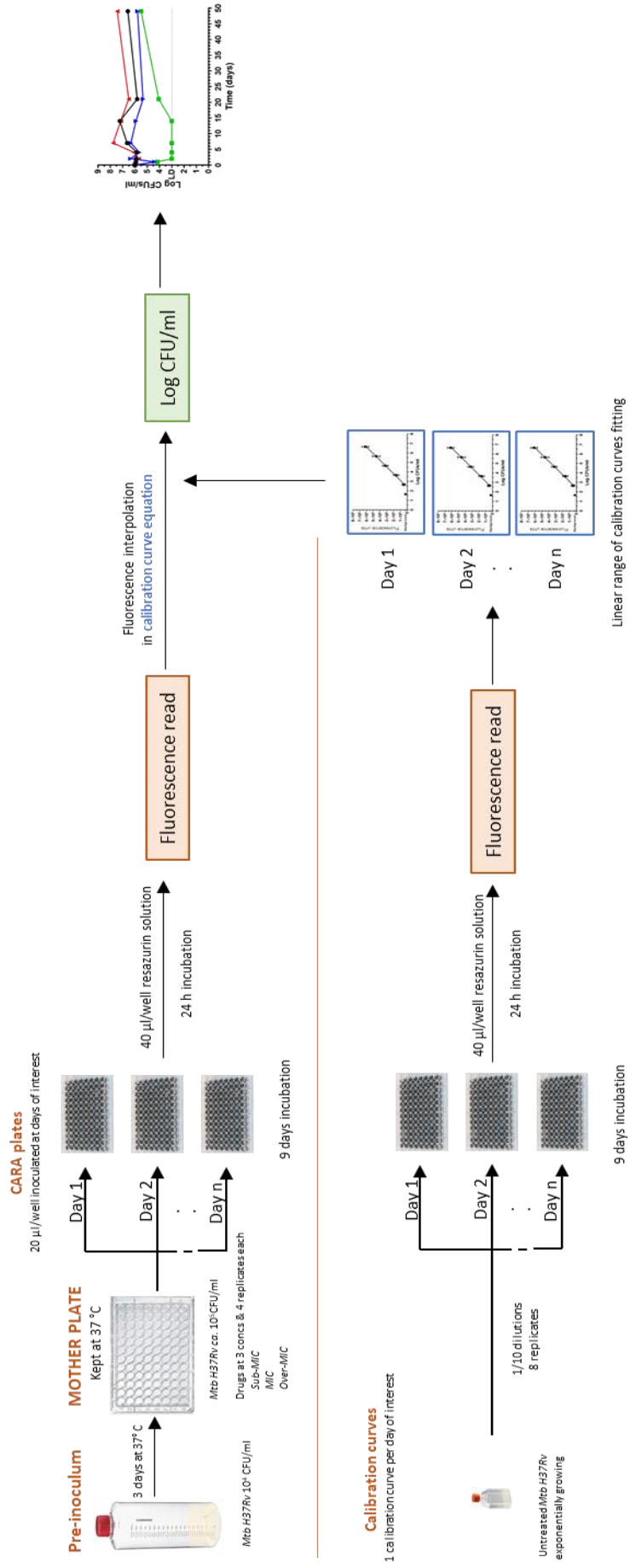

Figure 1.12. OPTIKA protocol schema. Compound plates are inoculated with a 3-day-old culture of *Mtb*. At designated time points, an aliquot of these mother plates is transferred to an empty CARA plate. In parallel, at every time point a calibration curve with a known concentration culture is built. After 9 days of incubation for bacterial growth, CARA plates are revealed following the resazurin assay. With the corresponding calibration curve, fluorescence is converted to $\log_{10}$ CFU/ml.

Table 1.5 compares OPTIKA versus traditional time kill assay based on CFU counting. Main differences are summarized below:

1. While samples in traditional TKA are typically kept in 10-ml culture flasks, OPTIKA uses 96-well plates. This allows a drastic increase of the assay capacity.

2. In traditional TKA, the cultures need to be serially diluted to get an acceptable number of CFU to be counted by the naked eye. This step also dilutes the compound that is present in the original culture flask. This tedious labour is removed in OPTIKA because the fluorescence-based resazurin readout is much more sensitive than the human eye. In OPTIKA, an aliquot of the treated culture is transferred directly to the agar plate for the bacterial outgrowth. In order to avoid the interference of the carry over compound, activated charcoal is added to the solid media to remove the compound transferred to the CARA plates [85].

3. Traditional TKA relies on CFU counting and OPTIKA is a fluorescence-based assay. To report data in traditional bacterial concentration units, OPTIKA includes a calibration curve of an untreated bacterial culture at every time point. The same protocol is followed for the calibration curve plate and for the sample plates, allowing association of the relative fluorescence units provided by the plate reader with the known bacterial concentration inoculated. The use of this readout eliminates the tedious and time-consuming CFU counting step and reduces the time to readout and results generation.

	TKA methods	
	CFU based	**OPTIKA**
Volume	10 ml (typically on a flask)	250 µl (on 96-well plates)
Handling	Serial 10-fold dilutions	Transfer by multichannel
	Manual seeding of chosen dilutions	
	Technical duplicates	Biological quadruplicates
	4-6 hours processing time	1-2 hours processing time
Reading	Manual CFU counts	Automated fluorescence (resazurin readout)
		88 samples/plate (up to 25 plates)
Throughput	*ca* . 30 samples	*ca.* 2200 samples
	15 unique conditions	550 unique conditions
Time to raw data	*ca.* 3 weeks	10 days

Table 1.5. Comparison of traditional time kill assays by CFU counts and OPTIKA methodologies. Treated cultures are maintained in 96-well plates instead of flasks. Biological quadruplicates are

assayed, and plates revealed by a resazurin-based assay. Throughput is drastically increased and time to generate results reduced.

Validation of OPTIKA was done comparing killing curves of eight single drugs and six combinations by the traditional CFU counting assay (section 1.2.4) and OPTIKA (section 1.2.5). The set of calibration curves of this OPTIKA experiment is shown in **Figure 1.13**.

The linear range of calibration curves for all time points (**Figure 1.13 A**) showed a window ranging from 4 log_{10}CFU/ml (day 21) to 6 log_{10}CFU/ml (days 4, 7 and 14). Goodness of fitness of experimental points to a linear regression was measured with the R^2 index calculated with Graphpad prism (**Figure 1.13 B**). The equation of fitted line was used to convert fluorescence units into log_{10}CFU/ml of all samples, and the lowest bacterial concentration included in the fluorescence linear range was used as the limit of detection of the corresponding time point.

A

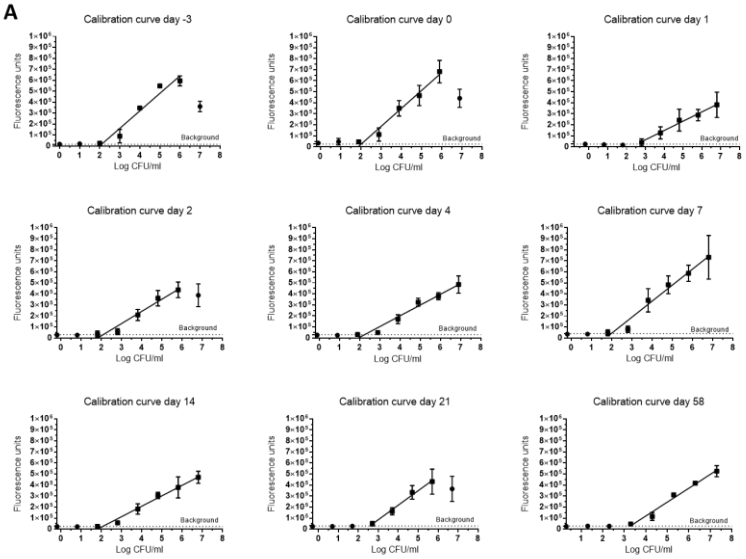

B

Time-point (day)	Calibration curve equation	R^2	Limit of detection (Log CFU/ml)
-3	Y = 159802*X - 318120	0.95	2.0
0	Y = 162584*X - 302447	0.98	1.9
1	Y = 84199*X - 187345	0.99	2.8
2	Y = 110408*X - 199089	0.96	1.8
4	Y = 97406*X - 188105	0.97	1.9
7	Y = 145216*X - 245915	0.97	1.8
14	Y = 94581*X - 169890	0.98	1.8
21	Y = 131612*X - 308805	0.99	2.7
58	Y = 125800*X - 383666	0.98	3.3

Figure 1.13. OPTIKA calibration curves. A: fluorescence units *vs* LogCFU/ml plots. Black line: straight fitting line of the linear range. B: equations of fitted linear range, R^2 index and limit of detection for all time points.

Figure 1.14 shows a head-to-head comparison of killing kinetic determinations measured by traditional CFU-based and OPTIKA assays.

Rifampicin was tested at three concentrations: two sub-MIC and one over-MIC. Only at 4x MIC it showed a significant bacterial reduction, with the other two sub-MIC concentrations presenting similar growth with respect to the untreated control in both traditional TKA and OPTIKA assays (**Figure 1.14 B**). Rifampicin combined with ethambutol was included in this assay as a control of synergistic interaction, as

previously described [83]. This favourable profile was confirmed in both assays (**Figure 1.14 C**). If rifampicin was combined with pretomanid, a possitive but moderate effect was also visible in traditional TKA and OPTIKA (**Figure 1.14 D**) .

Single drugs and combinations showed bacterial growth similar to the untreated control for the rest of the combinations. They were classified as no interaction by both methodologies (**Figures 1.14 E to 1.14 H**).

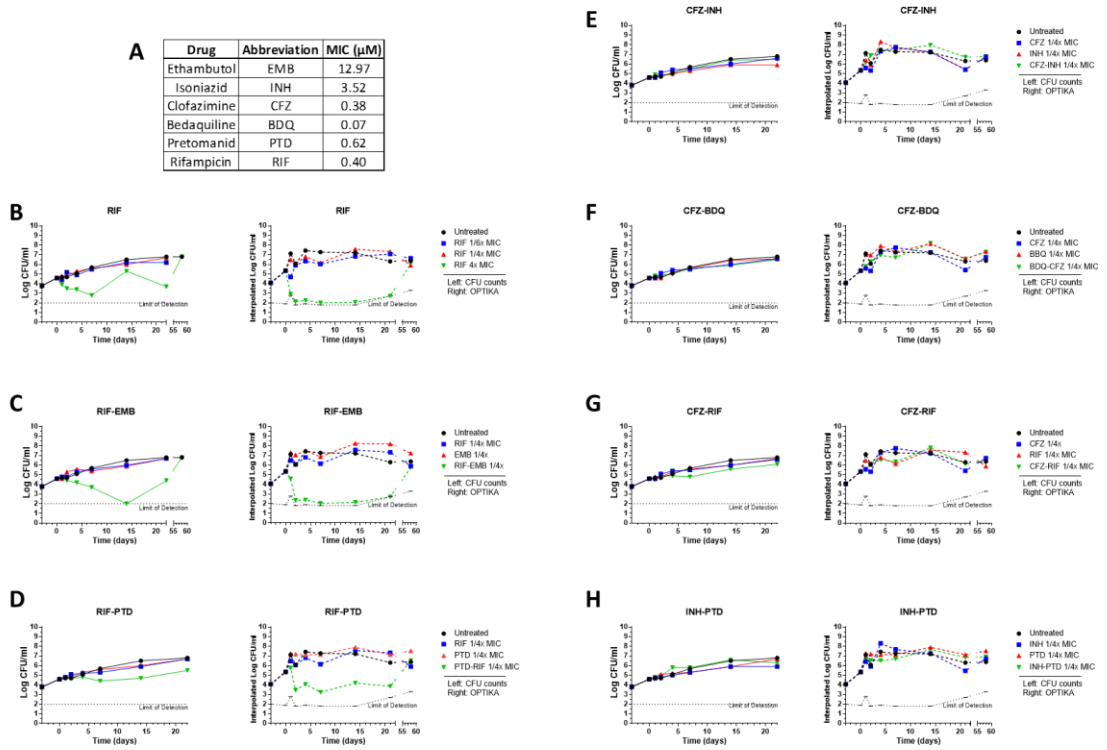

Figure 1.14. OPTIKA validation. Head-to-head comparison of killing kinetic determinations measured by traditional CFU-based and the OPTIKA assays. **(A)** Drugs and MIC values used. **(B to H)** Killing curve profiles by traditional TKA (left plot of every pair) and OPTIKA (right plot).

The good correlation of the killing curve profile under both experimental conditions gave us the confidence to propose OPTIKA as a new methodology to perform kill kinetic studies of drug combinations and was the basis for most of the following actions of this Thesis.

1.3.7 OPTIKA data analysis

OPTIKA allows performance of TKA with an increased throughput compared to the gold standard CFU-based counting assay. However, this implies the generation of large amount of data sets that need to be efficiently processed to infer results. This section describes a method developed to classify drug interactions and simplify data analysis based on five calculated parameters.

The classification of drug combinations is based on the comparison of the kill kinetic curve profile of the combinations against the corresponding single drugs (see section 1.2.5.1).

Interesting combinations were those that reached the limit of detection of bacterial growth and prevented bacterial regrowth at the end point. This is in contrast to single drugs that typically displayed different degrees of initial bacterial killing rates, followed by bacterial regrowth.

Figure 1.15 illustrates examples of different profiles of killing curves of single drugs and combinations obtained by OPTIKA.

1. **End point synergy**: the interaction of the combination isoniazid-rifampicin at 4x MIC (INH-RIF 4x MIC, **Figure 1.15 A**) could not be determined until day 21 because rifampicin showed the maximum reduction of the bacterial load at shorter time points. However, this combination showed a favourable interaction according to regrowth at day 21 and at the end point, because both single drugs showed bacterial rebound, and the combination maintained the bacterial growth under the limit of detection.

2. **Fast Killing**: in the case of isoniazid-rifampicin at 1x MIC (INH-RIF 1x MIC, **Figure 1.15 B**), there was a favourable interaction according to slope at day 2 because the combination killed faster than both single drugs alone. The low bacterial load reached by the combination was maintained until day 14. However, this was followed by a rapid rebound starting on day 14 and no difference was observed comparing the bacterial killing of the single drugs and the combination at the end point.

3. **Strong synergistic interaction**: ethambutol combined with rifampicin is a previously described example of synergy [83]. In our assay, this strong favourable interaction was confirmed (EMB-RIF 1x MIC, **Figure 1.15 C**). The limit of detection of bacterial killing was rapidly reached by the combination and maintained without bacterial regrowth until the end of the experiment. In contrast, respective single drugs assayed separately reached different degrees of bacterial killing, but they did not reach the limit of detection at any measured times.

4. **Paradoxical antagonism**: isoniazid-bedaquiline combination was an example of slow interaction (INH-BDQ 1x MIC, **Figure 1.15 D**). Comparing single drugs and the combination from day 0 to day 7, no positive interaction was observed. This correlated with the antagonism proposed by Cokol *et al.* [70]

because the combination showed less killing effect than isoniazid alone at day 5, which is the end point of the DiaMOND method. However, looking at the curve profile of the combination at longer times, it was observed that the decrease in the bacterial load was maintained until day 14. At that point, the limit of detection was reached, and no detectable bacterial load was maintained until the last time point analysed, with the final outcome classified as favourable interaction for this combination according to OPTIKA. Comparing with single drugs, bedaquiline showed a slow killing profile and the limit of detection was not reached at any time. In contrast, isoniazid presented a fast-killing rate at shorter times, reaching the limit of detection at day 4 and followed by a significant bacterial regrowth. Regarding the mechanism of interaction, it could be hypothesised that the combination may be preventing from the emergence of drug resistance, an important benefit of drug combinations [97]. Killing kinetics of isoniazid against *Mtb* are characterized by a fast-killing rate at early days, followed by a rebound of bacterial growth mainly due to the emergence of isoniazid resistant mutants [98-100]. The combination of isoniazid with bedaquiline could prevent from the emergence of isoniazid resistant bacteria according to OPTIKA data. shown in this work.

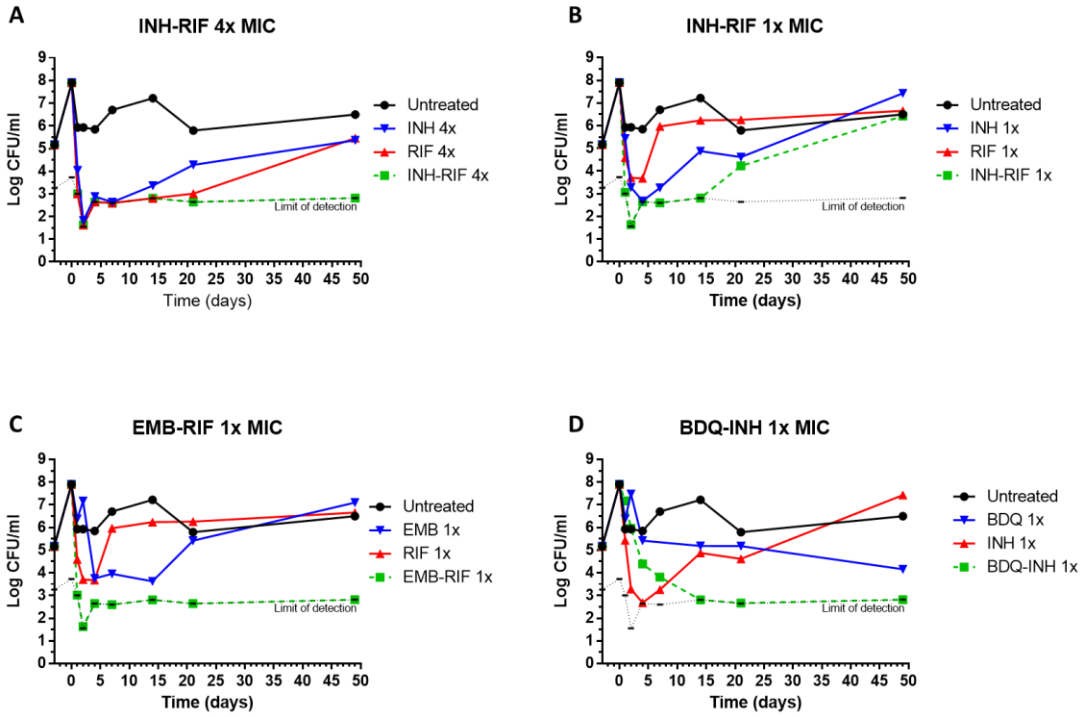

Figure 1.15. Examples of killing curve profiles by OPTIKA. (A) Isoniazid-rifampicin (INH-RIF) 4x: the interaction cannot be detected because maximum killing effect is reached by RIF alone until day 14. From day 21, the combination is classified as favourable. **(B)** Isoniazid-rifampicin (INH-RIF) 1x: a positive interaction is observed until day 14. **(C)** Ethambutol-rifampicin (EMB-RIF): favourable drug interaction is maintained until the end of the experiment. **(D)** Bedaquiline-

isoniazid (BDQ-INH) 1x: antagonism is observed until day 7, but synergy is observed from day 14 to the end of the experiment.

1.3.8 Definition of OPTIKA optimal indicators according to their killing curves profiles

OPTIKA was performed as described in section 1.2.5 for the 36 pair-wise combinations previously studied by Cokol *et al*.

Figure 1.16 shows the interaction classification of the combinations tested according to the parameters previously described for every concentration (sub-MIC, MIC and over-MIC). Combinations showed different profile classifications depending on the parameter and the concentration chosen; this could be explained considering the dynamic profile of the drug interactions.

First, a certain degree of interaction could be reached at shorter times and reverted at longer times or vice-versa. This happened, for example, in clofazimine-pretomanid (CFZ-PTD) at 1x MIC and bedaquiline-ethambutol (BDQ-EMB) at 1x MIC.

Second, considering only one parameter, combinations could display different classifications depending on the concentration tested. For example, the slope of moxifloxacin-isoniazid (MOX-INH) combination showed different classifications at sub-MIC, MIC or over-MIC.

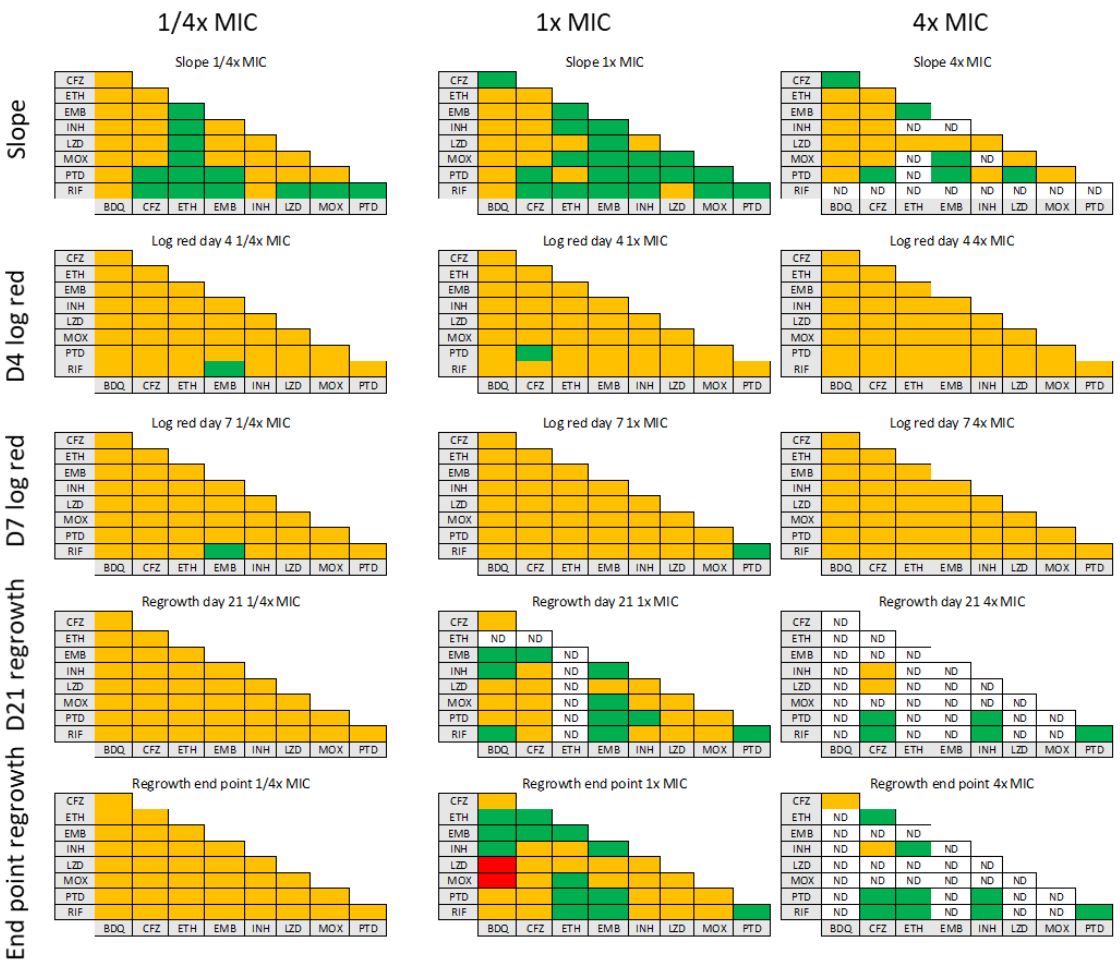

Figure 1.16. 36 pair-wise DiaMOND combinations assayed by OPTIKA. Each triangle represents the classification of the set of pair-wise combinations based on one OPTIKA parameter at one determined concentration. Left column: combinations assayed at 1/4x MIC. Middle column: combinations assayed at 1x MIC. Right column: combinations at 4x MIC. Rows represent different parameters, from top to bottom: slope at day 2, log reduction at day 4, log reduction at day 7, regrowth at day 21 and regrowth at day 49. Green: Favourable interaction. Yellow: No favourable Interaction. Red: Antagonism. ND: Not determined. Bedaquiline (BDQ), clofazimine (CFZ), ethambutol (EMB), ethionamide (ETH), isoniazid (INH), linezolid (LZD), moxifloxacin (MOX), pretomanid (PTD), rifampicin (RIF).

The combination of ethambutol with isoniazid was chosen as an example to explain in more detail this dynamic classification according to different parameters and drug concentrations (**Figure 1.17 A**).

1. At the sub-MIC concentration (**Figure 1.17 B**), the combination did not produce favourable interaction at any time point, and it was classified as no favourable interaction.

2. At the MIC concentration (**Figure 1.17 C**), ethambutol and isoniazid alone showed different killing rates, however both showed bacterial regrowth from days 7-14. This profile could be due to the development of resistant bacteria to isoniazid or ethambutol. The combination presented a strong initial favourable interaction, reaching a killing rate even faster than isoniazid at day two. This combination was classified as no favourable interaction using the log reduction parameter at day four and seven, because single drugs caused a strong reduction in the bacterial load and the remaining dynamic window was too little to allow for a two-log reduction by the combination. However, in contrast to the single drugs, the maximum killing effect was maintained until the last experimental time point, with bacterial load under the limit of detection, resulting in a favourable interaction. As the bedaquiline-isoniazid case shown in **Figure 1.15 D**, the combination of those two drugs could prevent the emergence of resistant *Mtb* bacteria.

3. Finally, the over-MIC concentration (**Figure 1.17 D**) was the least informative. Isoniazid showed the maximum detectable effect until day seven. Ethambutol showed a slower killing rate at initial days but reached the limit of detection at day four and maintained that killing level until the end point. The combination showed the maximum killing effect during the experiment. However, considering the asynchronous profiles of single drugs, it was not possible to discriminate whether the effect was caused by the combination or by the single drugs.

A

	EMB-INH OPTIKA Classification				
	Slope	Day 4 Log red	Day 7 Log red	Regrowth day 21	Regrowth end point
1/4x MIC					
1x MIC					
4xMIC	ND			ND	ND

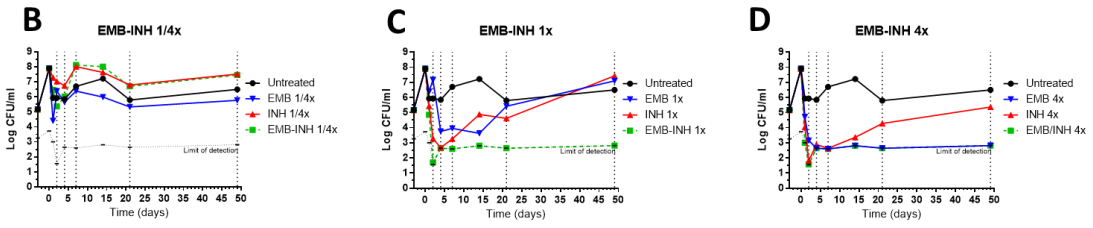

Figure 1.17. Detailed OPTIKA classification for ethambutol-isoniazid (EMB-INH) combination. **A:** Classification table. **B:** OPTIKA curves at sub-MIC concentration. **C:** OPTIKA curves at MIC concentration. **D:** OPTIKA curves at over-MIC concentration.

In summary, all indicators taken together permitted us to describe the curve profiling without a visual inspection of the killing curve plots. However, there was a need to establish a single parameter to classify the combinations. To overcome limitations of standard methods, long-term incubation was prioritized, being end point regrowth the

chosen parameter. To simplify, 1x MIC was the selected concentration to categorize the interactions, since it was the most informative concentration assayed for most of the combinations.

1.3.9 Study of 36 reference pair-wise combinations by OPTIKA and comparison with other methods

The interaction profile of the reference 36 pair-wise combinations by all methods described in this Chapter (*i.e.* CBA $FICI_{90}$, DiaMOND $FICI_{50}$, DiaMOND $FICI_{90}$, CBA FBCI, and OPTIKA) is summarised in **Table 1.6**.

All synergistic interactions detected by the CBA $FICI_{90}$, the standard method for drug combination evaluation, were classified as favourable by regrowth at the end point of the new OPTIKA method (bedaquiline-ethionamide, clofazimine-rifampicin, ethambutol-rifampicin, ethionamide-isoniazid, ethionamide-rifampicin and pretomanid-rifampicin). In addition to these six combinations, OPTIKA identified 12 favourable pair-wise combinations, being five of them (bedaquiline-ethambutol, bedaquiline-isoniazid, clofazimine-ethionamide, clofazimine-ethambutol and clofazimine-pretomanid) slow interactions with similar profile than the example described in **Figure 1.15 D,** only detectable by long term assays such as OPTIKA.

Slope was included in **Table 1.6** as the OPTIKA parameter that could be initially comparable to the FICI provided by CBA or DiaMOND, because it detected interactions at initial time points. However, the low correlation observed could indicate that it was not a good translational parameter.

Finally, two combinations were robustly classified as synergy by all methods studied here. The well-known favourable combination of rifampicin and ethambutol and the recently described [70] rifampicin plus pretomanid.

Combination	DiaMOND $FICI_{50}$ by Cokol *et al*	CBA $FICI_{90}$	DiaMOND $FICI_{50}$ in this work	DiaMOND $FICI_{90}$ in this work	CBA $FBCI_{99.9}$	OPTIKA slope day 2 1x MIC	OPTIKA regrowth end point 1x MIC	OPTIKA regrowth end point 4x MIC
BDQ-CFZ	Sy	NI	A	A	NI*	FI	NFI	NFI
BDQ-ETH	NI	Sy	NI	Sy	NI*	NFI	FI	ND
BDQ-EMB	A	NI	Sy	Sy	NI*	NFI	FI	ND
BDQ-INH	A	NI	A	A	NI*	NFI	FI	ND
BDQ-LZD	A	NI	A	A	NI*	NFI	A	ND
BDQ-MOX	A	NI	A	A	NI*	NFI	A	ND
BDQ-PTD	NI	NI	A	A	NI*	NFI	NFI	ND
BDQ-RIF	A	NI	A	A	Sy	NFI	NFI	ND
CFZ-ETH	Sy	NI	A	NI	NI*	NFI	FI	FI
CFZ-INH	Sy	NI	NI	Sy	Sy	NFI	NFI	NFI
CFZ-EMB	Sy	NI	A	Sy	NI*	NFI	FI	ND
CFZ-LZD	NI	NI	NI	Sy	NI*	NFI	NFI	ND
CFZ-RIF	Sy	Sy	Sy	Sy	NI*	FI	NFI	FI
CFZ-MOX	A	NI	NI	NI	NI*	NFI	NFI	ND
CFZ-PTD	NI	NI	A	A	NI*	FI	NFI	FI
EMB-PTD	Sy	NI	A	Sy	Sy	FI	FI	ND
EMB-ETH	A	NI	A	Sy	NI*	FI	FI	ND
EMB-RIF	Sy	Sy	Sy	Sy	Sy	FI	FI	ND
EMB-INH	A	NI	A	NI	NI	FI	FI	ND
EMB-LZD	A	NI	A	NI	NI*	FI	NFI	ND
EMB-MOX	A	NI	NI	Sy	NI	FI	NFI	ND
ETH-INH	NI	Sy	Sy	Sy	Sy	FI	NFI	FI
ETH-LZD	Sy	NI	NI	Sy	NI*	NFI	NFI	ND
ETH-MOX	A	NI	NI	Sy	NI*	FI	FI	ND
ETH-PTD	Sy	NI	A	NI	NI*	NFI	FI	FI
ETH-RIF	NI	Sy	Sy	Sy	Sy	FI	FI	FI
INH-LZD	NI	NI	A	NI	NI	NFI	NFI	ND
INH-MOX	A	NI	A	NI	NI	FI	NFI	ND
INH-PTD	NI	NI	A	Sy	NI*	FI	NFI	FI
INH-RIF	A	NI	NI	Sy	Sy	FI	NFI	FI
LZD-MOX	A	NI	A	A	NI*	FI	NFI	ND
LZD-PTD	A	NI	A	A	NI*	FI	NFI	ND
LZD-RIF	A	NI	A	NI	NI	NFI	NFI	ND
MOX-PTD	A	NI	NI	NI	NI*	FI	NFI	ND
MOX-RIF	A	NI	NI	A	NI*	FI	NFI	ND
PTD-RIF	Sy	Sy	Sy	Sy	Sy	FI	FI	FI

Table 1.6. Combination classification summary table. DiaMOND $FICI_{50}$ in Cokol *et al.*: $FICI_{50}$ reported in [70]. CBA $FICI_{90}$: $FICI_{90}$ by checkerboard assay. DiaMOND $FICI_{50}$ in this work: $FICI_{50}$ of our assay based on DiaMOND. CBA FBCI: $FBCI_{99.9}$ by checkerboard method. OPTIKA slope day 2: classification according to slope at day 2 for 1x MIC combinations. OPTIKA regrowth end point 1x MIC: classification according to regrowth at end point at 1x MIC. OPTIKA regrowth end point 4x MIC: classification according to regrowth at end point at 4x MIC. Sy: synergy (FICI or FBCI ≤ 0.5 for CBA. FICI < 0.85 for DiaMOND). A: antagonism (FICI or FBCI ≥4 for CBA. FICI > 1.1 for DiaMOND). NI: no interaction (FICI or FBCI values between synergy and antagonism). NI*: in those cases, $MBC_{99.9}$ was not reached by the combinations and FBCI values were calculated with 2x the maximum assay concentration used in the assay. FI: favourable interaction, NFI: no favourable interaction. ND: no determined. Bedaquiline (BDQ), clofazimine (CFZ), ethambutol (EMB), ethionamide (ETH), isoniazid (INH), linezolid (LZD), moxifloxacin (MOX), pretomanid (PTD), rifampicin (RIF).

1.3.10 OPTIKA applied to triple drug combinations

Ten triple drug combinations previously described by Cokol *et al.* [70] were assayed by OPTIKA.

Tested combinations were all possible triple combinations of five drugs (bedaquiline, clofazimine, isoniazid, pretomanid and rifampicin). Eight of them showed favourable interaction by OPTIKA according to regrowth at the end point parameter, at least in one of the three concentrations tested. In contrast, only two of them were classified as synergy by Cokol *et al.* (**Table 1.7**).

	Cokol *et al*	OPTIKA				
Combination	**Classification according to $FICI_{50}$**	**Slope day 2**	**Log Reduction day 4**	**Log Reduction day 7**	**Regrowth day 21**	**Regrowth end point**
INH-PTD-RIF 1/4x MIC	NI	NFI	NFI	NFI	NFI	NFI
INH-PTD-RIF 1x MIC		FI	NFI	NFI	FI	FI
INH-PTD-RIF 4x MIC		ND	NFI	NFI	FI	FI
BDQ-CFZ-INH 1/4x MIC	Sy	FI	NFI	NFI	NFI	NFI
BDQ-CFZ-INH 1x MIC		NFI	NFI	NFI	FI	FI
BDQ-CFZ-INH 4x MIC		NFI	NFI	NFI	ND	ND
BDQ-CFZ-PTD 1/4x MIC	NI	FI	NFI	NFI	NFI	NFI
BDQ-CFZ-PTD 1x MIC		FI	NFI	FI	FI	NFI
BDQ-CFZ-PTD 4x MIC		FI	NFI	NFI	ND	ND
BDQ-CFZ-RIF 1/4x MIC	Sy	FI	NFI	NFI	NFI	NFI
BDQ-CFZ-RIF 1x MIC		FI	NFI	FI	FI	NFI
BDQ-CFZ-RIF 4x MIC		ND	NFI	NFI	ND	ND
BDQ-INH-PTD 1/4x MIC	NI	ND	NFI	NFI	NFI	NFI
BDQ-INH-PTD 1x MIC		NFI	NFI	NFI	FI	FI
BDQ-INH-PTD 4x MIC		NFI	NFI	NFI	ND	ND
BDQ-INH-RIF 1/4x MIC	NI	FI	NFI	NFI	NFI	NFI
BDQ-INH-RIF 1x MIC		FI	NFI	NFI	FI	FI
BDQ-INH-RIF 4x MIC		ND	NFI	NFI	ND	ND
BDQ-PTD-RIF 1/4x MIC	NI	FI	NFI	NFI	NFI	NFI
BDQ-PTD-RIF 1x MIC		FI	NFI	FI	FI	FI
BDQ-PTD-RIF 4x MIC		ND	NFI	NFI	ND	ND
CFZ-INH-PTD 1/4x MIC	NI	NFI	NFI	NFI	NFI	NFI
CFZ-INH-PTD 1x MIC		FI	NFI	NFI	FI	NFI
CFZ-INH-PTD 4x MIC		NFI	NFI	NFI	FI	FI
CFZ-INH-RIF 1/4x MIC	NI	NFI	NFI	NFI	NFI	NFI
CFZ-INH-RIF 1x MIC		FI	NFI	NFI	FI	FI
CFZ-INH-RIF 4x MIC		ND	NFI	NFI	FI	FI
CFZ-PTD-RIF 1/4x MIC	NI	FI	NFI	NFI	NFI	NFI
CFZ-PTD-RIF 1x MIC		FI	NFI	FI	FI	NFI
CFZ-PTD-RIF 4x MIC		ND	NFI	NFI	FI	FI

Table 1.7. Classification of triple combinations. Cokol *et al*: data reported in [70]. Slope day 2: classification according to OPTIKA slope parameter. Log reduction days 4 and 7: classification according to OPTIKA log reduction parameter at days 4 and 7, respectively. Regrowth at day 21 and end point: classification according to OPTIKA regrowth parameter at days 21 and 49 respectively. NI: no interaction. Sy: synergy. FI: favourable interaction. NFI: no favourable interaction. ND: no determined. Bedaquiline (BDQ), clofazimine (CFZ), ethambutol (EMB), ethionamide (ETH), isoniazid (INH), linezolid (LZD), moxifloxacin (MOX), pretomanid (PTD), rifampicin (RIF).

The evaluation of triple-drug and their respective pair-wise combinations allowed us to determine the contribution of the pair-wise combinations. In the example shown in **Figure 1.18**, it was possible to understand the favourable triple combination that resulted from the mix of bedaquiline with isoniazid and rifampicin.

Analysing the curves of bedaquiline plus isoniazid, a positive drug interaction from day 14 was observed similar to the profile in the triple combination from day 14 to 49. As in the example of ethambutol-isoniazid shown above, this favourable outcome of the combination could be attributed to the prevention of isoniazid-resistant bacteria generation. Another explanation could be that the bacterial metabolism reduced by the effect of bedaquiline [101] could potentiate the bactericidal activity of isoniazid.

The addition of rifampicin to this slow pair-wise interaction caused a favourable faster interaction that produced the observed strong killing ability in the triple combination from day 1 to day 14. This first part of the curve matched with the corresponding part of the pair-wise combination formed by isoniazid plus rifampicin.

Finally, the combination of rifampicin with bedaquiline showed a positive but weaker interaction.

In summary, it could be deduced that rifampicin contributed positively at shorter time points, and bedaquiline with isoniazid contributed to the maintenance of the strong killing ability until day 49.

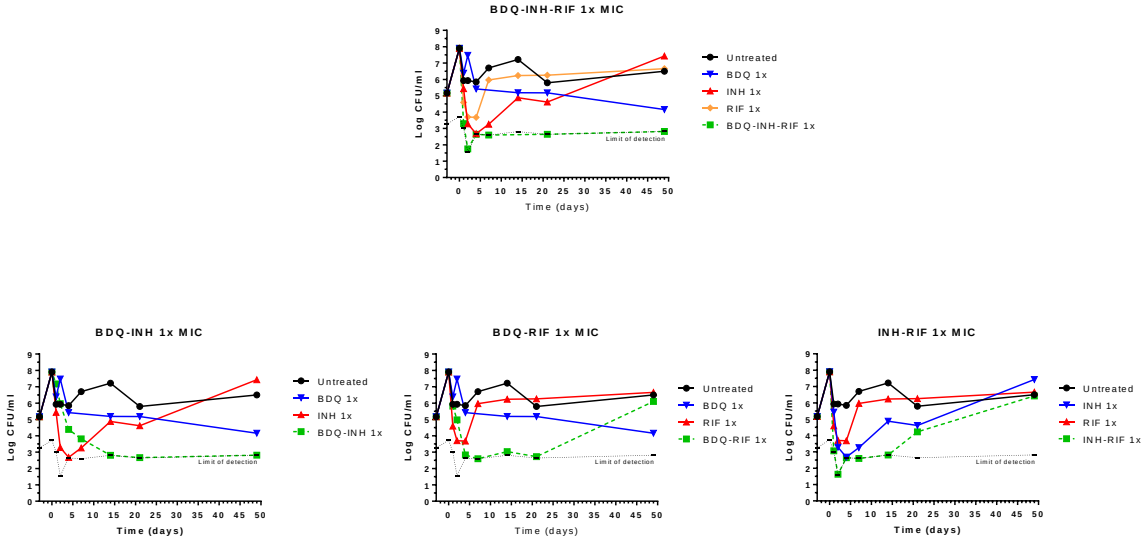

Figure 1.18. Example of deconvolution of BDQ-INH-RIF triple drug combination. Top: bedaquiline (BDQ) combined with isoniazid (INH) and rifampicin (RIF) resulted in a positive interaction at short and long times. Bottom left: BDQ combined with INH was favourable from day 14. Bottom centre: BDQ combined with rifampicin showed positive interaction from day 7 to day 21. Bottom right: INH combined with RIF showed a favourable profile until day 14.

1.4 General discussion

Recent years have seen a resurgence of new drug-like chemical entities with anti-mycobacterial activity, a number of which are progressing into clinical trials [67]. However, it is still unknown how to best combine these compounds into therapeutically effective multidrug regimens against TB.

Traditional efforts to identify new potential drug combinations involve empirical phenotypic screening for *in vitro* synergies at the microbiological level. This is typically done by checkerboard assays, which allows interrogation of 2-way drug interactions, but with limited power to identify 3-way or higher order drug interactions. A new technology called DiaMOND has overcome this limitation by reducing the number of experimental conditions that require testing, and vastly simplified the ability to identify favourable combinations of three, four or even a higher number of drugs [70].

Both CBA and DiaMOND are based on the calculation of the FICI, an index based on growth inhibition rather than bacterial killing, which remains unmeasured [82]. While CBA have typically relied on MIC (*i.e*. IC_{90}), DiaMOND uses IC_{50} to define the FICI. In this Chapter, we replicated the experiments described by Cokol *et al.* [70], where nine anti-TB drugs were combined in 36 pair-wise combinations. We found that the specific parameter used to describe *in vitro* drug interactions (*i.e.* IC_{50}, IC_{90} or MBC) influences the classification criteria of such drug combinations. Moreover, we found that the use of IC_{50} values as an indicator of drug interactions artificially enriched the classification of antagonistic combinations.

In addition, any synergistic combination identified by FICI-based readouts requires secondary validation by time kill assays that significantly, and in some cases prohibitively, increase the complexity and duration of combination testing [81]. TKA are the most valuable assay in static *in vitro* PK-PD studies and rely on CFU enumeration at different time points (instead of a fixed time point as in the case of CBA or DiaMOND). TKAs are also the basis of mathematical modelling of antimicrobial drug action [84]. However, their low throughput creates a barrier when it comes to validate triple or higher *n*-way interactions.

In this Chapter, we described the development of OPTIKA, an *in vitro* methodology that allows facile interrogation of *n*-way drug interactions. These measurements are dynamic and include direct measures of cidality. OPTIKA increased the capacity of traditional TKAs in more than 30-fold. It is based on the CARA assay [85, 86], which replaces the use of CFU by a resazurin-based fluorescence readout. We identified the critical parameters to define the degree of drug interaction by OPTIKA, being these (i) the slope of killing curve at day 2; (ii) the CFU log reduction at days 4 and

7, and (iii) bacterial regrowth (relapse) at days 21 and 50 (end point). The measurement of several interaction parameters at different time points extended to all drug exposure duration constitutes an indubitable added value of OPTIKA [98].

In-depth evaluation of different outputs from these parameters allowed us to prioritize regrowth at the end point as the most informative parameter to classify the interactions. Considering the long duration of OPTIKA and its roots in cell viability, favourable combinations at end point should be prioritized for further preclinical progression. Measurements around 50 days after drug exposure are not common in standard *in vitro* assays, partly due to thermal degradation of compounds at 37 °C in 7H9 media [102]. Although OPTIKA uses a static model, maintaining bacteria in the same culture medium, and drugs are only added at the beginning of the experiment, some combinations studied in this Chapter showed favourable drug interaction at the OPTIKA end point. Two hypotheses could explain this phenomenon: (i) drug combinations would be acting preventing the emergence of drug resistance to individual drugs, or (ii) the OPTIKA end point would be detecting post antibiotic effect (PAE) of drug combinations, as it was previously observed in other drug combinations against TB using traditional CFU based TKA [103]. In both scenarios, favourable drug combinations would produce irreversible damage to the bacteria in addition to the damage caused by single drugs, which definitely inhibited the bacterial viability. As described in Chapter 3 of this Thesis, transcriptomics is a valuable tool that could be applied to determine the mechanism of action of favourable drug interactions identified by OPTIKA at the end point.

OPTIKA is a TKA performed in a throughput manner based on fluorescence readouts. Similar to TKAs, it still presents some limitations:

First, experiments described here have been performed with a laboratory strain. Results from different strains including different lineages and clinical isolates that ensure genetically and drug susceptibility variability should be compared.

Second, all experiments described in this Chapter have been performed using standard *in vitro* growth conditions. However, the co-existence of *M. tuberculosis* sub-populations at distinct physiological states in patients with different drug susceptibility is the main reason for the need of a multidrug regimen against TB [104]. Before prioritizing favourable combinations identified by OPTIKA, this method should be adapted to different experimental *in vitro* conditions mimicking these microenvironments such as the carbon sources (*i.e*. glucose, cholesterol, fatty acids), low pH or metabolic states, using the non-replicating model [85], or the *M. tuberculosis* 18b strain [104].

Finally, PK-PD parameters such as the clinical achievable drug concentration or the drug penetration into the infected tissue have not been considered when developing OPTIKA. OPTIKA concentrations tested in this Chapter were selected based on the *in vitro* potency of individual drugs. Alternative parameters for choosing the concentrations for OPTIKA could be based on MBC instead of MIC readouts, or considering other PK-PD parameters such as plasma-free drug concentrations, as it is suggested in a recent study where several dose-response curve parameters have been evaluated as better indicators of favourable drug combinations when translating results from *in vitro* to *in vivo* [98, 105]. In addition, OPTIKA could be integrated with other *in vitro* models mimicking caseum environment [106, 107]. These models measure the drug concentration in necrotic granulomas and the acellular caseum. This could provide valuable insight to understand data generated by OPTIKA and to rationally propose effective new anti-TB regimens.

Regarding other potential applications, OPTIKA can robustly inform on the development of new anti-TB regimens. Most TB drug discovery programs are based on metrics of potency of static drug concentration assays such as the MIC values or the killing rate obtained from CFU based TKA. These approaches lack essential information such as the interaction of the drug, the microorganism, and the host. In addition, they are based on static MIC values and hardly reflect the continually changing drug concentrations to which the pathogen is actually exposed in *in vivo* systems [108]. In recent years, several translational approaches and tools have been developed and recognized as methods to efficiently progress anti-TB compounds [109, 110]. Translational PK-PD models are intended to reduce the high attrition rate of compounds when translating from *in vitro* assays into clinical stages [111, 112]. They identify the human dose that produces the exposure with a determined efficacy in an animal model. Their purpose is to define a relationship between dose and response to identify the optimal dosing to simulate alternate regimens. To successfully predict treatment outcomes, the dynamic concentration of drugs under study is a critical parameter. To simulate a desired PK profile, the Hollow Fiber System (HBS-TB) is a powerful tool [113]. This technology, which links *in vitro* data with simulation-based methods, has been recommended by the European Medicine Agency. Using repetitive sampling for drug concentrations and bacterial burden, the HFS-TB allows derivation of relationships among drug exposure, microbial kill rates, frequency of resistance, and exposure needed for resistance suppression for single drugs and drug combinations. Feeding from PK-PD data, the model can predict, through *in silico* modelling and simulation approaches, clinically relevant metrics (such as susceptibility breakpoints, target dosages, and optimal drug combinations) to understand, evaluate, and optimize performance of potential anti-TB regimens. However, HBS-TB presents a limited throughput. Drugs need to be thoroughly selected to optimize resources and efforts dedicated to these assays. According to the data presented in this Chapter, OPTIKA has demonstrated to be a valid

methodology to select starting combinations to be tested by the HFS-TB model, constituting a cell viability based-assay in contrast to standard growth inhibition-based assays.

1.5 Conclusions and future perspectives

In this Chapter, we developed OPTIKA, an *in vitro* methodology with capacity to robustly interrogate up to 550 conditions of drugs and drug combinations against *M. tuberculosis* in a single experiment. OPTIKA directly measures bacterial death and provides longitudinal kinetic data, revealing key aspects of the killing kinetics of the explored drug combinations, which fills the existing gap in the *in vitro* drug combination studies in the TB field. Favourable combinations identified with OPTIKA should be further profiled in other models to integrate pharmacokinetics and pharmacodynamics of compounds. Finally, the mechanism of action of the selected combinations could be further explored with other tools such as transcriptomics (as it has been done in Chapter 3 of this Thesis) or metabolomics.

Next steps in the optimization of OPTIKA are currently in progress. The work described in this Chapter has constituted the basis of a new project where this assay is being applied to evaluate drug interactions under different *in vitro* conditions such as glucose, cholesterol, fatty acids, low pH, non-replicating and different *Mtb* strains. Data from this project will be integrated in the ERA4TB consortium [30], the biggest European consortium focused on accelerating the development of new treatment regimens for tuberculosis, becoming an *in vitro* assay with high probabilities of being part of the current anti-TB drug discovery portfolio assays in the upcoming years.

1.6 APPENDIX I: Chapter 1 results summary table

Data for analyses done in sections 1.3.1, 1.3.2, 1.3.3 and 1.3.5

Plate #	Drug A	Drug B	Combination	Reference $MIC_{90}A$ (µM)	Experimental $MIC_{90}A$ (µM)	Max Conc A (µM)	Reference $MIC_{90}B$ (µM)	Experimental $MIC_{90}B$ (µM)	Max Conc B (µM)	DiaMOND $FICI_{50}$ in Cokol *et al*	DiaMOND $FICI_{50}$ in this work	DiaMOND $FICI_{90}$ in this work	CBA $FICI_{50}$	CBA $FICI_{90}$	$MBC_{99.9}$ A	$MBC_{99.9}$ B	CBA $FBCI_{99.9}$
1	BDQ	CFZ	BDQ-CFZ	0.11	0.06	0.22	0.31	0.62	0.62	0.50	1.77	1.29	1.50	1.50	> 0.22	> 0.62	2*
2	BDQ	ETH	BDQ-ETH	0.11	0.11	0.22	6.00	12.00	12.00	1.00	0.91	0.59	1.75	0.38	> 0.22	> 12.00	2*
3	BDQ	EMB	BDQ-EMB	0.11	0.11	0.22	12.50	12.50	25.00	1.20	0.51	0.38	0.75	0.63	> 0.22	> 25.00	2*
4	BDQ	INH	BDQ-INH	0.11	0.11	0.22	4.00	4.00	8.00	1.20	1.97	1.50	1.25	0.75	> 0.22	4.00	3*
5	BDQ	LZD	BDQ-LZD	0.11	0.11	0.22	1.50	1.50	3.00	1.40	1.83	1.83	1.50	1.00	> 0.22	> 3.00	2*
6	BDQ	MOX	BDQ-MOX	0.11	0.06	0.22	0.40	0.40	0.80	2.00	1.93	1.61	1.50	1.00	> 0.22	0.80	3*
7	BDQ	PTD	BDQ-PTD	0.11	0.11	0.22	0.50	1.00	1.00	1.00	1.27	1.26	1.00	1.00	> 0.22	> 1.00	2*
8	BDQ	RIF	BDQ-RIF	0.11	0.11	0.22	0.30	0.60	0.60	1.50	1.27	1.11	1.13	0.75	> 0.22	> 0.60	≤ 0.50
9	CFZ	ETH	CFZ-ETH	0.31	0.62	0.62	6.00	6.00	12.00	0.70	1.13	0.91	1.25	0.75	> 0.62	> 12.00	2*
10	CFZ	INH	CFZ-INH	0.31	0.62	0.62	4.00	4.00	8.00	0.30	0.97	0.71	1.25	0.63	> 0.62	8.00	≤ 0.50
11	CFZ	EMB	CFZ-EMB	0.31	0.62	0.62	12.50	12.50	25.00	0.70	1.69	0.83	1.06	1.00	> 0.62	> 25.00	2*
12	CFZ	LZD	CFZ-LZD	0.31	0.62	0.62	1.50	1.50	3.00	1.00	0.97	0.81	1.00	0.63	> 0.62	> 3.00	2*
13	CFZ	RIF	CFZ-RIF	0.31	0.62	0.62	0.30	0.60	0.60	0.80	0.79	0.39	0.75	0.38	> 0.62	> 0.60	2*
14	CFZ	MOX	CFZ-MOX	0.31	0.62	0.62	0.40	0.40	0.80	1.60	1.07	0.95	1.13	0.75	> 0.62	> 0.80	2*
15	CFZ	PTD	CFZ-PTD	0.31	0.62	0.62	0.50	1.00	1.00	1.10	2.14	2.63	1.50	1.02	> 0.62	> 1.00	2*
16	EMB	PTD	EMB-PTD	12.50	12.50	25.00	0.50	1.00	1.00	0.80	1.37	0.75	0.75	0.75	> 25.00	> 1.00	≤ 0.50
17	EMB	ETH	EMB-ETH	12.50	12.50	25.00	6.00	6.00	12.00	1.20	1.77	0.58	1.06	0.75	> 25.00	> 12.00	2*
18	EMB	RIF	EMB-RIF	12.50	12.50	25.00	0.30	0.60	0.60	0.70	0.33	0.22	0.31	0.27	> 25.00	> 0.60	≤ 0.25
19	EMB	INH	EMB-INH	12.50	12.50	25.00	4.00	4.00	8.00	1.60	2.03	0.92	1.13	0.75	> 25.00	8.00	≤ 0.75
20	EMB	LZD	EMB-LZD	12.50	12.50	25.00	1.50	1.50	3.00	1.30	2.23	1.01	1.50	1.00	> 25.00	> 3.00	2*
21	EMB	MOX	EMB-MOX	12.50	12.50	25.00	0.80	0.40	0.40	1.30	1.09	0.54	1.00	0.75	> 12.50	> 0.40	3*
22	ETH	INH	ETH-INH	6.00	6.00	12.00	4.00	4.00	8.00	1.00	0.71	0.55	0.63	0.38	> 12.00	> 8.00	≤ 0.25
23	ETH	LZD	ETH-LZD	6.00	6.00	12.00	1.50	1.50	3.00	0.80	0.98	0.73	1.13	1.00	> 12.00	> 3.00	2*
24	ETH	MOX	ETH-MOX	6.00	6.00	12.00	0.40	0.40	0.80	1.50	1.03	0.58	0.75	0.75	> 12.00	> 0.80	1.5
25	ETH	PTD	ETH-PTD	6.00	6.00	12.00	0.50	1.00	1.00	0.80	1.20	0.85	0.75	0.75	> 12.00	> 1.00	2*
26	ETH	RIF	ETH-RIF	6.00	6.00	12.00	0.30	0.60	0.60	1.00	0.50	0.40	0.50	0.27	> 12.00	> 0.60	≤ 0.13
27	INH	LZD	INH-LZD	4.00	4.00	8.00	1.50	1.50	3.00	1.00	1.41	0.98	1.25	1.00	4.00	> 3.00	≤ 1
28	INH	MOX	INH-MOX	4.00	4.00	8.00	0.40	0.40	0.80	1.60	1.56	1.04	1.03	1.00	4.00	> 0.80	≤ 0.8
29	INH	PTD	INH-PTD	4.00	4.00	8.00	0.50	1.00	1.00	1.10	1.17	0.72	1.00	0.75	> 8.00	> 1.00	2*
30	INH	RIF	INH-RIF	4.00	4.00	8.00	0.30	0.60	0.60	1.30	0.96	0.53	1.06	0.52	4.00	> 0.60	≤ 0.50
31	LZD	MOX	LZD-MOX	1.50	1.50	3.00	0.40	0.40	0.80	1.20	1.76	1.12	1.25	1.00	> 3.00	> 0.80	2*
32	LZD	PTD	LZD-PTD	1.50	1.50	3.00	0.50	1.00	1.70	1.70	2.19	1.49	1.02	1.02	> 3.00	> 1.00	2*
33	LZD	RIF	LZD-RIF	1.50	1.50	3.00	0.30	0.60	0.60	1.30	1.11	0.94	0.75	0.75	1.50	> 0.60	≤ 0.60
34	MOX	PTD	MOX-PTD	0.40	0.40	0.80	1.00	1.00	1.00	1.40	1.07	0.89	1.00	1.00	0.40	> 1.00	3*
35	MOX	RIF	MOX-RIF	0.40	0.40	0.80	0.30	0.60	0.60	1.60	0.98	1.39	1.00	1.00	0.80	> 0.60	3*
36	PTD	RIF	PTD-RIF	0.50	1.00	1.00	0.30	0.60	0.60	0.60	0.63	0.56	0.59	0.31	1.00	0.60	≤ 0.50

Drugs: Bedaquiline(BDQ), Clofazimine(CFZ), Ethionamide(EHT), Ethambutol (EMB), Isoniazid (INH), Linezolid (LZD),Moxifloxacin (MOX), Pretomanid (PTD) & Rifampicin (RIF). Reference MIC_{90}: MIC_{90} determined before drug combinations assay (MIC_{Ref}). Experimental MIC: MIC_{90} value of this experiment (MIC_{Exp}). DiaMOND $FICI_{50}$ in Cokol *et al.* : Data reported in DOI: 10.1126/sciadv.1701881 (REF 70). DiaMOND $FICI_{50}$ in this work: $FICI_{50}$ from this work by DiaMOND. DiaMOND $FICI_{90}$ in this work: $FICI_{90}$ from this work by DiaMOND. CBA $FICI_{50}$: $FICI_{50}$ from this work by CBA. CBA $FICI_{90}$: $FICI_{90}$ from this work by CBA. $MBC_{99.9}$: Minimal Bactericidal Concentration. CBA $FBCI_{99.9}$: Factorial Bactericidal Concentration Index, calculated from checkerboard. Modulator (> or ≤) $MBC_{99.9}$ is bigger than the highest concentration assayed. For calculations, 2x highest concentration is used. Red: Manually curated from normalized data. 2*: $MBC_{99.9}A$, $MBC_{99.9}B$ and $FBCI_{99.9}$ were no determined. 3*: $MBC_{99.9}A$ or $MBC_{99.9}B$ and FBCI were no determined.

1.7 APPENDIX II: Chapter 1 Killing curves supplementary tables

Supplementary table 1.1. Mean log CFU/ml ± SD of data plotted in **Figure 1.14**, OPTIKA assay.

	Mean Log CFU/ml ± SD								
Sample	**Day -3**	**Day 0**	**Day 1**	**Day 2**	**Day 4**	**Day 7**	**Day 14**	**Day 21**	**Day 58**
Untreated	4.08 ± 0.68	5.35 ± 0.87	7.13 ± 3.03	6.08 ± 1.01	7.44 ± 1.04	7.28 ± 0.53	7.22 ± 0.52	6.31 ± 0.88	6.39 ± 0.95
BDQ 1/4x	NA	NA	7.07 ± 0.26	6.97 ± 0.87	7.94 ± 0.70	7.29 ± 0.24	8.16 ± 0.81	6.58 ± 0.31	7.34 ± 0.57
BDQ-CFZ 1/4x	NA	NA	5.81 ± 0.49	6.30 ± 0.30	6.95 ± 0.23	6.73 ± 0.45	8.21 ± 0.64	6.57 ± 0.70	7.28 ± 0.21
CFZ 1/4x	NA	NA	5.59 ± 1.86	5.33 ± 0.76	7.32 ± 0.94	7.76 ± 0.67	7.26 ± 0.31	5.42 ± 0.34	6.75 ± 0.95
CFZ-INH 1/4x	NA	NA	6.15 ± 0.58	6.90 ± 0.60	7.46 ± 0.60	7.46 ± 0.32	7.96 ± 0.46	6.72 ± 0.40	6.78 ± 0.63
CFZ-RIF 1/4x	NA	NA	5.51 ± 1.88	6.14 ± 0.34	6.57 ± 0.41	6.36 ± 0.43	7.80 ± 0.32	6.14 ± 0.40	6.32 ± 0.90
EMB 1/4x	NA	NA	7.34 ± 3.11	7.06 ± 0.83	7.51 ± 0.68	6.87 ± 0.41	8.27 ± 0.68	8.21 ± 1.15	7.24 ± 0.68
INH 1/4x	NA	NA	6.41 ± 1.94	5.91 ± 0.79	8.32 ± 0.89	7.69 ± 0.57	7.26 ± 1.25	5.47 ± 0.65	6.73 ± 0.63
INH-PTD 1/4x	NA	NA	6.60 ± 0.24	6.55 ± 0.44	6.51 ± 0.48	6.71 ± 0.56	7.68 ± 0.49	6.86 ± 0.86	6.93 ± 0.39
PTD 1/4x	NA	NA	7.28 ± 0.33	7.20 ± 0.34	7.12 ± 0.51	7.17 ± 0.82	7.91 ± 0.35	7.15 ± 0.94	7.54 ± 0.58
PTD-RIF 1/4x	NA	NA	5.77 ± 0.81	3.46 ± 0.67	4.07 ± 0.24	3.24 ± 0.79	4.19 ± 1.23	3.87 ± 1.18	6.54 ± 0.56
RIF 1/4x	NA	NA	6.49 ± 0.90	6.08 ± 0.54	6.81 ± 1.00	6.15 ± 0.65	7.58 ± 0.56	7.34 ± 0.39	5.91 ± 0.41
RIF 1/6x	NA	NA	4.70 ± 0.97	5.90 ± 0.61	6.35 ± 0.58	6.03 ± 0.49	6.84 ± 0.26	7.07 ± 0.98	6.64 ± 0.61
RIF 4x	NA	NA	2.91 ± 0.21	2.13 ± 0.05	2.25 ± 0.07	2.00 ± 0.04	2.07 ± 0.02	2.70 ± 0.00	6.05 ± 0.89
RIF-EMB 1/4x	NA	NA	4.58 ± 2.04	2.34 ± 0.18	2.39 ± 0.10	2.03 ± 0.07	2.14 ± 0.01	2.70 ± 0.00	5.77 ± 0.73

Bedaquiline (BDQ), clofazimine (CFZ), ethambutol (EMB), isoniazid (INH), pretomanid (PTD), rifampicin (RIF). NA: not applicable.

Supplementary table 1.2. Mean log CFU/ml ± SD of data plotted in **Figure 1.14**, CFU counts assay.

	Mean Log CFU/ml ± SD								
Time (days)	**Day -3**	**Day 0**	**Day 1**	**Day 2**	**Day 4**	**Day 7**	**Day 14**	**Day 22**	**Day 58**
Untreated	3.82 ± 0.07	4.63 ± 0.06	4.7 ± 0.01	4.7 ± 0.13	5.1 ± 0.07	5.7 ± 0.11	6.5 ± 0.04	6.8 ± 0.11	6.8 ± 0.07
BDQ 1/4x	NA	NA	4.6 ± 0.00	4.6 ± 0.04	5.2 ± 0.02	5.6 ± 0.09	6.4 ± 0.03	6.6 ± 0.09	NA
CFZ 1/4x	NA	NA	4.6 ± 0.01	5.1 ± 0.03	5.4 ± 0.04	5.5 ± 0.12	6.0 ± 0.15	6.6 ± 0.12	NA
CFZ-BDQ 1/4x	NA	NA	4.8 ± 0.02	4.9 ± 0.01	5.0 ± 0.07	5.6 ± 0.12	5.9 ± 0.11	6.5 ± 0.12	NA
CFZ-INH 1/4x	NA	NA	4.9 ± 0.06	4.9 ± 0.03	4.9 ± 0.00	5.5 ± 0.10	6.4 ± 0.01	6.5 ± 0.10	NA
CFZ-RIF 1/4x	NA	NA	4.5 ± 0.23	4.9*	4.9 ± 0.00	4.8 ± 0.04	5.6 ± 0.01	6.1 ± 0.04	NA
EMB 1/4x	NA	NA	4.6 ± 0.02	5.3 ± 0.19	5.6 ± 0.17	5.4 ± 0.04	5.9 ± 0.01	6.7 ± 0.04	NA
INH 1/4x	NA	NA	4.7 ± 0.10	4.8 ± 0.08	5.0 ± 0.01	5.3 ± 0.11	5.9 ± 0.08	5.9 ± 0.11	NA
INH-PTD 1/4x	NA	NA	4.8 ± 0.09	4.9 ± 0.02	5.8 ± 0.03	5.8 ± 0.00	6.6 ± 0.12	6.3 ± 0.00	NA
PTD 1/4x	NA	NA	4.8 ± 0.09	5.1 ± 0.00	5.2 ± 0.04	5.3 ± 0.05	5.9 ± 0.03	6.7 ± 0.05	NA
PTD-RIF 1/4x	NA	NA	4.7 ± 0.08	4.7 ± 0.04	4.8 ± 0.01	4.4 ± 0.09	4.7 ± 0.02	5.5 ± 0.09	NA
RIF 1/4x	NA	NA	4.8 ± 0.05	4.8 ± 0.10	5.3 ± 0.06	5.6 ± 0.19	6.0 ± 0.07	6.7 ± 0.19	NA
RIF 1/6x	NA	NA	4.4 ± 0.07	5.2 ± 0.23	4.9 ± 0.03	5.5 ± 0.16	6.2 ± 0.00	6.2 ± 0.16	NA
RIF 4x	NA	NA	3.9 ± 0.10	3.5 ± 0.01	3.4 ± 0.03	2.8 ± 0.00	5.3 ± 0.04	3.7 ± 0.00	6.8 ± 0.04
RIF-EMB 1/4x	NA	NA	4.7 ± 0.01	4.4 ± 0.02	4.2 ± 0.17	3.7 ± 0.02	2.0 ± 0.00	4.4 ± 0.02	6.8 ± 0.06

Bedaquiline (BDQ), clofazimine (CFZ), ethambutol (EMB), isoniazid (INH), pretomanid (PTD), rifampicin (RIF). NA: not applicable *:Data from one replicate.

Supplementary table 1.3. Mean log CFU/ml ± SD of data plotted in **Figures 1.15 to 1.18.**

	Mean Log CFU/ml ± SD								
Sample	**Day -3**	**Day 0**	**Day 1**	**Day 2**	**Day 4**	**Day 7**	**Day 14**	**Day 21**	**Day 49**
Untreated	5.17 ± 0.46	7.90 ± 1.01	5.93 ± 1.55	5.93 ± 0.71	5.85 ± 0.80	6.70 ± 0.77	7.22 ± 0.65	5.80 ± 0.44	6.50 ± 0.60
BDQ 1X	NA	NA	6.38 ± 1.21	7.47 ± 0.57	5.42 ± 1.08	-	5.19 ± 2.86	5.18 ± 1.71	4.16 ± 0.83
BDQ-INH 1X	NA	NA	7.17 ± 0.71	5.97 ± 0.69	4.40 ± 0.15	3.81 ± 0.95	2.81 ± 0.00	2.67 ± 0.03	2.82 ± 0.00
BDQ-INH-RIF 1x	NA	NA	3.30 ± 0.20	1.75 ± 0.16	2.64 ± 0.00	2.60 ± 0.00	-	2.64 ± 0.00	2.82 ± 0.00
BDQ-RIF 1X	NA	NA	5.82 ± 0.42	4.98 ± 1.02	2.83 ± 0.15	2.60 ± 0.00	3.03 ± 0.26	2.73 ± 0.07	6.10 ± 2.45
EMB 1/4X	NA	NA	4.41 ± 0.28	6.38 ± 1.36	5.65 ± 0.40	6.39 ± 2.69	5.99 ± 2.29	5.33 ± 0.33	5.77 ± 0.38
EMB 1X	NA	NA	6.38 ± 1.14	7.17 ± 0.48	3.75 ± 1.08	3.95 ± 1.96	3.63 ± 1.63	5.42 ± 0.77	7.10 ± 0.46
EMB 4X	NA	NA	4.72 ± 1.31	3.15 ± 1.30	2.64 ± 0.00	2.60 ± 0.00	2.81 ± 0.00	2.64 ± 0.00	2.82 ± 0.00
EMB-INH 1/4x	NA	NA	6.46 ± 0.90	5.37 ± 0.92	6.02 ± 1.35	8.12 ± 0.79	8.02 ± 0.35	6.70 ± 0.59	7.46 ± 0.49
EMB-INH 1x	NA	NA	4.86 ± 0.31	1.70 ± 0.24	2.64 ± 0.00	2.60 ± 0.00	2.81 ± 0.00	2.64 ± 0.00	2.82 ± 0.00
EMB-INH 4x	NA	NA	3.00 ± 0.00	1.58 ± 0.03	2.64 ± 0.00	2.60 ± 0.00	2.81 ± 0.00	2.64 ± 0.00	2.82 ± 0.00
EMB-RIF 1x	NA	NA	3.02 ± 0.03	1.63 ± 0.08	2.64 ± 0.00	2.60 ± 0.00	2.81 ± 0.00	2.64 ± 0.00	2.82 ± 0.00
INH 1/4X	NA	NA	7.28 ± 0.60	7.03 ± 0.66	6.75 ± 0.96	8.01 ± 1.00	7.63 ± 0.26	6.79 ± 0.44	7.52 ± 0.47
INH 1X	NA	NA	5.44 ± 0.69	3.28 ± 0.83	2.68 ± 0.05	3.26 ± 1.32	4.88 ± 2.77	4.62 ± 2.29	7.43 ± 0.80
INH 4X	NA	NA	4.04 ± 0.86	1.82 ± 0.12	2.88 ± 0.48	2.64 ± 0.08	3.37 ± 1.12	4.28 ± 1.30	5.37 ± 1.71
INH-RIF 1x	NA	NA	3.06 ± 0.11	1.63 ± 0.04	2.64 ± 0.00	2.60 ± 0.00	2.81 ± 0.00	4.23 ± 1.70	6.42 ± 0.84
INH-RIF 4x	NA	NA	3.00 ± 0.00	1.63 ± 0.04	2.64 ± 0.00	2.60 ± 0.00	2.81 ± 0.00	2.64 ± 0.00	2.82 ± 0.00
RIF 1X	NA	NA	4.60 ± 0.53	3.70 ± 1.01	3.68 ± 0.88	5.97 ± 2.39	6.24 ± 2.29	6.26 ± 0.86	6.66 ± 1.92
RIF 4X	NA	NA	3.00 ± 0.00	1.63 ± 0.01	2.64 ± 0.00	2.60 ± 0.00	2.81 ± 0.00	3.01 ± 0.45	5.46 ± 1.35

Bedaquiline (BDQ), clofazimine (CFZ), ethambutol (EMB), isoniazid (INH), pretomanid (PTD), rifampicin (RIF). NA: not applicable -: Missing experimental data.

Chapter 2

In vitro identification and characterization of β-lactam synergistic partners against *Mycobacterium tuberculosis*

2.1 Introduction

In 1929, Alexander Fleming accidentally found that a strain of the mould *Penicillium* produced an antibacterial agent which he named penicillin [114]. This was the first observation of the antibacterial properties of β-lactams. He rapidly confirmed that it was not toxic if administered to mice and rabbits and it was used as an antiseptic for topical application. However, its antibacterial properties were not fully demonstrated until 1940, when it was observed that injected penicillin was effective to treat a lethal streptococcal infection in mice. The preparation of a stable form of penicillin along with a large-scale production occurred during World War II. Penicillin was active against a broad spectrum of infections, including those commonly found in military medicine. Before the 20th century, many soldiers died from bacterial infections after being wounded in action. The development and production of penicillin during World War II greatly reduced combatants´ mortality from infected wounds and its use prevented widespread venereal disease epidemics in the post-war era, playing a critical role in the early post-war recovery. In addition, penicillin was the first antibiotic produced in an industrially manner. The pioneering techniques developed for large-scale penicillin production, including fermentation, production and purification steps constituted the basis of modern bioreactors [115].

Penicillin is regarded as the initiator of the era of the antibiotics for many reasons: (i) it was the first successful chemotherapeutic agent produced by microbes, (ii) it is not destroyed in the body, and (iii) it is well tolerated by humans. In addition, newer antibiotics were discovered and produced using medicinal science and production methods created for the development of penicillin [116].

In 1940, the chemical structure of penicillin was determined. This molecule contains a highly reactive 3-carbon and 1-nitrogen ring (β-lactam ring) that gives its name to a large family of antibiotics, the β-lactams. This family includes several sub-families based on the number of atoms in the central nucleus and their substituents [115-118] (**Figure 2.1**):

1. Penicillins. Constituted by a nucleus of 6-aminopenicillanic acid and other chains in the ringside. Penicillin G was the first clinically used penicillin. It was approved in 1946 and it was mainly used to treat streptococcal and staphylococcal infections. However, the selection of penicillin-resistant staphylococci strains producing penicillinase, an enzyme that inactivates the β-lactam ring of penicillin, prompted the development of new less susceptible penicillins to the staphylococcal penicillinase, the semi-synthetic penicillins.

2. Cephalosporins. Containing a 7-aminocephalosporanic acid nucleus, and a side chain formed of 3,6-dihydro-2H-1,3-thiazane rings. Cephalosporin C, the first member of the now named cephalosporins, was discovered in 1953 and its stability to penicillin β-lactamase was found as an attractive property [119]. Many other cephalosporins were developed in the following years, being classified in classes or generations sequentially named according to their improved activity against gram-negative bacteria. The semi-synthetic cephalosporins constituted the most important group of antibiotics at that time.

3. Carbapenems. Similar to the penicillins, they contain an unsaturated five-membered ring containing a carbon atom instead of sulphur fused to the β-lactam ring. Carbapenems were discovered in the mid-1970s, being their stability to most of β-lactamases and their broad-spectrum potency remarkable properties. As it happened for other β-lactam classes, derivative compounds with improved potency and chemical stability were rapidly developed.

4. Monobactams [120]: here, the β-lactam ring is not fused to another ring. They were created by chemical synthesis and divided onto several classes depending on the substituents, which also determine their chemical reactivity.

5. β-lactamase inhibitors [121, 122]. Most of them contain the β-lactam ring in their structure. In the 1970s, some β-lactamase inhibitors were produced, such as clavulanic acid or sulbactam. Others such as tazobactam or avibactam are newer and others are currently being developed [122-124]. β-lactamase inhibitors display little antibiotic activity but are exceptional inhibitors of β-lactamases. They are co-administered with other β-lactams susceptible to β-lactamases.

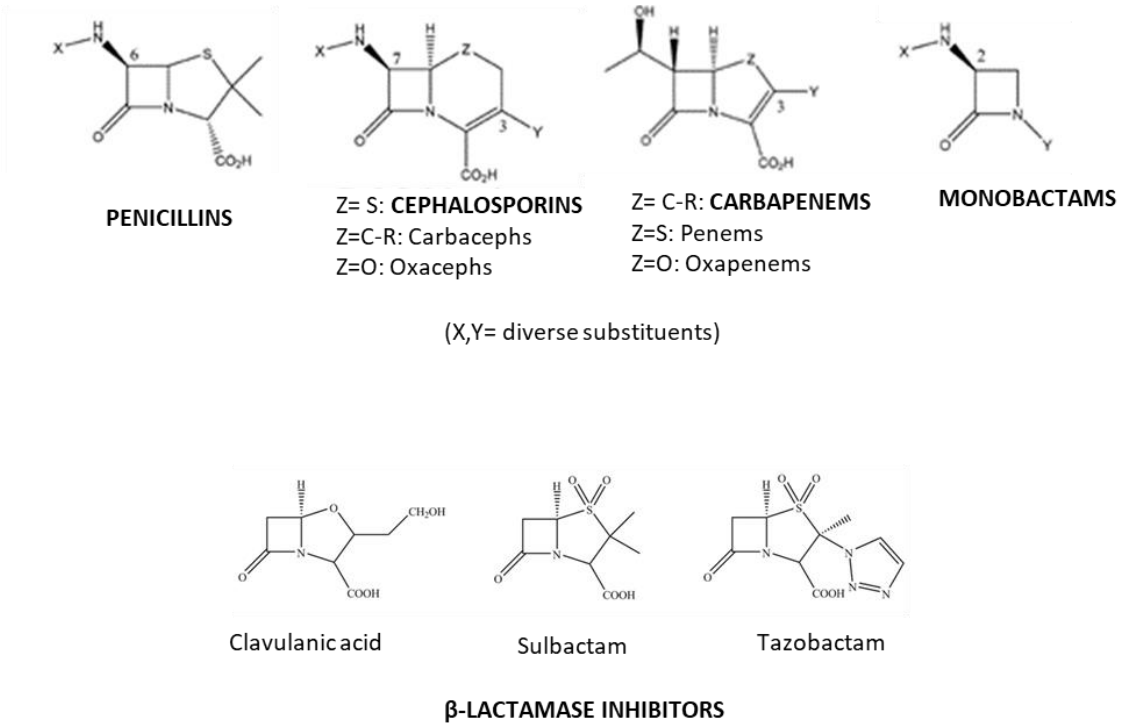

Figure 2.1 β-lactam subfamilies. Adapted from[118] and [122].

The mechanism of action of the β-lactams is inhibition of the cell wall formation by blocking peptidoglycan synthesis. The peptidoglycan is a polymer present in all type of bacteria. It forms a layer outside the cell membrane constituting the cell wall. The core structure of the peptidoglycan is shared across bacteria; it is formed by disaccharide strands (glycan) linked by short peptides. Cross-linking of the glycan strands and whether this peptidoglycan layer is localized within the cell wall varies across different type of bacteria [125, 126] (**Figure 2.2**).

- Gram-negative bacteria: the peptidoglycan is a thin structure comprised by one or two layers and it is located between the two cell membranes.

- Gram-positive bacteria: a multilayer exoskeleton above the cell membrane.

- Mycobacteria: they possess the most complex cell envelope formed by mycolic acids, arabinogalactan and peptidoglycan, which represent a giant macromolecule encasing the mycobacterial cell. Their peptidoglycan is formed by several layers covalently bound to the arabinogalactan, in turn bound to long-chain mycolic acids.

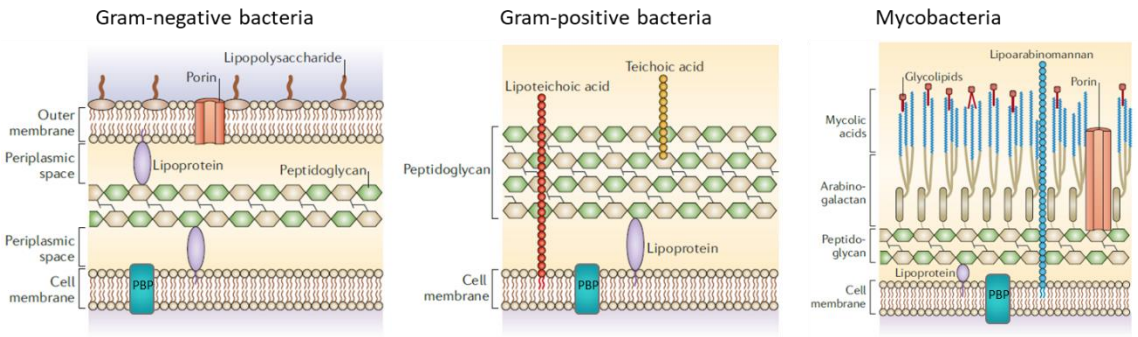

Figure 2.2. Cell wall structure of gram-negative bacteria, gram-positive bacteria, and mycobacteria. Adapted from [126].

The peptidoglycan is an essential molecule for bacterial survival, it provides a protective function by acting as a barrier against physical, chemical, and biological threats. In addition, it constitutes a scaffold for anchoring other cell envelope constituents, and confers cell shape and architecture [127]. The peptidoglycan is a very dynamic cell component that is constantly under remodelling in response to environmental changes or bacterial needs. These processes are very complex and are highly regulated by multiple and very specific interactions of cellular components [128, 129]. A major group of enzymes involved in the synthesis and remodelling of the peptidoglycan layer are the Penicillin Binding Proteins (PBPs). All bacteria possess their own family of PBPs, some of them are essential, but some others are not. PBPs are classified according to their molecular mass and catalytic function and their name reflects that they possess a great affinity for penicillin [130]. PBPs catalyse the final steps of peptidoglycan synthesis *i.e.* the cross-linking of glycan chains by short peptide bridges. There are several types of PBPs: (i) the most common D,D-transpeptidases (DDTs) responsible of the 4→3 cross-links and, (ii) L,D-transpeptidases (LDTs), specially important in mycobacteria and responsible of the 3→3 peptidoglycan cross-links [131] (for more information on LDTs, see Chapter 3 **Figure 3.3**).

Figure 2.3 shows a schema of the formation of a 4 → 3 cross-link catalysed by a PBP. There, a PBP nucleophilic serine residue attacks a pentapeptide on the donor strand, forming a peptide and releasing D-alanine. From the acceptor strand of the peptidoglycan, a second nucleophilic reaction occurs, in this example the L-lysine residue reacts with the enzyme complex, forming a cross-link and releasing the PBP enzyme.

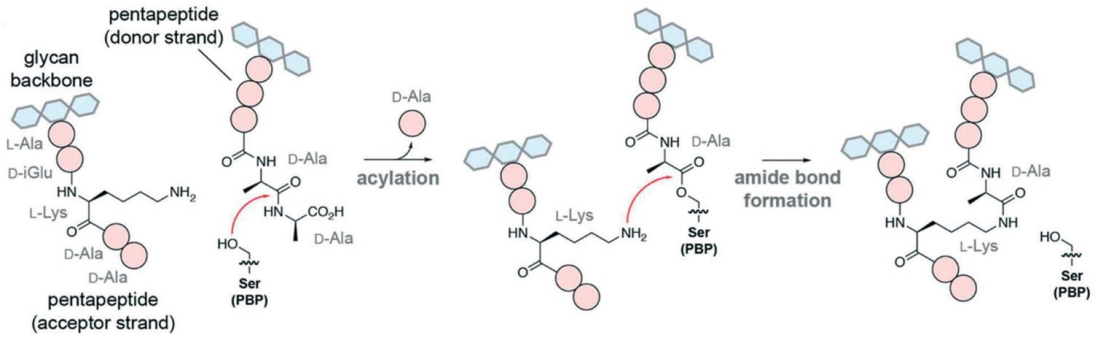

Figure 2.3. Mechanism of action of the PBP transpeptidase activity in the 4→3 peptidoglycan cross-link formation. From [131].

The β-lactam ring of penicillin (or other members of the β-lactam family) mimics the structure of the terminal D-Ala-D-Ala dipeptide in the nascent peptidoglycan of the dividing bacteria The nucleophilic serine residue of the PBP enzyme attacks the antibiotic β-lactam ring. The covalent PBP-β-lactam complexes are stable and produces a loss of PBP activity and, therefore, cell lysis (**Figure 2.4**) [131-133]. The fact that different PBPs are differentially inhibited by several β-lactams shows that this interaction is quite specific [117].

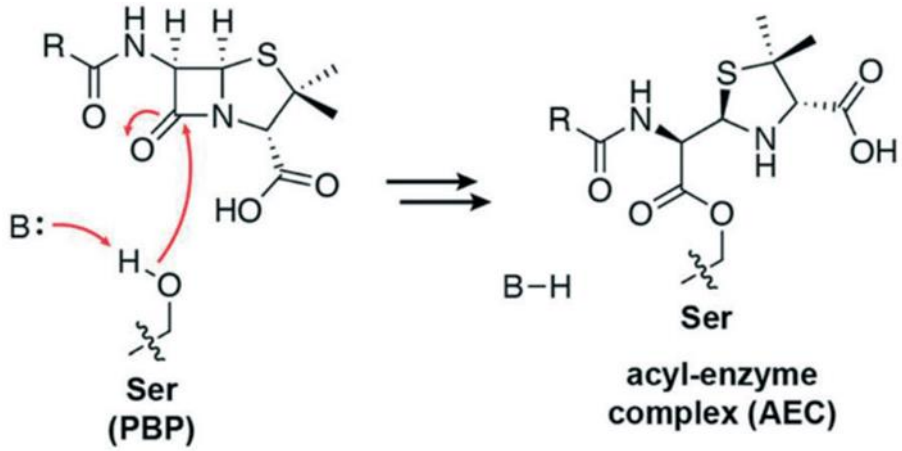

Figure 2.4. Scheme of the acylation of the transpeptidase serine with a penicillin antibiotic. From [131].

β-lactams is therefore one of the oldest and most successful family of antibiotics. They are a very diverse group of molecules well validated in medical practice with known PK-PD properties and possess great efficacy against a wide spectrum of gram-positive and gram-negative bacteria.

However, bacteria have acquired resistance to β-lactams through several mechanisms. Gram-negative bacteria produce enzymes that hydrolytically destroy the β-lactam, whereas the main mechanism of resistance of gram-positive bacteria is target modification. This consists on introducing structural changes in the enzymes that are targeted by the β-lactam, which makes these enzymes less reactive to these drugs [134].

In the context of TB, the situation is different. Historically, early β-lactams showed little activity against TB. This was erroneously attributed to the low permeability of the mycobacterial cell wall. Later, it was described that both low permeability of the cell wall and the presence of a highly active genetically encoded β-lactamase (BlaC) that inactivates β-lactams were the reason for their poor activity [135]. Different resistance mechanisms have been described for other bacteria and could be considered as well for mycobacteria [136] (**Figure 2.5**):

1. Changes in the population of porins or the characteristics of the outer membrane would increase the diffusion of β-lactams from the outside of the cell to the cytoplasm, decreasing the effective concentration of these drugs in their general site of action, *i.e.* the periplasm or cell wall zone.

2. β-lactams can be exported outside bacteria by multidrug efflux pumps, which reduce the effective β-lactam concentration.

3. The production of β-lactamases that degrades β-lactams is another effective mechanism to reduce the β-lactam activity.

4. Target site modification by introducing mutations in the PBPs would produce less affinity of β-lactams with their targets thus reducing its activity.

5. The number of PBPs could be modified in response to the presence of β-lactams. PBPs with low β-lactam affinity would be expressed as a mechanism of evasion to β-lactams.

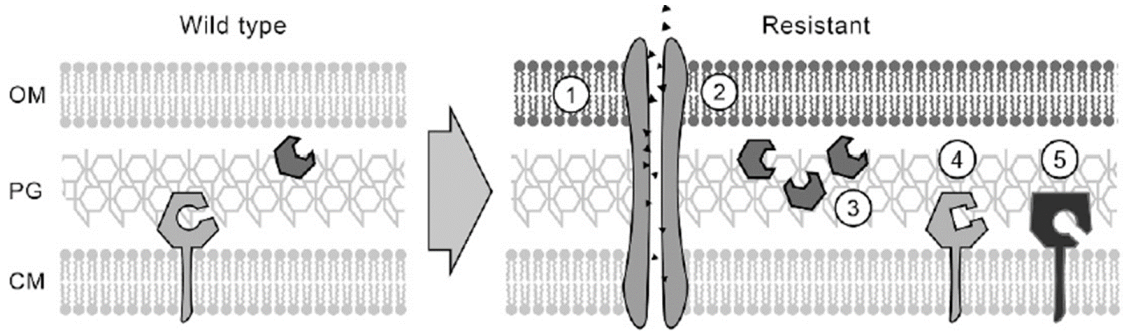

Figure 2.5. Mechanisms of β-lactams resistance in mycobacteria. From [136] Left: mycobacterial cell wall simplification includes the outer membrane (OM), the peptidoglycan

layer (PG) and the cell membrane (CM). Right: schema of β-lactams resistance mechanisms: modification of permeability of the outer membrane (1), increase of expression of efflux pumps (2), β-lactamase increased production, (3) target site modification, (4) and expression of β-lactam-refractory PBPs.

The activity of β-lactamases could be clinically reduced by the co-administration of β-lactamase inhibitors [137], being clavulanate the most effective against *Mtb* due to a stable inactivation of the enzyme [137, 138]. In 1983, an *in vitro* study demonstrated bactericidal activity of amoxicillin combined with the β-lactamase inhibitor clavulanate against 14 out of 15 clinical isolates of *Mtb* [139]. After this initial discovery, several clinical trials were performed with conflicting observations. In 1998, a clinical study evaluated the early bactericidal activity (EBA) of amoxicillin/clavulanate [140]. Patients received isoniazid (300 mg, once daily), ofloxacin (600 mg, once daily) or amoxicillin/clavulanate (1000 mg / 250 mg, three times a day) for seven days. Results showed that all three regimens reduced *Mtb* in sputum, with isoniazid as the most effective agent, and showed amoxicillin/clavulanate comparable activity to other antitubercular agents. However, in 2001 a later study found contradictory results [141]. In this study, patients received either amoxicillin/clavulanate (3000 mg / 750 mg, once daily) or no drugs for two days. The EBA of the two groups was compared and no statistically significant differences were found. A possible reason underlying these discrepant results could be the differences in the dosage of amoxicillin/clavulanate. Although in both studies patients received 3 g of amoxicillin and 750 mg of clavulanate daily, in the first study it was administered three times a day and, in the second one, once a day. However, the authors of the latter study concluded that amoxicillin/clavulanate was ineffective for the treatment of TB and it should be exclusively used in those cases of multidrug-resistant TB with no other treatment options.

Interest in β-lactams for the treatment of TB arose again some years later in the midst of an outbreak of XDR-TB (first reported in 2006 in Tugela Ferry, KwaZulu-Natal Province, South Africa) [142], when a report showed that carbapenems were poor substrates of *Mtb* β-lactamase and confirmed *in vitro* activity of meropenem/clavulanate against drug susceptible and XDR-TB strains [143]. In 2016, a clinical trial demonstrated that meropenem administered with amoxicillin/clavulanate had similar efficacy than the standard treatment (isoniazid, rifampicin, pyrazinamide and ethambutol). This, together with other mounting evidence [144-147], was an inflexion point on β-lactams perception as an anti-TB treatment option [148]. Currently, the WHO includes carbapenems in the list of recommended drugs to be used in longer MDR-TB regimes. Meropenem and imipenem-cilastatin are the carbapenems included in the latest group (group C), which contains drugs to be added to the regimen when medicines from groups A and B cannot be used. Carbapenems have to be administered

with the β-lactamase inhibitor clavulanic acid, which is available only in formulations combined with amoxicillin [149].

These findings confirming the anti-TB properties of β-lactams are especially encouraging because of a different mode of action than existing anti-TB therapies. Thus, β-lactams should be minimally impacted by the development of resistance to other therapies. Moreover, several types of PBPs have been described in *Mtb*. As in other bacteria, sub-classes of β-lactams show different affinity for them, *i.e.*, carbapenems inhibit LDTs while penicillins and cephalosporins target DDTs [150]. The combination of two sub-classes of β-lactams targeting different mycobacterial transpeptidases is regarded as a possibility to effectively disrupt the peptidoglycan biosynthesis [151, 152]. Reported *in vitro* synergy between penicillins and carbapenems (amoxicillin and meropenem, respectively) supports this hypothesis [153]. However, this is a field yet to be explored.

In this Chapter, we studied the *in vitro* activity of β-lactams in combination with an extended set of compounds against *Mtb,* as well as the β-lactam contribution in higher order drug combinations. This Chapter is divided into two parts:

1. **β-lactam synergy screening**. We described an *in vitro* combination screening against *Mtb* focused on β-lactams. Two β-lactams were chosen: meropenem, because of its anti-TB activity properties already demonstrated [143, 148], and cefadroxil, an oral cephalosporin that showed synergy with rifampicin [83]. These two primary compounds were tested in combination with a panel of 48 compounds with known mechanism of action against *Mtb*. This primary screening was performed with standard methodologies, based on growth inhibition assays. Compounds showing positive interaction with β-lactams from this primary assay were confirmed and further characterized based on bacterial killing using the OPTIKA assay described in Chapter 1. The improved throughput of OPTIKA, compared with standard time kill assays, allowed us to explore combinations up to three drugs and profiled their kinetics at extended time points (up to 50 days).

2. **Integration of β-lactams in current MDR-TB therapy.** We evaluated the contribution of β-lactams to drug combinations designed based on recent recommendations to treat MDR-TB. In 2019, the WHO launched the consolidated guidelines on drug-resistant tuberculosis treatment [149]. In these guidelines, a new drug classification to manage RR- and MDR-TB cases was included to achieve either a shorter regimen including injectable anti-TB drugs or a longer all-oral treatment. For the longer regimen, the WHO recommended to combine all three drugs belonging to group A

(levofloxacin/moxifloxacin, bedaquiline and pretomanid) plus at least one drug from group B (clofazimine or cycloserine/terizidone) for at least 18-20 months. These recommendations could be considered if there was no resistance to any of the drugs in group A. If there was resistance to fluoroquinolones (*i.e.,* levofloxacin or moxifloxacin), clofazimine constituted a valid alternative to them. When not possible to design a treatment with drugs from groups A and B, drugs from group C (ethambutol, delamanid, pyrazinamide, imipenem-cilastatin/meropenem, amikacin/streptomycin, ethionamide/prothionamide and *p*-aminosalicylic acid) should be used.

Considering these recommendations together with data from previous meta-analysis and observational studies, Caminero *et al.* [154] proposed a multidrug regimen using new drugs based on moxifloxacin-bedaquiline-linezolid or clofazimine-bedaquiline-linezolid for patients with fluoroquinolone resistant MDR-TB.

Our study was focused on a set of drugs chosen accordingly to the recommendations cited above. It was done completely based on bacterial killing, using OPTIKA, and following a different approach that allowed us to understand the individual contribution of single drugs in combinations up to five drugs at a time.

The **main objective of Chapter 2** is to identify favourable partners to combine with β-lactams against *Mtb* and understand its contribution when in multidrug anti-TB regimens. For this, we first performed an *in vitro* combination screening focused on β-lactams. Later, we did a second study to characterize the *in vitro* contribution of β-lactams to a set of drugs recently proposed by the WHO for MDR-TB treatment.

2.2 Material and methods

2.2.1 Bacterial strain, growth conditions, compound information and reagents

The bacterial strain, glycerol stocks and assay media described in Chapter 1 section 1.2.1, were used in this Chapter.

7H9 media was supplemented with detergent (tyloxapol 0.05% v/v) only for cultures used for OPTIKA calibration curves. Experiments including drugs were performed with detergent-free assay media.

The compound library (n= 48) included commercially available and drugs with known mechanism of action (secondary compounds, SC) (**Table 2.1**). The library was screened in pair-wise combinations with two β-lactams (primary compounds, PC): meropenem and cefadroxil against *Mtb*.

Stock solutions of compounds dissolved in their optimal solvent were always prepared fresh on the same day of plate inoculation. Compounds were dispensed using an HP D300e Digital Dispenser.

MTT and resazurin solutions were prepared as described in Material and Methods of Chapter 1, section 1.2.1.

Drug name	Abbreviation	Supplier	Class	Target	Application
Amikacin*	AMK	GSK-CS (KS202846-156A2)	Aminoglycoside	Protein synthesis	2nd line anti-TB
Bacitracin	BAC	GSK-CS (GDD/27938)	Polipeptides	Cell wall	Topical. Skin infections
Bedaquiline	BDQ	GSK-CS (EC/11613)	Diarylquinoline	Respiration	MDR-TB
Cefadroxil*	CFX	GSK-CS (KS202846-156B6)	Cephalosporin (1st gen)	Cell wall	Oral. Broad- spectrum
Cefdinir	CEF	Sigma (C7118)	Cephalosporin (3rd)	Cell wall	Oral. Broad- spectrum
Cefixime	CFM	GSK-CS (IM101056-009K0)	Cephalosporin (3rd)	Cell wall	Oral. Broad- spectrum
Cefotetan	CTT	GSK-CS (ST/1302758)	Cephamycin	Cell wall	Long $t_{1/2}$. Broad-spectrum
Ceftriaxone	CRO	GSK-CS (U519/151/1)	Cephalosporin (3rd)	Cell wall	Long $t_{1/2}$. Broad-spectrum
Cephradine	CFD	GSK-CS (EXSB/56-5CEP)	Cephalosporin (1st)	Cell wall	Oral. Broad- spectrum
Chloramphenicol	CAM	GSK-CS (M179/20/3)	Nitrobenzene	Protein synthesis	Broad-spectrum. High toxicity
Clarithromycin	CLA	GSK-CS (EXSB/5645-31B)	Macrolide	Protein synthesis	Broad-spectrum
Clindamycin	CLI	GSK-CS (0255Z81Y*A)	Lincosamide	Protein synthesis	Narrow spectrum
Clofazimine	CFZ	GSK-CS (H098750-035F3)	Riminophenazine	Multiple	2nd line MDR-TB
Cloxacillin	CLX	GSK-CS (EXSB/L-3146)	Penicillin	Cell wall	Narrow spectrum
Dapsone	DAP	GSK-CS (U15717/98/80)	Sulfonamide	Folate biosynthesis	M. leprae
Delamanid	DLM	ADOOQ (A12864)	Dihydro-nitroimidazooxazole	Cell wall	MDR-TB
Ertapenem	ETP	Amatek Chemical (DM-0004)	Carbapenem	Cell wall	Broad-spectrum
Ethambutol	EMB	GSK-CS (EC/5648)	Aminoalcohol	Cell wall	1st line anti-TB
Ethionamide	ETH	GSK-CS (EC11341)	Thioamide	Cell wall	2nd line anti-TB
Fidaxomicin	FDX	Selleckchem (S4227)	Macrolide	RNA polimerase	C.difficile
Fosfomycin	FOS	GSK-CS (GDD/61052)	Phosphonic acid derivate	Cell wall	Broad-spectrum
Fusidic acid	FUS	GSK-CS (EXSB/RIT-1427)	Fusidane	Protein synthesis	Skin infections
GV110352-157A3	481	GSK-CS (GV110352-157A3)	GSK set	Trp	-
Imipenem*	IMP	Ark Pharm (AK118710)	Carbapenem	Cell wall	Broad-spectrum
Isoniazid	INH	GSK-CS (KS202846-158A7)	Hydrazide	Cell wall	1st line anti-TB
Ketoconazole	KET	GSK-CS (H09875-035P0)	Imidazole	Ergosterol synthesis	Antifungal
Levofloxacin	LVX	GSK-CS (ST/1299957)	Fluoroquinolone	DNA replication	MDR-TB Phasell
Linezolid	LZD	GSK-CS (M183/95/1)	Oxazolidinone	Protein synthesis	MDR-TB
Meropenem	MER	Combi-Blocks (ST-9229)	Carbapenem	Cell wall	Broad-spectrum
Minocycline	MIN	GSK-CS (HO98750-035R1)	Tetracycline	Protein synthesis	Broad-spectrum
Moxifloxacin	MOX	GSK-CS (IM101056-054C8)	Fluoroquinolone	DNA replication	MDR-TB
N22692-27-A1	629	GSK-CS (N22692-27-A1)	GSK set	Leucyl tRNA synthese	-
N23902-22-1	366	GSK-CS (N23902-22-1)	GSK set	THPP	-
N28940-31-1	693	GSK-CS (N28940-31-1)	GSK set	InhA	-
N33478-41-2	588	GSK-CS (N33478-41-2)	GSK set	DprE1 reversible	-
N34945-11-2	150	GSK-CS (N34945-11-2)	GSK set	Spiro	-
N6601-28-2	260	GSK-CS (N6601-28-2)	GSK set	InhA	-
N9772-72-1	173	GSK-CS (N9772-72-1)	GSK set	MGI	-
Nitrofurantoin	NFT	GSK-CS (U1895/10/2)	Imidazolidine	Multiple	Urinary tract infections
p-amino salicilic acid	PAS	GSK-CS (U23919/187/1)	Benzenoids	Folate biosynthesis & mycobactin	2nd line anti-TB
Pretomanid	PTD	GSK-CS (ST/2496555)	Nitroimidazole	Cell wall	MDR-TB
Prothionamide	PTO	GSK-CS (R13147/156/26)	Thioamides	Cell wall	2nd line MDR-TB
Retapamulin	RET	GSK-CS (SB-275833)	Pleuromutilin	Protein synthesis	Skin infections
Rifampicin	RIF	GSK-CS (KS202846-159B5)	Rifamycin	RNA polimerase	1st line anti-TB
Spectinomycin	SPC	GSK-CS (ST/1302626)	Aminocyclitol	Protein synthesis	Gram -
Sulfamethoxazole	SMX	GSK-CS (0474C 64W*B)	Sulfonamide	Folate biosynthesis	Broad-spectrum
Sutezolid	SZD	Sigma (PZ0035)	Oxazolidinone	Protein synthesis	DR-TB Phase II
Tebipenem-Pivoxil	TBP	Amatek Sci (DM126)	Carbapenem	Cell wall	Broad-spectrum. Oral
Thioacetazone	THZ	GSK-CS (FUSI/32/29/4)	Thiosemicarbazole	Cell wall	2nd line anti-TB
Trimethoprim	TMP	GSK-CS (UC/24304)	Diaminopyrimidine	Folate biosynthesis	Broad-spectrum
Vancomycin	VCM	GSK-CS (ST/1302642)	Glycopeptide	Cell wall	Gram +

Table 2.1. Drugs used in Chapter 2. GSK-CS: compound store of GSK. Compounds were dissolved in DMSO except those marked with * (amikacin, cefadroxil and imipenem) that were dissolved in 66% DMSO + 33% H_2O.

2.2.2 Growth inhibition assays. MTT Readout

Drug susceptibility assays were performed in 384-well plates. MTT assay was performed as described in Chapter 1 (section 1.2.2).

2.2.2.1 Drug interaction studies. FICI determination

The compound library was screened in pair-wise combinations with meropenem and cefadroxil against *Mtb*. Two assay layouts were used for FICI determination in the primary screening.

(i) Primary Compound at sub-MIC concentration layout. The semi High Throughput Synergy Screen described by Ramón-García *et al* [83] was used.

Briefly, three dose response curves were assayed per pair-wise combination: two-fold dilutions of both single drugs and a third dose of mixed compounds. This was designed so that a fixed sub-MIC concentration (ideally 1/4x MIC) of the primary compound was assayed in combination with a two-fold serial dilution of the secondary compound. To overcome the inter-experiment typical 2-fold MIC variation [78] already mentioned in Chapter 1, several sub-MIC concentrations of the primary compound were included. Once plates were revealed, combinations containing the actual 1/4x MIC were used for FICI calculation.

Specifically, in the synergy screening described in this Chapter, three sub-MIC concentrations of meropenem (*i.e.* 1/2x, 1/4x and 1/8x MIC_{Ref}) and two sub-MIC concentrations of cefadroxil (*i.e.* 1/8x and 1/16x MIC_{Ref}) were assayed in combination with the two-fold serial dilutions of all secondary compounds.

(ii) DiaMOND layout. As described by Cokol *et al* [70], two-fold dilutions of single drugs and the equipotent serial dilution of the mixture were assayed per pair-wise combination.

In both assay layouts, MIC and MIC_{Combo} were interpolated in the four-parameter logistic model fitted curve equation. Curve fit of single drugs and combinations was done with the excel add-in XL fit version 5.5.0.5 (IDBS).

If % growth did not show the typical dose response curve [90] and 90% of growth inhibition was not observed, the next assay concentration would be used for calculations *(i.e.,* 2x Maximum assay concentration or 0.5x Minimum assay concentration). In these cases, the corresponding modulator appeared in the result table.

If the typical curve profile was observed, but 90% of growth inhibition was not determined by XL fit, the value was manually determined based on the shape of the curve.

To quantify the degree of pair-wise drug interaction, the Fractional Inhibitory Concentration Index ($FICI_{90}$) was calculated as described in Chapter 1 (section 1.2.2.1). The combination classification was done as described in section 1.2.2.1.

2.2.3 OPTIKA

OPTIKA was performed following the protocol described in Chapter 1 (section 1.2.5). Same drug concentrations were chosen (4x MIC, 1x MIC and 1/4x MIC). In the case of CLX, 4x MIC was not assayed because its high MIC. Same time points (*i.e.* day 0, 1, 2, 4, 7, 14, 21 and *ca*. 50) were taken.

It should be noted that , as in Chapter 1, SD was not included in killing curve plots for figure clearness. Mean Log CFU/ml and SD values can be found at appendix II of this Chapter. Otherwise indicated, this applies to all figures of this Chapter containing killing curves.

2.2.4 β-lactam synergy screening outline

The β-lactam synergy screening strategy used in this work follows a **bottom-up** approach in which triple combinations were built based on identified pair-wise interactions (**Figure 2.6**).

1. Meropenem (a carbapenem) and cefadroxil (a cephalosporin) were selected as primary compounds and screened in pair-wise combinations against secondary compounds of the compound library (see **Table 2.1**). This screening was based on growth inhibition and performed in liquid media, following two methodologies described above (section 2.2.2.1). Synergistic partners, *i.e.* secondary compounds showing an $FICI_{90}$ ≤0.5 in any of the two methodologies used were selected as hits.

2. The list of hits was refined based on literature revision. Favourable pair-wise drug interactions of primary compounds and selected hits were confirmed by a secondary screening based on bacterial killing using OPTIKA.

3. A focused OPTIKA triple drug combination screening was done. Triple combinations were designed so that they contained the primary compound combined with all possible pair-wise combinations of respective hits. Triple combinations showing positive interaction according to relapse at end point were selected and favourable interactions were confirmed by a second OPTIKA assay.

4. To understand the single drugs contribution to the combinations, an *in-depth* study of confirmed favourable triple interactions was done by OPTIKA, comparing the killing curve profile of triple and related pair-wise combinations.

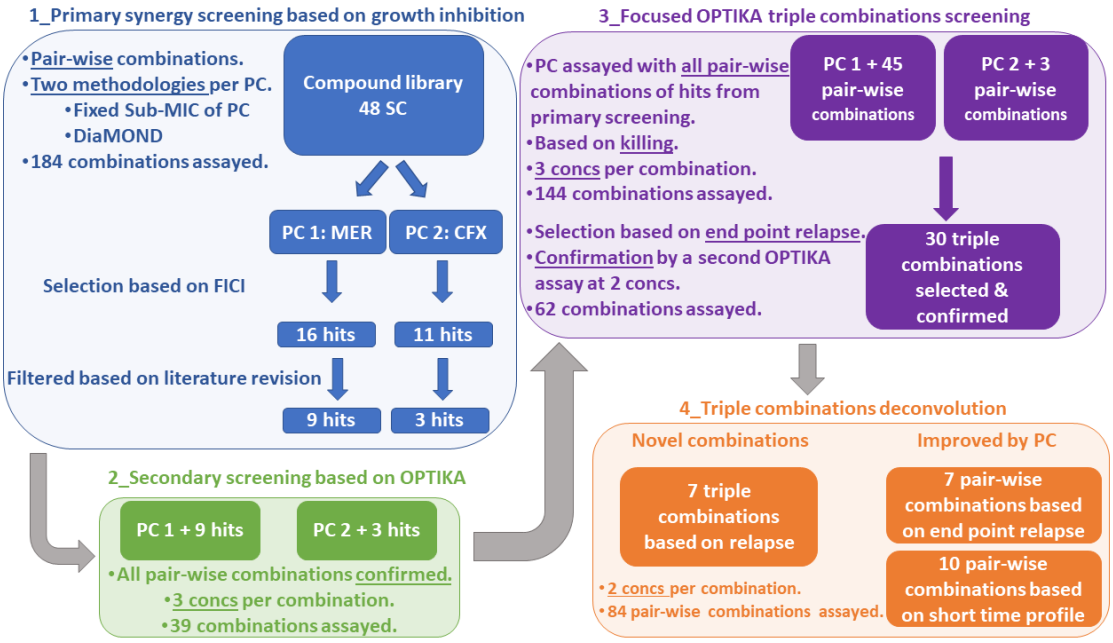

Figure 2.6. β-lactam synergy screening. Box 1. Primary screening based on growth inhibition: 48 Secondary Compounds (SC) and 2 Primary Compounds (PC 1: meropenem & PC 2: cefadroxil) were assayed in pair-wise combinations by two methodologies: Sub-MIC fixed concentration of PC and DiaMOND. Combinations showing $FICI_{90}$ ≤0.5 with any of the two methodologies were selected and subsequently filtered by literature revision of SC. Box 2. Secondary screening based on OPTIKA: synergistic combinations based on growth inhibition were confirmed based on bacterial killing. Box 3. Focused OPTIKA triple combinations screening: every PC was assayed with all possible pair-wise combinations of respective hits. Thirty triple combinations showing favourable interaction according to relapse at end point were selected and confirmed by a second OPTIKA assay. Box 4. Triple combinations deconvolution: contribution of single drugs to the thirty selected triple combinations was evaluated by assaying all related pair-wise combinations. Comparing curve profiles, seven novel triple combinations were identified. For them, the positive effect according to relapse at end point was not visible in any of the related pair-wise combinations. Seventeen triple combinations showed an enhanced positive interaction comparing with their respective pair-wise, seven of them according to relapse at end point and ten according to curve profile from day 0 to day 7.

2.2.5 Integration of β-lactams in current anti-TB therapy

To explore the β-lactam contribution to drug combinations proposed to treat MDR-TB, a **top-down** approach (**Figure 2.7**) was followed. Opposite to the β-lactam screening described above, where final triple-drug combinations were built by rational subsequent addition of compounds, here a set of five-drug combinations was directly assayed by OPTIKA. In order to understand the contribution of individual drugs to the final combination, all related four-, three- and two-drug possible combinations were assayed at the same time.

Combinations were designed considering the following key points:

1. Five-drug combinations were designed because MDR-TB treatment typically has an intensive phase with more than four drugs [155].

2. The five-drug combinations contained the nucleus recommended by Caminero *et al.* constituted by moxifloxacin/clofazimine-bedaquiline-linezolid.

3. In line with the main objective of this Chapter, β-lactams were included in the combinations to explore their contribution to combinations containing drugs already recommended to treat MDR-TB. Specifically, meropenem was chosen because it is included in group C of the WHO classification and cefadroxil was included as an oral cephalosporin.

4. Finally, delamanid was considered because it has been reported that it can be effective against MDR-TB when used with bedaquiline, linezolid, clofazimine and carbapenems [156].

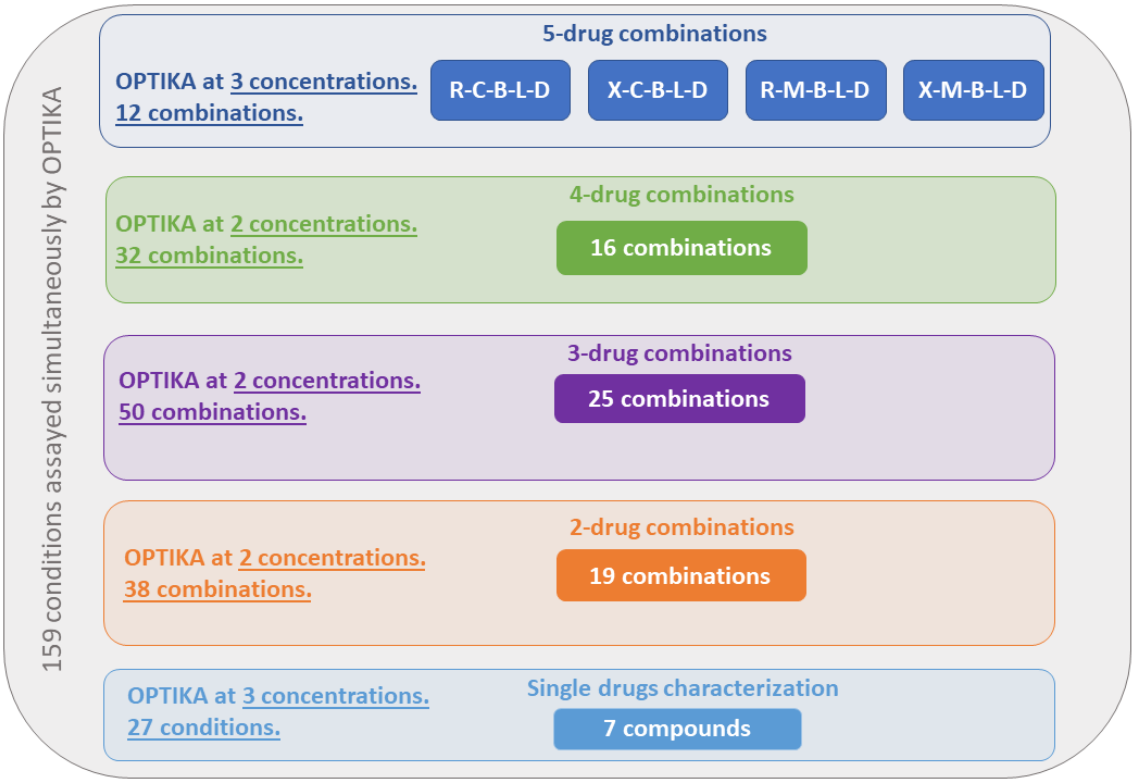

Figure 2.7. Integration of β-lactams in MDR-TB treatment screening outline. Seven anti-TB compounds: meropenem (R), clofazimine (C), bedaquiline (B), linezolid (L), delamanid (D), cefadroxil (X) and moxifloxacin (M) were combined so that four 5-drug combinations were evaluated against TB directly based on bacterial killing. All related four-, three- and two-drug combinations were assayed simultaneously to understand the individual drug contribution to the initial 5-drug combinations.

2.3 Results and discussion

2.3.1. β-lactam synergy screening outline

The β-lactam synergy screening was done following the bottom-up approach described in section 2.2.4. Before the synergy screening, the MIC of the compounds was determined by the MTT assay (section 2.2.2) to properly design subsequent experiments (**Chapter 2, appendix I**). Results and discussion are merged in the following sections.

2.3.1.1 β-lactam primary synergy screening

Primary pair-wise assays of the compound library combined with β-lactams were performed as described in section 2.2.2.1.

MIC_{Ref} of primary compounds were determined prior to the synergy screening, with values of 20 μM and 128 μM for meropenem and cefadroxil, respectively. Thus, sub-MIC concentrations chosen for the first approach of the synergy screening (fixed sub-MIC of primary compound) were:

- 10 μM, 5 μM and 2.5 μM in the case of meropenem. The MIC of meropenem was determined again in the screening assay, resulting in 40 μM. Combinations containing 10 μM of meropenem were used for $FICI_{90}$ calculation since they contained the primary compound at 1/4x MIC.

- In the case of cefadroxil, to avoid using too high drug concentrations, 32 μM and 8 μM were chosen for the synergy screening. In the screening assay, the MIC of cefadroxil was 64 μM. $FICI_{90}$ was calculated with combinations containing 8 μM of cefadroxil (1/8x MIC) because 32 μM would never produce FICI values below 0.5. As a consequence of this low concentration of the primary compound, some drug interactions were not detected.

$FICI_{90}$ was calculated for all combinations (**Chapter 2, appendix I**). Secondary compounds of combinations showing a $FICI_{90}$ of 0.5 or lower in at least one method were selected as hits (**Table 2.2**).

For meropenem, sixteen synergistic partners were identified; eleven of them were selected by both methods. In the case of cefadroxil, eleven hits were identified, with five of them selected with both methodologies. Tebipenem, rifampicin, thioacetazone, fusidic acid, and fidaxomicin showed interaction with both β-lactams.

		Meropenem (MER) synergy screening		Cefadroxil (CFX) synergy screening	
Secondary compound	**Abbreviation**	**FICI MER at 1/4x MIC**	**FICI DiaMOND**	**FICI CFX at 1/8x MIC**	**FICI DiaMOND**
Bacitracin	BAC			≤ 0.38	≤ 0.57
Cefdinir	CEF	0.22	0.78		
Cefixime	CFM	0.32	0.28		
Cefotetan	CTT			0.36	1.25
Ceftriaxone	CRO	0.40	0.25		
Cephradine	CFD	0.28	0.31		
Clindamycin	CLI	0.39	0.20		
Clofazimine	CFZ	0.58	0.42		
Cloxacillin	CLX	0.44	0.26		
Ethambutol	EMB	0.42	0.37		
Ethionamide	ETH	0.50	0.28		
Fidaxomicin	FDX	0.46	0.38	≤ 0.16	0.11
Fusidic acid	FUS	0.66	0.30	≥ 0.14	0.67
N23902-22-1	366			0.46	0.58
N6601-28-2	260	0.81	0.46		
N9772-72-1	173			0.82	0.41
Pretomanid	PTD	0.44	0.38		
Retapamulin	RET			0.17	0.47
Rifampicin	RIF	0.44	0.36	0.15	0.07
Tebipenem-Pivoxil	TBP	0.50	1.15	0.42	0.48
Thioacetazone	THZ	0.42	0.17	≤ 0.25	≤ 1.20
Vancomycin	VCM			≤ 0.13	≤ 0.03

MAX FICI (1.25)
FICI 0.5
MIN FICI (0.03)

Table 2.2. β-lactam synergy screenings hits. For every primary compound, combinations showing a $FICI_{90}$ of 0.5 or lower at least in one of the two methodologies were selected in this primary assay. The modulator "≤ or ≥" appeared if MIC of single drugs or combinations were not determined with the assay concentrations range (See Chapter 2, appendix 1).

It has been previously hypothesised that the combination of different sub-classes of β-lactams targeting different PBP enzymes would lead to a total inhibition of the peptidoglycan metabolism and, thus, of the bacterial death [151, 152]. Here, synergy was found among β-lactam sub-classes rather than among the same class of β-lactam. Except tebipenem, which showed a borderline synergy with meropenem only in the fixed sub-MIC approach, secondary compounds belonging to the carbapenems did not show favourable interaction when they were assayed in combination with meropenem (a carbapenem), and cephalosporins were not synergistic with cefadroxil (a cephalosporin). However, all cephalosporins (cefdinir, cefixime, ceftriaxone and cephradine) and one penicillin (cloxacillin) assayed in combination with meropenem were selected as hits. Similarly, one carbapenem (tebipenem) and one cephamycin (cefotetan) showed synergy with cefadroxil. Therefore, all this confirms that the combination of different sub-classes of β-lactams has a favourable interaction inhibiting the *in vitro* growth of *Mtb*.

The list of hits identified in the synergy primary assay was refined based on literature revision. Some of the selected compounds are drugs currently in use against TB (clofazimine, ethambutol, ethionamide, pretomanid and rifampicin). Others could be considered potential anti-TB drugs based on previous work (cefdinir) [83] or having family-related partners with good anti-TB properties (cloxacillin) [157]. Tebipenem was considered because it showed positive interaction with both primary compounds and belongs to the β-lactam family. Finally, thioacetazone was selected because it showed synergy with the two β-lactams and it was formerly used against TB.

Partners for meropenem were: ethambutol, clofazimine, pretomanid, tebipenem, rifampicin, thioacetazone, ethionamide, cefdinir and cloxacillin. Partners for cefadroxil were: tebipenem, rifampicin and thioacetazone.

In addition to these pair-wise combinations, the combination of meropenem with cefadroxil was also included in future studies because meropenem showed favourable interaction with other cephalosporins tested.

2.3.1.2 β-lactam synergy screening confirmation by OPTIKA

OPTIKA time kill assays were performed for meropenem and cefadroxil in pair-wise combinations with their respective hits.

Based on the slope at shorter times (**Table 2.3**), all synergistic pair-wise drug interactions selected in the primary assay were confirmed by OPTIKA. As it was mentioned in Chapter 1, the slope at day 2 could be initially considered the parameter to compare drug interactions observed in traditional combination assays based on growth inhibition. Comparing with results of the set of compounds tested in Chapter 1, here Log_{10} reduction detected more positive interactions, meaning that drug combinations included in this study showed a stronger interaction profile at shorter times than combinations of Chapter 1.

Eight out of 13 combinations showed a favourable drug interaction at regrowth at day 21. Considering the low stability of β-lactams in the assay media at 37°C [118], this could be attributed to a post-antibiotic effect.

Finally, most pair-wise combinations showed bacterial regrowth at end point (day 49), with only four of them maintaining bacterial load under the limit of detection.

Cephalosporins and carbapenems have been previously identified and characterized as good partners for rifampicin against *Mtb.* As it was described by Ramón-García *et al* [83], there is a strong *in vitro* interaction profile between rifampicin and cephalosporins, while a weaker but still positive interaction exists between rifampicin and carbapenems. These profiles were reproduced here by OPTIKA. Rifampicin showed a strong interaction with cefadroxil (a cephalosporin), which was maintained until the end point. Meropenem (a carbapenem) showed positive interaction with rifampicin, but this was lost after day 21.

	Slope			LogRed Day 4			LogRed Day 7			Regrowth day 21			Regrowth end point		
	1/4x MIC	1x MIC	4x MIC	1/4x MIC	1x MIC	4x MIC	1/4x MIC	1x MIC	4x MIC	1/4x MIC	1x MIC	4x MIC	1/4x MIC	1x MIC	4x MIC
MER-CFX															
MER-EMB												ND			ND
MER-CFZ															
MER-PTD															
MER-TBP		ND	ND												
MER-RIF			ND												
MER-THZ															
MER-ETH			ND								ND	ND			
MER-CEF															
MER-CLX			*NA*			*NA*			*NA*			*NA*			*NA*
CFX-TBP		ND	ND												
CFX-RIF			ND												
CFX-THZ			ND												

Table 2.3. Pair-wise combinations classification by OPTIKA. Classification according to Slope, Log reduction at days 4 and 7 and regrowth at days 21 and 49. Green: favourable, Yellow: No favourable, "ND" no determined, "*NA*" not available (*i.e.* no tested). Grey: combinations containing meropenem as primary compound. Blue: combinations containing cefadroxil as primary compound. Cefadroxil (CFX), cefdinir (CEF), clofazimine (CFZ), cloxacillin (CLX), ethambutol (EMB), ethionamide (ETH), meropenem (MER), pretomanid (PTD), rifampicin (RIF), tebipenem (TBP), thioacetazone (THZ).

2.3.1.3 OPTIKA screening of β-lactam triple drug combinations

Compounds selected in the primary screening and confirmed by OPTIKA pair-wise combination assay were tested in triple-drug combinations; designed so that primary compounds (meropenem or cefadroxil) were screened with all possible pair-wise combinations of their respective selected partners (*i.e.* cefadroxil, cefdinir, clofazimine, cloxacillin, ethambutol, ethionamide, pretomanid, rifampicin, tebipenem and thioacetazone for meropenem and rifampicin, tebipenem and thioacetazone for cefadroxil). These combinations were then assayed by OPTIKA.

Figure 2.8 shows OPTIKA classification of 45 triple combinations containing meropenem (grey) and three combinations containing cefadroxil (blue) as primary compounds. This classification was done, as described in Chapter 1, comparing the killing curves of each triple combination with their respective single drugs.

The interaction at short time points was observed in all cases. However, this effect was not always maintained at the end point. All combinations containing tebipenem showed positive interactions based on the slope at day 2, but only three of them prevented from the bacterial regrowth at day 49. These three combinations contained tebipenem, meropenem and either ethambutol, pretomanid or ethionamide.

In contrast, triple combinations containing meropenem-ethambutol or meropenem-pretomanid were favourable combinations that maintained the interaction

at longer time points with any of the compounds tested (based on regrowth at 4x MIC). Positive drug interactions between ethambutol and β-lactams sub-families have been previously described; *i.e.* with cefepime (a cephalosporin) against *M. avium* complex, with amoxicillin-clavulanate (a penicillin) against drug susceptible [158] and drug resistant [159] strains of *Mtb,* and finally with several carbapenems [83]. However, the favourable interaction of meropenem with pretomanid against *Mtb* was firstly described in this work.

Among all triple combinations containing cefadroxil as the primary compound, only cefadroxil combined with tebipenem and rifampicin (CFX-TBP-RIF) showed positive drug interaction at the end point. This triple combination presents some remarkable characteristics: (i) it highlights the favourable profile of combinations containing two sub-classes of β-lactams in this case, a cephalosporin (cefadroxil) and a carbapenem (tebipenem); (ii) it confirms the already described favourable interaction of rifampicin, the corner stone drug against TB, with β-lactams; and (iii) all the three drugs involved in this combination are orally-administered antibiotics, an attribute of high importance in the search of new regimens against TB.

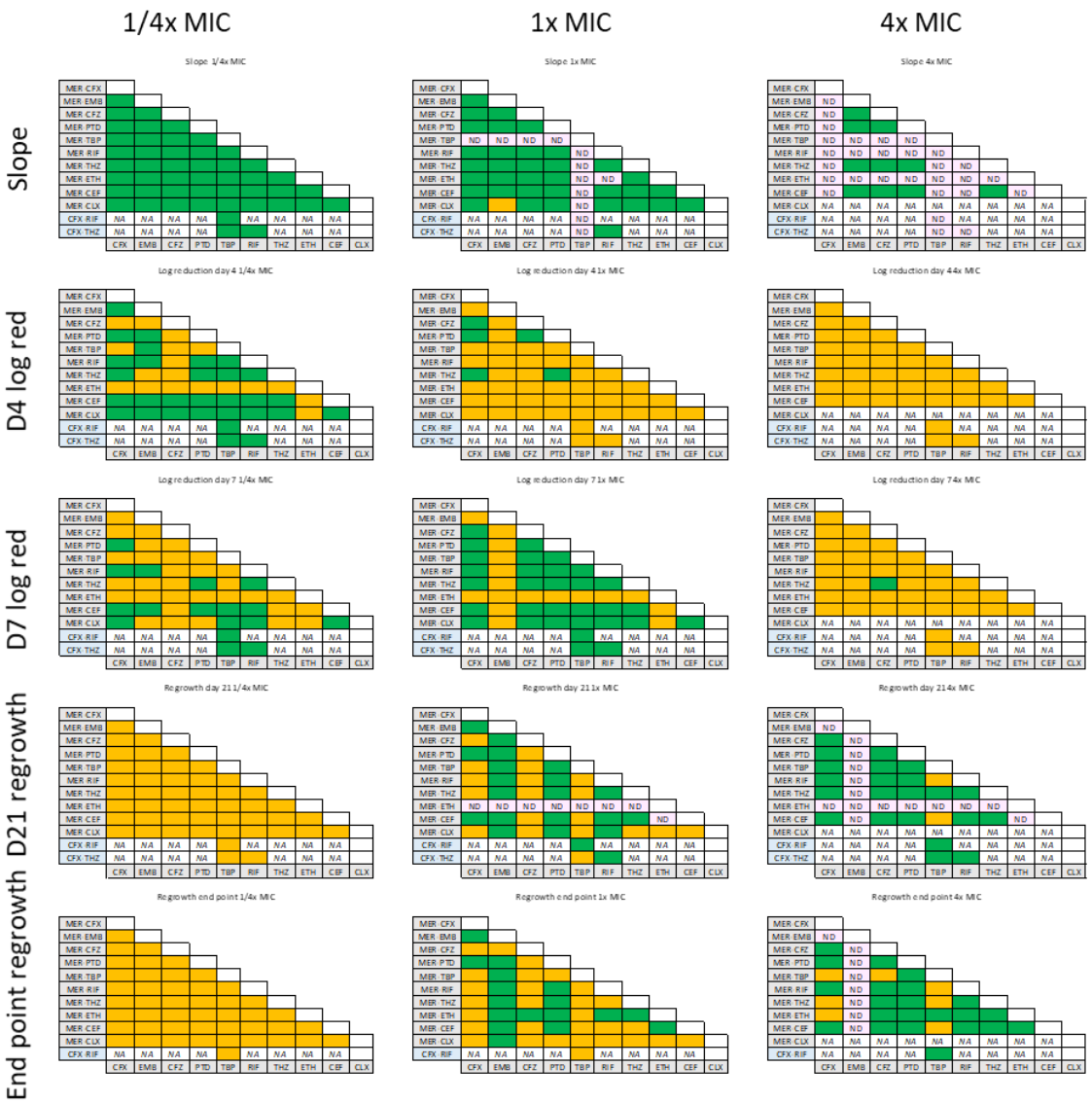

Figure 2.8. OPTIKA classification for triple combination screening. Each triangle represents the classification of the set of triple combinations based on one OPTIKA parameter at one determined concentration. Left column: combinations assayed at 1/4x MIC. Middle column: combinations assayed at 1x MIC. Right column: combinations at 4x MIC. Rows represent different parameters, from top to bottom: slope at day 2, log reduction at day 4, log reduction at day 7, regrowth at day 21 and regrowth at day 49. Grey: combinations containing the primary compound meropenem. Blue: combinations containing the primary compound cefadroxil. Green: synergy. Yellow: no synergy. ND: no determined. *NA*: not available (*i.e.* no tested combinations because they were not selected in primary screenings). Cefadroxil (CFX), cefdinir (CEF), clofazimine (CFZ), cloxacillin (CLX), ethambutol (EMB), ethionamide (ETH), meropenem (MER), pretomanid (PTD), rifampicin (RIF), tebipenem (TBP), thioacetazone (THZ).

In summary, thirty favourable triple combinations based on OPTIKA regrowth at end point (either at 1x or 4x MIC) were selected for a second OPTIKA experiment.

2.3.1.4 Triple-drug combinations secondary validation

Thirty favourable combinations were identified in the OPTIKA triple-drug combination screening according to regrowth end point. They were retested for confirmation by a second OPTIKA experiment. **Figure 2.9** shows combinations classification according to regrowth at end point in both experiments. All combinations except meropenem-ethionamide-tebipenem at 4x MIC confirmed the classification observed in the first assay.

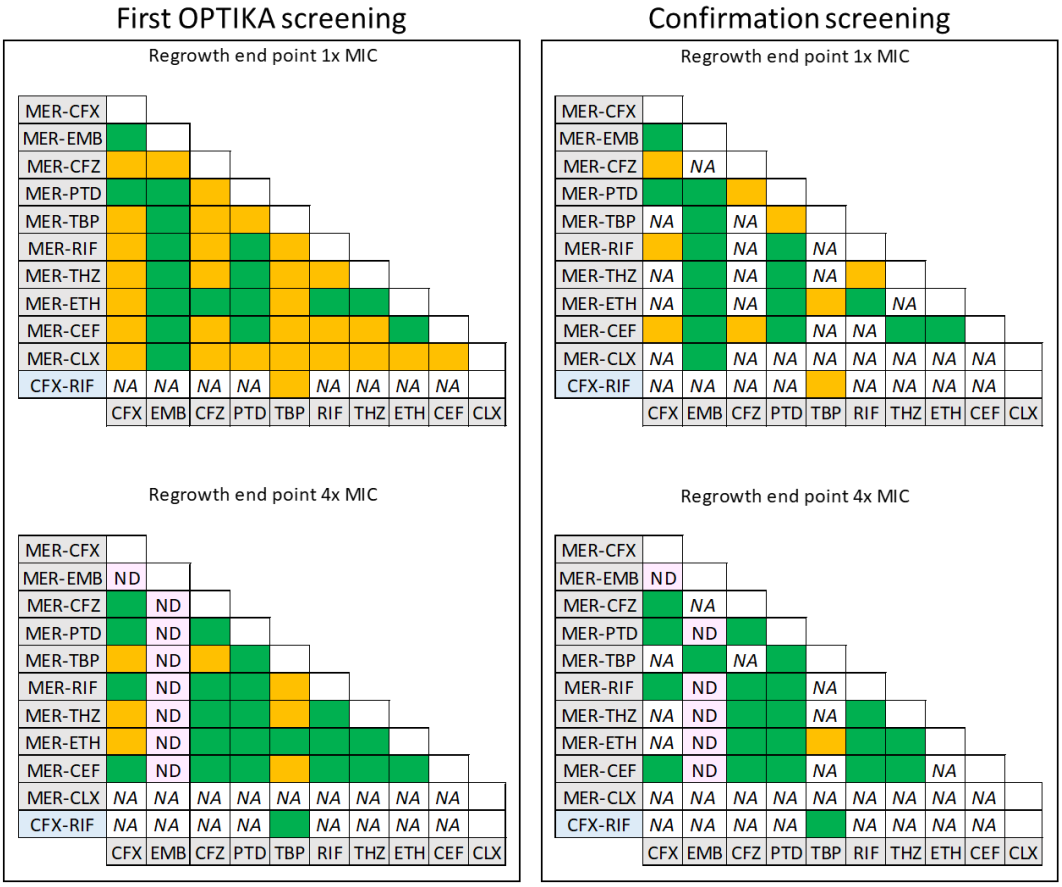

Figure 2.9. OPTIKA triple combinations confirmation. Based on relapse at day 49, classification of combinations at 1x MIC (top triangles) and 4x MIC (bottom triangles) of two independent assays were compared. Grey: combinations selected from the meropenem primary synergy screening. Blue: combination selected from the cefadroxil primary synergy screening. Green: synergy. Yellow: no interaction. ND: no determined. NA: not available (*i.e.* these combinations were not assayed because they were not selected in previous experiments). Cefadroxil (CFX), cefdinir (CEF), clofazimine (CFZ), cloxacillin (CLX), ethambutol (EMB), ethionamide (ETH), meropenem (MER), pretomanid (PTD), rifampicin (RIF), tebipenem (TBP), thioacetazone (THZ).

2.3.1.5 *In-depth* analysis of triple combinations containing β-lactam

In vitro killing kinetics of β-lactams are characterized by a fast initial killing rate followed by a bacterial rebound at different times depending on the concentration and the β-lactam itself [160]. This profile was confirmed in our assays. As it can be observed in the OPTIKA killing curve of meropenem in **Figure 2.10** (blue curve), a rapid initial killing rate was observed reaching the limit of detection at day 2, followed by a bacterial regrowth starting on day 4. On the contrary, the killing curves of the other two single drugs (pretomanid and thioacetazone, red and orange curves, respectively) showed a bacterial growth similar to the untreated control at every time point. When compounds not belonging to the β-lactam group were assayed together (purple curve of **Figure 2.10**), a favourable but slow interaction at short times was observed. Finally, similarly to meropenem killing kinetics, β-lactam containing pair-wise combinations and the triple combination (pink, light blue and green curves of **Figure 2.10,** respectively) showed a fast initial killing rate reaching the limit of detection at day two, suggesting that the fast killing rate of the triple combination was due to meropenem contribution. This analysis allowed us to understand the contribution of individual drugs to the triple combination interactions.

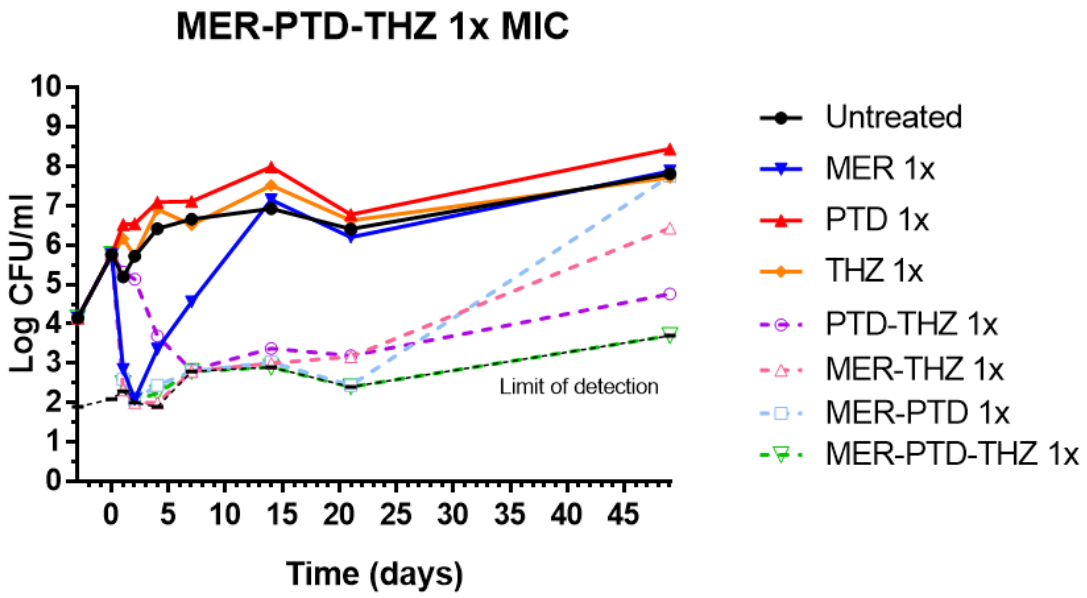

Figure 2.10. β-lactam contribution to triple combination killing profile. Meropenem (MER)-pretomanid (PTD)-thioacetazone (THZ) was classified as favourable by comparison of the killing profile of the triple combination (green curve) with the respective single drugs (blue, red and orange curves). The fast initial killing rate could be attributed to meropenem because the pair-wise combination PTD-THZ showed a slower initial killing profile (purple curve).

Deconvolution analysis showed in the example above was done for all the confirmed favourable triple combinations and it is discussed in the following section.

2.3.1.5.1 Deconvolution focused on regrowth at end point

Considering regrowth at end point, seven triple combinations were identified as favourable in contrast to their respective single drugs. As the favourable drug interaction of these combinations was not observed in related pair-wise combinations, they were denominated *novel* (**Table 2.4**).

Pretomanid, thioacetazone, cefdinir and rifampicin were identified as the best partners for meropenem when they were combined with a third drug.

	Regrowth at end point			
	A-B-C	A-B	A-C	B-C
MER-CFZ-CEF 1x				
MER-PTD-CEF 1x				
MER-PTD-RIF 1x				
MER-PTD-TBP 1x				
MER-PTD-THZ 1x				
MER-RIF-THZ 4x				
MER-THZ-CEF 1x				

Table 2.4. Novel triple meropenem-containing combinations. Triple combinations were classified according to relapse at end point and compared with the classification of related pair-wise combinations. A, B & C: individual drugs of the triple combination: drug on the left, in the middle and on the right position, respectively. Green: favourable interaction. Yellow: no favourable interaction. Cefdinir (CEF), clofazimine (CFZ), meropenem (MER), pretomanid (PTD), rifampicin (RIF), tebipenem (TBP), thioacetazone (THZ).

2.3.1.5.2 Deconvolution focused on meropenem addition to pair-wise combinations

When meropenem was added to some pair-wise combinations, it caused a drastic improvement at short-time interaction (general curve profile from day 0 to day 7) or at regrowth at end point. **Table 2.5** shows a set of pair-wise combinations whose interaction profile was enhanced by meropenem.

Pair-wise combination	Short time (D0-D7)	Regrowth at end point
CFX-CEF 1x		✓
CFX-EMB 1x		✓
CFX-PTD 4x		✓
CFZ-ETH 1x (& 4x)	✓	
CFZ-PTD 1x (& 4x)	✓	
CFZ-RIF 1x	✓	
CFZ-THZ 1x (& 4x)	✓	
EMB-CLX 1x		✓
EMB-PTD 1x	✓	
EMB-TBP 1x		✓
EMB-THZ 1x	✓	✓
PTD-ETH 1x (& 4x)	✓	
PTD-RIF 1x	✓	
PTD-THZ 1x (& 4x)	✓	✓ (Only 4x)
RIF-THZ 1x	✓	

Table 2.5. Improved pair-wise combinations by meropenem. Meropenem enhanced the killing profile of these pair-wise combinations at short times or at regrowth at day 49 (green check mark). Cefadroxil (CFX), cefdinir (CEF), clofazimine (CFZ), cloxacillin (CLX), ethambutol (EMB), ethionamide (ETH), pretomanid (PTD), rifampicin (RIF), tebipenem (TBP), thioacetazone (THZ).

Figure 2.11 shows an example of a favourable pair-wise combination improved by meropenem. The combination of ethambutol-pretomanid (**Figure 2.11 A**) was, in general, positive, but it showed a slow killing rate at short times. From day 14 and on, it reached the limit of detection of bacterial growth and this killing effect was maintained until the last experimental time point. When meropenem was added, the triple combination of meropenem-ethambutol-pretomanid (**Figure 2.11 B**) was clearly favourable reaching the limit of detection of bacterial growth at day 1 and maintaining this effect until day 49.

Would this behaviour translate into the clinic, β-lactams could be included in anti-TB regimens by administering them during the first days of treatment. Applying this concept to the combination considered here, meropenem would be administered for the first two weeks and the treatment would continue with EMB-PTD for longer times.

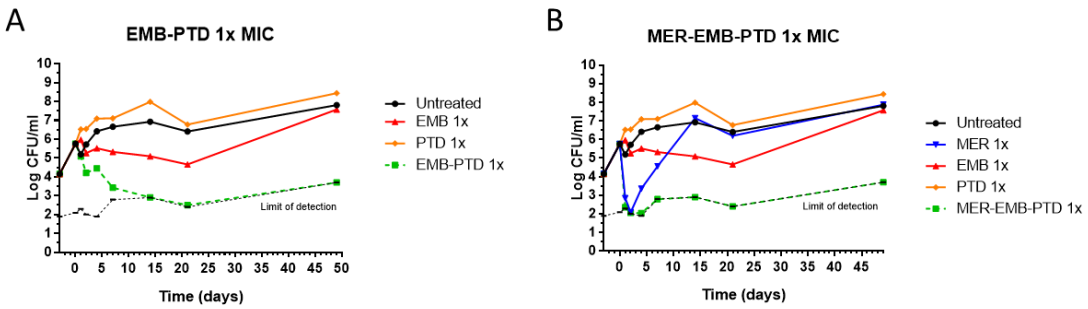

Figure 2.11. Example of meropenem effect in short time interaction of pair-wise combinations. (A) Ethambutol-pretomanid showed a slower killing rate from day 0 to day 7. **(B)** This interaction was improved if meropenem was added to the combination. Ethambutol (EMB), meropenem (MER), pretomanid (PTD).

2.3.1.5.3 Deconvolution focused on ethambutol and meropenem

Among all drugs tested, only ethambutol showed favourable interaction at 1x MIC with all compounds assayed in pair-wise combinations (**Figure 2.12**).

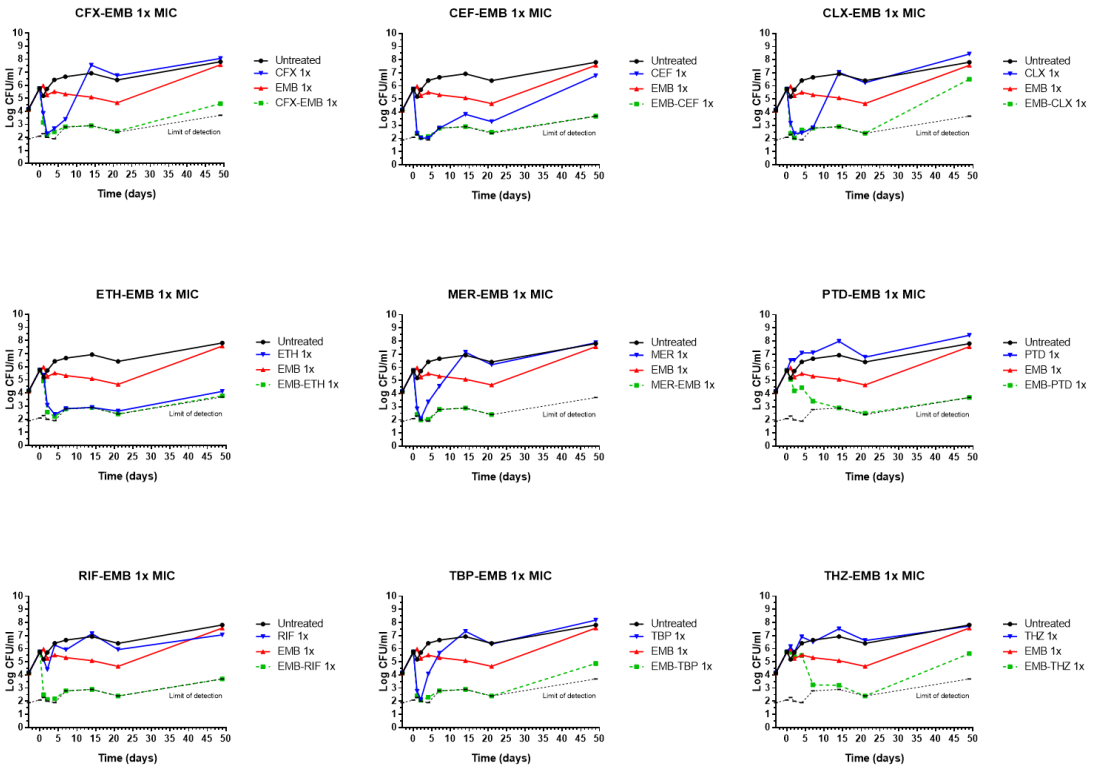

Figure 2.12. Ethambutol containing pair-wise combinations. Low bacterial load was robustly maintained in all pair-wise combinations containing ethambutol, although different killing rates were observed depending on the other partner of the combination. It should be noted that the last point of the MER-EMB killing curve was missing. However, according to other experimental data showed in this thesis regarding the end point regrowth, this combination can be classified as synergy. Cefadroxil (CFX), cefdinir (CEF), cloxacillin (CLX), ethambutol (EMB), ethionamide

(ETH), meropenem (MER), pretomanid (PTD), rifampicin (RIF), tebipenem (TBP), thioacetazone (THZ).

When meropenem was added this positive interaction was maintained in all cases until the end of the experiment. As described above for pretomanid-ethambutol (**Figure 2.13 A**), the addition of meropenem to the pair-wise combination produced a triple-drug combination that showed a faster killing rate at short times maintaining the low bacterial load at day 49. In other cases, such as cefadroxil-ethambutol, tebipenem-ethambutol and cloxacillin-ethambutol (**Figure 2.13 B**), the bacterial regrowth showed by the pair-wise combination was prevented by the addition of meropenem. Finally, in the case of thioacetazone-ethambutol (**Figure 2.13 C**), both effects described above were observed when meropenem was added.

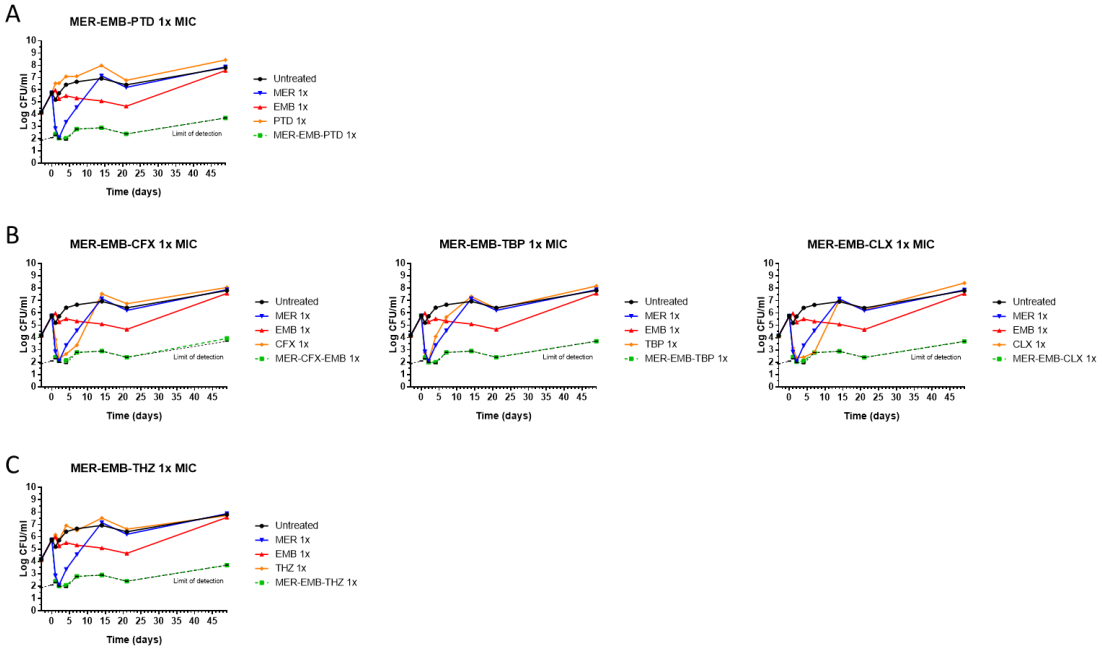

Figure 2.13. Triple-drug combinations where the interaction of ethambutol-containing combinations was enhanced by meropenem. Meropenem **(A)** enhanced the slope at short times, **(B)** reduced the bacterial regrowth, or **(C)** both effects when added to combinations containing ethambutol. Cefadroxil (CFX), cloxacillin (CLX), ethambutol (EMB), meropenem (MER), pretomanid (PTD), tebipenem (TBP), thioacetazone (THZ).

2.3.2 β-lactams within currently recommended MDR-TB therapy

This study followed the top-down approach described in **Figure 2.7**, section 2.2.5. Selected five-drug combinations as well as all four-, three- and two-drug possible combinations were assayed simultaneously by OPTIKA. The inclusion of all intermediate combinations allowed us to understand individual drug contributions to final combinations and propose new recommendations for future anti-TB regimes based on *in vitro* killing activity.

Compounds were chosen based on the WHO [149] and other recommendations [154, 156] to treat MDR-TB. Combinations were constituted by the core moxifloxacin/clofazimine-bedaquiline-linezolid plus a β-lactam (meropenem/ cefadroxil) and delamanid.

2.3.2.1 Five-drug combinations killing ability

Five-drug combinations were assayed by OPTIKA at 1/4x MIC, MIC and 4x MIC values of related single drugs.

With sub-MIC (1/4x) and over-MIC (4x) concentrations, no conclusions were drawn. In the first case, all combinations showed similar growth levels than single drugs and the untreated control. While in the second case, the effect of the combination could not be distinguished from that of the single drugs, which reached the limit of detection.

At 1x MIC, different degrees of drug interaction were observed (**Figure 2.14**). According to the general killing profile, the best five-drug combination was formed by meropenem-clofazimine-bedaquiline-linezolid-delamanid. However, the favourable interaction of this combination was not maintained at extended time points.

In contrast, a better killing profile was obtained in the β-lactam screening that combined only three drugs. This suggests that triple combinations tested were properly selected in the primary assays, proving thus the applicability of the methodology followed in the first section of this Chapter.

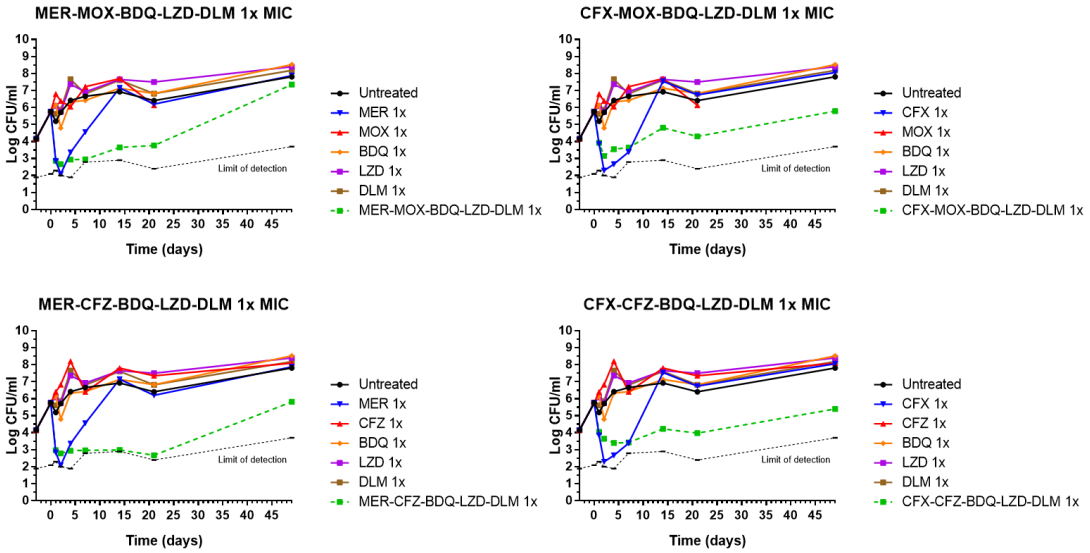

Figure 2.14. Five-drug combinations killing curves. At 1x MIC, five drugs combined (dotted green curves) showed better killing profile than their respective single drugs (solid curves). This effect was not maintained at longer time points. Bedaquiline (BDQ), cefadroxil (CFX), clofazimine (CFZ), delamanid (DLM), linezolid (LZD), meropenem (MER), moxifloxacin (MOX).

2.3.2.2 Evaluation of delamanid (or β-lactam) contribution to triple and four-drug combinations

The effect of delamanid or β-lactam (meropenem or cefadroxil) addition to the proposed triple combinations (bedaquiline-linezolid plus moxifloxacin or clofazimine for fluoroquinolones resistant strains) was evaluated by comparison of the curve profiles (**Figure 2.15**).

Figure 2.15 A and **Figure 2.15 C** show killing curves of triple combinations and their respective single drugs. In both cases, a weak positive interaction in the triple-drug combination was observed. The addition of meropenem to these triple combinations (blue curve of **Figure 2.15 B** and **Figure 2.15 D**) produced a significant reduction of the bacterial load. This interaction became more positive at longer time points in the triple combination when containing clofazimine instead of moxifloxacin.

Similar results were observed if cefadroxil was added to the triple combination containing clofazimine (red curve of **Figure 2.15 B**). However, the addition of cefadroxil to the triple combination containing moxifloxacin did not produce a significant change (red curve of **Figure 2.15 D**).

Finally, the addition of delamanid (purple curve of **Figure 2.15 B** and **Figure 2.15 D**) did not produce any favourable effect on the killing ability of the triple combinations.

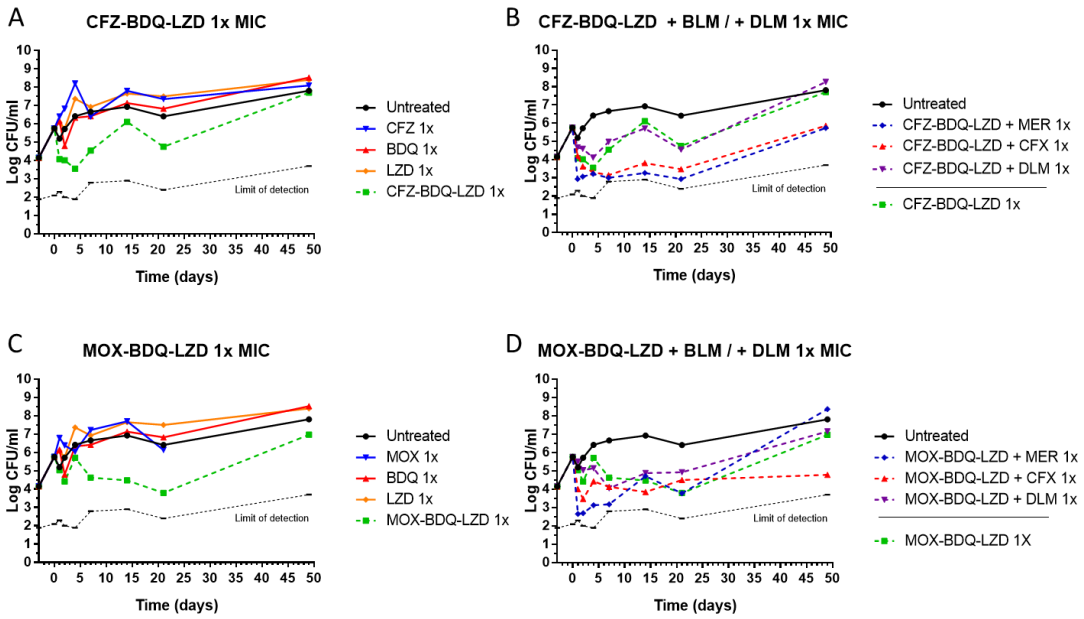

Figure 2.15. Killing curves of triple combinations with β-lactam or delamanid addition. A: plot of clofazimine-bedaquiline-linezolid and respective single drugs. Weak favourable effect was observed when they were combined. **B:** effect of meropenem, cefadroxil or delamanid addition to the triple combination. Four-drug combinations plotted in B show the positive effect caused by meropenem or cefadroxil (blue and red dotted curves respectively) and no benefit of the delamanid addition (purple dotted curve). A similar behaviour is observed in plots **C** and **D**, where the initial triple combination contained moxifloxacin instead of clofazimine. Bedaquiline (BDQ), cefadroxil (CFX), clofazimine (CFZ), delamanid (DLM), linezolid (LZD), meropenem (MER), moxifloxacin (MOX).

A similar behaviour was observed when the β-lactam or delamanid was added to four-drug combinations (**Figure 2.16**).

Considering the example shown in **Figure 2.16 A** (combination of meropenem-clofazimine-bedaquiline-linezolid-delamanid), meropenem enhanced the killing profile of clofazimine-bedaquiline-linezolid (blue curve in left plot of **Figure 2.16 A**). However, when delamanid was added to this four-drug combination (green curve in left plot of **Figure 2.16 A**), the new curve was superposed to the previous one and with no additional effect. Delamanid thus did not produce any favourable effect to the clofazimine-bedaquiline-linezolid combination (blue curve in right plot of **Figure 2.16 A**). However, a better killing profile was observed when meropenem was added to this four-drug combination.

In summary, the positive effect of the five-drug combination compared to the triple combination lacking delamanid and meropenem was due exclusively to meropenem. This effect was also reproduced with cefadroxil instead or meropenem

(**Figure 2.16 B**). Our data also suggest that delamanid could be removed from the combination with no negative consequences.

For the β-lactam or delamanid addition to combinations containing moxifloxacin (**Figure 2.16 C** and **Figure 2.16 D**), the positive effect was weaker than in clofazimine containing combinations, being this effect visible only in the slope at short times. However, as it happened for combinations containing clofazimine, it was exclusively due to the β-lactam contribution.

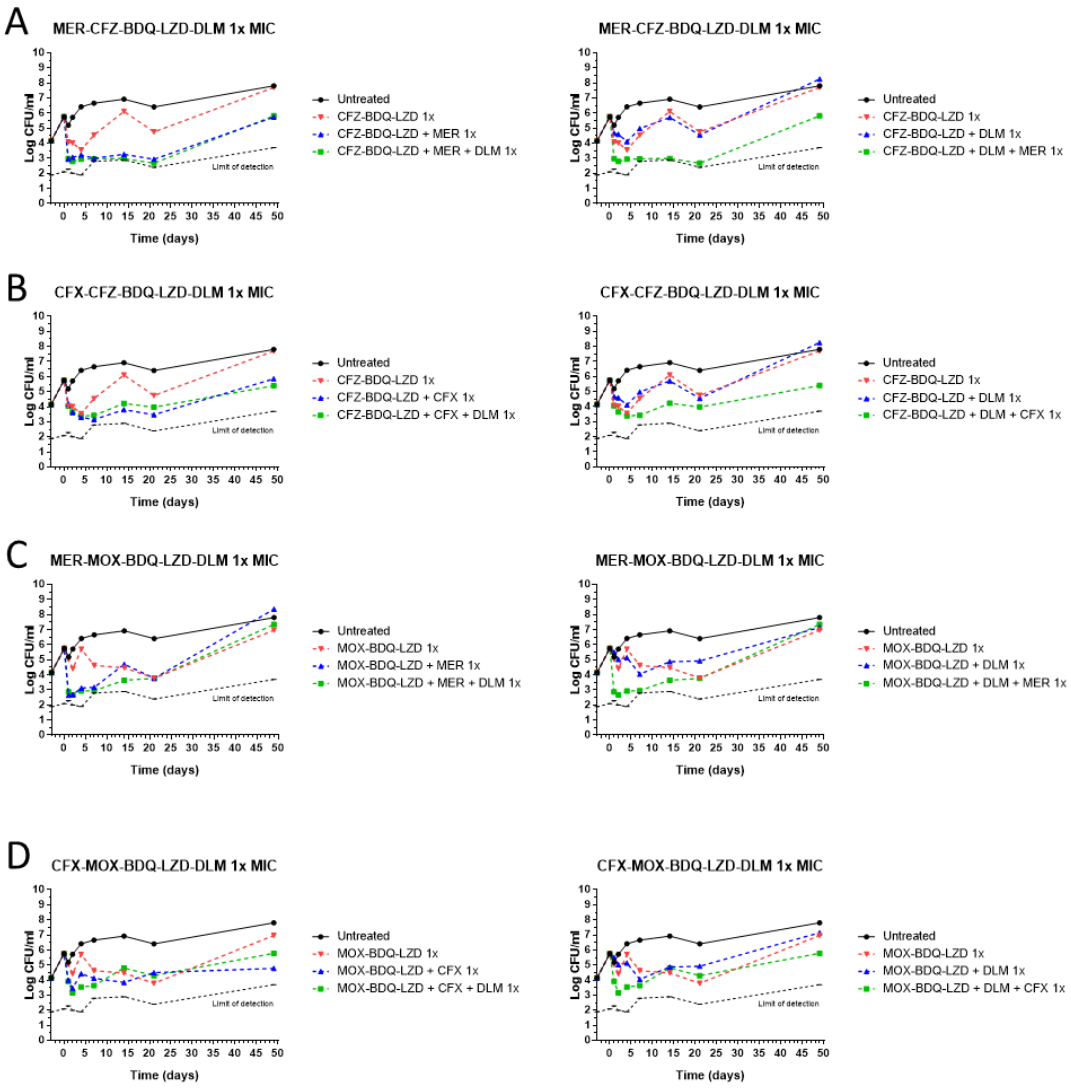

Figure 2.16. Delamanid or β-lactam addition to four combinations. Red curves represent triple combination lacking delamanid or β-lactam. Blue curves in plots of the left show the effect of β-lactam addition to triple combinations, *i.e.* a general improvement in the killing profile especially at short times. Green curves of plots on the left represent the addition of delamanid to the four-drug combinations; here, the killing profile of four-drug combinations was not enhanced by delamanid. Blue curves of plots on the right correspond to the killing profile of triple combinations plus delamanid. In general, blue curves are superposed to red curves, showing no additional effect in the killing profile. Green curves represent β-lactam addition to four-drug

combination. In this case, the killing profile of the triple and four-drug combinations was improved. Bedaquiline (BDQ), cefadroxil (CFX), clofazimine (CFZ), delamanid (DLM), linezolid (LZD), meropenem (MER), moxifloxacin (MOX).

2.3.2.3 Negative effect of linezolid in five-drug combinations

A similar analysis to that of the section 2.3.2.2 was done to understand the contribution of linezolid in five-drug combinations.

Figure 2.17 A (left plot) shows the killing profile of the core combination clofazimine-bedaquiline-delamanid (red curve). When meropenem was added to this triple combination (**Figure 2.17** left plot, blue curve), there was a clear improvement in the slope at shorter times. When linezolid was added to this four-drug combination (**2.17 A** left plot, green curve), the resulting curve superposed the previous one, showing no improvement in the killing profile.

However, considering the same combination and changing the order of drugs addition, if linezolid was added to the core triple drug combination (**Figure 2.17 A** right, blue curve), the killing profile of the resulting four-drugs combination worsened. Finally, when meropenem was added to this unfavourable four-drug combination (**Figure 2.17 A** right, green line), the killing profile of the initial triple combination was recovered and improved in slope at short time.

This effect was observed in other cases (**Figure 2.17 B**, **Figure 2.17 C** and **Figure 2.17 D**), where the presence of linezolid reduced the killing profile of the combination, even increasing the total number of drugs in the final combination.

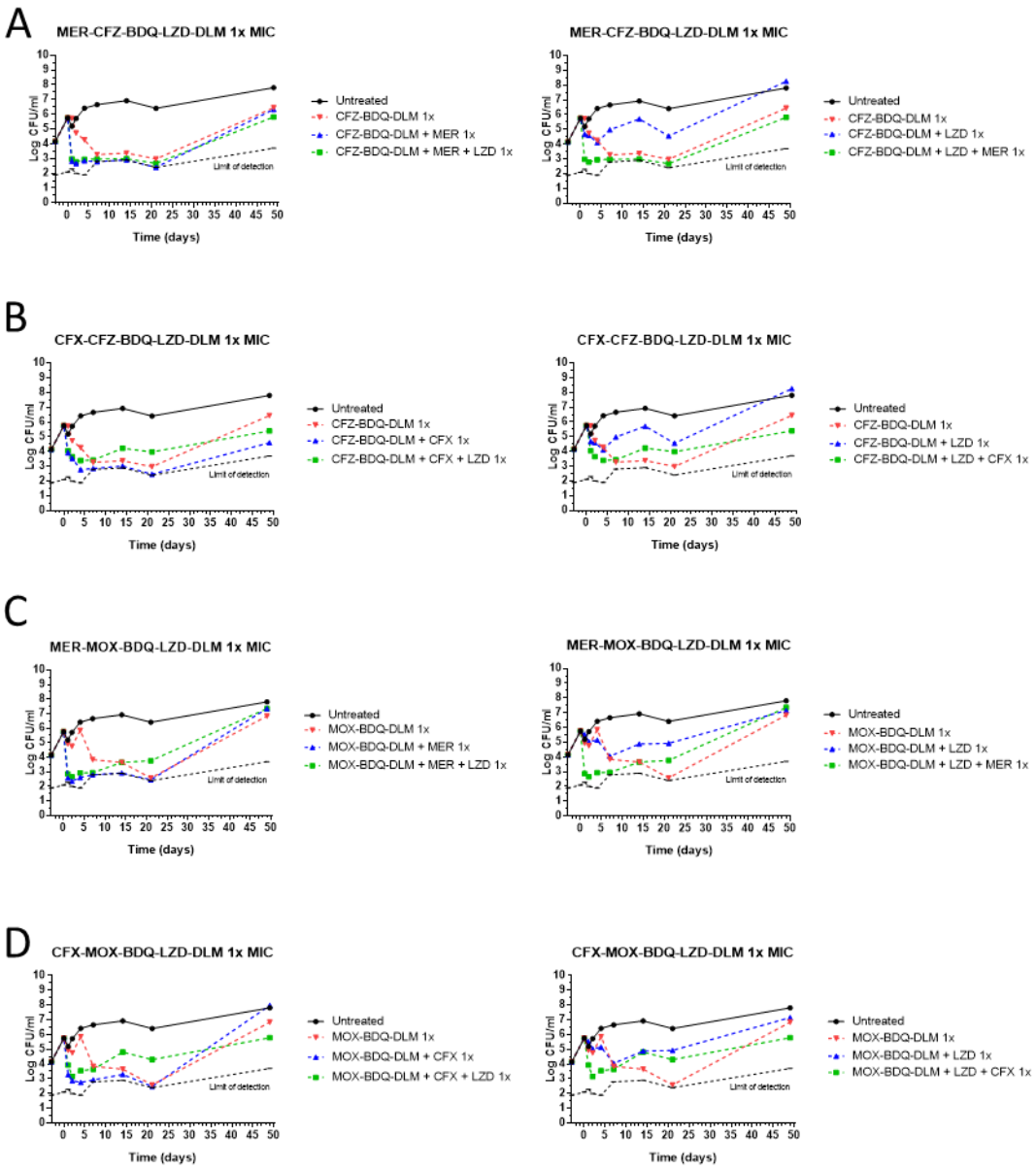

Figure 2.17. Negative effect of linezolid in five-drug combinations. Red curves represent triple combinations lacking linezolid or β-lactams. Blue curves in left plots show the effect of β-lactam addition to triple combinations, *i.e.* a general improvement in the killing profile especially at short times. Green curves of left plots represent the addition of linezolid to the four-drug combinations, *i.e.* the killing profile of four-drug combinations was not enhanced by linezolid being in some cases worse than the four-drug combination itself. Blue curves of right plots correspond to the killing profile of triple combinations plus linezolid. In general, blue curves show higher levels of bacterial concentrations than red curves, showing worse profile of killing ability. Green curves represent β-lactam addition to the four-drug combinations. In this case, the killing profile of the four-drug combinations was improved by the β-lactam, although the killing profile of the triple combination was in some cases better than the five-drug combo. Bedaquiline (BDQ), cefadroxil (CFX), clofazimine (CFZ), delamanid (DLM), linezolid (LZD), meropenem (MER), moxifloxacin (MOX).

2.3.2.4 Bedaquiline-pretomanid-linezolid (BPaL) deconvolution

A shorter all-oral regimen against MDR-TB composed of bedaquiline-pretomanid-linezolid was developed by the TB Alliance and recently recommended by the WHO under *operational research conditions* [149]. According to results from the NiX-TB clinical trial, 90% of patients treated with this regimen for six months had a favourable outcome [161], which can be comparable with the success outcome of DS-TB patients treated with the standard of care in modern trials treatment [162-164]. These results were very encouraging to treat XDR-TB, a form of the disease that lacks a standard regimen. Here, patients are typically treated with individualized regimens, which includes up to seven drugs for two years or even more and with extensive side effects, little success, and high mortality rate [149, 161].

The bacterial killing of this triple-drug combination and all related pair-wise combinations were tested here by OPTIKA including sub-MIC, MIC and over-MIC concentrations. However, as it was observed in previous combinations described in this Chapter, only MIC concentration was useful to draw conclusions. (**Figure 2.18**).

The triple combination showed a weak favourable interaction from day 2 to day 7, reducing the bacterial load around 2-logs comparing with the single drugs and the untreated control. This slight interaction was lost at longer times, showing the killing curve of the combination similar concentration of viable bacteria than the untreated control. An interesting profile was found when deconvoluting this triple combination by the evaluation of the bacterial killing ability of related pair-wise combinations. The combination of bedaquiline plus pretomanid showed a better interaction profile than the triple combination, reaching a bacterial concentration close to the limit of detection at day 21. This, in line with previous observations done in this Chapter, confirms the negative effect of linezolid when added to *in vitro* favourable drug combinations.

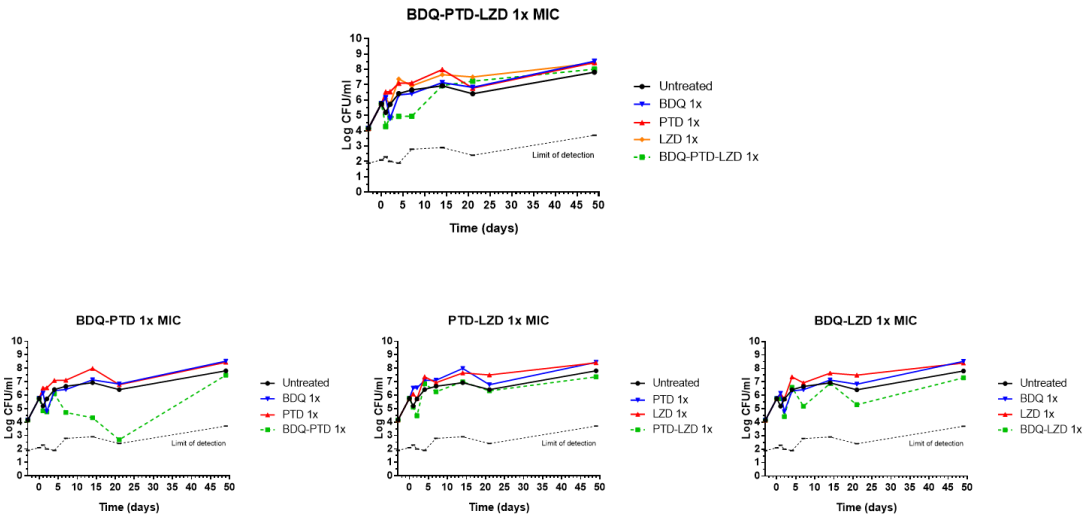

Figure 2.18. BPaL deconvolution. The combination of bedaquiline-pretomanid was the only pair-wise combination that showed positive interaction reaching values close to the limit of detection at day 21 and being followed by a fast rebound. None of the other combinations showed favourable interaction at any time point. Bedaquiline (BDQ), linezolid (LZD), pretomanid (PTD).

2.4 General discussion and future perspectives

This Chapter aimed to identify favourable *in vitro* β-lactam containing drug combinations against *Mtb*. Typically, due to the low throughput of standard cell viability assays, *in vitro* synergy screenings are performed based on primary growth inhibition assays and the most favourable drug interactions identified are confirmed by traditional killing curves based on CFU [81, 82]. This approach is time and effort consuming and implies missing favourable drug interactions because they could not be detected by single-point growth inhibition assays or because the low throughput of CFU-based time kill assays entails the selection of the most favourable drug interactions to be confirmed based on cell viability. However, to evaluate drug combinations described here we used our recently developed OPTIKA methodology (Chapter 1), which allowed us to interrogate a large number of *n*-drugs combinations based on bacterial killing in longitudinal assays. This would have been unfeasible using standard CFU-based TKA methodologies.

In the first screening, we aimed to identify favourable partners in combination with β-lactams using a focused bottom-up approach. Three-drug combinations were progressively built by rational drugs addition to simpler favourable combinations. This methodology allowed us to remove compounds with lower potential to be good partners and to explore more variety of potentially interesting combinations. In order to evaluate *in-depth* the drug interaction of β-lactams with other drugs, two different β-lactams (*i.e.* primary compounds) belonging to different sub-classes were selected to be assayed in combination with the same panel of secondary compounds. Specifically, meropenem (a carbapenem) and cefadroxil (a cephalosporin) were chosen as primary compounds.

Based on $FICI_{90}$ in the primary screening, similar numbers of hits were selected for both meropenem and cefadroxil. However, after a selection done based on literature revision, nine compounds were progressed to be further evaluated by OPTIKA in combination with meropenem, and three in the case of cefadroxil, making the subsequent studies being focused mainly on meropenem.

The first outcome of our β-lactam containing synergy screening was the improvement of the killing profile at short times of combinations containing meropenem. Translation to a clinical application of our findings, β-lactams could be added in new anti-TB treatments at the beginning of the therapy. For *Mycobacterium ulcerans*, the causative agent of Buruli ulcer, the bacterial load at the beginning of the therapy is closely related with the time to heal [165]. In line with the results shown here, a recent study with *M. ulcerans* found synergistic interactions between β-lactams and drugs currently recommended by the WHO to treat this disease, suggesting that the

inclusion of β-lactams in that therapy would lead to a most effective and shorter regimen [166]. Translating knowledge from these closely related mycobacteria, our proposal of including meropenem at initial days of TB treatments would contribute to get a shorter anti-TB regimen.

Another major finding after this combination screening was the robust favourable interaction of meropenem combined with pretomanid. Pretomanid belongs to the nitroimidazole family of drugs. It is a pro-drug that possesses a complex mode of action. Once activated, it inhibits the mycolic acid biosynthesis and thus blocks the cell wall formation in actively replicating bacteria. In addition, it acts as a nitric oxide (NO) donor in anaerobic conditions, killing bacteria in non-replicating stages [167, 168]. It was first identified in 1995 by PathoGenesis (now Novartis) and it was developed by the TB Alliance [167, 169]. It presents good bioavailability data and is well tolerated by healthy volunteers [28].

Pretomanid has been recently authorised by the US Food and Drug Administration (FDA), the Drug Controller General of India (DCGI) and the European Medicines Agency (EMA) to be used as part of the BPaL regimen against XDR-TB. It is currently tested in combination with other anti-TB drugs under several phase II and phase III clinical trials [14]:

- TB-PRACTECAL (ClinicalTrials.gov NCT02589782). This trial looks for a shorter, effective and tolerable regimen for patients suffering from drug resistant TB. Here, bedaquiline, pretomanid and linezolid are combined with either moxifloxacin or clofazimine.

- APT Trial (ClinicalTrials.gov NCT02256696). It evaluates if the inclusion of pretomanid in the first-line treatment for DS-TB could shorten the standard regimen. Here, pretomanid is combined with isoniazid, pyrazinamide and either rifampicin or rifabutin to determine whether it can be used with rifamycins, key sterilizing first-line drugs against TB [170].

- SimpliciTB (ClinicalTrials.gov NCT03338621). In this trial the efficacy, safety and tolerability of the all-oral bedaquiline-pretomanid-moxifloxacin-pyrazinamide regimen is evaluated. The treatment is administered for four months to patients with DS-TB and six months to patients with DR-TB.

- NiX-TB Trial (ClinicalTrials.gov NCT02333799). This recently completed trial showed a positive outcome for MDR-TB. It consisted of combining

bedaquiline (400 mg once daily for two weeks then 200 mg three times per week) plus pretomanid (200 mf once daily) plus linezolid (1200 mg once daily) administered for six months. After completion of this trial, 90% of patients treated with this regimen had a favourable outcome. Despite of the effectiveness of this treatment, an important rate of adverse events related to linezolid was observed [161].

- ZeNiX (ClinicalTrials.gov NCT03086486). Here the efficacy, safety and tolerability of linezolid as well as its dose and treatment duration in combination with pretomanid and bedaquiline is evaluated. This trial arose from the linezolid-associated toxicity observed in the previous NiX-TB trial when evaluating the all-oral triple regimen BPaL. Doses of bedaquiline and pretomanid are maintained as in the BPaL regimen (100 mg and 200 mg daily, respectively), and four different administrations of linezolid are evaluated: 1200 mg once daily for 26 weeks, 1200 mg once daily for 9 weeks, 600 mg once daily for 26 weeks and 600 mg once daily for 9 weeks.

The *in vitro* drug interaction between β-lactams and pretomanid found here has not been reported before. It agrees with the previously described synergy between β-lactams and compounds targeting the cell wall formation such as ethambutol [83, 158, 159]. Pretomanid is used in combination regimens against TB. The work described here suggests that the inclusion of β-lactams in those pretomanid-containing combination regimens could enhance its antimycobacterial properties.

In the second screening described in this Chapter, we used the opposite strategy to evaluate *in vitro* drug interaction, a top-down approach. Here, anti-TB drugs currently proposed by the WHO to treat MDR-TB were tested along with β-lactams in combinations up to five drugs. We assayed the most complex drug combinations and all related simpler combinations simultaneously, which eliminated the experimental inoculum-variation inherent to microbiological tests. Including all possible intermediate combinations independently of the potential, positive or negative contribution allowed us to deduce the contribution of single drugs or small combinations to the final five-drugs combination.

Regarding the bacterial killing profile observed, tested combinations showed weaker synergistic profile than combinations included in the β-lactams screening even though combinations were formed by a higher number of drugs. Individual drug contribution analysis revealed that delamanid could be removed from combinations without negative effects. Moreover, this would reduce the cardiotoxicity associated to the bedaquiline-delamanid combination previously described [171]. However, the *in*

vitro contribution of β-lactams (meropenem or cefadroxil) was clearly favourable, robustly increasing the killing rate at short times. On the contrary, when linezolid was added, the killing ability of combinations was dismissed.

Linezolid is an oxazolidinone active against gram-positive bacteria [172]. It was repurposed for the treatment of TB as an alternative to overcome emerging resistance to other first-line drugs [173]. Linezolid inhibits the initiation of protein production by binding to the bacterial ribosomal 50S subunit. The blocking of this early step of protein production seems to be unique, which explains the lack of described cross-resistance with other clinically approved anti-TB drugs. In addition, it possesses good pharmacokinetic properties with excellent oral bioavailability [171]. Currently, linezolid is being used in combination with other anti-TB drugs against MDR-TB [14]. Even though positive outcomes of MDR-TB treatments including linezolid have being observed, its toxicity is limiting its use. As an example, ZeNiX trial arose as a consequence of adverse events related with linezolid observed in the original NiX-TB trial. The main objective of the ZeNiX trial is to evaluate whether the efficacy of the BPaL regimen can be maintained while reducing toxicity with a lower dose and duration of linezolid.

Taking together the already described good safety data of β-lactams and *in vitro* drug interactions described in this Chapter, next steps in line with this work could be: (i) the *in vitro* evaluation of five-drug proposed combinations changing linezolid by pretomanid; (ii) the exploration of other sub-families of β-lactams aiming to include two β-lactams in the final combination; or (iii) the evaluation of combinations of all-oral drugs to build an injectable-free regimen. In this line, β-lactams offer a large family of compounds, and many of them can be orally administered.

Nevertheless, it has to be considered that experiments performed in this Chapter present some limitations.

1. They were performed at standard *in vitro* culture conditions of *M. tuberculosis*. Favourable interactions identified here should be retested under other *in vitro* conditions mimicking the different physiological states of the bacteria during infection such as cholesterol, glucose, acetate, low pH, fatty acids, stationary phase, non-replicating or intracellular assays.

2. Time kill assays are static PK/PD models. In OPTIKA, drugs were only added at the beginning of the assays and do not reproduce clinical therapy. Favourable combinations could be assayed in dynamic PK/PD models such as the hollow fibre system, where the posology and the

length of treatment can be mimicked *in vitro* and might provide data with higher prediction of clinical outcomes [113].

3. As an *in vitro* study, it has its inherent limitations. OPTIKA data of the BPaL triple combination presented in this Chapter exemplifies confronting data. This combination did not show a positive interaction in OPTIKA when the three drugs were assayed together. In fact, the combination of bedaquiline and pretomanid showed a more favourable profile than the triple combination. In line with our data, another *in vitro* study based on growth inhibition [105] classified this triple combination as antagonism against an *Mtb* Erdman strain. However, there is strong evidence of a positive bactericidal and sterilizing drug interaction described by several *in vivo* assays [174-176] and little doubts about its clinical efficacy to treat patients with MDR-TB [161]. Nevertheless, it should be considered that results shown here are derived from a unique *in vitro* assay, which lacks the role of the immune system that is present in *in vivo* models and clinical trials [177]. In addition, OPTIKA assays performed in this Chapter have only been done with the standard growth medium of *Mtb*. This combination should be evaluated by OPTIKA under other carbon sources such as glucose, cholesterol, valerate, butyrate, acetate or propionate to get a more robust conclusion [178].

Screenings described here could serve as a proof of concept to initially test a large number of combinations and extrapolate general guidelines to compound combinations depending on their mechanism of action or chemical properties. Later, more experiments could be designed using other systems with low throughput such us the dynamic hollow fibre system where human PK profiles could be simulated.

2.5 Conclusions

Novel regimens against MDR-TB are urgently needed. The recently approved BPaL and other regimens under clinical development have shown promising results [47, 67]. One limitation of the BPaL regimen is the high rate of the reported adverse effects of linezolid. The efficacy of the BPaL regimen lowing the dose of linezolid is being evaluated in the ZeNiX trial [161]. However, new treatments replacing linezolid by other drugs with better tolerability properties could also constitute valid options to get a universal regimen.

β-lactams are one of the largest groups of antibiotics available today with an exceptional record of clinical safety in humans [115]. Based on *in vitro* data using cell viability as readout shown in this Chapter, β-lactams could be explored as potential drugs to be included in the anti-TB treatment for several reasons.

First, it has been robustly observed that β-lactams produced a fast reduction of the bacterial load at initial days, which allows us to suggest their use in early days of the treatment. In addition, for many combinations including β-lactams, bacterial regrowth was not observed at longer times.

Second, the favourable drug interaction between the β-lactam meropenem and the recently approved anti-TB drug pretomanid suggested that this family of compounds could be explored as part of multi-drug regimens against MDR-TB containing pretomanid. Although the combination of pretomanid and the oral β-lactam cefadroxil was not detected in this work, this may be due to the experimental design of the primary combination screening. There, cefadroxil was tested at a too low concentration and, as a consequence, only very strong favourable interactions were detected. In the same line, bedaquiline (the third drug of the BPaL combination) was not selected as a synergistic partner of meropenem or cefadroxil in primary combination screenings based on growth inhibition. As a consequence, the combinations bedaquiline-meropenem and bedaquiline-cefadroxil were not assayed by OPTIKA. Nevertheless, the slow killing profile between bedaquiline and isoniazid shown in Chapter 1 suggested that this favourable drug combination at long times would have not been detected based on single-point standard assays. More experimental work is needed to confirm this interaction profile between pretomanid and other β-lactams, such as cefadroxil and between bedaquiline and β-lactams.

Third, comparing results from the first and second screenings described in this Chapter, we could conclude that higher order drug combinations do not necessarily produce a better *in vitro* killing profile than combinations rationally designed containing only three drugs.

Finally, favourable identified combinations following methodologies described here should be confirmed using other carbon sources, dynamic PK/PD or *in vivo* models to get a better prediction of clinical outcomes.

2.6 APPENDIX I: Chapter 2 results summary table

Data for sections 2.3.1 and 2.3.1.1

SC abrevation	Secondary compound (SC)	Meropenem synergy screening												Cefadroxil synergy screening											
		MER at fixed sub-MIC						DiaMOND						CFX at fixed sub-MIC						DiaMOND					
		SC MIC_{Ref} (µM)	MIC_{MER} (µM)	MIC_{SC} (µM)	MIC_{SC} @ 1/4x MIC_{MER}	MIC_{SC} fold red	FICI	Class	MIC_{SC} (µM)	DiaMOND MIC_{MER} (µM)	MIC_{MER} Fold red	MIC_{SC} fold red	FICI	Class	SC MIC_{Ref} (µM)	MIC_{CFX} (µM)	MIC_{SC} (µM)	MIC_{SC} @ 1/8X MIC_{CFX}	MIC_{SC} Fold red	FICI	Class	MIC_{SC} (µM)	DiaMOND MIC_{CFX} (µM)	DiaMOND MIC_{SC} (µM)	MIC_{CFX} Fold red	MIC_{SC} Fold red	FICI	Class
AMK	Amikacin	3.13	20.00	1.64	1.46	1	1.13	NI	1.64	5.99	0.94	3	2	0.86	NI	3.13	64.00	1.64	1.55	1	1.07	NI	1.64	18.65	0.91	3	2	0.85	NI
BAC	Bacitracin	100.00	47.43	103.95	39.46	3	0.59	NI	93.46	10.32	51.61	5	2	0.77	NI	100.00	64.00	> 400	200.00	4	≤ 0.38	Sy	>400	32.50	50.77	2	16	≤ 0.57	NI
BDQ	Bedaquiline	0.13	47.43	0.03	0.02	1	0.78	NI	0.03	2.97	0.02	16	2	0.74	NI	0.03	64.00	0.11	0.05	2	0.60	NI	0.11	39.50	0.02	2	6	0.79	NI
CEF	Cefdinir	12.50	47.43	58.03	0.56	104	0.22	Sy	15.75	12.79	7.99	4	2	0.78	NI	12.50	64.00	13.58	9.86	1	0.85	NI	13.58	39.03	7.62	2	2	1.17	NI
CFM	Cefixime	100.00	47.43	419.39	45.15	9	0.32	Sy	447.98	8.73	43.65	5	10	0.28	Sy	400.00	64.00	401.00	373.64	1	1.06	NI	401.00	32.37	202.30	2	2	1.01	NI
CTT	Cefotetan (YM09330)	100.00	47.43	> 400	> 400	1	ND	ND	>400	23.83	119.15	2	7	≤ 0.65	NI	100.00	64.00	400.00	94.78	4	0.36	Sy	400.00	64.00	100.00	1	4	1.25	NI
CRO	Ceftriaxone	50.00	20.00	18.61	2.90	6	0.40	Sy	18.61	1.37	3.43	15	5	0.25	Sy	50.00	64.00	18.61	11.39	2	0.74	NI	18.61	8.51	6.65	8	3	0.49	NI
CFD	Cephradine	400.00	47.43	730.06	53.93	14	0.28	Sy	1378.00	8.73	174.68	5	8	0.31	Sy	400.00	64.00	> 400	400.00	2	≤ 0.63	NI	>400	33.28	208.00	2	4	≤ 0.59	NI
CAM	Chloramphenicol	12.50	47.43	16.60	15.42	1	1.14	NI	12.66	12.75	7.97	4	2	0.90	NI	12.50	64.00	11.85	12.50	1	1.18	NI	11.85	64.00	12.50	1	1	2.05	NI
CLA	Clarithromycin	100.00	47.43	23.76	8.81	3	0.58	NI	34.12	3.71	18.55	13	2	0.62	NI	25.00	64.00	77.14	100.00	1	1.42	NI	77.14	64.00	25.00	1	3	1.32	NI
CLI	Clindamycin	100.00	47.43	320.86	59.00	5	0.39	Sy	161.67	3.92	19.62	12	8	0.20	Sy	100.00	64.00	400.00	400.00	1	1.36	NI	400.00	256.00	400.00	0	1	5.00	NI
CFZ	Clofazimine	0.31	47.43	0.11	0.04	3	0.58	NI	0.35	6.38	0.10	7	4	0.42	Sy	0.31	64.00	0.53	1.24	0	2.45	NI	0.53	30.19	0.15	2	4	0.75	NI
CLX	Cloxacillin	100.00	47.43	290.03	66.79	4	0.44	Sy	186.81	5.43	27.17	9	7	0.26	Sy	200.00	64.00	100.00	100.00	1	1.13	NI	100.00	33.28	104.00	2	1	1.56	NI
DAP	Dapsone	20.00	47.43	10.36	27.15	0	2.83	NI	23.83	12.39	12.39	4	2	0.78	NI	20.00	64.00	23.40	80.00	0	3.54	NI	23.40	93.41	29.19	1	1	2.71	NI
ETP	Ertapenem	100.00	47.43	109.13	76.00	1	0.91	NI	100.00	11.40	57.00	4	2	0.81	NI	*NT*	*NT*	*NT*	*NT*	*NT*	*NT*	*NT*	*NT*	*NT*	*NT*	*NT*	*NT*	*NT*	*NT*
EMB	Ethambutol	12.50	47.43	7.42	1.55	5	0.42	Sy	8.56	3.98	2.49	12	3	0.37	Sy	12.50	64.00	23.88	15.13	2	0.76	NI	23.88	29.31	5.72	2	4	0.70	NI
ETH	Ethionamide	6.00	47.43	6.12	1.76	3	0.50	Sy	6.95	4.28	1.29	11	5	0.28	Sy	6.00	64.00	3.85	4.15	1	1.20	NI	3.85	48.86	4.58	1	1	1.95	NI
FDX	Fidaxomicin	3.13	20.00	1.33	0.29	5	0.46	Sy	1.33	2.27	0.35	9	4	0.38	Sy	3.13	64.00	1.33	< 0.10	27	≤ 0.16	Sy	1.33	2.19	0.11	29	12	0.11	Sy
FOS	Fosfomycin	100.00	47.43	> 400	> 400	1	ND	ND	>400	36.46	182.31	1	4	≤ 1.00	NI	100.00	64.00	> 400	> 400	1	ND	ND	>400	>256	>400	0	1	ND	ND
FUS	Fusidic acid	100.00	47.43	347.72	156.82	2	0.66	NI	316.08	7.99	39.97	6	8	0.30	Sy	100.00	64.00	101.91	< 3.13	65	≥ 0.14	Sy	101.91	22.04	34.44	3	3	0.67	NI
481	GVI10352-157A3	0.50	47.43	0.41	0.41	1	1.21	NI	0.60	15.98	0.40	3	2	1.01	NI	0.50	64.00	0.49	0.44	1	1.01	NI	0.49	42.85	0.33	1	1	1.35	NI
IPM	Imipenem	50.00	20.00	124.14	88.16	1	0.95	NI	124.14	9.58	23.95	2	5	0.66	NI	50.00	64.00	50.00	81.42	1	1.75	NI	50.00	29.93	23.38	2	2	0.94	NI
INH	Isoniazid	4.00	47.43	7.27	5.26	1	0.93	NI	6.75	23.71	4.74	2	1	1.20	NI	4.00	64.00	2.55	2.02	1	0.92	NI	2.55	33.48	2.09	2	1	1.34	NI
KET	Ketoconazole	25.00	47.43	13.06	11.67	1	1.10	NI	25.32	7.43	9.29	6	3	0.52	NI	*NT*	*NT*	*NT*	*NT*	*NT*	*NT*	*NT*	*NT*	*NT*	*NT*	*NT*	*NT*	*NT*	*NT*
LVX	Levofloxacin	1.25	47.43	0.86	0.60	1	0.92	NI	0.94	11.77	0.74	4	1	1.03	NI	1.25	64.00	0.27	0.25	1	1.04	NI	0.27	10.74	0.21	6	1	0.94	NI
LZD	Linezolid	0.31	47.43	1.24	1.53	1	1.45	NI	1.39	21.91	0.34	2	4	0.71	NI	1.50	64.00	1.55	1.76	1	1.26	NI	1.55	128.00	3.00	1	1	3.94	NI
MIN	Minocycline	6.25	47.43	4.93	1.72	3	0.56	NI	6.53	8.98	2.81	5	2	0.62	NI	6.25	64.00	7.08	3.36	2	0.60	NI	7.08	33.80	3.30	2	2	0.99	NI
MOX	Moxifloxacin	0.40	47.43	0.53	0.39	1	0.94	NI	0.37	11.40	0.23	4	2	0.86	NI	0.40	64.00	0.22	0.11	2	0.62	NI	0.22	31.35	0.20	2	1	1.38	NI
629	N22692-27-A1	0.06	47.43	0.07	0.08	1	1.33	NI	0.07	24.74	0.07	2	1	1.65	NI	*NT*	*NT*	*NT*	*NT*	*NT*	*NT*	*NT*	*NT*	*NT*	*NT*	*NT*	*NT*	*NT*	*NT*
366	N23902-22-1	0.31	47.43	0.45	0.26	2	0.79	NI	0.30	10.02	0.16	5	2	0.72	NI	0.31	64.00	0.27	0.09	3	0.46	Sy	0.27	17.25	0.08	4	3	0.58	NI
693	N28940-31-1	0.50	47.43	0.26	0.18	1	0.92	NI	0.43	8.12	0.20	6	2	0.64	NI	0.50	64.00	0.27	0.12	2	0.56	NI	0.27	18.48	0.14	3	2	0.83	NI
588	N33478-41-2	0.13	47.43	0.08	0.04	2	0.76	NI	0.11	7.31	0.05	6	2	0.60	NI	0.13	64.00	0.13	0.07	2	0.65	NI	0.13	22.68	0.05	3	3	0.70	NI
150	N34945-11-2	0.63	47.43	0.60	0.25	2	0.63	NI	0.45	5.88	0.19	8	2	0.53	NI	0.63	64.00	1.01	0.39	3	0.52	NI	1.01	28.22	0.28	2	4	0.72	NI
260	N6601-28-2	400.00	47.43	38.96	23.29	2	0.81	NI	65.45	1.40	27.98	34	2	0.46	Sy	*NT*	*NT*	*NT*	*NT*	*NT*	*NT*	*NT*	*NT*	*NT*	*NT*	*NT*	*NT*	*NT*	*NT*
173	N9772-72-1	1.00	47.43	0.56	0.57	1	1.24	NI	0.96	7.98	0.40	6	2	0.58	NI	1.00	64.00	0.59	0.40	1	0.82	NI	0.59	9.58	0.15	7	4	0.41	Sy
NFT	Nitrofurantoin	50.00	47.43	84.66	52.65	2	0.83	NI	87.32	17.36	43.39	3	2	0.86	NI	50.00	64.00	44.91	25.64	2	0.70	NI	44.91	22.63	17.68	3	3	0.75	NI
PAS	p-amino salicilic acid	0.50	47.43	0.32	0.13	2	0.62	NI	0.28	4.64	0.12	10	2	0.51	NI	0.50	64.00	0.45	0.41	1	1.05	NI	0.45	46.79	0.37	1	1	1.55	NI
PTD	Pretomanid	1.00	47.43	0.64	0.15	4	0.44	Sy	0.47	5.05	0.13	9	4	0.38	Sy	0.50	64.00	0.51	0.31	2	0.73	NI	0.51	22.27	0.17	3	3	0.69	NI
PTO	Prothionamide	3.13	47.43	1.16	0.48	2	0.62	NI	0.94	4.11	0.64	12	1	0.77	NI	3.13	64.00	1.46	1.73	1	1.30	NI	1.46	21.44	1.05	3	1	1.05	NI
RET	Retapamulin	100.00	47.43	9.37	9.30	1	1.20	NI	21.42	2.54	12.70	19	2	0.65	NI	12.50	64.00	31.25	1.34	23	0.17	Sy	31.25	21.64	4.23	3	7	0.47	Sy
RIF	Rifampicin	0.30	47.43	0.28	0.06	5	0.44	Sy	0.20	3.73	0.06	13	4	0.36	Sy	0.30	64.00	0.34	0.01	34	0.15	Sy	0.34	2.44	0.01	26	34	0.07	Sy
SPC	Spectinomycin	100.00	20.00	69.72	47.20	1	1.16	NI	69.72	9.44	47.20	2	1	1.14	NI	100.00	64.00	69.72	107.93	1	1.67	NI	69.72	140.96	220.25	0	0	5.36	A
SMX	Sulfamethoxazole	12.50	47.43	5.16	4.76	1	1.13	NI	15.97	21.91	13.70	2	1	1.32	NI	12.50	64.00	6.30	50.00	0	8.06	A	6.30	21.00	4.00	3	2	0.97	NI
SZD	Sutezolid	0.63	47.43	0.42	0.26	2	0.84	NI	0.29	9.08	0.29	5	1	1.16	NI	0.63	64.00	0.63	0.70	1	1.24	NI	0.63	72.28	0.71	1	1	2.27	NI
TBP-PI	Tebipenem-Pivoxil	25.00	47.43	22.68	6.61	3	0.50	Sy	13.80	10.30	12.88	5	1	1.15	NI	25.00	64.00	7.47	2.19	3	0.42	Sy	7.47	7.14	2.79	9	3	0.48	Sy
THZ	Thiacetazone	2.00	47.43	1.53	0.32	5	0.42	Sy	4.43	3.85	0.39	12	12	0.17	Sy	2.00	64.00	> 8	1.98	8	≤ 0.25	Sy	> 8	68.15	2.13	1	8	≤ 1.20	NI
TMP	Trimethoprim	100.00	47.43	> 400	> 400	1	ND	ND	>400	28.28	141.41	2	6	≤ 0.77	NI	100.00	64.00	> 400	> 400	1	ND	ND	>400	119.00	186.00	1	4	≤ 2.10	NI
VCM	Vancomycin hydrochloride	100.00	47.43	278.05	91.23	3	0.54	NI	351.50	16.15	80.74	3	4	0.57	NI	100.00	64.00	252.51	< 3.13	161	≤ 0.13	Sy	252.51	1.28	2.00	50	126	≤ 0.03	Sy

MIC_{Ref}: MIC used for experimental design. SC: secondary compound. MIC fold red: For every drug, ratio between MIC when assayed alone and MIC in the corresponding combination. Class: classification. *NT*: No Tested compounds.

2.7 APPENDIX II: Chapter 2 OPTIKA killing curves supplementary tables

Supplementary table 2.1. Mean log CFU/ml ± SD of data plotted in **Figures 2.10 to 2.13.**

	Mean Log CFU/ml ± SD								
Sample	**Day -3**	**Day 0**	**Day 1**	**Day 2**	**Day 4**	**Day 7**	**Day 14**	**Day 21**	**Day 49**
Untreated	4.15 ± 0.58	5.76 ± 0.77	5.2 ± 0.77	5.72 ± 0.8	6.42 ± 0.78	6.66 ± 0.56	6.93 ± 0.4	6.41 ± 0.41	7.81 ± 1.18
CEF 1x	NA	NA	2.41 ± 0.01	2.03 ± 0.02	2.03 ± 0.02	2.80 ± 0.00	3.85 ± 1.52	3.29 ± 1.54	6.79 ± 1.23
CFX 1x	NA	NA	3.85 ± 0.39	2.29 ± 0.19	2.67 ± 0.67	3.39 ± 0.35	7.55 ± 0.31	6.75 ± 0.39	8.06 ± 1.03
CLX 1x	NA	NA	3.17 ± 0.48	2.38 ± 0.32	2.42 ± 0.23	2.82 ± 0.05	7.04 ± 0.17	6.25 ± 1.16	8.43 ± 1.18
EMB 1x	NA	NA	5.98 ± 0.40	5.27 ± 1.72	5.52 ± 1.11	5.33 ± 1.43	5.10 ± 1.97	4.66 ± 2.61	7.58 ± 0.13
EMB-PTD 1x	NA	NA	5.09 ± 0.25	4.21 ± 0.50	4.46 ± 0.22	3.43 ± 0.39	2.92 ± 0.03	2.51 ± 0.21	3.70 ± 0.00
ETH 1x	NA	NA	5.36 ± 0.49	3.08 ± 0.42	2.38 ± 0.21	2.81 ± 0.02	2.90 ± 0.00	2.63 ± 0.40	4.13 ± 0.86
MER 1x	NA	NA	2.85 ± 0.17	2.09 ± 0.09	3.37 ± 0.72	4.56 ± 0.29	7.16 ± 0.38	6.20 ± 0.95	7.88 ± 0.44
MER-CFX-EMB 1x	NA	NA	2.40 ± 0.03	2.13 ± 0.01	2.15 ± 0.02	2.80 ± 0.00	2.90 ± 0.00	2.40 ± 0.00	3.93 ± 0.33
MER-EMB-CLX 1x	NA	NA	2.42 ± 0.05	2.05 ± 0.02	2.12 ± 0.06	2.80 ± 0.00	2.90 ± 0.00	2.40 ± 0.00	3.70 ± 0.00
MER-EMB-PTD 1x	NA	NA	2.37 ± 0.05	2.05 ± 0.04	2.05 ± 0.05	2.80 ± 0.00	2.90 ± 0.00	2.40 ± 0.00	3.70 ± 0.00
MER-EMB-TBP 1x	NA	NA	2.36 ± 0.03	2.00 ± 0.00	2.01 ± 0.06	2.80 ± 0.00	2.90 ± 0.00	2.40 ± 0.00	3.70 ± 0.00
MER-EMB-THZ 1x	NA	NA	2.39 ± 0.05	2.02 ± 0.02	2.07 ± 0.03	2.80 ± 0.00	2.90 ± 0.00	2.40 ± 0.00	3.70 ± 0.00
MER-PTD 1x	NA	NA	2.60 ± 0.34	2.07 ± 0.03	2.45 ± 0.42	2.80 ± 0.00	3.03 ± 0.27	2.45 ± 0.06	7.75 ± 1.70
MER-PTD-THZ 1x	NA	NA	2.49 ± 0.04	2.06 ± 0.03	2.25 ± 0.27	2.80 ± 0.00	2.90 ± 0.00	2.40 ± 0.00	3.70 ± 0.00
MER-THZ 1x	NA	NA	2.33 ± 0.04	2.00 ± 0.00	2.00 ± 0.06	2.80 ± 0.00	3.01 ± 0.14	3.17 ± 0.16	6.44 ± 0.72
PTD 1x	NA	NA	6.53 ± 0.23	6.55 ± 0.97	7.10 ± 0.30	7.11 ± 1.00	7.99 ± 0.27	6.78 ± 0.19	8.45 ± 0.41
PTD-THZ 1x	NA	NA	5.33 ± 0.65	5.14 ± 0.55	3.70 ± 0.11	2.83 ± 0.07	3.38 ± 0.96	3.20 ± 1.59	4.76 ± 1.94
RIF 1x	NA	NA	5.17 ± 0.07	4.43 ± 0.58	6.29 ± 0.89	5.92 ± 0.74	7.16 ± 0.28	5.94 ± 0.20	7.06 ± 0.67
TBP 1x	NA	NA	2.77 ± 0.09	2.12 ± 0.05	4.08 ± 0.36	5.66 ± 1.21	7.33 ± 0.34	6.36 ± 0.28	8.18 ± 0.64
THZ 1x	NA	NA	6.16 ± 0.51	5.74 ± 0.54	6.92 ± 0.15	6.52 ± 0.70	7.53 ± 0.27	6.63 ± 0.26	7.72 ± 1.02
CFX-EMB 1x	NA	NA	3.16 ± 0.42	2.19 ± 0.07	2.43 ± 0.13	2.82 ± 0.04	2.90 ± 0.00	2.48 ± 0.15	4.59 ± 1.79
EMB-CEF 1x	NA	NA	2.39 ± 0.03	2.07 ± 0.01	2.16 ± 0.03	2.80 ± 0.00	2.90 ± 0.00	2.48 ± 0.16	3.70 ± 0.00
EMB-ETH 1x	NA	NA	4.92 ± 0.17	2.54 ± 0.26	2.21 ± 0.06	2.80 ± 0.00	2.90 ± 0.00	2.40 ± 0.00	3.79 ± 0.18
EMB-RIF 1x	NA	NA	2.49 ± 0.05	2.15 ± 0.07	2.20 ± 0.03	2.80 ± 0.00	2.90 ± 0.00	2.40 ± 0.00	3.70 ± 0.00
EMB-TBP 1x	NA	NA	2.41 ± 0.04	2.09 ± 0.01	2.30 ± 0.10	2.80 ± 0.00	2.90 ± 0.00	2.40 ± 0.00	4.88 ± 1.49
EMB-THZ 1x	NA	NA	5.74 ± 0.41	5.42 ± 0.38	5.49 ± 0.37	3.25 ± 0.39	3.22 ± 0.42	2.40 ± 0.00	5.63 ± 2.55
EMB-CLX 1x	NA	NA	2.39 ± 0.05	2.07 ± 0.02	2.65 ± 0.51	2.80 ± 0.00	2.90 ± 0.00	2.40 ± 0.00	6.52 ± 2.45
EMB-PTD 1x	NA	NA	5.09 ± 0.25	4.21 ± 0.50	4.46 ± 0.22	3.43 ± 0.39	2.92 ± 0.03	2.51 ± 0.21	3.70 ± 0.00
MER-EMB 1x	NA	NA	2.42 ± 0.09	2.01 ± 0.01	2.05 ± 0.01	2.80 ± 0.00	2.90 ± 0.00	2.40 ± 0.00	-

Cefdinir (CEF), cefadroxil (CFX), cloxacillin (CLX), ethambutol (EMB), ethionamide (ETH), meropenem (MER), pretomanid (PTD), rifampicin (RIF), tebipenem (TBP), thioacetazone (THZ). NA: Not applicable. -: Missing experimental data.

Supplementary table 2.2. Mean log CFU/ml ± SD of data plotted in **Figures 2.14 to 2.18**

	Log CFU/ml ± SD								
Sample	**Day -3**	**Day 0**	**Day 1**	**Day 2**	**Day 4**	**Day 7**	**Day 14**	**Day 21**	**Day 49**
Untreated	4.15 ± 0.58	5.76 ± 0.77	5.2 ± 0.77	5.72 ± 0.8	6.42 ± 0.78	6.66 ± 0.56	6.93 ± 0.4	6.41 ± 0.41	7.81 ± 1.18
BDQ 1x	NA	NA	6.16 ± 0.38	4.79 ± 1.14	6.34 ± 0.86	6.42 ± 1.44	7.14 ± 0.08	6.83 ± 0.74	8.53 ± 0.66
BDQ-LZD 1x	NA	NA	5.76 ± 0.45	4.43 ± 1.19	6.60 ± 0.22	5.19 ± 0.30	6.89 ± 0.45	5.30 ± 0.15	7.30 ± 0.24
BDQ-PTD 1x	NA	NA	4.84 ± 0.39	4.76 ± 1.21	6.11 ± 0.69	4.72 ± 1.05	4.32 ± 1.25	2.69 ± 0.33	7.49 ± 0.28
BDQ-PTD-LZD 1x	NA	NA	4.28 ± 0.99	4.88 ± 1.10	4.94 ± 1.26	4.95 ± 0.87	6.94 ± 0.43	7.23 ± 0.62	8.01 ± 0.22
CFX 1x	NA	NA	3.85 ± 0.39	2.29 ± 0.19	2.67 ± 0.67	3.39 ± 0.35	7.55 ± 0.31	6.75 ± 0.39	8.06 ± 1.03
CFX-CFZ-BDQ-DLM 1x	NA	NA	3.93 ± 0.14	3.54 ± 0.18	2.78 ± 0.43	2.86 ± 0.12	3.02 ± 0.23	2.47 ± 0.14	4.61 ± 1.82
CFX-CFZ-BDQ-LZD 1x	NA	NA	4.21 ± 0.46	3.63 ± 0.17	3.31 ± 0.64	3.16 ± 0.28	3.81 ± 0.48	3.48 ± 0.74	5.86 ± 2.99
CFX-CFZ-BDQ-LZD-DLM 1x	NA	NA	4.05 ± 1.14	3.65 ± 0.55	3.40 ± 0.40	3.43 ± 0.68	4.23 ± 1.07	3.98 ± 1.14	5.41 ± 2.19
CFX-MOX-BDQ-DLM 1x	NA	NA	3.28 ± 0.28	2.88 ± 0.16	2.76 ± 0.86	2.93 ± 0.26	3.30 ± 0.38	2.49 ± 0.06	7.98 ± 0.04
CFX-MOX-BDQ-LZD 1x	NA	NA	4.01 ± 0.55	3.48 ± 0.27	4.43 ± 0.15	4.13 ± 0.94	3.86 ± 0.93	4.51 ± 0.14	4.79 ± 1.42
CFX-MOX-BDQ-LZD-DLM 1x	NA	NA	3.93 ± 1.26	3.15 ± 0.42	3.56 ± 0.94	3.65 ± 0.34	4.81 ± 0.64	4.30 ± 0.54	5.79 ± 2.09
CFZ 1x	NA	NA	6.41 ± 0.67	6.83 ± 1.10	8.21 ± 0.37	6.40 ± 1.49	7.80 ± 0.31	7.35 ± 0.18	8.10 ± 0.65
CFZ-BDQ-DLM 1x	NA	NA	5.73 ± 0.44	4.74 ± 0.90	4.27 ± 1.36	3.27 ± 0.54	3.38 ± 0.46	2.98 ± 0.89	6.45 ± 1.69
CFZ-BDQ-LZD 1x	NA	NA	4.08 ± 0.23	4.02 ± 0.58	3.56 ± 1.21	4.55 ± 0.53	6.11 ± 0.69	4.75 ± 1.00	7.71 ± 0.30
CFZ-BDQ-LZD-DLM 1x	NA	NA	4.67 ± 0.60	4.60 ± 0.47	4.12 ± 1.60	4.98 ± 1.36	5.71 ± 0.39	4.55 ± 1.12	8.26 ± 1.17
DLM 1x	NA	NA	5.62 ± 0.34	5.87 ± 0.67	7.66 ± 0.38	6.81 ± 0.67	7.61 ± 0.35	6.82 ± 0.43	8.19 ± 0.94
LZD 1x	NA	NA	6.09 ± 0.06	5.74 ± 0.52	7.37 ± 0.20	6.93 ± 0.43	7.66 ± 0.62	7.50 ± 0.10	8.41 ± 0.99
MER 1x	NA	NA	2.85 ± 0.17	2.09 ± 0.09	3.37 ± 0.72	4.56 ± 0.29	7.16 ± 0.38	6.20 ± 0.95	7.88 ± 0.44
MER-CFZ-BDQ-DLM 1x	NA	NA	2.82 ± 0.22	2.67 ± 0.36	2.86 ± 0.48	2.80 ± 0.00	2.90 ± 0.00	2.40 ± 0.00	6.34 ± 1.24
MER-CFZ-BDQ-LZD 1x	NA	NA	2.94 ± 0.17	3.07 ± 0.32	3.23 ± 0.41	3.01 ± 0.19	3.27 ± 0.43	2.94 ± 0.54	5.74 ± 2.42
MER-CFZ-BDQ-LZD-DLM 1x	NA	NA	2.98 ± 0.61	2.79 ± 0.43	2.94 ± 0.63	2.97 ± 0.21	2.99 ± 0.10	2.68 ± 0.50	5.82 ± 2.56
MER-MOX-BDQ-DLM 1x	NA	NA	2.59 ± 0.13	2.37 ± 0.25	2.62 ± 0.38	2.81 ± 0.01	2.93 ± 0.06	2.46 ± 0.08	7.35 ± 0.62
MER-MOX-BDQ-LZD 1x	NA	NA	2.66 ± 0.14	2.69 ± 0.56	3.13 ± 0.28	3.18 ± 0.22	4.71 ± 0.94	3.78 ± 0.82	8.37 ± 0.34
MER-MOX-BDQ-LZD-DLM 1x	NA	NA	2.87 ± 0.73	2.67 ± 0.41	2.94 ± 0.63	2.95 ± 0.31	3.65 ± 0.54	3.77 ± 0.47	7.35 ± 1.20
MOX 1x	NA	NA	6.80 ± 0.71	6.39 ± 0.30	6.05 ± 0.70	7.23 ± 1.07	7.71 ± 0.30	6.14 ± 0.29	-
MOX-BDQ-DLM 1x	NA	NA	4.94 ± 0.42	4.77 ± 0.45	5.85 ± 0.27	3.85 ± 0.49	3.65 ± 0.79	2.59 ± 0.38	6.84 ± 0.35
MOX-BDQ-DLM 1x	NA	NA	3.33 ± 0.41	3.09 ± 0.29	3.06 ± 0.89	3.37 ± 0.72	5.33 ± 0.88	3.20 ± 0.57	5.94 ± 0.34
MOX-BDQ-LZD 1x	NA	NA	5.04 ± 0.31	4.42 ± 0.54	5.71 ± 0.73	4.63 ± 0.91	4.48 ± 1.68	3.80 ± 1.71	6.97 ± 1.22
MOX-BDQ-LZD-DLM 1x	NA	NA	5.51 ± 0.57	5.04 ± 0.32	5.14 ± 0.62	4.05 ± 0.96	4.88 ± 1.34	4.93 ± 0.48	7.15 ± 2.04
PTD 1x	NA	NA	6.53 ± 0.23	6.55 ± 0.97	7.10 ± 0.30	7.11 ± 1.00	7.99 ± 0.27	6.78 ± 0.19	8.45 ± 0.41
PTD-LZD 1x	NA	NA	5.11 ± 0.25	4.47 ± 0.81	6.85 ± 0.29	6.26 ± 0.22	7.00 ± 0.20	6.32 ± 0.45	7.36 ± 0.30

Bedaquiline (BDQ), cefadroxil (CFX), clofazimine (CFZ), delamanid (DLM), linezolid (LZD), meropenem (MER), moxifloxacin (MOX), pretomanid (PTD). NA: Not applicable. -: Missing experimental data.

Chapter 3

Mechanism of action elucidation studies of the rifampicin/β-lactam synergy in mycobacteria

3.1 Introduction

Rifampicin, the corner stone drug for TB treatment, shows *in vitro* synergy with drugs that target the mycobacterial cell wall, such as ethambutol and β-lactams [83]. One hypothesis for the mechanism of action underlying this synergy is that the destabilization of the cell wall by ethambutol and β-lactams could lead to an increased uptake and higher intracellular accumulation of rifampicin [179]. However, levels of intracellular accumulation of rifampicin were insufficient to explain the strong drug interaction with these drug, especially in the case of cephalosporins [83].

The aim of this Chapter is to shed light through transcriptomics into the mechanism of action of these synergistic combinations.

Traditional approaches for biological research were limited to the study of one or a few genes at a time. However, with the emergence of high throughput approaches and the development of bioinformatics, the study of the whole genome, transcriptome, proteome, or metabolome of the organism of interest under a certain biological condition is already a reality. The massive sequencing development, also known as next-generation sequencing (NGS), led to the *omics* technologies onset.

Genomics is the field of biology that studies genes and genomes of organisms sequenced with high-throughput technologies, and thanks to it, evolutionary relationships between organisms can be established [180].

Proteomics and metabolomics use mass spectrometry and magnetic resonance imaging to identify and quantify proteins or metabolites present in an organism. The proteome and the metabolome provide information about its functioning and cell responses to determined conditions [181].

Finally, transcriptomics analyses cellular gene expressions. RNA-Seq is the method of choice to interrogate in a high-throughput manner the expression levels of genes in the genome with enough sensitivity to perform transcriptome profiling. RNA-Seq is typically used to understand transcriptomic variations with respect a control under different conditions such as oxygen levels, carbon sources or drug exposure to elucidate the biological mechanism behind them [182, 183].

In RNA-Seq studies, RNA samples are subjected to a complex process summarized in **Figure 3.1**. Briefly, starting from total RNA, mRNA is purified, and then, cDNA is synthetized, fragmented and sequenced. A quality process filters RNA-Seq data where low-quality reads are discarded. Afterwards, it is aligned to the reference genome

of the organism under study (if available and in our case *M. bovis* BCG). Finally, data is normalized, and a differential analysis performed by comparison with a control sample.

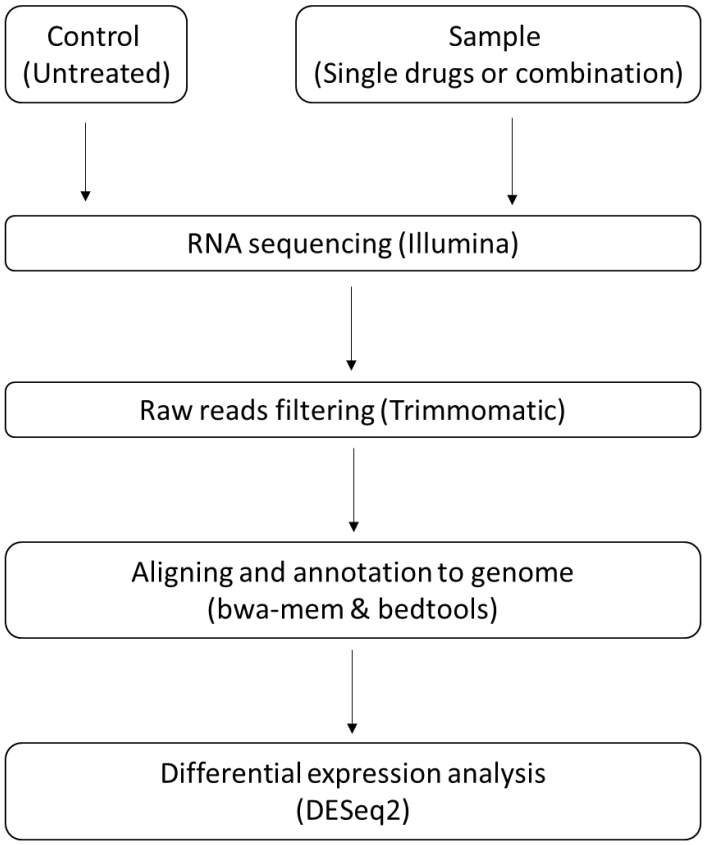

Figure 3.1. RNA-Seq and bioinformatic analysis schema. Extracted mycobacterial mRNA is sequenced. Bioinformatic analysis includes removal of low-quality reads, alignment of the sequenced data with the reference genome, determination of coding regions and finally comparison of the gene expression of the sample *versus* the control to obtain differentially expressed genes. Brackets indicate specific tools used in this Chapter 3.

The experimental design is of utmost importance when performing transcriptomic studies to elucidate the mode of action of antimicrobial compounds. Drug doses and the time of incubation need to be carefully defined before embarking on costly RNA-Seq studies.

Ethambutol and two β-lactams (*i.e.* meropenem and cefadroxil) were chosen to perform experiments described in this chapter for two main reasons: (i) all of them had shown *in vitro* synergy with rifampicin and, (ii) they are cell wall inhibitors with different molecular target.

The molecular target of all drugs included in this Chapter is shown in **Figure 3.2.**

- Rifampicin inhibits the RNA polymerase, blocking the bacterial RNA synthesis. It acts in synergy with the first-line anti-TB drug ethambutol. In addition, the synergy between β-lactams and rifampicin has been described in several mycobacterium species and different clinical isolates of *M. tuberculosis* [83, 184].

- Ethambutol acts at the cell wall formation level, inhibiting the arabinogalactan biosynthesis [185].

- β-lactams, unlike ethambutol, bind to transpeptidases that catalyse the peptidoglycan crosslinking and inhibit its biosynthesis. β-lactams included in this Chapter are meropenem (a carbapenem) and cefadroxil (a cephalosporin).

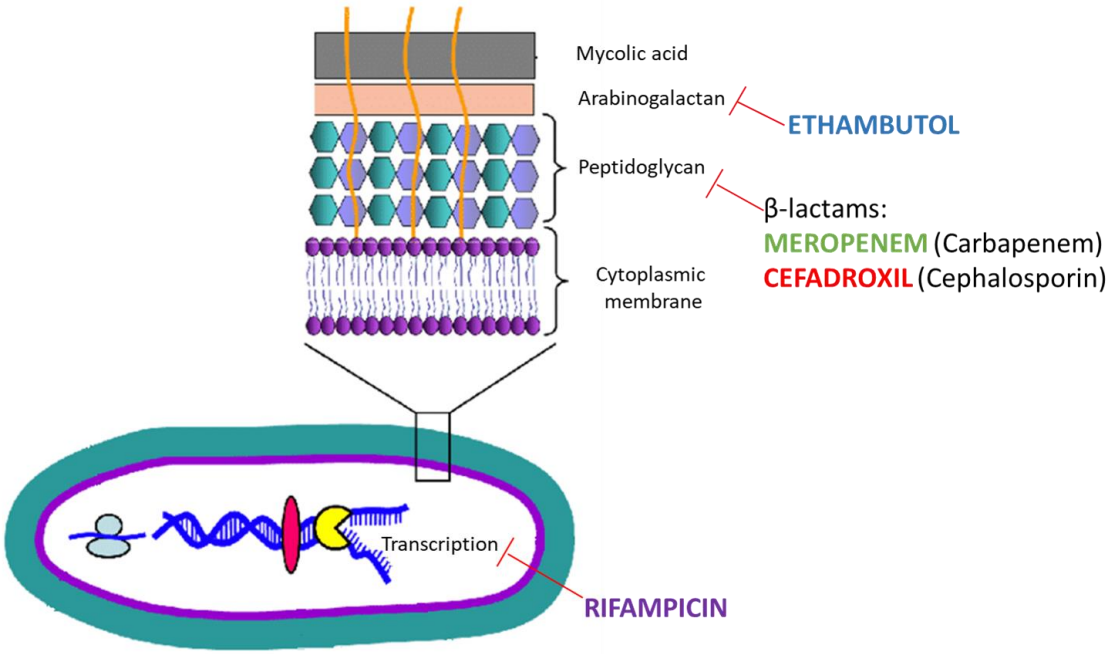

Figure 3.2. Rifampicin, ethambutol, meropenem and cefadroxil molecular targets. Adapted from [186]. Rifampicin targets the transcription. Ethambutol inhibits the arabinogalactan biosynthesis. β-lactams: meropenem (a carbapenem) and cefadroxil (a cephalosporin) alter the peptidoglycan layer biosynthesis.

The peptidoglycan constitutes the bacterial exoskeleton. It encapsulates the plasma membrane and gives rigidity to bacterial cells. Many molecules and cell wall components such as arabinogalactans are linked to this peptidoglycan layer [152].

Most bacteria show 4→3 links in their peptidoglycan layer. However, mycobacterial peptidoglycan is comprised by two different cross-links (**Figure 3.3**):

- 4→3 cross-links constitute around 20% of mycobacterial peptidoglycan. This cross-linking process is catalysed by serine D,D-transpeptidases, also called PBPs. At least, four PBPs have been described for *Mtb* (PBP1-PBP4). In general, PBP1 and PBP2 show high affinity with β-lactams. Nevertheless, two cephalosporins, cephalotin (1st generation) and cefoperazone (3rd generation), showed low affinity with PBP1 and PBP2. Most β-lactams show great affinity with PBP3 and low affinity with PBP4 [187].

- 3→3 cross-links constitute an 80% of the branches in the peptidoglycan layer. This process is catalysed by the lately discovered non-canonical cysteine L,D- transpeptidases (LDTs). Five LDTs have been found in the *M. tuberculosis* genome (Ldt_{Mt1} - Ldt_{Mt5}), four of which are strongly inactivated by carbapenems [188]. Members of the Ldt_{Mt1} family could be inactivated by cephalosporins, but with 1,000-fold lower efficacy than carbapenems [189].

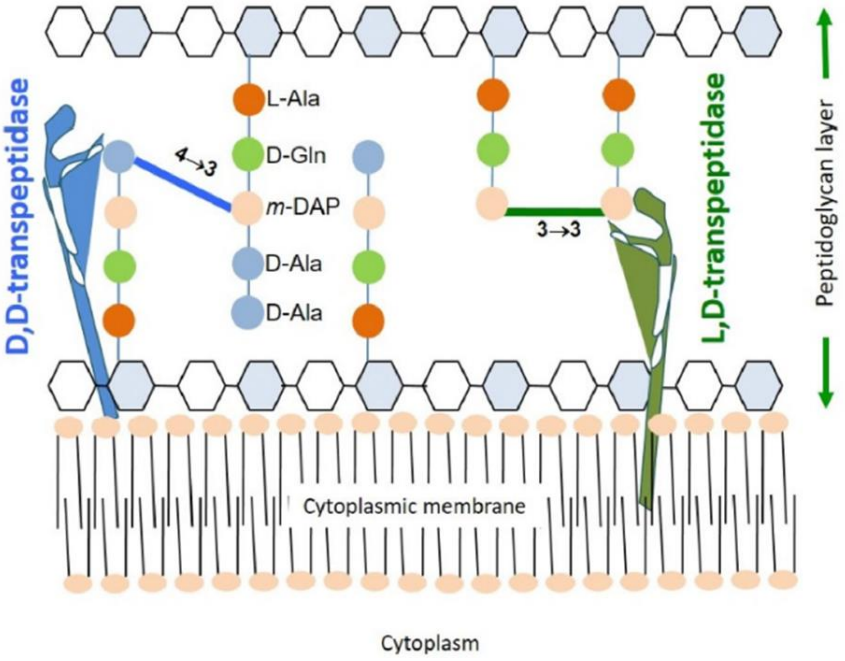

Figure 3.3. Mycobacterial peptidoglycan structure. Sugar chains of peptidoglycan are comprised of N-acetylglucosamine (white hexagons) and N-acetylmuramic acid residues (blue hexagons). Polypeptide chains are linked to these residues, and branches between these peptide chains are introduced by transpeptidases. 4→3 and 3→3 cross-links are catalysed by D,D-transpeptidases and L,D-transpeptidases, respectively. Figure from [152].

In the work described in this Chapter 3, we aimed to identify potential mechanisms of action that could explain the robustly observed synergy between rifampicin and β-lactams against mycobacteria. The global strategy is summarized as follows:

1. We used *M. bovis* BCG as a surrogate model of *Mtb*. The synergy observed in the reference work [83] was reproduced in *M. bovis* BCG, validating this strain for transcriptomic studies. Cultures were treated with rifampicin in three pair-wise combinations with drugs targeting the cell wall: ethambutol, meropenem and cefadroxil.

2. To detect bacterial adaptation in response to the antibiotic insult, cells needed to be perturbed but the cell death needed to be avoided. Thus, cells were treated at sub-inhibitory concentrations of the drugs for extended times prior to RNA sequencing.

3. The transcriptomic analysis was performed using an untreated culture as the control to analyse the differential gene expression. First, comparing with the gene expression of the untreated control, we identified genes differentially expressed in samples treated with single drugs and combinations. Second, the comparison of the transcriptomes of cultures treated with single drugs and those treated with drug combinations allowed us to identify general drug-dependant bacterial responses. Finally, our analysis was focused on the search of differentially expressed genes, operons or biological pathways, always comparing single drugs and combinations.

3.2 Material and methods

3.2.1 Bacterial strain, growth conditions, compounds information and reagents

M. bovis BCG (Pasteur 1173P2) strain was used for all experiments described in Chapter 3. Mycobacteria were routinely propagated at 37°C in 7H9 supplemented with 10% ADC, 0.2% glycerol and 0.05% (vol/vol) tyloxapol. Inoculum concentration was calculated with the standard relationship: OD_{600} nm of 0.125 corresponds to 10^7 CFU/ml.

The stock solutions of drugs and assay plates used in this study were prepared as described in previous Chapters (sections 1.2.1 and 2.2.1).

The MTT solution was prepared dissolving 5 mg/ml in Milli-Q water. Once dissolved, this solution was filtered through a 0.2 µm pore size, and aliquots were stored at -20°C until use.

SDS (Sodium Dodecyl Sulphate. Sigma, L4509) was dissolved at 10% in milliQ water, filtered through a 0.2 µm pore size and stored at room temperature until use.

3.2.2 FICI determination. MTT assay

Traditional checkerboard methodology was used for FICI determination as described in Chapter 1 (section 1.2.2.1) with small differences:

1. Drug interaction assays were performed in an 8x12 grid checkerboard layout in 384-well plates (Greiner 781091), so that one plate served to interrogate four pair-wise combinations. Assay plates were inoculated with *M. bovis* BCG (50 µl/well) at designated bacterial density (*i.e. ca.* 10^5 or 10^7 CFU/ml) and incubated at 37°C.

2. After 7 days, 25 µl/well of the MTT solution were added and further incubated at 37°C for 24 hours. Then, 25 µl/well of the SDS solution were added and overnight incubated at 37°C. Plates were then equilibrated at room temperature for 30 min and adhesive seals were placed. Absorbance at 580 nm was measured with Spectramax M5 Plate reader (Molecular Devices).

Calculations and the combination classification were done as described in Chapter 1 (sections 1.2.2 and 1.2.2.1).

3.2.3 CFU-based time kill assays

Exponentially growing cultures of *M. bovis* BCG were used for TKA. This pre-inoculum culture was distributed (10 ml) in 25 cm^2 tissue culture flasks and desired cell concentration adjusted with fresh assay media (7H9 + Gly + ADC + Tx 0.01%). Drug solutions were then added to the cultures at the designated final concentrations and TKA were performed as described in Chapter 1 (Section 1.2.4).

It should be noted that, as in other Chapters, SD was not included in killing curve plots for figure clearness. Mean Log CFU/ml and SD values can be found at appendix I of this Chapter.

3.2.4 Mechanism of action studies / experimental design

Bacteria were exposed to sub-inhibitory concentration of antibiotics for two days. Briefly, an exponentially growing culture of *M. bovis* BCG was split in 175 cm^2 culture flasks (Corning 431080). Per sample, the bacterial density was adjusted to 10^7 CFU/ml with fresh media (7H9 + Gly + ADC + Tx 0.01%) in a final volume of 100 ml. Drugs were added at the desired concentration according to **Table 3.1**. Flasks were incubated in horizontal position at 37°C for two days.

Sample	Treatment	Drug & concentration (µg/ml)
1	Untreated	NA
2	RIF 0.5x MIC	RIF 0.064
3	EMB 0.5x MIC	EMB 4
4	CFX 0.5x MIC	CFX 8
5	MER 0.5x MIC	MER 8
6	RIF-EMB 0.5x MIC	RIF 0.064 - EMB 4
7	RIF-MER 0.5x MIC	RIF 0.064 - MER 8
8	RIF-CFX 0.5x MIC	RIF 0.064 - CFX 8

Table 3.1. Selected conditions for transcriptomic studies. MIC values correspond to 10^7 CFU/ml cell density. Cefadroxil (CFX), ethambutol (EMB), meropenem (MER), rifampicin (RIF).

3.2.4.1 Mycobacterial RNA extraction

The total RNA was extracted from treated cultures after two days of drug exposure following the protocol kindly provided by Jesus Gonzalo Asensio (UNIZAR)

[190]. Briefly, cultures were pelleted by centrifugation. To protect RNA, pellets were resuspended in 1 ml of RNA protect bacteria reagent (Qiagen), incubated at room temperature for 5 minutes and then pelleted again by centrifugation.

Next steps of the protocol were performed on ice. Pellets resuspended on 400 µl of fresh lysis buffer (20 mM sodium acetate pH 5.5, 0.1 mM EDTA, 0.5% SDS in DEPC water) and 1 ml of acid phenol:chloroform 1:1 was added and then transferred to a lysis matrix tube. Cells were lysed using Fast Prep in three cycles of 15 seconds at speed 6.5. Samples were incubated on ice 5 minutes between cycles.

The tubes were centrifuged and supernatants were transferred to the tubes containing 900 µl of chloroform:isoamylalcohol 24:1. They were then carefully mixed by inversion and centrifuged. Upper phases were transferred to cold tubes containing 900 µl of isopropanol and 90 µl of acid sodium acetate. Precipitated nucleic acids were centrifuged. Pellets were washed with 1 ml of ethanol 70% and dried in a hood at room temperature for 10 minutes. Finally, they were dissolved in 90 µl of DEPC treated water.

The DNA was removed with DNase (Ambion) by incubation at 37°C for 1 hour. 1 ml of acid phenol:clorophorm 1:1 was added, and tubes were centrifuged. Supernatants were precipitated with 900 µl of isopropanol and 90 µl of cold acid sodium acetate. Precipitated RNAs were collected by centrifugation and resuspended in 30 µl of DEPC treated water. The RNA concentration in samples was determined with nanodrop and the RNA integrity was assessed by agarose gel electrophoresis.

3.2.5 Transcriptomics

Both mRNA sequencing and the bioinformatic analysis were done by FISABIO (Foundation for the Promotion of Health and Biomedical Research of Valencia Region). Samples were sequenced in technical duplicates.

The RNA was sequenced through *Illumina* system following the recommendations of the supplier (**Figure 3.1**). Bioinformatic analysis included a filtering by *trimmomatric* for the removal of low-quality leading and tailing reads and the drop of reads below 40 bases long. Reads were aligned with *bwa-mem* and strand-specific coverage annotation was performed with *bedtools*.

Differential expression analysis was done with *DESeq2* package [191]. The analysis of the differential expression of genes was performed considering untreated control *versus* all different treatments. *Log2FoldChange* and *p-adj* parameters were generated for each gene and drug condition.

3.2.5.1 Selection of differentially expressed genes with statistical significance. Volcano plots

Among all genes in the coding DNA sequence (CDS), those whose Log2FoldChange showed a value of -1.5 or lower were selected as downregulated. Similarly, genes with a Log2FoldChange value of 1.5 or higher were selected as overexpressed. Statistically significant results were those showing an adjusted p-value (p-adj) of 0.01 or lower.

These cut-off criteria for p-adj and Log2FoldChange parameters were maintained for all analyses.

Volcano plots were built to visualize statistical differentially expressed genes. For each gene, $-Log_{10}$Padj *vs* Log_2Fold Change were plotted.

3.2.5.2 Functional category analysis

Functional classification of genes was done according to functional categories described in Tuberculist (http://genolist.pasteur.fr/TubercuList/).

Since Tuberculist is a database containing information of *M. tuberculosis* H37Rv strain, *M. bovis* BCG genes were correlated with annotated *M. tuberculosis* H37Rv genes to perform functional category analysis. Orthologous genomes of *M. tuberculosis* H37Rv and *M. bovis* BCG were downloaded from MycoInDB (http://bif.uohyd.ac.in/mycoindb). Orthologous genes missing in MycoInDB were obtained from https://www.genome.jp.

M. bovis BCG genome was divided into 13 categories, 11 of them described in Tuberculist. Genes codifying ribosomal proteins according to *M. bovis* BCG annotation in MycoInDB were considered an additional category. Finally, 40 *M. bovis* BCG genes not annotated in *M. tuberculosis* H37Rv genome were categorized as *empty*. Most of them were pseudogenes. The thirteen resulting categories are listed below:

1. Virulence, detoxification, adaptation.
2. Lipid metabolism.
3. Information pathways.
4. Cell wall and cell processes.
5. Stable RNAs.
6. Insertion seqs and phagues.
7. PE/PPE.
8. Intermediary metabolism and respiration.

9. Unknown.
10. Regulatory proteins.
11. Conserved hypotheticals.
12. Ribosomal proteins.
13. Empty.

3.2.5.3 Enrichment analysis

The enrichment analysis was performed with selected sets of statistical differentially expressed genes.

This analysis was done with BiNGO software [192]. BiNGO relies on the Gene Ontology (GO) database [193], which includes gene biological annotations terms and pathways.

M. bovis BCG is not a model organism with an annotation file available in BiNGO. The gene annotation file (*gene_association.BCG*) was downloaded and manually enriched with information obtained from https://www.ebi.ac.uk/QuickGO/. This file contains the whole list of genes of the organism of interest and each gene is associated to the corresponding GO terms.

The ontology file (*go-basic.obo*) was downloaded from http://geneontology.org/ and links the gene ontology terms with their biological functions.

BiNGO provides biological pathways that are statistically overrepresented in a set of genes. It performs singular enrichment analysis (SEA), which provides individual annotated terms below the *enrichment p-value* threshold.

In this chapter, a *hypergeometric test* applying *Benjamini & Hochberg False Discovery Rate (FDR) correction* with a significance level of *0.05* using *whole annotation as reference set* was performed.

The results of the overrepresented biological pathways obtained from BiNGO analysis were visualized with TIBCO® Spotfire® Analyst software.

3.3 Results and discussion

3.3.1 Confirmation of drug interaction between rifampicin and compounds targeting the cell wall in *M. bovis* BCG

Prior to the transcriptomic studies, synergistic interactions already described in *Mtb* strains [83] were confirmed in the *M. bovis* BCG strain used in this Chapter 3. These experiments validated the use of *M. bovis* BCG as a surrogate model of *M. tuberculosis* H37Rv.

The isobologram in **Figure 3.4** shows the synergy profile observed in all pair-wise combinations selected at standard inoculum size conditions (*i.e.* 10^5 CFU/ml) by traditional checkerboard methodology based on growth inhibition (see material and methods section 3.2.2). As reported in the reference work [83] and confirmed here, rifampicin showed the strongest synergistic interaction with cefadroxil, followed by ethambutol and finally by meropenem.

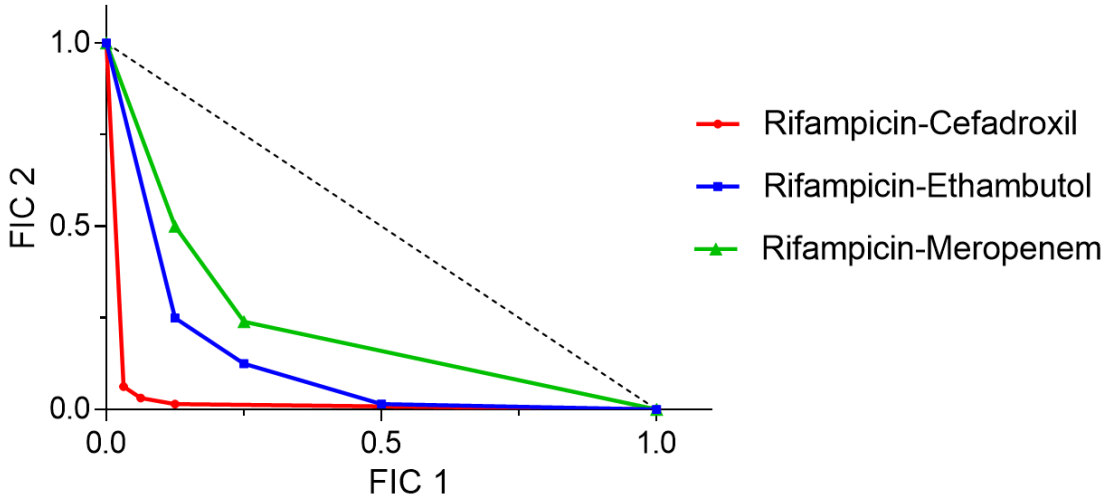

Figure 3.4. Fractional Inhibitory Concentrations isobologram. All combinations tested showed a concave contour with all FICI determined points under the no interaction limit (straight dotted line). Considering the curves' distance to the origin, the most synergistic combination was rifampicin-cefadroxil (red curve), followed by rifampicin-ethambutol (blue curve), and finally rifampicin-meropenem (green curve).

To assess the killing profile of combinations, TKA of combinations and single drugs were performed for three days by a traditional CFU counting assay (**Figure 3.5**).

Poor killing effect was observed at 1/4x MIC concentrations for single drugs or combinations. A similar behaviour was observed for single drugs at 1x MIC. However, at

1x MIC, all the combinations reached the limit of detection by day three. Rifampicin combined with meropenem showed the fastest profile, with low bacterial levels since day one. The rifampicin-ethambutol combination showed a slower profile, where the limit of detection was reached at day two. Finally, rifampicin combined with cefadroxil had the slowest effect and reached the limit of detection of bacterial growth at day three. These results confirmed the killing interaction profile described in the reference work [83] and validated the use of *M. bovis* BCG strain as a surrogate model of *M. tuberculosis* H37Rv to perform transcriptomic studies.

Surprisingly, the combination with the strongest interaction based on growth inhibition was the slowest one in terms of bacterial killing rate and vice-versa. This highlights the importance of considering not only results based on growth inhibition, but also killing ability and kinetics to prioritize combinations.

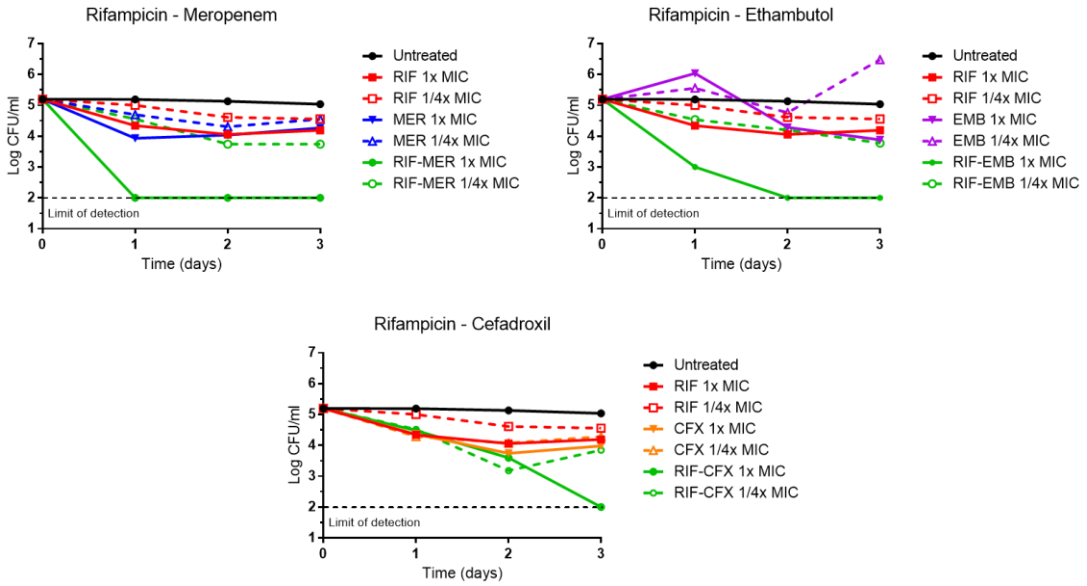

Figure 3.5. Killing curves of selected combinations. Combinations enhanced the killing profile of single drugs. The limit of detection was reached at 1x MIC of combinations at day 1 when rifampicin (RIF) was combined with meropenem (MER); at day 2 when it was combined with ethambutol (EMB) and after 3 days if it was combined with cefadroxil (CFX). MIC_{RIF} = 16 ng/ml, MIC_{MER} = 250 ng/ml, MIC_{EMB} = 4000 ng/ml, MIC_{CFX} = 8000 ng/ml.

TKA are usually performed at a starting inoculum of 10^5 CFU/ml. However, in order to improve the efficiency of the RNA extraction protocol, experiments (*i.e.* MIC and TKA) were repeated at a higher cell density (10^7 CFU/ml).

Cefadroxil is not soluble in DMSO and it was dissolved in DMSO:H_2O (1:1). This caused dispensation issues in the HP digital dispenser when tested at high concentrations. The MIC of cefadroxil at 10^7 CFU/ml could not be determined and the

maximum concentration tested (16000 ng/ml) was used as the MIC. This could have an impact on the experiment design because if the actual concentration was lower than 1/2x MIC, the effect on bacteria could be reduced or the killing kinetics may be slower than desired.

The duration of drug treatment was chosen once drug interactions of the selected pair-wise combinations were confirmed against *M. bovis* BCG. For this, bacterial cells need to be collected before the bacterial death occurs, but after a sufficient period of time to detect the drug effect.

Kill kinetics were also performed at high cell density (**Figure 3.6**). At day three, some combinations already reached the limit of detection; according to our transcriptomic strategy above described, this time point was too late since cells had started to die. Consequently, cells were collected and RNA was sequenced at day two (black arrow in **Figure 3.6**). This time point would allow us to detect transcriptional changes due to drug effect just before cell death.

The combination containing cefadroxil showed a slower killing rate when compared with the other combinations. In fact, at day two the difference between treated and untreated samples was minimum, although a clear synergistic effect was observed at day 30. This could be due to the already mentioned overestimation of the MIC of cefadroxil. Nevertheless, day two time point was chosen for all drugs in order to compared results afterwards.

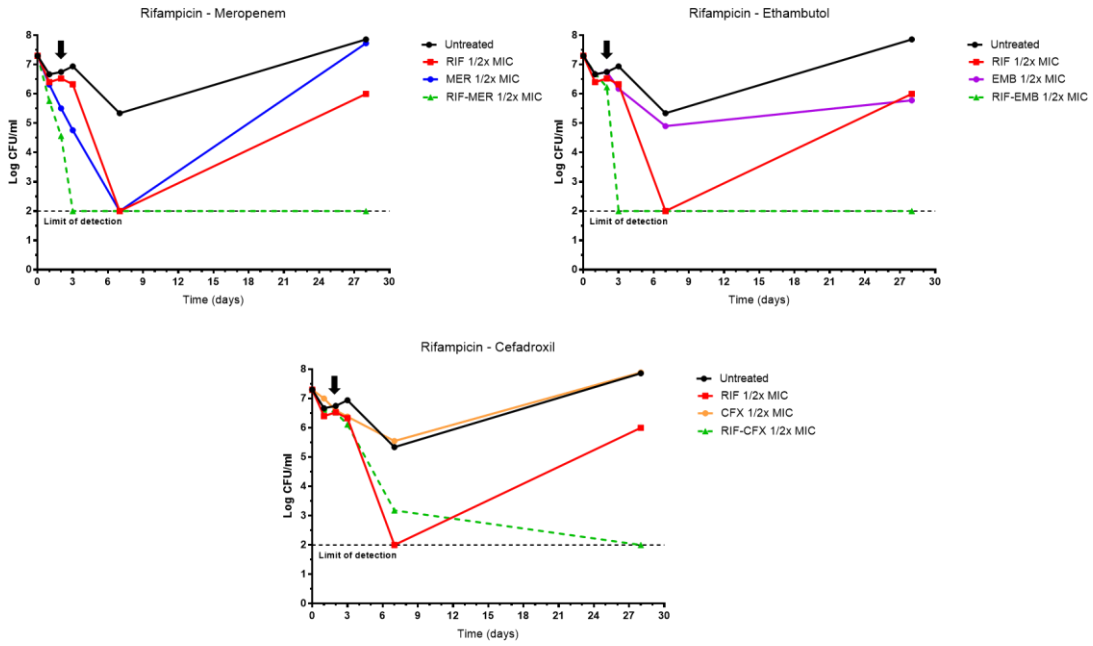

Figure 3.6. TKA at high cell density. Chosen drug concentrations presented the pursued effect showing strong killing ability when they were combined and low killing ability when assayed

alone at 0.5x MIC. Black arrow indicates the time point of cells collection for transcriptomics. MIC_{RIF} = 128 ng/ml, MIC_{MER} = 16000 ng/ml, MIC_{EMB} = 8000 ng/ml, MIC_{CFX} = 16000 ng/ml.

3.3.2 General transcriptomic profile analysis

RNA-Seq data was mined by Principal Component Analysis (PCA) in collaboration with FISABIO. Each point in the PCA plot represents the general transcriptomic profile of a particular condition. (**Figure 3.7**).

Transcriptomic responses were specific and combination dependent. Samples treated with single drugs were clearly separated from each other and from the untreated control. Cultures treated with drug combinations displayed far from the respective single drugs, indicating that the general transcriptomic profile was different and, therefore, bacterial response to treatment.

Samples treated with cefadroxil and rifampicin-cefadroxil were the closest to the untreated control, correlating with the low effect on bacterial killing observed at day two.

Interestingly, samples treated with rifampicin-ethambutol and rifampicin-meropenem displayed together and far from their respective single drugs, indicating that the transcriptional response of those combinations was very different from the individual response of the single drugs.

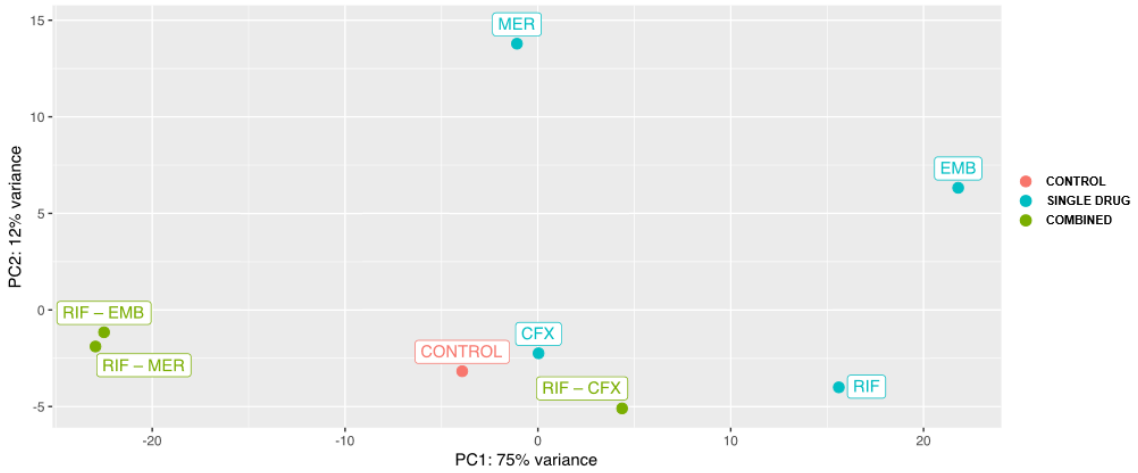

Figure 3.7. Principal component analysis (PCA) plot. Transcriptomic profile of untreated control, treatment with cefadroxil, ethambutol, meropenem, rifampicin, rifampicin-cefadroxil, rifampicin-ethambutol or rifampicin-meropenem. Samples treated with single drugs showed different transcriptional response. Combinations of rifampicin with ethambutol or meropenem showed similar response. Samples treated with cefadroxil or rifampicin-cefadroxil showed little transcriptional response comparing with the untreated control. In collaboration with Álvaro Chiner (IBV-CSIC). Cefadroxil (CFX), ethambutol (EMB), meropenem (MER), rifampicin (RIF),

rifampicin-cefadroxil (RIF-CFX), rifampicin-ethambutol (RIF-EMB), rifampicin-meropenem (RIF-MER).

3.3.3 Analysis of gene differential expression

Statistically significant differentially expressed genes were selected according to cut-offs defined in section 3.2.5.1 (*i.e.* p-adj ≤0.01 and Log2Fold Change ≥/≤ ±1.5). **Figure 3.8** displays volcano plots of all conditions used to represent the global transcriptomic response at the single gene level. The most statistically significant and differentially expressed genes were represented in the upper corners of the plots. The number of statistically differentially expressed genes was different depending on the treatment tested. All conditions showed more genes inhibited than overexpressed.

In line with the observation in the PCA plot, volcano plots of rifampicin-meropenem and rifampicin-ethambutol (**Figure 3.8 E** and **Figure 3.8 F**) showed similar profiles. For the cefadroxil and rifampicin-cefadroxil samples (**Figure 3.8 D** and **Figure 3.8 G**), genes were minimally differentially expressed comparing with the untreated control, which correlated with results from the PCA plot, where these two samples were placed close to the control. This observation could be related to the already mentioned slower effect of these treatments and the little effect that they showed at day two. For this particular case, the Log2Fold change cut-off could be lowered to a value closer to ±1. However, this would only allow selection of some genes in the case of rifampicin-cefadroxil. Only one gene of the cefadroxil sample showed a Log2Fold Change < -1.2, while all other genes were not differentially expressed above or below ± 0.8. However, changing the cut-off would imply the use of different criteria for different samples and results may not be comparable.

Due to the large number of repressed and overexpressed genes of samples not containing cefadroxil, instead of an individual gene analysis, a general transcriptomic analysis was performed focused on cellular processes and pathways.

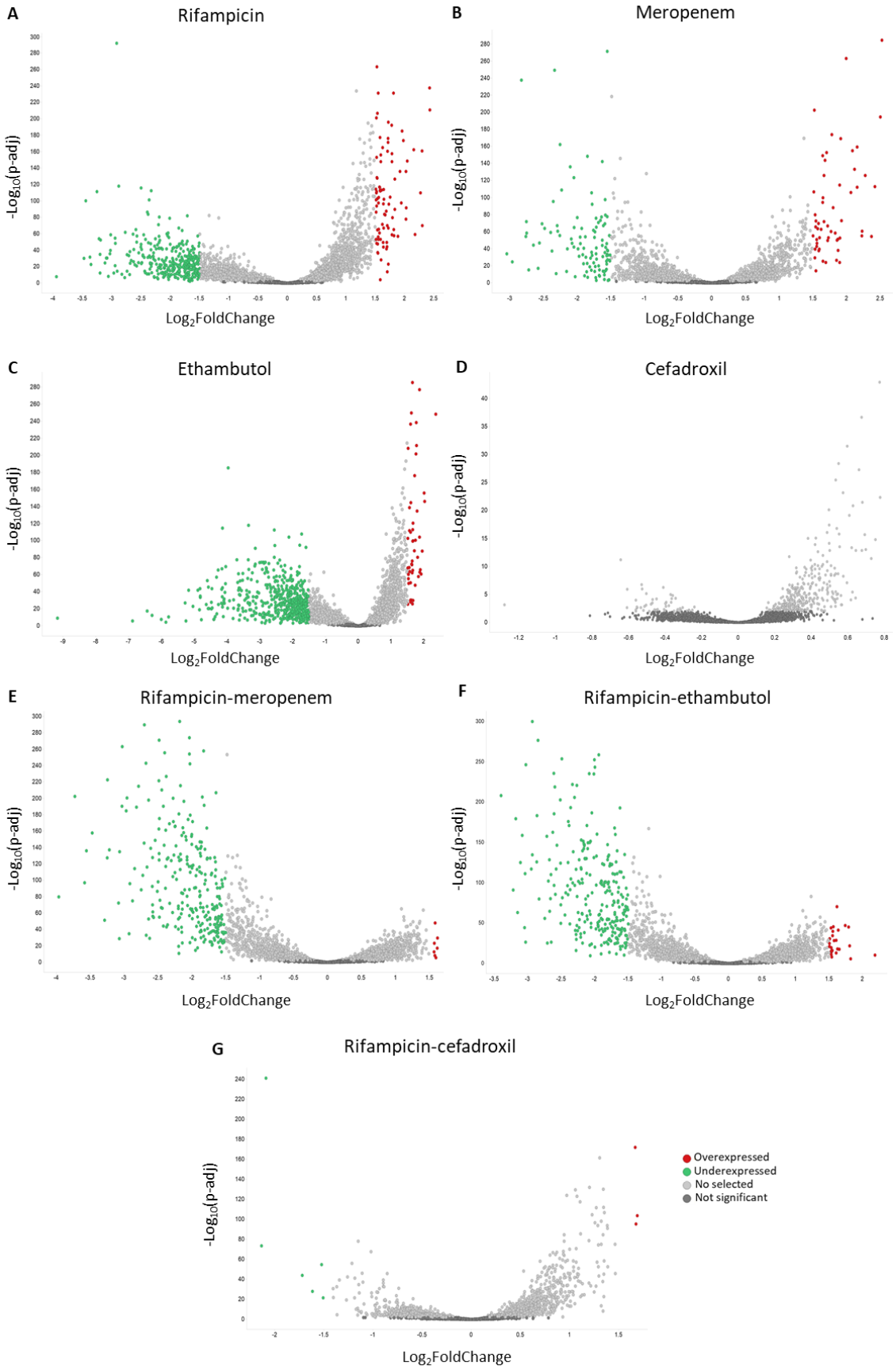

Figure 3.8. Differential gene expression volcano plots. Genes are plotted based on their differential expression and statistical significance under different treatments: **(A)** Rifampicin, **(B)**

Meropenem, **(C)** Ethambutol, **(D)** Cefadroxil, **(E)** Rifampicin-Meropenem, **(F)** Rifampicin-Ethambutol, **(G)** Rifampicin-Cefadroxil. Genes are coloured based on their classification: red for overexpressed (Log2Fold Change ≥ 1.5), green for downregulated (Log2Fold Change ≤ -1.5), dark grey for genes excluded because of low statistical significance (P-adj > 0.01) and light grey for genes statistically significant (P-adj ≤ 0.01) but not differentially expressed (-1.5 < Log2Fold Change > 1.5).

Figure 3.9 shows the number of genes differentially expressed per drug treatment grouped according to their functional category classification (section 3.2.5.2).

In the case of cefadroxil, no genes were selected applying filters of statistical significance and differential expression. In the case of cefadroxil combined with rifampicin, there were only nine genes. However, when comparing with rifampicin, there was a clear reduction in the number of genes differentially expressed under samples treated with rifampicin and those treated with rifampicin combined with cefadroxil. This reduction allowed us to hypothesize that, in combination with cefadroxil, the bacterial response to rifampicin was dominated by cefadroxil response, inducing silencing of rifampicin transcriptional response.

For the rest of the samples, most of the genes differentially expressed belonged to the conserved hypotheticals, cell wall and cell processes, and intermediary metabolism and respiration categories. This was expected considering that most genes in the *M. bovis* BCG genome were included in these three categories.

The following differences in bacterial response were identified:

1. Bacterial response to the single drugs rifampicin and ethambutol produced a comparable number of genes differentially expressed in every category. However, there were some differences to highlight:

    a) Cell wall and cell processes: bacterial response to rifampicin produced more overexpressed genes than ethambutol (22 *vs* 13), whereas the response to ethambutol caused more downregulation than rifampicin (96 *vs* 51) in genes belonging to this group.

    b) Intermediary metabolism and respiration: similarly to cell wall and cell processes, the bacterial response to rifampicin led to more genes of this category overexpressed (21 *vs* 5), and response to ethambutol produced more downregulated genes (83 *vs* 56).

2. In the case of meropenem, a smaller number of genes were differentially expressed compared to rifampicin and ethambutol.

3. Rifampicin-ethambutol and rifampicin-meropenem combinations showed a very similar profile, confirming that the similarities observed in the PCA plot between these two conditions were due to a similar bacterial response to treatment.

4. Response to rifampicin-ethambutol and rifampicin-meropenem: genes belonging to the cell wall and cell processes were less repressed than for single drugs treatment. Similarly, genes of the information pathway category were more downregulated comparing with single drugs.

5. In contrast to the response to rifampicin, bacteria exposed to rifampicin combined with either ethambutol or meropenem showed a great inhibition of genes belonging to the ribosomal protein category. This agrees with the hypothesis that bacterial adaptation to rifampicin was supressed when bacteria were exposed to rifampicin in combination with a synergistic partner, *i.e.* ethambutol or meropenem in this case. The inhibition of gene expression of ribosomal genes could be used as a biomarker, being an early indicator of bacterial death.

Figure 3.9. Functional classification of differentially expressed genes under different drug conditions. Statistically differentially expressed genes per drug treatment and category. Circle size represents the number of genes. Per category, colour represents the expression: green for downregulation, and red for overexpression. The total number of genes of each category in the whole genome is shown in brackets, adjacent to the category name. Cefadroxil (CFX), ethambutol (EMB), meropenem (MER), rifampicin (RIF), rifampicin-cefadroxil (RIF-CFX), rifampicin-ethambutol (RIF-EMB), rifampicin-meropenem (RIF-MER).

Figure 3.10 A shows a heat map of statistically significant expression of genes of samples treated with rifampicin, ethambutol, meropenem, cefadroxil, rifampicin-ethambutol, rifampicin-meropenem and rifampicin-cefadroxil. As in other plots already shown in this Chapter, upregulation and downregulation in samples treated with cefadroxil and rifampicin-cefadroxil was considerably lower than in the other samples. A new heatmap was done excluding these samples.

Figure 3.10 B shows a heat map of statistically significant expression of genes of samples treated with rifampicin, ethambutol, meropenem, rifampicin-ethambutol and rifampicin-meropenem. In this case, 922 genes were selected and, similar to **Figure 3.9,** it was observed an inversion in the level of expression of genes of samples treated with drug combinations comparing with single drugs. This effect was especially notable in two clusters, the PE/PPE and the ribosomal proteins genes (**Figure 3. 10 C** and **Figure 3.10 D**, respectively).

1. PE/PPE is a group of proteins exclusive of *Mycobacteriaceae* and actinobacteria members. Structurally, these proteins present proline-glutamic acid or proline-proline-glutamic acid residues at their conserved N-terminal domain, denominated PE and PPE proteins, respectively [194]. Numerous studies in this field [195-198] revealed different insights: (i) PE/PPE interact to act as heterodimers, (ii) they are linked with Type VII secretion system, (iii) they are implicated in nutrient transport across the cell wall and, (iv) they are involved in mycobacterial virulence. Immunogenicity showed by some of PE/PPE proteins suggested their potential as vaccine candidates against TB.

   However, details on the molecular mechanism of some of these processes remains unknown. The same happens with the regulation of the expression of PE/PPE proteins, where it has been found that PE and PPE proteins are not regulated as a group [199].

   Figure 3.10 C shows the heatmap of PE/PPE genes statistically differentially expressed under rifampicin, ethambutol, meropenem, rifampicin-ethambutol and rifampicin-meropenem exposure. From 169 PE/PPE genes in the whole genome, 43 of them were significantly differentially expressed under any of these conditions. The different degree of expression observed among them could be explained considering the already described independence of function and regulation of genes in this category [199].

2. In the case of the ribosomal proteins cluster (**Figure 3.11 C**), 42 out of 60 genes were significantly differentially expressed, being all of them slightly upregulated in the presence of rifampicin or ethambutol and strongly downregulated in the

presence of drug combinations. For meropenem, downregulation was observed in all genes, but it was weaker than within the combinations. This inversion in the response, depending on whether bacteria were treated with single drugs or combinations, suggested that drug combinations produced a bacterial perturbation that prevented the bacterial response observed when they were exposed to single drugs, similar to what we have previously described in the PE/PPE cluster. In other words, drug combinations would supress the bacterial adaptation to single drugs:

- First, the overexpression of ribosomal proteins of bacteria treated with rifampicin could constitute the bacterial adaptation to this drug.

- Second, the inhibition of almost the entire group of ribosomal proteins by drug combinations could imply a general turn-off of the transcriptional machinery.

- Finally, taking together the arguments exposed above, favourable drug interactions between rifampicin and either ethambutol or meropenem described by *in vitro* assays can be explained by the fact that bacterial adaptation to rifampicin increases the expression of ribosomal proteins. This adaptation is blocked in the presence of drug combinations, which leads to bacterial death. This could constitute the transcriptional indicator of bacterial death previously observed in whole cell time-kill assays.

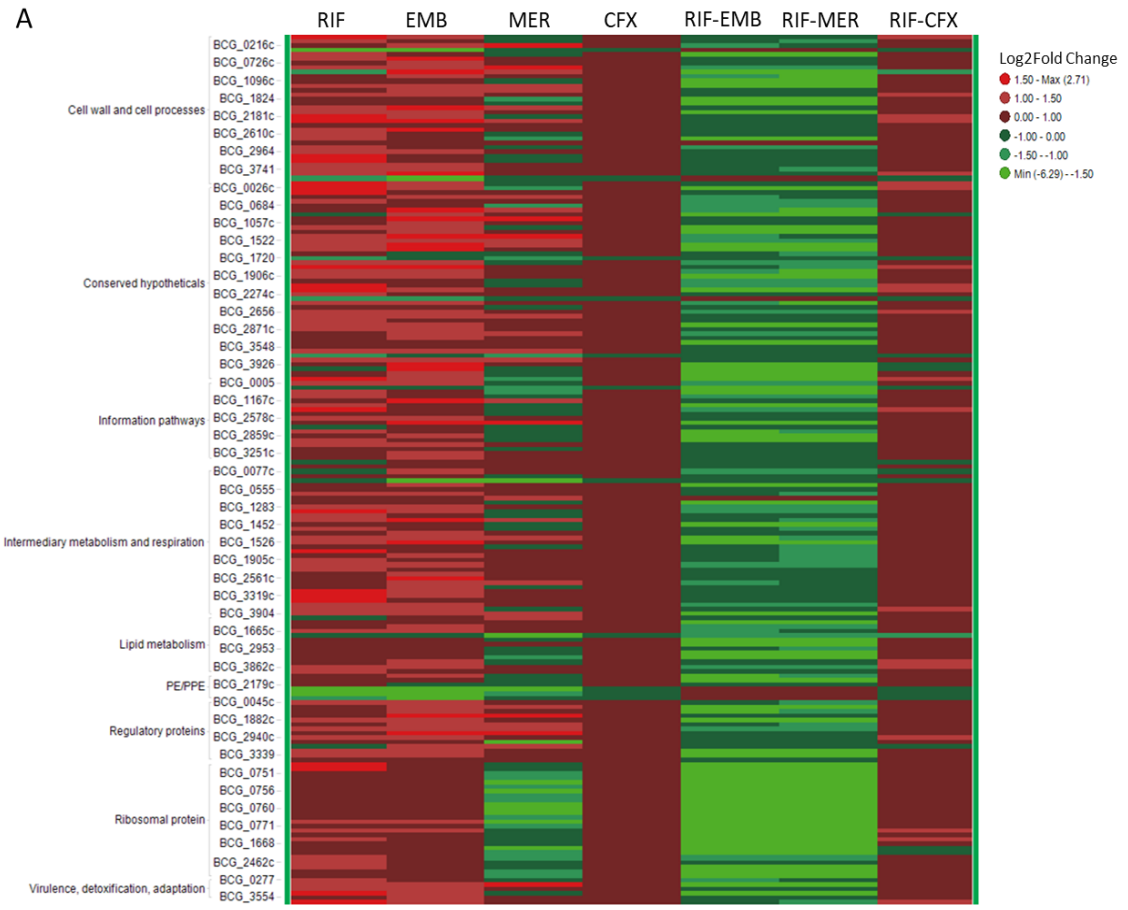
A
RIF
EMB
MER
CFX
RIF-EMB
RIF-MER
RIF-CFX
Log2Fold Change
1.50 - Max (2.71)
1.00 - 1.50
0.00 - 1.00
-1.00 - 0.00
-1.50 - -1.00
Min (-6.29) - -1.50
Cell wall and cell processes
Conserved hypotheticals
Information pathways
Intermediary metabolism and respiration
Lipid metabolism
PE/PPE
Regulatory proteins
Ribosomal protein
Virulence, detoxification, adaptation
BCG_0216c
BCG_0726c
BCG_1096c
BCG_1824
BCG_2181c
BCG_2610c
BCG_2964
BCG_3741
BCG_0026c
BCG_0684
BCG_1057c
BCG_1522
BCG_1720
BCG_1906c
BCG_2274c
BCG_2656
BCG_2871c
BCG_3548
BCG_3926
BCG_0005
BCG_1167c
BCG_2578c
BCG_2859c
BCG_3251c
BCG_0077c
BCG_0555
BCG_1283
BCG_1452
BCG_1526
BCG_1905c
BCG_2561c
BCG_3319c
BCG_3904
BCG_1665c
BCG_2953
BCG_3862c
BCG_2179c
BCG_0045c
BCG_1882c
BCG_2940c
BCG_3339
BCG_0751
BCG_0756
BCG_0760
BCG_0771
BCG_1668
BCG_2462c
BCG_0277
BCG_3554

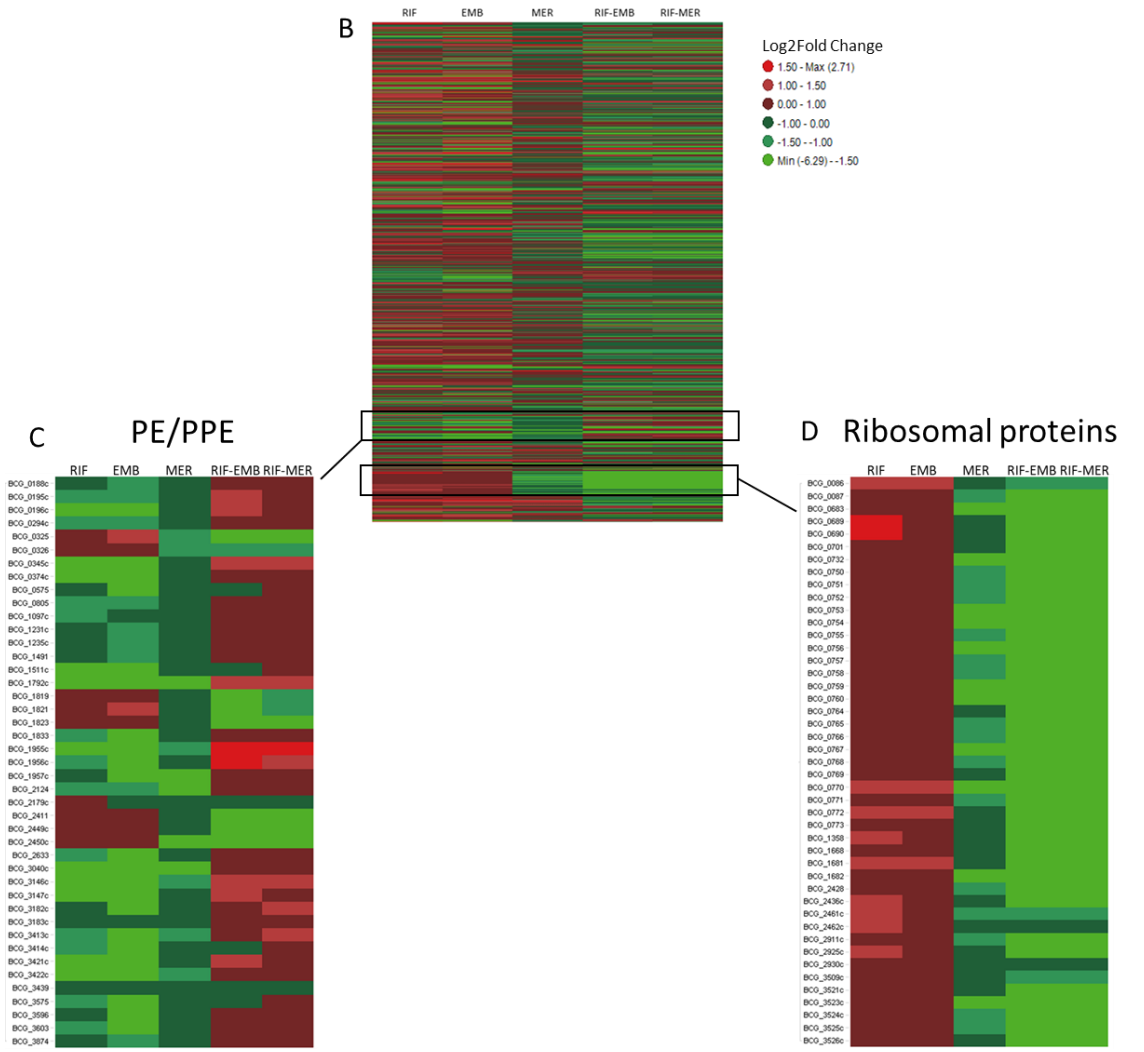

Figure 3.10 Heatmap of statistically significant genes. (A) Including cefadroxil. **(B), (C), and (D):** excluding cefadroxil. **(A):** 196 genes selected with p-adj ≤ 0.01 in all conditions. **(B):** 922 genes selected with p-adj ≤ 0.01 in all conditions containing RIF, EMB and MER. **(C):** 43 genes significantly expressed belonging to the PE/PPE category. **(D):** 42 genes significantly expressed belonging to the ribosomal protein category. Colour represents differential expression level; red for overexpression and green for downregulation. In both cases, darker colours indicate Log2Fold Change closer to 0 and lighter colours more differential expression. Cefadroxil (CFX), ethambutol (EMB), meropenem (MER), rifampicin (RIF), rifampicin-cefadroxil (RIF-CFX), rifampicin-ethambutol (RIF-EMB), rifampicin-meropenem (RIF-MER).

3.3.4 Enrichment analysis of molecular pathways

Enrichment analysis in transcriptomic studies is used to identify biological processes overrepresented in a set of genes. The study of biological processes, which involves several genes instead of individual ones, enhances the predictive power of transcriptomic studies. There are different methods and numerous tools to perform this analysis [200].

An enrichment analysis relies on the gene annotation in databases such as the Gene Ontology annotation terms. It compares the distribution of genes included in a determined set with their background distribution in the whole genome. Through enrichment analysis, terms that are statistically overrepresented among genes included in the selected set are identified and ranked by statistical significance, measured with the calculated *enrichment p-value* [201].

In this work, a molecular pathway enrichment analysis was performed using the BiNGO software (section 3.2.5.3). BiNGO is a tool that selects overrepresented molecular pathways from a set of genes. In the analysis performed in this Chapter 3, per drug condition, genes with statistical overexpression and downregulation (p-adj≤ 0.01 and Log2foldChange≥ 1.5 and ≤-1.5, respectively) were selected for BiNGO analysis.

BiNGO analysis is based on previously annotated gene information. Nowadays, term annotation is a live process, and it remains unfinished. Unfortunately, in the case of *M. bovis* BCG, a considerable number of genes are not annotated with the corresponding gene ontology term. This constitutes the main limitation of this analysis, which produces a lack of information of biological pathways of those selected genes with no information in the database. **Table 3.2** shows the number of selected genes and the number of these genes that BiNGO excluded from the analysis, per drug condition.

	Underexpression		Overexpression	
	Selected genes	Genes with no information	Selected genes	Genes with no information
RIF	329	181	88	39
EMB	271	109	53	34
MER	108	58	58	35
CFX	0	0	0	0
RIF-EMB	271	109	27	16
RIF-MER	283	107	7	6
RIF-CFX	6	3	3	1

Table 3.2. Number of selected genes per condition used for BiNGO analysis. Green and red represent statistical differentially expressed genes selected with the cut-off: p-adj ≤ 0.01 & log2Fold Change ≤-1.5 and p-adj ≤ 0.01 & log2Fold Change ≥1.5. In all cases, a considerable number of genes did not have GO information annotated, and thus, they were excluded from BiNGO analysis (*genes with no information* column). Cefadroxil (CFX), ethambutol (EMB), meropenem (MER), rifampicin (RIF), rifampicin-cefadroxil (RIF-CFX), rifampicin-ethambutol (RIF-EMB), rifampicin-meropenem (RIF-MER).

Overrepresented pathways among downregulated genes annotated in the database are shown in **Figure 3.11**. Samples treated with cefadroxil did not show any gene differentially downregulated. Six genes were selected for rifampicin-cefadroxil samples, but BiNGO analysis did not produce any overrepresented biological pathway related with them.

Ethambutol, meropenem, rifampicin-ethambutol and rifampicin-meropenem showed significant inhibition of general processes related with biosynthesis of different macromolecules. However, the rifampicin exposure produced inhibition of processes related with DNA synthesis, recombination and transposition.

This data revealed that bacterial adaptations to drugs at the conditions selected in this Chapter resulted in a general inhibition of biological pathways involved in cell replication and synthesis of biomolecules.

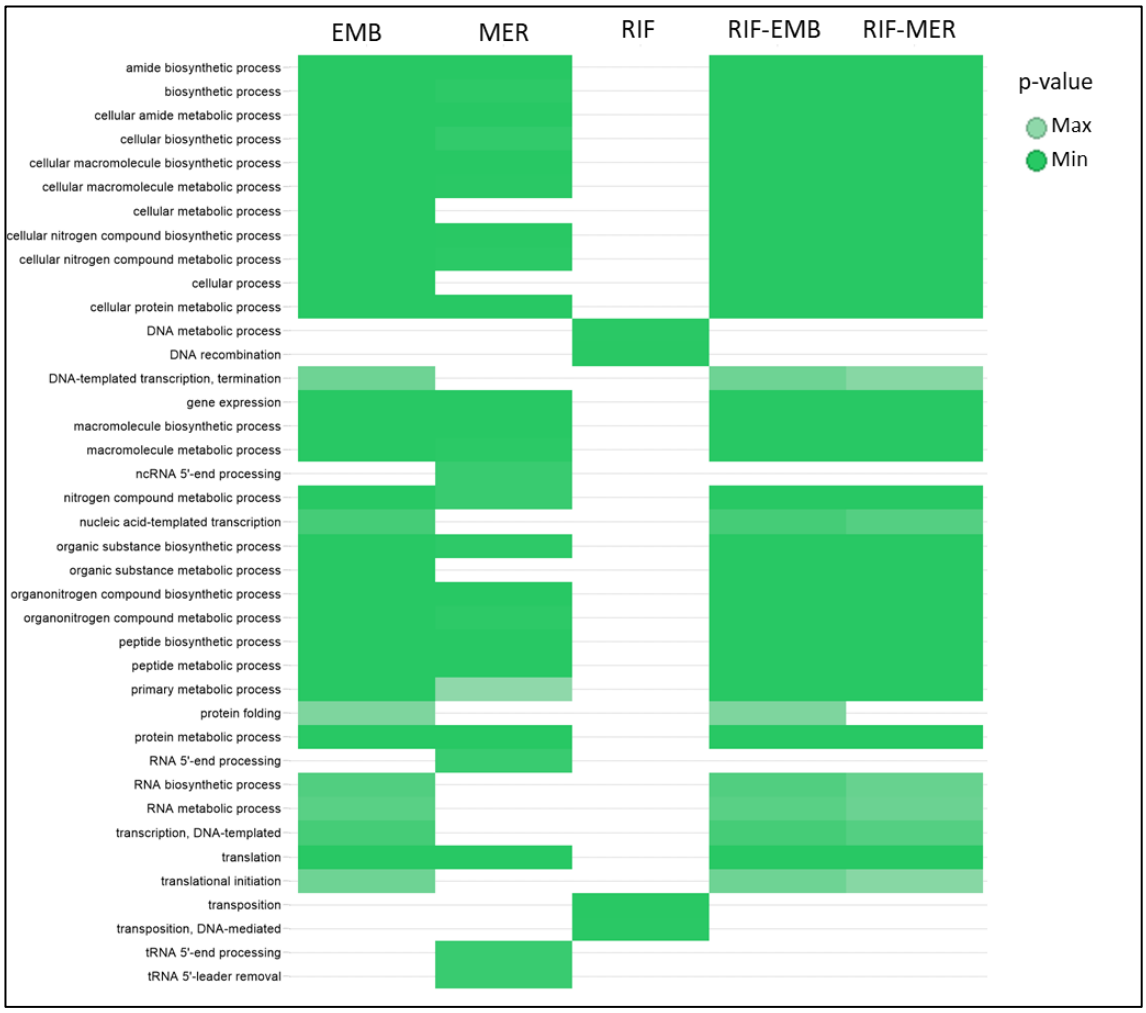

Figure 3.11. Biological pathways overrepresented in downregulated genes. BiNGO analysis of differentially downregulated genes with statistical significance (log2Fold Change ≤-1.5 & p-adj ≤ 0.01) identified statistically significant overrepresented molecular pathways, per drug condition. Processes are coloured according to an *enrichment p*-value being more intense for more statistically significant and lighter for less significant results. Cefadroxil (CFX), ethambutol (EMB), meropenem (MER), rifampicin (RIF), rifampicin-cefadroxil (RIF-CFX), rifampicin-ethambutol (RIF-EMB), rifampicin-meropenem (RIF-MER).

Overrepresented biological pathways of overexpressed genes are shown in **Figure 3.12**. Comparing with **Figure 3.11**, more variety among samples was found in the analysis of upregulated genes.

Figure 3.12. Biological pathways overrepresented in upregulated genes. BiNGO analysis of differentially overexpressed genes with statistical significance (log2Fold Change ≥1.5 & p-adj ≤ 0.01) per condition identified statistically significant overrepresented molecular pathways. Processes are coloured according to the enrichment p-value, being more intense for more statistically significant and lighter for less significant results. Cefadroxil (CFX), ethambutol (EMB),

meropenem (MER), rifampicin (RIF), rifampicin-cefadroxil (RIF-CFX), rifampicin-ethambutol (RIF-EMB), rifampicin-meropenem (RIF-MER).

In-depth analysis of the pathways overrepresented under different drug exposure showed some interesting findings that are discussed below:

1. **Arginine biosynthesis** was identified as an overrepresented pathway among upregulated genes. Interestingly, it was only present under rifampicin exposure (**Figure 3.12**).

   The d*e novo* l-arginine amino acid biosynthesis from l-glutamate amino acid is shown in **Figure 3.13**. This process consists of eight steps, which are catalysed by eight enzymes, *i.e.* argA to argJ.

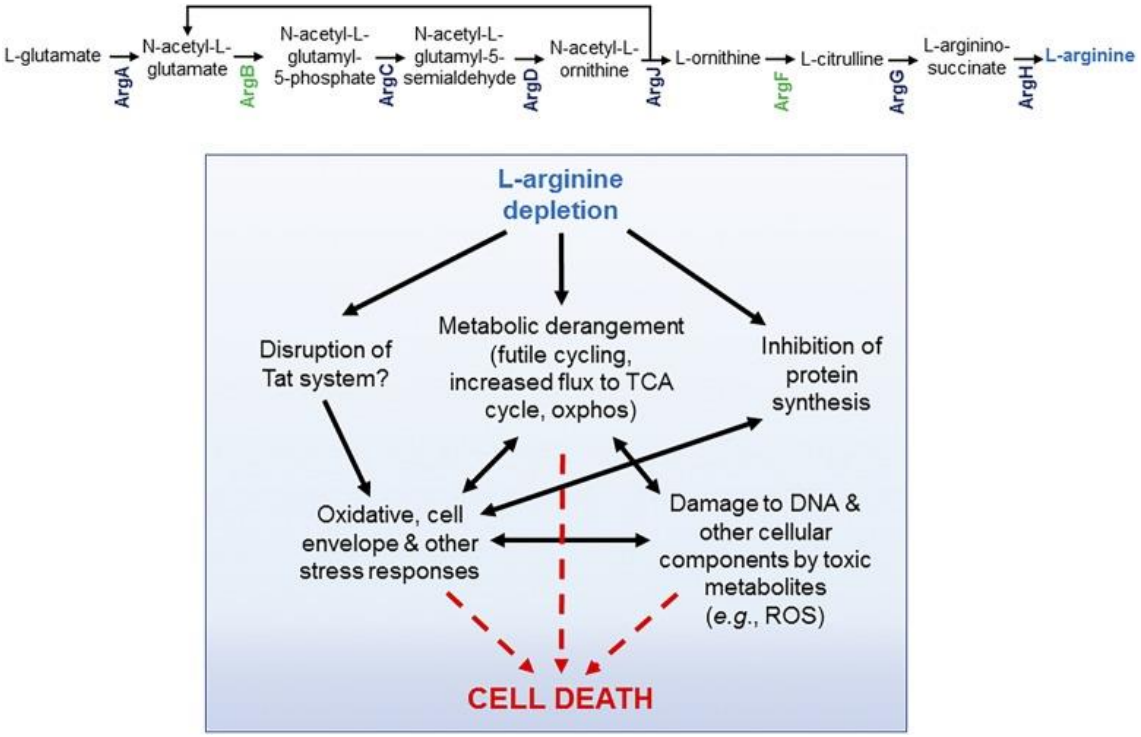

Figure 3.13. *De novo* L-arginine biosynthesis route. From [202].

The expression of seven genes of this pathway under different drug exposure studied in this Chapter 3 is shown in **Figure 3.14**. The already described inversion in single drugs *vs* the combination expression pattern was observed also here at the individual gene expression level.

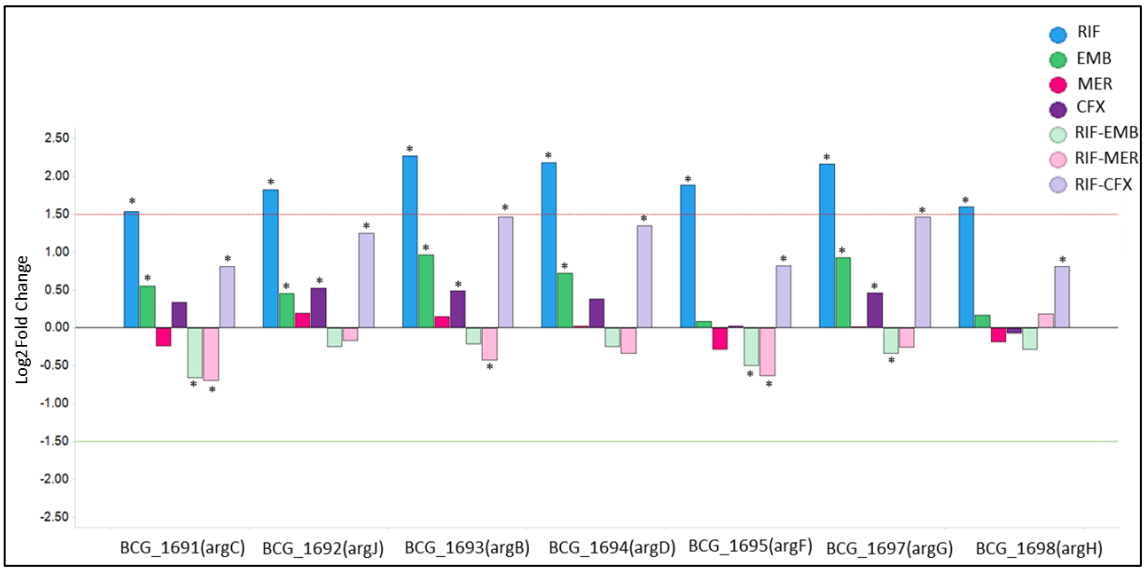

Figure 3.14. Differential expression of genes involved in arginine biosynthesis. Log2Fold Change of BCG_1691, BCG_1692, BCG_1693, BCG_1694, BCG_1695, BCG_1697 and BCG_1698 under rifampicin (blue), ethambutol (green), meropenem (pink), cefadroxil (purple), rifampicin-ethambutol (light green), rifampicin-meropenem (light pink) and rifampicin-cefadroxil (light purple) drug exposure. Statistically significant results (p-adj ≤ 0.01) are marked with an asterisk. Differential gene expression cut-offs are marked with red and green lines for overexpression and downregulation, respectively. ArgA is not included because Log2Fold Change was between -1.5 and 1.5 for all conditions.

The *de novo* arginine biosynthesis is a bacterial adaptative response to oxidative stress. Upregulation of this pathway was found when bacteria were exposed to bactericidal agents such as isoniazid or vitamin C [203]. Moreover, in mutants lacking this *de novo* arginine biosynthesis (ΔArgB or ΔArgF), a reduction of antioxidants was observed, with the presence of oxidative damage and subsequent bacterial death.

The upregulation of genes involved in the *de novo* biosynthesis of arginine under rifampicin treatment identified in our data set could be explained as a rapid bacterial adaptative response to the stress generated by this drug. Supporting our hypothesis, the damage produced by drug combinations prevented bacteria from mounting this response, potentiating the bactericidal effect of the combination.

2. **The phosphorelay signal transduction system** was overrepresented under meropenem and ethambutol conditions (**Figure 3.12**). Two-component regulatory systems are important bacterial mechanisms to respond to environmental changes. They are comprised by a histidine kinase protein typically placed in the membrane, which detects the external signal such as phosphate concentration, pH, and redox states among others. This sensor

interacts with the response regulator, a cytoplasmic protein that binds to the DNA and modifies the gene expression depending on the environmental change detected [204, 205].

Selected genes of this pathway included four genes belonging to the OmpR family, a class of response regulators of two-component regulatory systems (**Figure 3.15**).

Samples treated with meropenem or ethambutol showed overexpression in four genes belonging to the OmpR family, two of them were not characterized and the other two belonged to the PrrAB and MprAB systems. These two systems are involved in virulence of *M. tuberculosis*. MprAB is responsible of the cell wall maintenance, responding to envelope stress conditions. PrrAB is responsible for the intracellular adaptation and it is essential for *in vitro* growth, sensing and responding to nitrogen limitation [204].

As it happened in the arginine synthesis, this response was not observed in the combinations, suggesting that samples treated with single drugs, specifically those targeting the cell wall, *i.e.* meropenem and ethambutol, detected the antibiotic stress and mounted an adaptative response. However, cells exposed to drug combinations could not regulate this pathway to escape from this antibiotic stress.

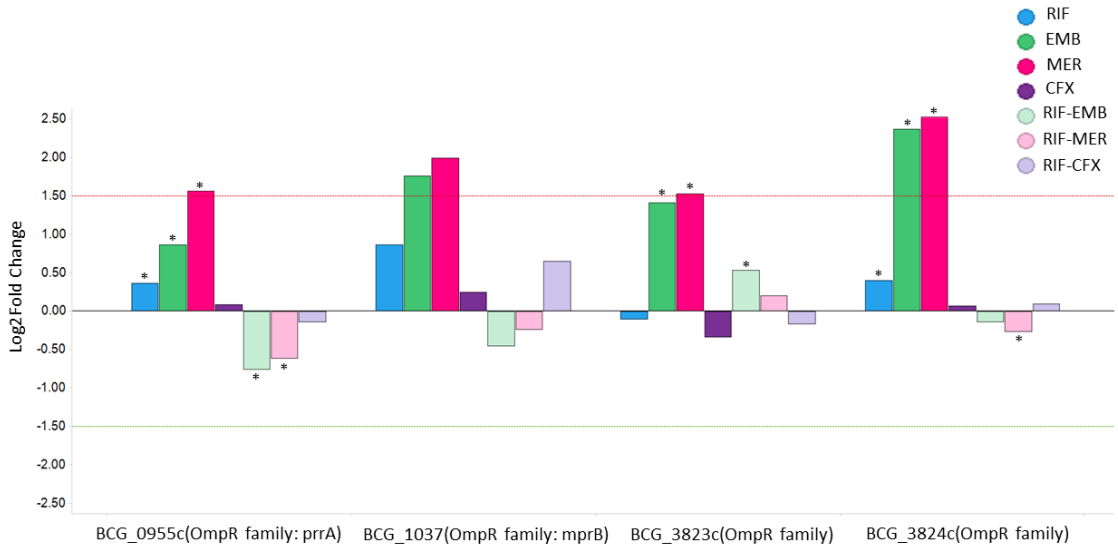

Figure 3.15. Differential expression of some genes involved in phosphorelay signal transduction system pathway belonging to the OmpR family. Log2Fold Change of BCG_0955c, BCG_1037, BCG_3823c and BCG_3824c under rifampicin (blue), ethambutol (green), meropenem (pink), cefadroxil (purple), rifampicin-ethambutol (light green), rifampicin-meropenem (light pink) and rifampicin-cefadroxil (light purple) drug exposure. Statistically

significant results (p-adj ≤ 0.01) are marked with an asterisk. Differential gene expression cut-offs are marked with red and green lines for overexpression and downregulation, respectively.

3. **BCG_1415c** gene showed downregulation under exposure to rifampicin or ethambutol and upregulation close to the cut-off when rifampicin was combined with ethambutol or meropenem (**Figure 3.16**). Although the expression of BCG_1415c under rifampicin-ethambutol and rifampicin-meropenem was weak, it should be considered that, in general, the upregulation response was weaker than downregulation under conditions described in this chapter.

   BCG_1415c is described as a transcriptional regulatory protein in the database. The Rv1353c gene, its orthologous in *M. tuberculosis* H37Rv, was recently described as a transcriptional regulator whose upregulation has been identified as an indicator of synergistic combinations [206].

   Our data support this finding. Comparing the expression of this gene under single drugs and already known synergistic combinations, it can be observed that it is upregulated in the case of the combinations. Unfortunately, the mechanism of action of this regulation remains unknown.

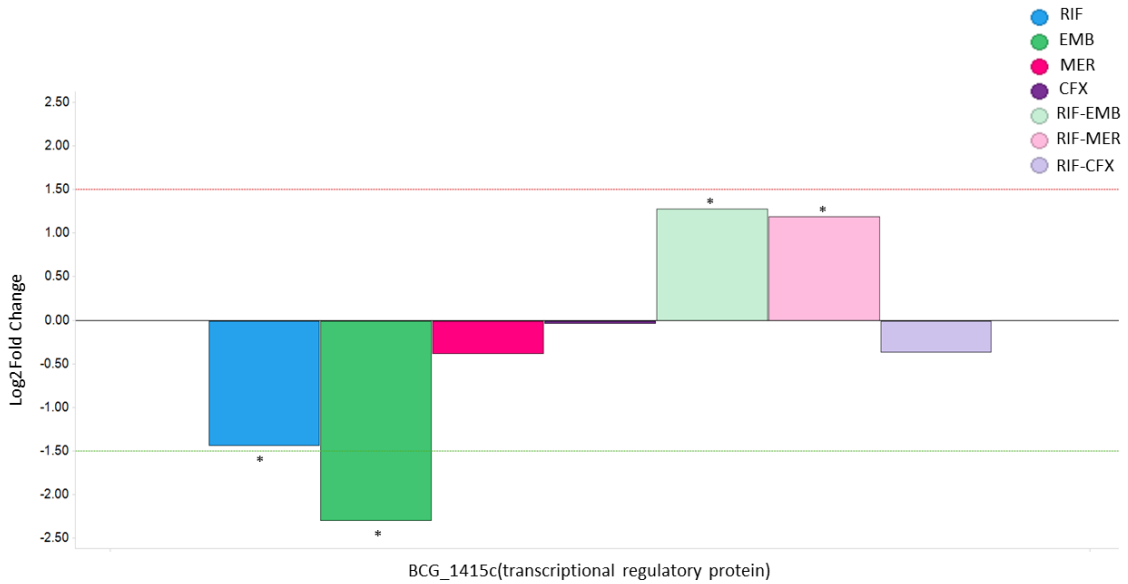

Figure 3.16. Differential expression of BCG_1415c gene. Under rifampicin (blue), ethambutol (green), meropenem (pink), cefadroxil (purple), rifampicin-ethambutol (light green), rifampicin-meropenem (light pink) and rifampicin-cefadroxil (light purple) drug exposure. Statistically significant results (p-adj ≤ 0.01) are marked with an asterisk. Differential gene expression cut-offs are marked with red and green lines for overexpression and downregulation, respectively.

4. Lastly, the ***ini*BAC operon** expression was clearly influenced by conditions tested in this work (**Figure 3.17**).

This operon is comprised by three genes: BCG_0380 or *iniB*, BCG_0381 or *iniA,* and BCG_0382 or *iniC*.

IniBAC promoter is induced by the presence of different drugs that specifically target the cell wall biosynthesis such as isoniazid, ethambutol, ethionamide, and ampicillin among others. This induction was found to be specific to the cell wall biosynthesis inhibition because it was not observed under other biological stresses such as heat shock, oxidative stress, cell wall degradation or treatment with drugs that do not target the cell wall (*i.e.* rifampicin) [207].

Considering overexpression of *iniB, iniA and iniC* genes a consequence of the promoter induction, data shown here agrees with previous findings. Only bacteria treated with cell wall inhibitors (*i.e.* ethambutol and meropenem) showed significant overexpression of all genes of this operon (**Figure 3.17**). The induction caused by ethambutol has been previously described, as well as the repression under rifampicin treatment [207]. However, upregulation caused by meropenem has not been described before. Samples treated with cefadroxil did not produce statistically significant results and samples treated with drug combinations showed downregulated genes.

The function of these genes remains unknown. Initially, its induction was linked to cell death. Afterwards, *iniA* was described as an efflux pump component that mediated multi-drug tolerance [208]. This last observation would explain the *iniBAC* overexpression under ethambutol or meropenem conditions as an adaptative bacterial response to escape of the drugs damage. In contrast, bacteria treated with ethambutol or meropenem combined with rifampicin would not be able to mount this response, being more exposed to the damage caused by these drugs.

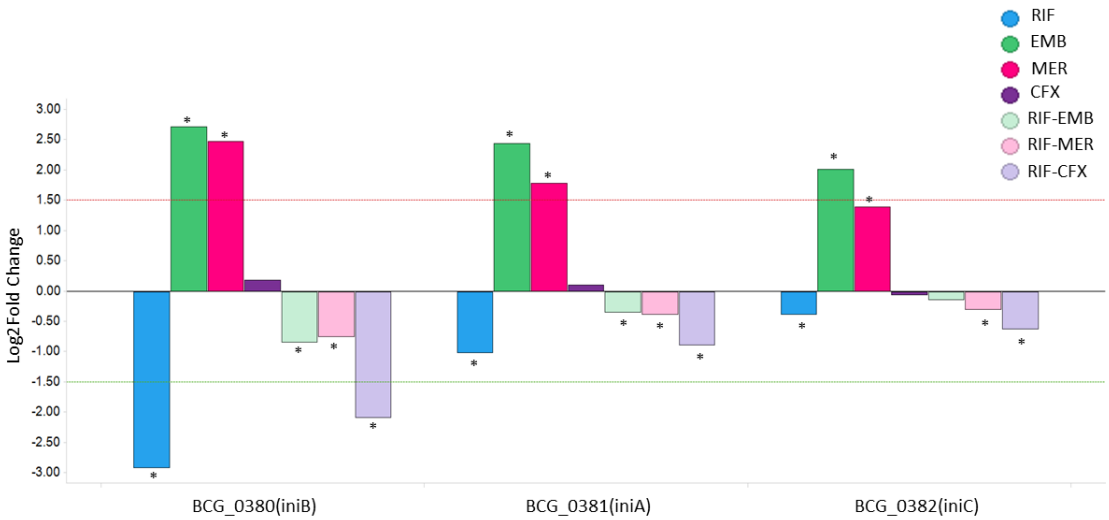

Figure 3.17. Differential expression of *iniBAC* operon. Log2Fold Change of BCG_0380, BCG_0381, and BCG_0382 under rifampicin (blue), ethambutol (green), meropenem (pink), cefadroxil (purple), rifampicin-ethambutol (light green), rifampicin-meropenem (light pink) and rifampicin-cefadroxil (light purple) drug exposure. Statistically significant results (p-adj ≤ 0.01) are marked with an asterisk. Differential gene expression cut-offs are marked with red and green lines for overexpression and downregulation, respectively.

3.4 General discussion and future perspectives

Antibiotics are largely known as molecules that kill bacteria. For many of them, their interaction with a specific protein or molecular component (*i.e.* their mechanism of action) is well characterized and drugs are associated to their molecular target [209].

However, antibiotics not only affect bacteria at their target level. It has already been described that antibiotic tolerance implies similar bacterial responses at a molecular level independently of the antibiotic and their specific target [210]. Antibiotic exposure induces bacterial physiological changes, such as elongation produced by DNA synthesis inhibition or increased ribosome concentrations caused by translation inhibitors. Other changes modulate the concentration of second messengers and transcription factors that ultimately alter the gene expression [211].

Antibiotics are typically stress agents that alter the global gene expression of bacteria in many different ways. For example, (i) by inducing the expression of their target to overcome its inhibition, (ii) by increasing the expression of genes involved in reparation of the specific damage or (iii) expressing efflux pumps to avoid the antibiotic intracellular accumulation. Other processes are directed to reduce the damage caused by oxidative stress, such as the expression of (i) two-component systems, (ii) iron-sulfur cluster containing proteins or (iii) SOS response activation, among others [183, 209, 211, 212].

Bacteria can modulate their general gene expression to increase survival rates during adverse conditions. Variations in mRNA expression levels can be used as a tool to infer bacterial phenotype information. This global gene expression adaptation occurs not only under different physiological conditions that compromise the cell homeostasis integrity, but also in the presence of antibiotics. Moreover, this expression depends on the concentration and the time of treatment and the antibiotic itself [183].

In this Chapter 3 we aimed to gain insights on the mechanism of action of synergistic combinations containing rifampicin and cell wall inhibitors:

1. First, we validated our *M. bovis* BCG strain, confirming the synergy in standard *in vitro* assays, *i.e.,* checkerboard and time-kill assays.

2. Second, transcriptomic conditions were defined as sub-inhibitory concentrations of drugs and long times of exposure. These were key parameters which allowed us to collect cells perturbed by drugs, but still viable. This increased the dynamic

window, which was needed to measure the bacterial adaptive response to the combinations and single drugs.

3. Third, although inhibition of direct targets of the selected drugs was not observed, after the transcriptomic analysis it was possible to identify specific molecular pathways to drugs or combinations, as well as discriminating between general transcriptional changes and those drug specific. Cultures treated with synergistic combinations were not able to mount an adaptive response unlike bacteria exposed to single drugs. In addition, in line with recent observations [213, 214], metabolic changes identified in this Chapter 3 may constitute a mechanism of drug-adaptation.

With data generated in the bioinformatic and transcriptomic analysis done in this Chapter 3 we created a repository accessible upon request. This repository is a valuable tool that can be consulted in future studies where expression levels of determined genes could be needed to confirm hypothesis or understand experimental drug interactions. An example of its applicability was the BCG_1415c gene previously described. This gene would not be initially selected in a general analysis of the whole transcriptome of all samples because the defined cut-off was only achieved under ethambutol treatment. In addition, its description in the database was vague (*i.e.* transcriptional regulatory protein). However, it was identified after literature revision, and the study of the gene expression under all conditions allowed us to find overexpression levels close to the cut-off when bacteria were treated with drug combinations. This overexpression was exclusively found in drug combinations, which agrees with the hypothesis of the original work that described the overexpression of this gene an indicator of synergistic combinations.

One limitation of this study is that concentrations for cefadroxil containing samples were not accurately chosen. According to the results of the TKA and transcriptomic analysis, the actual MIC of cefadroxil was probably higher than considered. Therefore, transcriptional changes of samples containing cefadroxil could not be detected and they had to be excluded from the rest of the analysis.

Another limitation is that data are inferred from one biological and two technical replicates. The transcriptomic experiment was designed so that single cultures were treated with selected drug conditions. Thus, only one biological replicate per drug condition was performed due to the high number of samples processed. Technical duplicates were used to minimize technical error. However, the error inherent to biological variation could not be detected. This error is typically reduced including multiple biological samples of the same condition [215]. Here, we tried to reduce this impact by using a stricter cut off than the standard (*i.e.* p-adj 0.01 *vs* the standard 0.05).

Future steps for this work would include transcriptomics data validation by quantitative RT-qPCR [87, 216]. The correlation of quantification through qPCR and level of expression detected in transcriptomics constitutes the standard validation method for RNA-Seq results. For this, new samples treated as described in this work will be needed. Some genes differentially expressed would be amplified from the total RNA of all samples and quantification could be correlated with level of expression from our transcriptomic study.

3.5 Conclusions

The work presented in this chapter highlights different adaptive responses of bacteria exposed to single drugs or synergistic combinations.

The positive interaction between rifampicin and cell-wall inhibitors against *Mtb* is well-known. Here, we found an important modulation of the metabolic activity of bacteria exposed to rifampicin, in contrast to bacteria exposed to rifampicin in combination with a synergistic partner. This adaptive response would permit the bacterial adaptation to single drugs. However, bacteria exposed to synergistic combinations are not able to generate such response, suffering severe damage that invariably culminates in cell death. This constitutes our main rational of the mechanism of action of the synergistic combinations studied in this work.

3.6 APPENDIX I: Chapter 3 Killing curves supplementary tables

Supplementary table 3.1. Mean log CFU/ml ± SD of data plotted in **Figure 3.5**.

	Mean Log CFU/ml ± SD			
Sample	**Day 0**	**Day 1**	**Day 2**	**Day 3**
Untreated	5.20 ± 0.04	5.19 ± 0.06	5.13 ± 0.12	5.04 ± 0.00
RIF 1/4x	NA	5.00 ± 0.08	4.61 ± 0.01	4.56 ± 0.09
RIF 1x	NA	4.34 ± 0.03	4.06 ± 0.03	4.19 ± 0.23
EMB 1/4x	NA	5.56 ± 0.10	4.76 ± 0.04	6.48 ± 0.39
EMB 1x	NA	6.04 ± 0.05	4.29 ± 0.02	3.88 ± 0.04
CFX 1/4x	NA	4.29 ± 0.14	4.08 ± 0.00	4.28 ± 0.00
CFX 1x	NA	4.36 ± 0.16	3.74 ± 0.06	3.98 ± 0.32
MER 1/4x	NA	4.70 ± 0.05	4.31 ± 0.05	4.55 ± 0.27
MER 1x	NA	3.93 ± 0.11	4.04 ± 0.17	4.27 ± 0.08
RIF-EMB 1/4x	NA	4.54 ± 0.17	4.20 ± 0.00	3.78 ± 0.74
RIF-EMB 1x	NA	3.00 ± 0.00	2.00	2.00
RIF-MER 1/4x	NA	4.56 ± 0.00	3.74 ± 0.06	3.74 ± 0.06
RIF-MER 1x	NA	2.00	2.00	2.00
RIF-CFX 1/4x	NA	4.52 ± 0.04	3.18 ± 0.21	3.86*
RIF-CFX 1x	NA	4.48 ± 0.07	3.60 ± 0.34	2.00

Cefadroxil (CFX), ethambutol (EMB), meropenem (MER), rifampicin (RIF) NA: not applicable. *: Data from one replicate.

Supplementary table 3.2. Mean log CFU/ml ± SD of data plotted in **Figure 3.6.**

	Mean Log CFU/ml ± SD					
Sample	**Day 0**	**Day 1**	**Day 2**	**Day 3**	**Day 7**	**Day 28**
Untreated	7.30 ± 0.16	6.67*	6.75 ± 0.02	6.94 ± 0.08	5.34*	7.86 ± 0.04
RIF 1/2x	NA	6.40*	6.53 ± 0.04	6.33 ± 0.16	2.00	6.00 ± 0.04
EMB 1/2x	NA	6.67*	6.75 ± 0.03	6.18 ± 0.04	4.90*	5.78 ± 0.22
MER 1/2x	NA	6.32*	5.51 ± 0.09	4.76 ± 0.05	2.00	7.73 ± 0.06
CFX 1/2x	NA	7.00*	6.60 ± 0.11	6.38 ± 0.00	5.55 ± 0.04	7.89 ± 0.06
RIF-EMB 1/2x	NA	6.70*	6.23 ± 0.04	2.00	2.00	2.00
RIF-MER 1/2x	NA	5.76*	4.57 ± 0.08	2.00	2.00	2.00
RIF-CFX 1/2x	NA	6.63*	6.53 ± 0.12	6.11 ± 0.17	2.00	2.00

Cefadroxil (CFX), ethambutol (EMB), meropenem (MER), rifampicin (RIF) NA: not applicable. *: Data from one replicate.

General conclusions and future perspectives

In this Thesis, we developed OPTIKA, an *in vitro* assay to perform drug combination studies against *Mtb*. OPTIKA presents two main advantages compared to standard methodologies for drug combination studies:

1. OPTIKA measures bacterial death, unlike checkerboard assays or DiaMOND, that are growth inhibition-based methods.

2. OPTIKA is performed in a 96-well plate format using a resazurin readout, in contrast to the traditional time kill assays method, that is based on CFU and presents a very low throughput.

OPTIKA is a powerful technique whose throughput is more than 30-fold increased if compared to the standard CFU based time-kill assays. This allows a direct kinetic evaluation of n-way drug combinations in a single step.

From the combination screening focused on β-lactam containing combinations using OPTIKA, we got some conclusions that are summarized below:

- We confirmed the typical killing curve profile of β-lactams assayed against *Mtb*. This is characterized by a fast-killing rate at initial days followed by a bacterial growth rebound at different time points depending on the drug itself and the concentration.

- Ethambutol arose as a good partner for β-lactams, as previously described. Interestingly, we found that all triple-drug combinations tested containing at least one β-lactam and ethambutol showed a maintained killing effect at long times.

- As suggested in other studies, we found that combinations of different sub-classes of β-lactams showed a favourable drug interaction.

- Many of the favourable drug combinations containing β-lactams maintained a low bacterial load at long times.

- Among the drugs tested, we identified pretomanid as a drug that robustly showed favourable drug interaction with meropenem, suggesting that more complex drug combinations containing the core meropenem-pretomanid should be explored.

- Combinations containing linezolid showed a dismissed killing ability than the same combinations without linezolid.

- The fast initial killing rate observed in β-lactams killing curves was also found in combinations containing β-lactams and it was not observed in combinations without them. This was robustly observed in combinations of three, four and five drugs, which allowed us to conclude that, if this behaviour would translate into the clinical, β-lactams should be used at initial days of anti-TB regimens.

Next steps in line with the work described in the screening of drug combinations containing β-lactam would include:

1. The confirmation of the favourable drug interactions identified here under other experimental conditions such as *Mtb* clinical strains, low pH or different carbon sources. This could be done with OPTIKA adapting the growth media of the mother plate to the desired conditions.

2. Evaluation of drug combinations containing two β-lactams exploring other sub-families not tested here.

3. Exploring more complex drug combinations containing the core pretomanid-meropenem.

4. Replacing linezolid by pretomanid to evaluate its contribution in the set of drugs that we screened based on MDR-TB treatment recommendations.

5. Further characterizing favourable drug combinations identified here in other platforms that allow PK profiles simulation such as the Hollow Fibre System. This would allow both: (i) to confirm the favourable drug interactions identified through OPTIKA using a more translational approach, and (ii) to provide more robust *in vitro* data to feed PK/PD models.

Finally, in the last chapter of this Thesis, the transcriptomic analysis of synergistic drug combinations of rifampicin and β-lactams revealed a clear different bacterial response to single drugs and drug combinations. Our transcriptomic analysis was done at sub-inhibitory concentrations for long times, which allowed us to collect the bacterial RNA when bacteria were perturbated by the drugs, but the population was still alive.

We found several transcriptomic differences that indicated that bacteria exposed to single drugs generated an adaptative response which involves metabolic changes such as overexpression of genes to reduce bacterial stress. However, when bacteria were exposed to favourable drug combinations, this adaptative response was not observed, leading to an irreparable cellular damage which led to the bacterial death.

After the transcriptomic study, our hypothesis of the mechanism of action of synergistic drug combinations is that favourable drug combinations prevent the bacteria

from mounting an adaptative response to overcome the damage caused by the single drugs. In addition, with data from our transcriptomic analysis, we generated a repository (accessible upon request) that can be consulted in future studies to confirm hypothesis from literature or from future experimental work.

Conclusiones generales

- Tras la evaluación de las metodologías actuales para el estudio *in vitro* de combinaciones, se encontraron las principales limitaciones:
    - Realizan medidas de inhibición de crecimiento, indicador que presenta una baja traslación a muerte celular.
    - Debido a la variación propia de los ensayos de determinación de MIC o IC_{50}, la selección de condiciones que propone DiaMOND no siempre es la zona más informativa.
    - Aquellos ensayos basados en muerte celular presentan una baja capacidad que imposibilita el estudio de un número elevado de combinaciones.

- Se ha desarrollado OPTIKA, una metodología para estudiar combinaciones *in vitro* frente an *M. tuberculosis*. Esta técnica presenta mucha mayor capacidad que los métodos tradicionales, permite realizar cribados de combinaciones de hasta cinco compuestos y está basada en medidas de muerte celular a distintos tiempos, proporcionando resultados muy valiosos para alimentar modelos matemáticos encaminados al desarrollo de nuevas terapias frente a tuberculosis.

- El perfil de los β-lactámicos en curvas de muerte tradicionales se ha confirmado por OPTIKA.

- Las combinaciones de dos β-lactámicos de distintas subfamilias han mostrado potencial interacción favorable.

- Las combinaciones de β-lactámicos con etambutol han demostrado ser favorables. Además, combinaciones triples que contienen un β-lactámico y etambutol han mantenido esta interacción a tiempos largos.

- La combinación de meropenem con pretomanid se ha identificado como una interacción favorable muy robusta.

- Por el contrario, la contribución de linezolid a los ensayos *in vitro* descritos en esta tesis ha sido, en general no favorable.

- Si el rápido efecto de los β-lactámicos observado en esta tesis traslada a otros sistemas más complejos, éstos deberían ser administrados en los primeros días del tratamiento en futuros regímenes contra la tuberculosis.

- En los ensayos de transcriptómica se ha observado que bacterias expuestas a fármacos a bajas concentraciones generan una respuesta adaptativa que les permite sobrevivir en presencia de dichos fármacos. Sin embargo, cuando son tratadas con combinaciones favorables de dichos fármacos a las mismas concentraciones no son capaces de generar dicha respuesta.

References

1. Jordao L, Vieira OV: **Tuberculosis: New Aspects of an Old Disease.** *International Journal of Cell Biology* 2011, **2011:**403623.
2. Herzog H: **History of tuberculosis.** *Respiration* 1998, **65:**5-15.
3. Barberis I, Bragazzi NL, Galluzzo L, Martini M: **The history of tuberculosis: from the first historical records to the isolation of Koch's bacillus.** *J Prev Med Hyg* 2017, **58:**E9-E12.
4. Daniel TM: **The history of tuberculosis.** *Respir Med* 2006, **100:**1862-1870.
5. Karamanou M, Androutsos G: **The masterful description of pulmonary tuberculosis by Soranus of Ephesus (c. 98-138 A.D.).** *Am J Respir Crit Care Med* 2012, **186:**571.
6. Frith J: **History of Tuberculosis. Part 1 - Phthisis, consumption and the White Plague.** *Journal of Military and Veterans' Health* 2014, **22:**29-35.
7. Daniel TM: **Jean-Antoine Villemin and the infectious nature of tuberculosis.** *Int J Tuberc Lung Dis* 2015, **19:**267-268.
8. Sakula A: **Robert Koch: centenary of the discovery of the tubercle bacillus, 1882.** *Thorax* 1982, **37:**246-251.
9. Gutierrez MC, Brisse S, Brosch R, Fabre M, Omais B, Marmiesse M, Supply P, Vincent V: **Ancient origin and gene mosaicism of the progenitor of Mycobacterium tuberculosis.** *PLoS Pathog* 2005, **1:**e5.
10. Comas I, Coscolla M, Luo T, Borrell S, Holt KE, Kato-Maeda M, Parkhill J, Malla B, Berg S, Thwaites G, et al: **Out-of-Africa migration and Neolithic coexpansion of Mycobacterium tuberculosis with modern humans.** *Nat Genet* 2013, **45:**1176-1182.
11. Daniel TM: **Hermann Brehmer and the origins of tuberculosis sanatoria.** *Int J Tuberc Lung Dis* 2011, **15:**161-162, i.
12. Luca S, Mihaescu T: **History of BCG Vaccine.** *Maedica (Bucur)* 2013, **8:**53-58.
13. Abdallah AM, Behr MA: **Evolution and Strain Variation in BCG.** *Strain Variation in the Mycobacterium tuberculosis Complex: Its Role in Biology, Epidemiology and Control* 2017**:**155-169.
14. WHO: **Global tuberculosis report 2020.** 2020.
15. TBVI: **TuBerculosis Vaccine Initiative.** *https://wwwtbvieu/* Accessed 29/10/2021.
16. Sakula A: **Selman Waksman (1888–1973), discoverer of streptomycin: A centenary review.** *British Journal of Diseases of the Chest* 1988, **82:**23-31.
17. TBFACTS.ORG: **History of TB drugs.** *https://tbfactsorg/history-of-tb-drugs/* Accessed 29/10/2021.
18. Daniels M, Hill AB: **Chemotherapy of pulmonary tuberculosis in young adults; an analysis of the combined results of three Medical Research Council trials.** *Br Med J* 1952, **1:**1162-1168.
19. Ma Z, Lienhardt C, McIlleron H, Nunn AJ, Wang X: **Global tuberculosis drug development pipeline: the need and the reality.** *Lancet* 2010, **375:**2100-2109.

20. Olaru ID, von Groote-Bidlingmaier F, Heyckendorf J, Yew WW, Lange C, Chang KC: **Novel drugs against tuberculosis: a clinician's perspective.** *Eur Respir J* 2015, **45:**1119-1131.
21. Murray JF, Schraufnagel DE, Hopewell PC: **Treatment of Tuberculosis. A Historical Perspective.** *Ann Am Thorac Soc* 2015, **12:**1749-1759.
22. **Tuberculosis morbidity--United States, 1996.** *MMWR Morb Mortal Wkly Rep* 1997, **46:**695-700.
23. WHO: **World Health Organization. Global Tuberculosis Programme. TB: A global emmergency.** 1994.
24. WHO: **World Health Organization. Tuberculosis Programme: framework for effective tuberculosis control.** 1994.
25. Uplekar M, Stop TB Partnership & World Health Organization: **The Stop TB Strategy: building on and enhancing DOTS to meet the TB-related Millennium Development Goals.** 2006.
26. Kaufmann SH, Parida SK: **Changing funding patterns in tuberculosis.** *Nat Med* 2007, **13:**299-303.
27. Comas I, Gagneux S: **The past and future of tuberculosis research.** *PLoS Pathog* 2009, **5:**e1000600.
28. Ginsberg AM, Laurenzi MW, Rouse DJ, Whitney KD, Spigelman MK: **Assessment of the effects of the nitroimidazo-oxazine PA-824 on renal function in healthy subjects.** *Antimicrob Agents Chemother* 2009, **53:**3726-3733.
29. Aldridge BB, Barros-Aguirre D, Barry CE, 3rd, Bates RH, Berthel SJ, Boshoff HI, Chibale K, Chu XJ, Cooper CB, Dartois V, et al: **The Tuberculosis Drug Accelerator at year 10: what have we learned?** *Nat Med* 2021, **27:**1333-1337.
30. ERA4TB: **EUROPEAN REGIMEN ACCELERATOR FOR TUBERCULOSIS** *https://era4tborg/the-project/* Accessed 29/10/2021.
31. Black TA, Buchwald UK: **The pipeline of new molecules and regimens against drug-resistant tuberculosis.** *Journal of Clinical Tuberculosis and Other Mycobacterial Diseases* 2021, **25:**100285.
32. Queval CJ, Brosch R, Simeone R: **The Macrophage: A Disputed Fortress in the Battle against Mycobacterium tuberculosis.** *Front Microbiol* 2017, **8:**2284.
33. Silva Miranda M, Breiman A, Allain S, Deknuydt F, Altare F: **The tuberculous granuloma: an unsuccessful host defence mechanism providing a safety shelter for the bacteria?** *Clin Dev Immunol* 2012, **2012:**139127.
34. Ducati RG, Ruffino-Netto A, Basso LA, Santos DS: **The resumption of consumption -- a review on tuberculosis.** *Mem Inst Oswaldo Cruz* 2006, **101:**697-714.
35. Chai Q, Zhang Y, Liu CH: **Mycobacterium tuberculosis: An Adaptable Pathogen Associated With Multiple Human Diseases.** *Front Cell Infect Microbiol* 2018, **8:**158.
36. Paulson T: **Epidemiology: A mortal foe.** *Nature* 2013, **502:**S2-3.

37. Furin J, Cox H, Pai M: **Tuberculosis.** *Lancet* 2019, **393:**1642-1656.
38. Nayak S, Acharjya B: **Mantoux test and its interpretation.** *Indian Dermatol Online J* 2012, **3:**2-6.
39. Sotgiu G, Saderi L, Petruccioli E, Aliberti S, Piana A, Petrone L, Goletti D: **QuantiFERON TB Gold Plus for the diagnosis of tuberculosis: a systematic review and meta-analysis.** *J Infect* 2019, **79:**444-453.
40. Pai M, Behr MA, Dowdy D, Dheda K, Divangahi M, Boehme CC, Ginsberg A, Swaminathan S, Spigelman M, Getahun H, et al: **Tuberculosis.** *Nat Rev Dis Primers* 2016, **2:**16076.
41. Cudahy P, Shenoi SV: **Diagnostics for pulmonary tuberculosis.** *Postgrad Med J* 2016, **92:**187-193.
42. Nguyen TNA, Anton-Le Berre V, Banuls AL, Nguyen TVA: **Molecular Diagnosis of Drug-Resistant Tuberculosis; A Literature Review.** *Front Microbiol* 2019, **10:**794.
43. WHO: **World Tuberculosis Day 2021** *https://wwwwhoint/campaigns/world-tb-day/2021* Accessed 29/10/2021.
44. WHO: **Global Tuberculosis report 2021.** 2021.
45. The Lancet M: **Is the tuberculosis response another casualty of COVID-19?** *Lancet Microbe* 2021, **2:**e485.
46. Pai M, Kasaeva T, Swaminathan S: **Covid-19's Devastating Effect on Tuberculosis Care - A Path to Recovery.** *N Engl J Med* 2022.
47. TBAlliance: *https://wwwtballianceorg/why-new-tb-drugs/global-pandemic* Accessed 29/10/2021.
48. TBFACTS.ORG: *https://tbfactsorg/tb-statistics/* Accessed 29/10/2021.
49. Iseman MD: **Tuberculosis therapy: past, present and future.** *Eur Respir J Suppl* 2002, **36:**87s-94s.
50. WHO: **World Health Organization. Treatment of drug-susceptible tuberculosis: rapid communication.** 2021.
51. Tiberi S, du Plessis N, Walzl G, Vjecha MJ, Rao M, Ntoumi F, Mfinanga S, Kapata N, Mwaba P, McHugh TD, et al: **Tuberculosis: progress and advances in development of new drugs, treatment regimens, and host-directed therapies.** *Lancet Infect Dis* 2018, **18:**e183-e198.
52. Sheikh BA, Bhat BA, Mehraj U, Mir W, Hamadani S, Mir MA: **Development of New Therapeutics to Meet the Current Challenge of Drug Resistant Tuberculosis.** *Curr Pharm Biotechnol* 2021, **22:**480-500.
53. WHO: **World Health Organization. Meeting report of the WHO expert consultation on the definition of extensively drug-resistant tuberculosis, 27-29 October 2020.** 2021.
54. Almeida A, Adjuntsov M, Bushura W, Delgado E, Drasher M, Fernando-Pancho M, Gasane M, Ianosi MV, Lessem E, Musah A, et al: **Hear us! Accounts of people treated with injectables for drug-resistant TB.** *Public Health Action* 2021, **11:**146-154.

55. WHO: **World Health Organization. Ooperational handbook on tuberculosis. Module 4: treatment - drug-resistant tuberculosis treatment.** 2020.
56. Stephanie F, Saragih M, Tambunan USF: **Recent Progress and Challenges for Drug-Resistant Tuberculosis Treatment.** *Pharmaceutics* 2021, **13**.
57. Bandodkar B, Shandil RK, Bhat J, Balganesh TS: **Two Decades of TB Drug Discovery Efforts—What Have We Learned?** 2020, **10:**5704.
58. Lienhardt C, Nahid P: **Advances in clinical trial design for development of new TB treatments: A call for innovation.** *PLoS Med* 2019, **16:**e1002769.
59. Koul A, Arnoult E, Lounis N, Guillemont J, Andries K: **The challenge of new drug discovery for tuberculosis.** *Nature* 2011, **469:**483-490.
60. Bogatcheva E, Hanrahan C, Nikonenko B, Samala R, Chen P, Gearhart J, Barbosa F, Einck L, Nacy CA, Protopopova M: **Identification of new diamine scaffolds with activity against Mycobacterium tuberculosis.** *J Med Chem* 2006, **49:**3045-3048.
61. Ashburn TT, Thor KB: **Drug repositioning: identifying and developing new uses for existing drugs.** *Nat Rev Drug Discov* 2004, **3:**673-683.
62. Tiberi S, Munoz-Torrico M, Duarte R, Dalcolmo M, D'Ambrosio L, Migliori GB: **New drugs and perspectives for new anti-tuberculosis regimens.** *Pulmonology* 2018, **24:**86-98.
63. Grace AG, Mittal A, Jain S, Tripathy JP, Satyanarayana S, Tharyan P, Kirubakaran R: **Shortened treatment regimens versus the standard regimen for drug-sensitive pulmonary tuberculosis.** *Cochrane Database of Systematic Reviews* 2019.
64. Gillespie SH: **The role of moxifloxacin in tuberculosis therapy.** *Eur Respir Rev* 2016, **25:**19-28.
65. Manjunatha UH, Smith PW: **Perspective: Challenges and opportunities in TB drug discovery from phenotypic screening.** *Bioorg Med Chem* 2015, **23:**5087-5097.
66. Mahajan R: **Bedaquiline: First FDA-approved tuberculosis drug in 40 years.** *Int J Appl Basic Med Res* 2013, **3:**1-2.
67. WGONTB: **WORKING GROUPS ON NEW TB DRUGS.** *https://wwwnewtbdrugsorg/* Accessed 29/10/2021.
68. Parish T: **In vitro drug discovery models for Mycobacterium tuberculosis relevant for host infection.** *Expert Opin Drug Discov* 2020, **15:**349-358.
69. Spigelman M, Woosley R, Gheuens J: **New initiative speeds tuberculosis drug development: novel drug regimens become possible in years, not decades.** *Int J Tuberc Lung Dis* 2010, **14:**663-664.
70. Cokol M, Kuru N, Bicak E, Larkins-Ford J, Aldridge BB: **Efficient measurement and factorization of high-order drug interactions in Mycobacterium tuberculosis.** *Sci Adv* 2017, **3:**e1701881.

71. Larkins-Ford J, Greenstein T, Van N, Degefu YN, Olson MC, Sokolov A, Aldridge BB: **Systematic measurement of combination-drug landscapes to predict in vivo treatment outcomes for tuberculosis.** *Cell Syst* 2021, **12:**1046-1063 e1047.
72. Dooley KE, Hanna D, Mave V, Eisenach K, Savic RM: **Advancing the development of new tuberculosis treatment regimens: The essential role of translational and clinical pharmacology and microbiology.** *PLoS Med* 2019, **16:**e1002842.
73. WHO: **World Health Organization. THE END TB STRATEGY.** 2014.
74. Foucquier J, Guedj M: **Analysis of drug combinations: current methodological landscape.** *Pharmacol Res Perspect* 2015, **3:**e00149.
75. Odds FC: **Synergy, antagonism, and what the chequerboard puts between them.** *J Antimicrob Chemother* 2003, **52:**1.
76. Berenbaum MC: **A method for testing for synergy with any number of agents.** *J Infect Dis* 1978, **137:**122-130.
77. Kim SJ: **Drug-susceptibility testing in tuberculosis: methods and reliability of results.** 2005, **25:**564-569.
78. Rand KH, Houck HJ, Brown P, Bennett D: **Reproducibility of the microdilution checkerboard method for antibiotic synergy.** *Antimicrob Agents Chemother* 1993, **37:**613-615.
79. Tang J, Wennerberg K, Aittokallio T: **What is synergy? The Saariselka agreement revisited.** *Front Pharmacol* 2015, **6:**181.
80. Greco WR, Bravo G, Parsons JC: **The search for synergy: a critical review from a response surface perspective.** *Pharmacol Rev* 1995, **47:**331-385.
81. Doern CD: **When does 2 plus 2 equal 5? A review of antimicrobial synergy testing.** *J Clin Microbiol* 2014, **52:**4124-4128.
82. Gomara M, Ramon-Garcia S: **The FICI paradigm: Correcting flaws in antimicrobial in vitro synergy screens at their inception.** *Biochem Pharmacol* 2019, **163:**299-307.
83. Ramon-Garcia S, Gonzalez Del Rio R, Villarejo AS, Sweet GD, Cunningham F, Barros D, Ballell L, Mendoza-Losana A, Ferrer-Bazaga S, Thompson CJ: **Repurposing clinically approved cephalosporins for tuberculosis therapy.** *Sci Rep* 2016, **6:**34293.
84. Nielsen EI, Friberg LE: **Pharmacokinetic-pharmacodynamic modeling of antibacterial drugs.** *Pharmacol Rev* 2013, **65:**1053-1090.
85. Gold B, Roberts J, Ling Y, Quezada LL, Glasheen J, Ballinger E, Somersan-Karakaya S, Warrier T, Warren JD, Nathan C: **Rapid, Semiquantitative Assay To Discriminate among Compounds with Activity against Replicating or Nonreplicating Mycobacterium tuberculosis.** *Antimicrob Agents Chemother* 2015, **59:**6521-6538.
86. Gold B, Roberts J, Ling Y, Lopez Quezada L, Glasheen J, Ballinger E, Somersan-Karakaya S, Warrier T, Nathan C: **Visualization of the Charcoal Agar Resazurin**

Assay for Semi-quantitative, Medium-throughput Enumeration of Mycobacteria. *J Vis Exp* 2016.

87. Everaert C, Luypaert M, Maag JLV, Cheng QX, Dinger ME, Hellemans J, Mestdagh P: **Benchmarking of RNA-sequencing analysis workflows using whole-transcriptome RT-qPCR expression data.** *Sci Rep* 2017, **7:**1559.
88. Riss TL, Moravec RA, Niles AL, Duellman S, Benink HA, Worzella TJ, Minor L: **Cell Viability Assays.** *Assay Guidance Manual* 2004.
89. Berenbaum MC: **What is synergy?** *Pharmacol Rev* 1989, **41:**93-141.
90. Goutelle S, Maurin M, Rougier F, Barbaut X, Bourguignon L, Ducher M, Maire P: **The Hill equation: a review of its capabilities in pharmacological modelling.** *Fundam Clin Pharmacol* 2008, **22:**633-648.
91. Leisching G, Pietersen RD, Wiid I, Baker B: **Virulence, biochemistry, morphology and host-interacting properties of detergent-free cultured mycobacteria: An update.** *Tuberculosis (Edinb)* 2016, **100:**53-60.
92. Pietersen RD, du Preez I, Loots DT, van Reenen M, Beukes D, Leisching G, Baker B: **Tween 80 induces a carbon flux rerouting in Mycobacterium tuberculosis.** *J Microbiol Methods* 2020, **170:**105795.
93. Mouton JM, Heunis T, Dippenaar A, Gallant JL, Kleynhans L, Sampson SL: **Comprehensive Characterization of the Attenuated Double Auxotroph Mycobacterium tuberculosisDeltaleuDDeltapanCD as an Alternative to H37Rv.** *Front Microbiol* 2019, **10:**1922.
94. Brochado AR, Telzerow A, Bobonis J, Banzhaf M, Mateus A, Selkrig J, Huth E, Bassler S, Zamarreno Beas J, Zietek M, et al: **Species-specific activity of antibacterial drug combinations.** *Nature* 2018, **559:**259-263.
95. Dubos RJ, Davis BD: **Factors affecting the growth of tubercle bacilli in liquid media.** *J Exp Med* 1946, **83:**409-423.
96. Dubos RJ, Middlebrook G: **The effect of wetting agents on the growth of tubercle bacilli.** *J Exp Med* 1948, **88:**81-88.
97. Moellering RC: **Antimicrobial Combinations.** *Rinsho yakuri/Japanese Journal of Clinical Pharmacology and Therapeutics* 1993, **24:**293-300.
98. Bax HI, Bakker-Woudenberg I, de Vogel CP, van der Meijden A, Verbon A, de Steenwinkel JEM: **The role of the time-kill kinetics assay as part of a preclinical modeling framework for assessing the activity of anti-tuberculosis drugs.** *Tuberculosis (Edinb)* 2017, **105:**80-85.
99. Gumbo T, Louie A, Liu W, Ambrose PG, Bhavnani SM, Brown D, Drusano GL: **Isoniazid's bactericidal activity ceases because of the emergence of resistance, not depletion of Mycobacterium tuberculosis in the log phase of growth.** *J Infect Dis* 2007, **195:**194-201.
100. Vilcheze C, Jacobs WR, Jr.: **The Isoniazid Paradigm of Killing, Resistance, and Persistence in Mycobacterium tuberculosis.** *J Mol Biol* 2019, **431:**3450-3461.

101. Khoshnood S, Goudarzi M, Taki E, Darbandi A, Kouhsari E, Heidary M, Motahar M, Moradi M, Bazyar H: **Bedaquiline: Current status and future perspectives.** *J Glob Antimicrob Resist* 2021, **25:**48-59.
102. Yu X, Jiang G, Li H, Zhao Y, Zhang H, Zhao L, Ma Y, Coulter C, Huang H: **Rifampin stability in 7H9 broth and Lowenstein-Jensen medium.** *J Clin Microbiol* 2011, **49:**784-789.
103. Chan CY, Au-Yeang C, Yew WW, Hui M, Cheng AF: **Postantibiotic effects of antituberculosis agents alone and in combination.** *Antimicrob Agents Chemother* 2001, **45:**3631-3634.
104. Sala C, Dhar N, Hartkoorn RC, Zhang M, Ha YH, Schneider P, Cole ST: **Simple model for testing drugs against nonreplicating Mycobacterium tuberculosis.** *Antimicrob Agents Chemother* 2010, **54:**4150-4158.
105. Larkins-Ford J, Greenstein T, Van N, Degefu YN, Olson MC, Sokolov A, Aldridge BB: **Systematic measurement of combination-drug landscapes to predict in vivo treatment outcomes for tuberculosis.** *Cell Syst* 2021.
106. Prideaux B, Via LE, Zimmerman MD, Eum S, Sarathy J, O'Brien P, Chen C, Kaya F, Weiner DM, Chen PY, et al: **The association between sterilizing activity and drug distribution into tuberculosis lesions.** *Nat Med* 2015, **21:**1223-1227.
107. Dartois V: **The path of anti-tuberculosis drugs: from blood to lesions to mycobacterial cells.** *Nat Rev Microbiol* 2014, **12:**159-167.
108. Budha NR, Lee RB, Hurdle JG, Lee RE, Meibohm B: **A simple in vitro PK/PD model system to determine time-kill curves of drugs against Mycobacteria.** *Tuberculosis (Edinb)* 2009, **89:**378-385.
109. Ernest JP, Strydom N, Wang Q, Zhang N, Nuermberger E, Dartois V, Savic RM: **Development of New Tuberculosis Drugs: Translation to Regimen Composition for Drug-Sensitive and Multidrug-Resistant Tuberculosis.** 2021, **61:**495-516.
110. Clewe O, Aulin L, Hu Y, Coates AR, Simonsson US: **A multistate tuberculosis pharmacometric model: a framework for studying anti-tubercular drug effects in vitro.** *J Antimicrob Chemother* 2016, **71:**964-974.
111. Davies GR, Nuermberger EL: **Pharmacokinetics and pharmacodynamics in the development of anti-tuberculosis drugs.** *Tuberculosis (Edinb)* 2008, **88 Suppl 1:**S65-74.
112. Craig WA, Ebert SC: **Killing and regrowth of bacteria in vitro: a review.** *Scand J Infect Dis Suppl* 1990, **74:**63-70.
113. Cavaleri M, Manolis E: **Hollow Fiber System Model for Tuberculosis: The European Medicines Agency Experience.** *Clin Infect Dis* 2015, **61 Suppl 1:**S1-4.
114. Fleming A: **On the antibacterial action of cultures of a penicillium, with special reference to their use in the isolation of B. influenzae. 1929.** *Bull World Health Organ* 2001, **79:**780-790.
115. Rolinson GN: **Forty years of beta-lactam research.** *J Antimicrob Chemother* 1998, **41:**589-603.

116. Kardos N, Demain AL: **Penicillin: the medicine with the greatest impact on therapeutic outcomes.** *Appl Microbiol Biotechnol* 2011, **92:**677-687.
117. Bush K, Bradford PA: **beta-Lactams and beta-Lactamase Inhibitors: An Overview.** *Cold Spring Harb Perspect Med* 2016, **6**.
118. Smith PW, Zuccotto F, Bates RH, Martinez-Martinez MS, Read KD, Peet C, Epemolu O: **Pharmacokinetics of beta-Lactam Antibiotics: Clues from the Past To Help Discover Long-Acting Oral Drugs in the Future.** *ACS Infect Dis* 2018, **4:**1439-1447.
119. Abraham EP: **Cephalosporins 1945-1986.** *Drugs* 1987, **34 Suppl 2:**1-14.
120. Grabrijan K, Strasek N, Gobec S: **Monocyclic beta-lactams for therapeutic uses: a patent overview (2010-2020).** *Expert Opin Ther Pat* 2021, **31:**247-266.
121. van den Akker F, Bonomo RA: **Exploring Additional Dimensions of Complexity in Inhibitor Design for Serine β-Lactamases: Mechanistic and Intra- and Inter-molecular Chemistry Approaches.** 2018, **9**.
122. Watkins R, Papp-Wallace K, Drawz S, Bonomo R: **Novel β-lactamase inhibitors: a therapeutic hope against the scourge of multidrug resistance.** 2013, **4**.
123. Geddes AM, Klugman KP, Rolinson GN: **Introduction: historical perspective and development of amoxicillin/clavulanate.** *Int J Antimicrob Agents* 2007, **30 Suppl 2:**S109-112.
124. Tooke CL, Hinchliffe P, Bragginton EC, Colenso CK, Hirvonen VHA, Takebayashi Y, Spencer J: **β-Lactamases and β-Lactamase Inhibitors in the 21st Century.** *Journal of molecular biology* 2019, **431:**3472-3500.
125. Fisher JF, Mobashery S: **beta-Lactam Resistance Mechanisms: Gram-Positive Bacteria and Mycobacterium tuberculosis.** *Cold Spring Harb Perspect Med* 2016, **6**.
126. Brown L, Wolf JM, Prados-Rosales R, Casadevall A: **Through the wall: extracellular vesicles in Gram-positive bacteria, mycobacteria and fungi.** *Nat Rev Microbiol* 2015, **13:**620-630.
127. Irazoki O, Hernandez SB, Cava F: **Peptidoglycan Muropeptides: Release, Perception, and Functions as Signaling Molecules.** *Front Microbiol* 2019, **10:**500.
128. Horcajo P, de Pedro MA, Cava F: **Peptidoglycan plasticity in bacteria: stress-induced peptidoglycan editing by noncanonical D-amino acids.** *Microb Drug Resist* 2012, **18:**306-313.
129. Egan AJF, Errington J, Vollmer W: **Regulation of peptidoglycan synthesis and remodelling.** *Nat Rev Microbiol* 2020, **18:**446-460.
130. Macheboeuf P, Contreras-Martel C, Job V, Dideberg O, Dessen A: **Penicillin Binding Proteins: key players in bacterial cell cycle and drug resistance processes.** *FEMS Microbiology Reviews* 2006, **30:**673-691.
131. Mora-Ochomogo M, Lohans CT: **β-Lactam antibiotic targets and resistance mechanisms: from covalent inhibitors to substrates.** *RSC Med Chem* 2021, **12:**1623-1639.

132. Tipper DJ, Strominger JL: **Mechanism of action of penicillins: a proposal based on their structural similarity to acyl-D-alanyl-D-alanine.** *Proc Natl Acad Sci U S A* 1965, **54:**1133-1141.
133. Georgopapadakou N, Hammarstrom S, Strominger JL: **Isolation of the penicillin-binding peptide from D-alanine carboxypeptidase of Bacillus subtilis.** *Proc Natl Acad Sci U S A* 1977, **74:**1009-1012.
134. Ogawara H: **Penicillin-binding proteins in Actinobacteria.** *J Antibiot (Tokyo)* 2015, **68:**223-245.
135. Wang F, Cassidy C, Sacchettini JC: **Crystal structure and activity studies of the Mycobacterium tuberculosis beta-lactamase reveal its critical role in resistance to beta-lactam antibiotics.** *Antimicrob Agents Chemother* 2006, **50:**2762-2771.
136. Wivagg CN, Bhattacharyya RP, Hung DT: **Mechanisms of beta-lactam killing and resistance in the context of Mycobacterium tuberculosis.** *J Antibiot (Tokyo)* 2014, **67:**645-654.
137. Khanna NR, Gerriets V: **Beta Lactamase Inhibitors.** *StatPearls* 2021.
138. Hugonnet JE, Blanchard JS: **Irreversible inhibition of the Mycobacterium tuberculosis beta-lactamase by clavulanate.** *Biochemistry* 2007, **46:**11998-12004.
139. Cynamon MH, Palmer GS: **In vitro activity of amoxicillin in combination with clavulanic acid against Mycobacterium tuberculosis.** *Antimicrob Agents Chemother* 1983, **24:**429-431.
140. Chambers HF, Kocagoz T, Sipit T, Turner J, Hopewell PC: **Activity of amoxicillin/clavulanate in patients with tuberculosis.** *Clin Infect Dis* 1998, **26:**874-877.
141. Donald PR, Sirgel FA, Venter A, Parkin DP, Van de Wal BW, Barendse A, Smit E, Carman D, Talent J, Maritz J: **Early bactericidal activity of amoxicillin in combination with clavulanic acid in patients with sputum smear-positive pulmonary tuberculosis.** *Scand J Infect Dis* 2001, **33:**466-469.
142. Singh JA, Upshur R, Padayatchi N: **XDR-TB in South Africa: no time for denial or complacency.** *PLoS medicine* 2007, **4:**e50-e50.
143. Hugonnet JE, Tremblay LW, Boshoff HI, Barry CE, 3rd, Blanchard JS: **Meropenem-clavulanate is effective against extensively drug-resistant Mycobacterium tuberculosis.** *Science* 2009, **323:**1215-1218.
144. England K, Boshoff HI, Arora K, Weiner D, Dayao E, Schimel D, Via LE, Barry CE, 3rd: **Meropenem-clavulanic acid shows activity against Mycobacterium tuberculosis in vivo.** *Antimicrob Agents Chemother* 2012, **56:**3384-3387.
145. Jaganath D, Lamichhane G, Shah M: **Carbapenems against Mycobacterium tuberculosis: a review of the evidence.** *Int J Tuberc Lung Dis* 2016, **20:**1436-1447.

146. Chambers HF, Turner J, Schecter GF, Kawamura M, Hopewell PC: **Imipenem for treatment of tuberculosis in mice and humans.** *Antimicrob Agents Chemother* 2005, **49:**2816-2821.
147. Veziris N, Truffot C, Mainardi JL, Jarlier V: **Activity of carbapenems combined with clavulanate against murine tuberculosis.** *Antimicrob Agents Chemother* 2011, **55:**2597-2600.
148. Diacon AH, van der Merwe L, Barnard M, von Groote-Bidlingmaier F, Lange C, Garcia-Basteiro AL, Sevene E, Ballell L, Barros-Aguirre D: **beta-Lactams against Tuberculosis--New Trick for an Old Dog?** *N Engl J Med* 2016, **375:**393-394.
149. WHO: **World Health Organization. Consolidated guidelines on drug-resistant tuberculosis treatment.** 2019.
150. Levine SR, Beatty KE: **Investigating beta-Lactam Drug Targets in Mycobacterium tuberculosis Using Chemical Probes.** *ACS Infect Dis* 2021, **7:**461-470.
151. Kumar P, Kaushik A, Lloyd EP, Li SG, Mattoo R, Ammerman NC, Bell DT, Perryman AL, Zandi TA, Ekins S, et al: **Non-classical transpeptidases yield insight into new antibacterials.** *Nat Chem Biol* 2017, **13:**54-61.
152. Story-Roller E, Lamichhane G: **Have we realized the full potential of beta-lactams for treating drug-resistant TB?** *IUBMB Life* 2018, **70:**881-888.
153. Gonzalo X, Drobniewski F: **Is there a place for beta-lactams in the treatment of multidrug-resistant/extensively drug-resistant tuberculosis? Synergy between meropenem and amoxicillin/clavulanate.** *J Antimicrob Chemother* 2013, **68:**366-369.
154. Caminero JA, Garcia-Basteiro AL, Rendon A, Piubello A, Pontali E, Migliori GB: **The future of drug-resistant tuberculosis treatment: learning from the past and the 2019 World Health Organization consolidated guidelines.** *Eur Respir J* 2019, **54**.
155. Collaborative Group for the Meta-Analysis of Individual Patient Data in MDRTBt, Ahmad N, Ahuja SD, Akkerman OW, Alffenaar JC, Anderson LF, Baghaei P, Bang D, Barry PM, Bastos ML, et al: **Treatment correlates of successful outcomes in pulmonary multidrug-resistant tuberculosis: an individual patient data meta-analysis.** *Lancet* 2018, **392:**821-834.
156. Seung KJ, Khan P, Franke MF, Ahmed S, Aiylchiev S, Alam M, Putri FA, Bastard M, Docteur W, Gottlieb G, et al: **Culture Conversion at 6 Months in Patients Receiving Delamanid-containing Regimens for the Treatment of Multidrug-resistant Tuberculosis.** *Clin Infect Dis* 2020, **71:**415-418.
157. de Jager VR, Vanker N, van der Merwe L, van Brakel E, Muliaditan M, Diacon AH: **Optimizing beta-Lactams against Tuberculosis.** *Am J Respir Crit Care Med* 2020, **201:**1155-1157.
158. Pagliotto AD, Caleffi-Ferracioli KR, Lopes MA, Baldin VP, Leite CQ, Pavan FR, Scodro RB, Siqueira VL, Cardoso RF: **Anti-Mycobacterium tuberculosis activity of antituberculosis drugs and amoxicillin/clavulanate combination.** *J Microbiol Immunol Infect* 2016, **49:**980-983.

159. Abate G, Miorner H: **Susceptibility of multidrug-resistant strains of Mycobacterium tuberculosis to amoxycillin in combination with clavulanic acid and ethambutol.** *J Antimicrob Chemother* 1998, **42:**735-740.
160. Turnidge JD: **The pharmacodynamics of beta-lactams.** *Clin Infect Dis* 1998, **27:**10-22.
161. Conradie F, Diacon AH, Ngubane N, Howell P, Everitt D, Crook AM, Mendel CM, Egizi E, Moreira J, Timm J, et al: **Treatment of Highly Drug-Resistant Pulmonary Tuberculosis.** *N Engl J Med* 2020, **382:**893-902.
162. Gillespie SH, Crook AM, McHugh TD, Mendel CM, Meredith SK, Murray SR, Pappas F, Phillips PP, Nunn AJ, Consortium RE: **Four-month moxifloxacin-based regimens for drug-sensitive tuberculosis.** *N Engl J Med* 2014, **371:**1577-1587.
163. Jindani A, Harrison TS, Nunn AJ, Phillips PP, Churchyard GJ, Charalambous S, Hatherill M, Geldenhuys H, McIlleron HM, Zvada SP, et al: **High-dose rifapentine with moxifloxacin for pulmonary tuberculosis.** *N Engl J Med* 2014, **371:**1599-1608.
164. Merle CS, Fielding K, Sow OB, Gninafon M, Lo MB, Mthiyane T, Odhiambo J, Amukoye E, Bah B, Kassa F, et al: **A four-month gatifloxacin-containing regimen for treating tuberculosis.** *N Engl J Med* 2014, **371:**1588-1598.
165. Sarpong-Duah M, Frimpong M, Beissner M, Saar M, Laing K, Sarpong F, Loglo AD, Abass KM, Frempong M, Sarfo FS, et al: **Clearance of viable Mycobacterium ulcerans from Buruli ulcer lesions during antibiotic treatment as determined by combined 16S rRNA reverse transcriptase /IS 2404 qPCR assay.** *PLoS Negl Trop Dis* 2017, **11:**e0005695.
166. Arenaz-Callao MP, Gonzalez Del Rio R, Lucia Quintana A, Thompson CJ, Mendoza-Losana A, Ramon-Garcia S: **Triple oral beta-lactam containing therapy for Buruli ulcer treatment shortening.** *PLoS Negl Trop Dis* 2019, **13:**e0007126.
167. Keam SJ: **Pretomanid: First Approval.** *Drugs* 2019, **79:**1797-1803.
168. Singh R, Manjunatha U, Boshoff HI, Ha YH, Niyomrattanakit P, Ledwidge R, Dowd CS, Lee IY, Kim P, Zhang L, et al: **PA-824 kills nonreplicating Mycobacterium tuberculosis by intracellular NO release.** *Science* 2008, **322:**1392-1395.
169. Stover CK, Warrener P, VanDevanter DR, Sherman DR, Arain TM, Langhorne MH, Anderson SW, Towell JA, Yuan Y, McMurray DN, et al: **A small-molecule nitroimidazopyran drug candidate for the treatment of tuberculosis.** *Nature* 2000, **405:**962-966.
170. Ignatius EH, Abdelwahab MT, Hendricks B, Gupte N, Narunsky K, Wiesner L, Barnes G, Dawson R, Dooley KE, Denti P: **Pretomanid Pharmacokinetics in the Presence of Rifamycins: Interim Results from a Randomized Trial among Patients with Tuberculosis.** *Antimicrob Agents Chemother* 2021, **65**.
171. Bahuguna A, Rawat DS: **An overview of new antitubercular drugs, drug candidates, and their targets.** *Med Res Rev* 2020, **40:**263-292.

172. Chen H, Du Y, Xia Q, Li Y, Song S, Huang X: **Role of linezolid combination therapy for serious infections: review of the current evidence.** *Eur J Clin Microbiol Infect Dis* 2020, **39:**1043-1052.
173. Sharma D, Dhuriya YK, Deo N, Bisht D: **Repurposing and Revival of the Drugs: A New Approach to Combat the Drug Resistant Tuberculosis.** *Front Microbiol* 2017, **8:**2452.
174. Tasneen R, Betoudji F, Tyagi S, Li SY, Williams K, Converse PJ, Dartois V, Yang T, Mendel CM, Mdluli KE, Nuermberger EL: **Contribution of Oxazolidinones to the Efficacy of Novel Regimens Containing Bedaquiline and Pretomanid in a Mouse Model of Tuberculosis.** *Antimicrob Agents Chemother* 2016, **60:**270-277.
175. Nuermberger E, Tyagi S, Tasneen R, Williams KN, Almeida D, Rosenthal I, Grosset JH: **Powerful bactericidal and sterilizing activity of a regimen containing PA-824, moxifloxacin, and pyrazinamide in a murine model of tuberculosis.** *Antimicrob Agents Chemother* 2008, **52:**1522-1524.
176. De Groote MA, Gruppo V, Woolhiser LK, Orme IM, Gilliland JC, Lenaerts AJ: **Importance of confirming data on the in vivo efficacy of novel antibacterial drug regimens against various strains of Mycobacterium tuberculosis.** *Antimicrob Agents Chemother* 2012, **56:**731-738.
177. Munguia J, Nizet V: **Pharmacological Targeting of the Host-Pathogen Interaction: Alternatives to Classical Antibiotics to Combat Drug-Resistant Superbugs.** *Trends Pharmacol Sci* 2017, **38:**473-488.
178. Early JV, Casey A, Martinez-Grau MA, Gonzalez Valcarcel IC, Vieth M, Ollinger J, Bailey MA, Alling T, Files M, Ovechkina Y, Parish T: **Oxadiazoles Have Butyrate-Specific Conditional Activity against Mycobacterium tuberculosis.** *Antimicrob Agents Chemother* 2016, **60:**3608-3616.
179. Piddock LJ, Williams KJ, Ricci V: **Accumulation of rifampicin by Mycobacterium aurum, Mycobacterium smegmatis and Mycobacterium tuberculosis.** *J Antimicrob Chemother* 2000, **45:**159-165.
180. Chiner-Oms A, Comas I: **Large genomics datasets shed light on the evolution of the Mycobacterium tuberculosis complex.** *Infect Genet Evol* 2019, **72:**10-15.
181. Edson Machado CC, Antonio Basílio de Miranda and Marcos Catanho **Web Resources on Tuberculosis: Information, Research, and Data Analysis, Mycobacterium - Research and Development.** 2018.
182. Aguilar-Ayala DA, Tilleman L, Van Nieuwerburgh F, Deforce D, Palomino JC, Vandamme P, Gonzalez-Y-Merchand JA, Martin A: **The transcriptome of Mycobacterium tuberculosis in a lipid-rich dormancy model through RNAseq analysis.** *Scientific Reports* 2017, **7:**17665.
183. Briffotaux J, Liu S, Gicquel B: **Genome-Wide Transcriptional Responses of Mycobacterium to Antibiotics.** *Front Microbiol* 2019, **10:**249.

184. Kaushik A, Makkar N, Pandey P, Parrish N, Singh U, Lamichhane G: **Carbapenems and Rifampin Exhibit Synergy against Mycobacterium tuberculosis and Mycobacterium abscessus.** *Antimicrob Agents Chemother* 2015, **59:**6561-6567.
185. Chakraborty S, Rhee KY: **Tuberculosis Drug Development: History and Evolution of the Mechanism-Based Paradigm.** *Cold Spring Harb Perspect Med* 2015, **5:**a021147.
186. Sukhithasri V, Vinod V, Varma S, Biswas R: **Mycobacterium tuberculosis treatment modalities and recent insights.** *Curr Drug Deliv* 2014, **11:**744-752.
187. Gun MA, Bozdogan B, Coban AY: **Tuberculosis and beta-lactam antibiotics.** *Future Microbiol* 2020, **15:**937-944.
188. Cordillot M, Dubee V, Triboulet S, Dubost L, Marie A, Hugonnet JE, Arthur M, Mainardi JL: **In vitro cross-linking of Mycobacterium tuberculosis peptidoglycan by L,D-transpeptidases and inactivation of these enzymes by carbapenems.** *Antimicrob Agents Chemother* 2013, **57:**5940-5945.
189. Dubee V, Triboulet S, Mainardi JL, Etheve-Quelquejeu M, Gutmann L, Marie A, Dubost L, Hugonnet JE, Arthur M: **Inactivation of Mycobacterium tuberculosis l,d-transpeptidase LdtMt(1) by carbapenems and cephalosporins.** *Antimicrob Agents Chemother* 2012, **56:**4189-4195.
190. Gonzalo-Asensio J, Perez I, Aguilo N, Uranga S, Pico A, Lampreave C, Cebollada A, Otal I, Samper S, Martin C: **New insights into the transposition mechanisms of IS6110 and its dynamic distribution between Mycobacterium tuberculosis Complex lineages.** *PLoS Genet* 2018, **14:**e1007282.
191. Love MI, Huber W, Anders S: **Moderated estimation of fold change and dispersion for RNA-seq data with DESeq2.** *Genome Biology* 2014, **15:**550.
192. Maere S, Heymans K, Kuiper M: **BiNGO: a Cytoscape plugin to assess overrepresentation of gene ontology categories in biological networks.** *Bioinformatics* 2005, **21:**3448-3449.
193. Ashburner M, Ball CA, Blake JA, Botstein D, Butler H, Cherry JM, Davis AP, Dolinski K, Dwight SS, Eppig JT, et al: **Gene ontology: tool for the unification of biology. The Gene Ontology Consortium.** *Nat Genet* 2000, **25:**25-29.
194. Rathnaiah G. ZDK, Barletta R.G: **Role of Mycobacterium tuberculosis PE and PPE Proteins in Pathogen-Host Interactions.** 2019.
195. Li W, Deng W, Xie J: **Expression and regulatory networks of Mycobacterium tuberculosis PE/PPE family antigens.** *J Cell Physiol* 2019, **234:**7742-7751.
196. Ates LS: **New insights into the mycobacterial PE and PPE proteins provide a framework for future research.** *Mol Microbiol* 2020, **113:**4-21.
197. Wang Q, Boshoff HIM, Harrison JR, Ray PC, Green SR, Wyatt PG, Barry CE, 3rd: **PE/PPE proteins mediate nutrient transport across the outer membrane of Mycobacterium tuberculosis.** *Science* 2020, **367:**1147-1151.

198. Namouchi A, Gomez-Munoz M, Frye SA, Moen LV, Rognes T, Tonjum T, Balasingham SV: **The Mycobacterium tuberculosis transcriptional landscape under genotoxic stress.** *BMC Genomics* 2016, **17:**791.
199. M.I. Voskuil DS, R. Rutherford, Y. Liu, G.K. Schoolnik, : **Regulation of the Mycobacterium tuberculosis PE/PPE genes.** 2004, **84:**256-262.
200. Huang da W, Sherman BT, Lempicki RA: **Bioinformatics enrichment tools: paths toward the comprehensive functional analysis of large gene lists.** *Nucleic Acids Res* 2009, **37:**1-13.
201. Tipney H, Hunter L: **An introduction to effective use of enrichment analysis software.** *Hum Genomics* 2010, **4:**202-206.
202. Mizrahi V, Warner DF: **Death of Mycobacterium tuberculosis by l-arginine starvation.** *Proc Natl Acad Sci U S A* 2018, **115:**9658-9660.
203. Tiwari S, van Tonder AJ, Vilcheze C, Mendes V, Thomas SE, Malek A, Chen B, Chen M, Kim J, Blundell TL, et al: **Arginine-deprivation-induced oxidative damage sterilizes Mycobacterium tuberculosis.** *Proc Natl Acad Sci U S A* 2018, **115:**9779-9784.
204. Parish T: **Two-Component Regulatory Systems of Mycobacteria.** *Microbiol Spectr* 2014, **2:**MGM2-0010-2013.
205. Itou H, Tanaka I: **The OmpR-family of proteins: insight into the tertiary structure and functions of two-component regulator proteins.** *J Biochem* 2001, **129:**343-350.
206. Ma S, Jaipalli S, Larkins-Ford J, Lohmiller J, Aldridge BB, Sherman DR, Chandrasekaran S: **Transcriptomic Signatures Predict Regulators of Drug Synergy and Clinical Regimen Efficacy against Tuberculosis.** *mBio* 2019, **10**.
207. Alland D, Steyn AJ, Weisbrod T, Aldrich K, Jacobs WR: **Characterization of the Mycobacterium tuberculosis iniBAC Promoter, a Promoter That Responds to Cell Wall Biosynthesis Inhibition.** 2000, **182:**1802-1811.
208. Colangeli R, Helb D, Sridharan S, Sun J, Varma-Basil M, Hazbon MH, Harbacheuski R, Megjugorac NJ, Jacobs WR, Jr., Holzenburg A, et al: **The Mycobacterium tuberculosis iniA gene is essential for activity of an efflux pump that confers drug tolerance to both isoniazid and ethambutol.** *Mol Microbiol* 2005, **55:**1829-1840.
209. Kohanski MA, Dwyer DJ, Hayete B, Lawrence CA, Collins JJ: **A common mechanism of cellular death induced by bactericidal antibiotics.** *Cell* 2007, **130:**797-810.
210. Nandakumar M, Nathan C, Rhee KY: **Isocitrate lyase mediates broad antibiotic tolerance in Mycobacterium tuberculosis.** *Nat Commun* 2014, **5:**4306.
211. Mitosch K, Bollenbach T: **Bacterial responses to antibiotics and their combinations.** *Environ Microbiol Rep* 2014, **6:**545-557.
212. Hatzios SK, Bertozzi CR: **The regulation of sulfur metabolism in Mycobacterium tuberculosis.** *PLoS Pathog* 2011, **7:**e1002036.

213. Schrader SM, Botella H, Jansen R, Ehrt S, Rhee K, Nathan C, Vaubourgeix J: **Multiform antimicrobial resistance from a metabolic mutation.** *Sci Adv* 2021, **7**.
214. Lopatkin AJ, Bening SC, Manson AL, Stokes JM, Kohanski MA, Badran AH, Earl AM, Cheney NJ, Yang JH, Collins JJ: **Clinically relevant mutations in core metabolic genes confer antibiotic resistance.** *Science* 2021, **371**.
215. Hansen KD, Wu Z, Irizarry RA, Leek JT: **Sequencing technology does not eliminate biological variability.** *Nat Biotechnol* 2011, **29:**572-573.
216. Coenye T: **Do results obtained with RNA-sequencing require independent verification?** *Biofilm* 2021, **3:**100043.